

**Identification and functional characterization of genes
conferring resistance to Fusarium head blight,
underlying QTL-Fhb1, based on forward and reverse
genetics approach**

Nancy Soni

Department of Plant Science
McGill University, Montreal, Canada

February 2021

**A thesis submitted to the McGill University in partial fulfilment of the requirements of the
degree of Doctor of Philosophy**

©Nancy Soni (2021)

Dedicated to my family and wheat growers

TABLE OF CONTENTS

TABLE OF CONTENTS	iii
LIST OF TABLES	viii
LIST OF FIGURES	ix
LIST OF APPENDICES	xi
LIST OF ABBREVIATIONS	xii
ABSTRACT	xiv
RÉSUMÉ	xvi
ACKNOWLEDGEMENTS	xviii
PREFACE AND CONTRIBUTION OF THE AUTHORS	1
Contributions of Authors	1
Contributions to Knowledge	1
CHAPTER I: INTRODUCTION	5
1.1 OBJECTIVES AND HYPOTHESES	10
Hypotheses	10
Global Objective	10
Specific Objectives	10
CHAPTER II: REVIEW OF LITERATURE	11
2.1 Fusarium head blight	11
2.1.1 Fusarium head blight epidemiology	11
2.1.2 Pathogen growth and colonization	11
2.1.3 Impacts of FHB in wheat production	12
2.1.4 Management practices for FHB	13
2.1.5 Types of FHB resistance	14
2.2 Wheat crop breeding	15
2.2.1 Marker-assisted selection (MAS).....	15
2.2.2. Quantitative trait locus (QTL) for FHB resistance.....	16
2.3 Wheat chromosome 3B and QTL-Fhb1	17
2.3.1 Gene discovery in QTL-Fhb1.....	18
2.4 Forward genetics approach to identify novel candidates in FHB resistance	19
2.4.1 QTL-sequencing.....	19
2.4.2 Metabolomics	20

2.4.2.1 Metabolite extraction and analytical platforms.....	21
2.4.2.2 Computational framework and advancement of metabolomics.....	23
2.5 Reverse genetics approach for functional genomics.....	23
2.5.1 Virus-induced gene silencing (VIGS).....	23
CONNECTING STATEMENT FOR CHAPTER III.....	26
CHAPTER III.....	27
Combined metabolo-genomics approach-based identification of genetic determinants of Fusarium head blight resistance in wheat QTL-Fhb1.....	27
3.1 Abstract.....	28
3.2 Introduction.....	29
3.3 Materials and methods.....	31
3.3.1 Plant production and experimental design.....	31
3.3.2 Pathogen production and inoculation.....	31
3.3.3 Disease severity assessment.....	31
3.3.4 Sample collection, metabolite extraction, and Liquid chromatography-mass spectrometry (LC-MS) analysis.....	32
3.3.4.1 LC-MS data processing, statistical analysis and metabolites identification.....	32
3.3.4 QTL-Fhb1 sequencing.....	33
3.3.4.1 Bioinformatics analysis and <i>In-silico</i> annotation of a gene identified.....	33
3.3.4.2 Comparative mapping.....	33
3.3.4.3 First-strand cDNA synthesis and semi-quantitative PCR analysis.....	34
3.3.4.4 Single nucleotide polymorphism (SNP) analysis.....	34
3.4 Results.....	35
3.4.1 Resistant NIL had reduced disease severity.....	35
3.4.2 Resistant-related (RR) metabolites in response to <i>Fg</i> infection in wheat NILs.....	35
3.4.3 Genes identified in QTL-Fhb1.....	35
3.4.4 GO enrichment analyses revealed over-represented GO term(s).....	36
3.4.5 Gene synteny among relative species.....	36
3.4.6 Gene expression profiling post- <i>Fg</i> infection.....	36
3.4.7 Genetic variants among NILs.....	37
3.4.8 Prioritization of Candidate Genes.....	37
3.5 Discussion.....	38
3.5.1 Functional genomic analysis of constitutive and inducible defense responses to <i>Fg</i> infection in wheat NILs with contrasting FHB resistance.....	39
3.5.2 Novel candidates for FHB resistance.....	39
3.5.2.1 Glutamate metabolic process.....	39

3.5.2.2 Response to oxidative stress/ Oxidation-Reduction	40
3.5.2.3 Carbohydrate metabolic process	40
3.5.2.4 Receptor-like kinases	41
3.5.2.5 Regulation of transcription	42
3.5.3 Metabolic profiling provided key insights to metabolic pathways actively participating in pathogen invasion	43
3.6 Author contribution statement	46
3.7 Compliance with ethical standards	46
3.8 Conflict of interest	46
3.9 Acknowledgments	46
REFERENCES	47
CONNECTING STATEMENT FOR CHAPTER IV	73
CHAPTER IV	74
Role of laccase gene in wheat NILs differing at QTL-Fhb1 for resistance against Fusarium head blight	74
4.1 Abstract	75
4.2 Introduction	75
4.3 Materials and methods	77
4.3.1 Plant production and experimental design	77
4.3.2 Pathogen production and inoculation	78
4.3.3 Candidate gene identification in QTL-Fhb1	78
4.3.4 Gene expression analysis	79
4.3.5 Phylogenetic analysis	79
4.3.6 Molecular docking of TaLAC4 with lignin model compounds	79
4.3.7 Gene cloning, sequencing, and polymorphism analysis	80
4.3.8 Construction of BSMV vectors and virus-induced gene silencing (VIGS) of <i>TaLAC4</i>	81
4.3.9 Comparison of <i>TaLAC4</i> non-silenced and silenced NIL-R	82
4.3.9.1 qRT-PCR, fungal biomass, and disease severity	82
4.3.9.2 Phloroglucinol-HCL staining or weisner test	82
4.3.9.3 Acetyl bromide soluble lignin (ABSL) assay	83
4.3.10 Metabolite profiling of <i>TaLAC4</i> non-silenced and silenced NIL-R	83
4.3.10.1 Metabolites extraction, LC-HRMS and data processing	84
4.3.10.2 Statistical analysis and putative metabolite identification	84
4.4 Results	85
4.4.1 Characterization of <i>TaLAC</i> gene	85
4.4.2 Molecular docking revealed binding substrates of TaLAC4	85

4.4.3 Polymorphism and differential gene expression of <i>TaLAC4</i> in NIL-R and NIL-S	86
4.4.4 <i>TaLAC4</i> gene expression in silenced and non-silenced NIL-R.....	87
4.4.5 Silencing of <i>TaLAC4</i> gene in NIL-R increased disease severity and fungal biomass in rachis.....	87
4.4.6 Total lignin and its structure altered in NIL-R, following silencing of <i>TaLAC4</i>	88
4.4.7 Effect of <i>TaLAC4</i> silencing on the abundances of PRr metabolites in NIL-R.....	88
4.5 Discussion	88
4.5.1 <i>TaLAC4</i> in plant defense against <i>Fg</i>	88
4.5.2 Metabolic changes in the laccase silenced NIL-R plants.....	89
4.5.3 <i>TaLAC4</i> contributes to basal immunity by mediating induced lignins	91
4.6 Author contribution statement.....	92
4.7 Compliance with ethical standards	93
4.8 Declaration of Competing Interest.....	93
4.9 Acknowledgments	93
REFERENCES.....	93
CONNECTING STATEMENT FOR CHAPTER V	114
CHAPTER V	115
<i>TaNAC032</i> transcription factor regulates lignin-biosynthetic genes to combat Fusarium head blight in wheat	115
5.1 Abstract	116
5.2 Introduction.....	116
5.3 Materials and methods.....	119
5.3.1 Plant materials and experimental design.....	119
5.3.2 Fungal inoculum production and inoculation.....	119
5.3.3 Metabolite extraction and LC-high resolution MS/MS analysis.....	120
5.3.4 Identification of NAC as a candidate gene underlying QTL-Fhb1	120
5.3.5 Sanger sequencing and genetic polymorphism analysis	121
5.3.6 Real-time Quantitative PCR (qRT-PCR)	121
5.3.7 <i>In-silico</i> promoter analysis of RR metabolites biosynthetic genes (<i>R_{RRM}</i>) and their interaction with <i>TaNAC032</i>	122
5.3.8 Constructing knockdown vectors, in vitro transcription of viral RNA, and plant inoculation	122
5.3.8.1 <i>TaNAC032</i> gene silencing confirmation and disease evaluation	123
5.3.8.2 Lignin detection using Weisner test.....	123
5.3.8.3 Lignin quantification based on acetyl bromide soluble lignin (ABSL) assay	124
5.4 Results.....	124
5.4.1 Sequencing and <i>Ab-initio</i> characterization of a novel <i>TaNAC032</i> transcription factor identified in wheat NILs.....	124

5.4.2 <i>TaNAC032</i> gene expression following pathogen inoculation	125
5.4.3 Polymorphism in <i>TaNAC032</i> protein	125
5.4.4 In silico promoter analysis and physical interaction of RR metabolite biosynthetic genes (RRRM) with <i>TaNAC032</i>	126
5.4.5 Silencing of pathogen-induced <i>TaNAC032</i> increased susceptibility in wheat resistant NIL to <i>Fg</i> infection	126
5.4.6 Semi-comprehensive metabolomics revealed biosynthesis of phenylpropanoids and lignan glycosides by the downstream <i>R_{RRM}</i> genes that were regulated by <i>TaNAC032</i> in wheat	127
5.4.7 The silenced <i>Tanac032</i> in NIL-R revealed altered lignin composition in rachis.....	128
5.5 Discussion	128
5.6 Author Contributions	132
5.7 Compliance with ethical standards	133
5.8 Declaration of Competing Interest.....	133
5.9 Acknowledgments	133
REFERENCES.....	133
CHAPTER VI.....	157
GENERAL DISCUSSION, CONCLUSION AND FUTURE DIRECTIONS	157
6.1 General discussion and conclusions	157
6.2 Future works	159
REFERENCES.....	163
APPENDICES	174
Supplementary Tables.....	174
Supplementary Text	182
PERMISSION FOR MANUSCRIPT USE.....	184
Personal use.....	184
Commercial use.....	184
Internal institutional use	185
BIOSAFETY RELATED DOCUMENTS	186

LIST OF TABLES

Table 3.1 Resistance related induced (RRI) and resistance related constitutive (RRC) metabolites putatively identified upon <i>Fg</i> and mock inoculation in NILs rachis with resistant and susceptible QTL-Fhb1.	54
Table 3.2 Genes located in the QTL-Fhb1 region derived from Sumai 3*5/Thatcher population flanking between markers XSTS3B-138 and XSTS3B-142.....	56
Table 3.3 List of primers used in the gene expression study.	59
Table 3.4 List of candidates possessing multiple genomic variants based on SNP variant analysis.	61
Table 4.1 List of high fold change resistance-related induced metabolites identified in NIL-R+BSMV: <i>Talac4</i> (<i>TaLAC4</i> silenced NILs).....	100
Table 4.2 GenBank accession numbers of proteins used in the phylogeny study.	100
Table 4.3 List of primers used in the experiments.	102
Table 5.1 Promoter sequence analysis of downstream resistance-related metabolite biosynthetic genes (R _{RRM}) harboring secondary wall NAC binding element (SNBE).	139
Table 5.2 List of primers used in this study.....	139
Table 5.3 Genbank accession numbers of proteins used in the phylogeny study.	140

LIST OF FIGURES

Figure 3.1 Phenotyping of NILs differing at QTL-Fhb1..	64
Figure 3.2 Gene ontology (GO) term enrichment analysis.....	65
Figure 3.3 Comparative mapping of chromosome 3B linkage map with the corresponding 3B physical bin map and novel genes underlying QTL-Fhb1 between XSTS3B-138 and XSTS3B-142 flanking markers..	66
Figure 3.4 Heatmap of differentially expressed genes.....	68
Figure 3.5 MultAlin software based amino acid sequence alignment of resistant and susceptible NIL.....	69
Figure 3.6 The workflow of combined metabolo-genomics approach to identify potential FHB resistance genes in wheat NILs.....	72
Figure 4.1 Physical map of the QTL-Fhb1 on the short arm of wheat chromosome 3B.....	103
Figure 4.2 Ab-initio characterization of <i>TaLAC4</i> gene..	104
Figure 4.3 Molecular docking of <i>TaLAC4</i> with lignin model compounds..	106
Figure 4.4 Sequencing of <i>TaLAC4</i> gene in the NILs with contrasting alleles.....	107
Figure 4.5 Virus-induced gene silencing (VIGS) fragments were designed to specifically knock-down the <i>TaLAC4</i> gene.....	109
Figure 4.6 BSMV based virus-induced gene silencing of the phytoene desaturase (PDS) gene..	110
Figure 4.7 BSMV based virus-induced gene silencing of <i>TaLAC4</i> gene..	111
Figure 4.8 Effect of <i>TaLAC4</i> silencing in FHB resistant near-isogenic line (NIL-R), inoculated with <i>F. graminearum</i> or mock-solution.....	112
Figure 4.9 Total lignin quantification using acetyl bromide method and phloroglucinol-HCL staining.....	113
Figure 5.1 <i>In silico</i> analysis of the <i>TaNAC032</i> gene.	142
Figure 5.2 <i>TaNAC032</i> sequencing and sequence analysis.....	144

Figure 5.3 <i>TaNAC032</i> sequencing and sequence analysis in wheat genotypes (Sumai 3, NIL-R (S/T), NIL-S (S/T), NIL-R (HC/98), NIL-S (HC/98), Frontana, Pasteur and Thatcher) with varying levels of FHB resistance.	145
Figure 5.4 Canonical lignin biosynthesis pathway in plants.....	147
Figure 5.5 <i>In-silico</i> DNA-protein interaction using the GeneMANIA server.....	148
Figure 5.6 Virus-induced gene silencing (VIGS) of the <i>TaNAC032</i> gene..	149
Figure 5.7 Effect of <i>TaNAC032</i> silencing in FHB resistant near-isogenic line (NIL-R), inoculated with <i>F. graminearum</i> or mock-solution.....	150
Figure 5.8 BoxPlot represents relative metabolite abundances of RRI metabolites in silenced (BSMV: <i>Tanac032</i>) and non-silenced (BSMV: 00) NIL-R at 3 dpi after <i>Fg</i> inoculation.....	153
Figure 5.9 Lignification induced by <i>TaNAC032</i> in rachis.....	154
Figure 5.10 Proposed model showing <i>TaNAC032</i> transcription factor regulating the biosynthesis of lignin specific pathway biosynthetic <i>R_{RRM}</i> genes to produce resistant-related metabolites (RMs).	156

LIST OF APPENDICES

Supplementary Table 3. 1 Resistance related (RR) metabolites (P<0.05) detected in the wheat NILs rachis following <i>F. graminearum</i> (<i>Fg</i>) or mock-solution inoculation.....	174
Supplementary Table 3. 2 Putative candidate genes and gene ontology (GO) underlying QTL-Fhb1.	176
Supplementary Table 4.1 Lists the predicted minimum binding energy scores (kJ/mol), RMSD of best-fit predicted laccase models with lignin model compounds obtained from AutoDock Vina software.....	179
Supplementary Table 4.2 List of high fold change metabolites identified in NIL-R+BSMV: <i>Talac4</i> (<i>TaLAC4</i> silenced NILs).	179

LIST OF ABBREVIATIONS

ABSL	Acetyl bromide soluble lignin
AME	Accurate mass error
AUDPC	Area under disease progress curve
BAC	Bacterial artificial chromosome
BLAST	Basic local alignment search tool
BSMV	Barley stripe mosaic virus
cDNA	Complimentary deoxyribonucleic acid
CFIA	Canadian Food Inspection Agency
CRISPR	Clustered regularly interspaced short palindromic repeats
D3G	DON-3-O-glucoside
DNA	Deoxyribonucleic acid
DON	Deoxynivalenol
dpi	Days post inoculation
FAO	Food and agriculture organization
FC	Fold-change
FDA	Food and Drug Administration
FHB	Fusarium head blight
GC-MS	Gas chromatography mass spectrometry
HCAAs	Hydroxycinnamic acid amides
hpi	Hours post inoculation
IWGSC	International wheat genome sequencing consortium
LC-MS	Liquid chromatography mass spectrometry
LC-HRMS	Liquid chromatography high resolution mass spectrometry
m/z	Mass to charge ratio
MS	Mass spectrometry
NCBI	National Center for Biotechnology Information
NIL	Near-isogenic line
NMR	Nuclear magnetic resonance
PCD	Programmed cell death

PCR	Polymerase chain reaction
PDS	Phytoene desaturase
PR	Pathogenesis related
PSD	Proportion of spikelets diseased
qPCR	Quantitative polymerase chain reaction
QTL	Quantitative trait loci
RCBD	Randomized complete block design
RM	Mock inoculated resistant genotype
RNA	Ribonucleic Acid
RNAi	RNA interference
RP	Pathogen inoculated resistant genotype
RR	Resistance related
RRC	Resistance related constitutive metabolite
RRI	Resistance related induced metabolite
RT-qPCR	Quantitative reverse transcription PCR
SM	Mock inoculated susceptible genotype
SNP	Single nucleotide polymorphism
SP	Pathogen inoculated susceptible genotype
SSR	Simple Sequence Repeat
<i>TaCCR</i>	<i>Triticum aestivum</i> Cinnamoyl-CoA reductase
<i>TaCAD</i>	<i>Triticum aestivum</i> Cinnamyl alcohol dehydrogenase
T-DNA	The transfer DNA
<i>TaLAC4</i>	<i>Triticum aestivum</i> Laccase-4-like
<i>TaNAC032</i>	<i>Triticum aestivum</i> NAC transcription factor 32-like
Tri6	Trichodiene synthase-6
VIGS	Virus-induced gene silencing

ABSTRACT

Fusarium head blight (FHB) is among the most destructive diseases of wheat (*Triticum aestivum* L.), predominantly caused by *Fusarium graminearum* (Fg). Amongst hundreds of quantitative trait loci (QTLs) identified for FHB resistance, QTL-Fhb1 is of significant interest even today, contributing a major effect in FHB resistance. A few genetic determinants of FHB resistance have been identified in the recent past, but their resistance mechanisms have not been deciphered. Therefore, this study aimed to identify candidate gene(s) and to decode resistance mechanisms based on a combined metabolo-genomics approach in wheat near-isogenic lines (NILs) differing at QTL-Fhb1. The resistance-related (RR) metabolites identified in NIL-R with high fold-change in abundance were mainly phenylpropanoids, flavonoids, and lignan glycosides. The dissection of QTL-Fhb1 based on flanking marker sequencing led to the identification of laccase-4-like, cell wall invertase, G-type lectin S-receptor-like serine/threonine-protein kinase, NAC transcription factor 32-like and glutamate synthase 1 as the potential candidate genes. Plant laccases are implicated in the lignification of secondary cell walls as an innate defense response against pathogens. The Fg was limited to the inoculated pair of spikelets in NIL-R spikes, but it spread to other spikelets when the *TaLAC4* was silenced in NIL-R, based on virus-induced gene silencing (VIGS). Histopathology revealed thickened cell walls, mainly due to G-lignin, in non-silenced NIL-R, relative to the silenced, and as well a higher total lignin content. Metabolic profiling of *TaLAC4* silenced NIL-R identified the accumulation of several precursor metabolites higher in abundances upstream *TaLAC4*, confirming the role of *TaLAC4* in pathogen-induced lignification of secondary cell walls in the rachis. Also, in-silico promoter analysis of phenylpropanoid pathway-related genes identified *TaLAC4*, *TaCCR*, *TaCAD*, and *TaMYB* carrying secondary wall NAC binding element (SNBE) sites, which were further confirmed based on protein-DNA docking. Henceforth, the *TaNAC032* was functionally characterized based on VIGS to understand the transcription regulation of *TaLAC4*. *TaNAC032* silenced NIL-R confirmed an increase in fungal biomass and disease severity but displayed decreased expression of downstream resistance genes *TaCCR*, *TaCAD*, *TaLAC4*, and *TaMYB*.

Furthermore, the silenced NIL-R was also associated with reduced total lignin content and the total lignin deposited in cell walls. This was also associated with a decrease in the abundance of RR metabolites related to monolignols and lignan glycosides, confirming the plausible role of *TaNAC032* in the regulation of lignin biosynthetic genes, including *TaLAC4* in wheat resistant

NIL. Among the genes identified in QTL-Fhb1, this is the first study to report the role of *TaNAC032* and *TaLAC4* in FHB resistance through reinforcement of secondary cell walls. Both *TaNAC032* and *TaLAC4* significantly contributed to QTL-Fhb1 resistance. If mutated, both functionally validated candidate genes can be edited in susceptible genotypes, employing genome editing tools to enhance FHB resistance.

RÉSUMÉ

La fusariose de l'épi (FHB) est une maladie du blé (*Triticum aestivum* L.) hautement destructrice causée par *Fusarium graminearum* (Fg). Parmi des centaines de locus de caractères quantitatifs (QTL), QTL-Fhb1 est d'un intérêt particulier, puisque celui-ci contribue à un effet majeur dans la résistance à la FHB. Récemment, quelques déterminants génétiques de la résistance à la FHB ont été identifiés, mais leurs mécanismes de résistance spécifiques n'ont pas été découverts. Cette étude visait à identifier les gène(s) candidat(s) et décoder les mécanismes de résistance en se basant sur une approche métabolo-génomique combinée avec des lignées de blé quasi-isogéniques (NILs) caractérisées par une différence au niveau de QTL-Fhb1. Les métabolites de résistance reliée (RR) avec un fort changement en abondance identifiés dans la lignée NIL-R étaient principalement les phénylpropanoïdes, les flavonoïdes et les glycosides de lignane. La dissection de QTL-Fhb1 basée sur le séquençage de marqueurs de flancs a mené à l'identification de laccase-4-like, cell wall invertase, G-type lectin S-receptor-like serine/threonine-protein kinase, NAC transcription factor 32-like et glutamate synthase 1 comme potentiel gènes candidats. Les laccases végétales sont impliquées dans la lignification des parois cellulaires secondaires comme réponse défensive innée contre le pathogène. Le Fg était limité à une paire d'épilletts inoculée chez NIL-R, mais se propageait aux autres épilletts lorsque *TaLAC4* était éteint dans NIL-R par extinction de gène par virus (VIGS). L'analyse histopathologique a révélé un épaissement de la paroi cellulaire, principalement dû à la G-lignine, dans la lignée NIL-R non éteinte, en comparaison à la lignée éteinte, en conjonction avec une quantité totale de lignine supérieure. Le profilage de métabolites de *TaLAC4* dans les lignées NILs éteintes a identifié une accumulation de plusieurs métabolites précurseurs avec une abondance supérieure en amont de *TaLAC4*, confirmant ainsi le rôle de *TaLAC4* dans la lignification induite par un pathogène des parois cellulaires secondaires du rachis. De plus, l'analyse *in-silico* du promoteur des gènes impliqués dans la voie du phénylpropanoïde a identifié *TaLAC4*, *TaCCR*, *TaCAD*, et *TaMYB* comme comportant des sites d'éléments de liaison NAC pour parois secondaires (SNBE), ce qui a été aussi confirmé par amarrage de protéines-ADN. Conséquemment, *TaNAC032* a été fonctionnellement caractérisé par VIGS pour comprendre le processus de régulation de la transcription de *TaLAC4*. La lignée *TaNAC032* éteinte NIL-R a confirmé une augmentation de la biomasse fongique et de la gravité de la maladie, mais une réduction dans l'expression des gènes de résistance *TaCCR*, *TaCAD*, *TaLAC4*, et *TaMYB*, situés en aval, a aussi été observée.

De surcroît, la quantité totale de lignine, ainsi que la lignine totale déposée dans les parois cellulaires, ont été réduites dans la lignée NIL-R éteinte. Ceci était associé avec une réduction dans l'abondance des métabolites RR reliés aux monolignols et des glycosides de lignane, confirmant le rôle plausible de *TaNAC032* dans la régulation de gènes impliqués dans la biosynthèse de la lignine, ce qui inclut *TaLAC4* dans la souche NIL. Parmi les gènes identifiés dans QTL-Fhb1, il s'agit de la première étude à reporter le rôle de *TaNAC032* et *TaLAC4* dans la résistance à la FHB par le renforcement des parois cellulaires secondaires. Dans l'ensemble, *TaNAC032* et *TaLAC4* ont significativement contribué à la résistance de QTL-Fhb1. Les gènes fonctionnellement validés pourront être édités dans les génotypes susceptibles, si mutés, en employant des outils pour l'édition du génome.

ACKNOWLEDGEMENTS

My experience at McGill University has been nothing short of amazing. Since my first day, I have been received a warm welcome from all my lab mates. This thesis epitomizes not only my work in the lab and at the keyboard but also the result of collective experiences I have encountered at McGill from dozens of remarkable individuals whom I also wish to acknowledge. First and foremost, I wish to express my sincere gratitude and profound indebtedness to my advisor, professor **Ajjamada C. Kushalappa**, for his patience, motivation, and immense knowledge. His guidance and continuous support have given me the freedom to pursue this research without objection. He has provided insightful discussions about the research all the time we met, whether it's the coffee room or hallway. His saying “defend science, and not defend yourself” has always encouraged me to gain in-depth knowledge about the related subject. He has helped and supported me immensely during every phase of my Ph.D. life. Please accept my heartfelt thanks!

I am genuinely grateful to my advisory committee members, **Dr. Jean-Benoit Charron** and **Dr. Robin Beech** for their insightful comments, criticism, suggestions, and encouragement which helped me gaining confidence, expand my knowledge and enhance my thinking abilities. I would like to convey my acknowledgment to **Dr. Raj Duggavathi** for permitting me to use lab space for qRT-PCR and microtome equipment for histochemical studies. I am grateful to our Dean **Anja Geitmann** for granting permission to use lab space for microscopy and **Dr. Bara Altartouri** for providing great help in microscopy. I am thankful to our collaborator **Mr. Yves Dion**, Centre de recherche sur les grains (CÉROM) for his valuable guidance and support. I would like to thank **Dr. S. Fox**, AAFC, Winnipeg, Canada for providing wheat NILs and **Dr. S. Rio**, CÉROM for providing *Fusarium graminearum* isolate (GZ-3639). I would like to express my appreciation to **Dr. Denis Faubert** and his team members **Mrs. Boulos Marguerite** and **Dr. Sylvian** from IRCM, Montreal for the LC-MS analysis. I would like to thank all the plant science staff, **Guy Rimmer**, **Ian Ritchie**, and **S. Dernovici**, for their invaluable assistance and providing access to the laboratory and research facilities in the greenhouse. Without their precious support, it would not be possible to conduct this research. I sincerely thank **Susan Gregus**, **L. Flood**, **D. Chan-hum**, for their much-needed assistance in administrative tasks.

I am overwhelmed by all my lab mates for their unconditional help and support, both professionally and personally. I would like to start with Niranjana; he was a true and amazing friend ever since we began to share the lab space. He has inspired me every single day and helped me

motivated. I can't forget those sleepless nights working in the lab and going back home the next morning, incredible days of my life! I would like to thank Sripad for always being supportive and guiding me to the right path. He has always boosted my confidence. Also, I thank Russiachand, Krishna Kumar and Chaitra Nagaraju for all your support, motivation and encouragement. Bikram Paudel, I cannot thank you enough for your great help whether it is taking me to the hospital or grocery shopping.

I would like to express my sincere gratitude to all the previous post-docs and lab mates, I have shared lab space with, Dr. Arun Kumar, Dr. Yogendra Kalenahalli, Dr. Shivappa, Dr. Shailesh Karre, Dr. Uday Kage and Dr. Dhananjay Dhokane, Harini, Hanan, Fatemeh, Dr. Farhard and Dr. Huali for continually motivating me to do better research through sharing their scientific work experiences. Thanks for the engagement in fruitful scientific discussions and accompanying me for coffee break and lunch. I would like to extend my deepest gratitude to Dr. Deepa Madalageri for taking care of me like a sister, like a best friend.

I am more than grateful to Achal Dhariwal for always being a great support to me. Thank you for keeping my spirit high, and I am sure, you will become a great scientist. I thank all my beloved friends, Ashish Subba, Mohit, Rasika, Richa, Kshitija, Nilesh, Bhakti, Sadanand, Vanya, Jia, Varinder, Meha, Karuna, Irfan, Diljot, Sukhjiwan, Diksha, Maria, Dina, Julian, and Dana. The memories we have shared shall be cherished forever. Thank you for all your immense care and love. My special thanks to Jérôme Gélinas Bélanger for translating abstract to French.

I am obliged to the McGill University for providing me financial support when I was in need through research assistantship, graduate excellence award, the GREAT award for attending an international conference, Frank P Jones bursary, and Francis James loan. I am also grateful to Associate Dean, Dr. Ian Strachan for providing me the Graduate mobility award to enhance graduate research experience at ETH Zurich. I am obliged to the Natural Sciences and Engineering Research Council of Canada (NSERC), McGill Sustainability Systems Initiative (MSSI) and Ministère de l'Agriculture, des Pêcheries et de l'Alimentation du Québec (MAPAQ), Québec, Canada for providing funding to conduct this research. I am sincerely grateful to the Department of Plant Agriculture, University of Guelph for providing the Corteva Plant Sciences Symposium travel grant and having me there as one of the plenary speakers.

I finish with India, where I have an amazing family as the most crucial part of my life. My family is unique and perfect in many ways. Their immense love, care, unconditional support and

sacrifice is unmatched. They have supported me whenever I needed it and cherished with me every great moment.

PREFACE AND CONTRIBUTION OF THE AUTHORS

Contributions of Authors

The following thesis was prepared according to the “Guidelines Concerning Thesis Preparation” of McGill University. The thesis contains three Chapters (Chapters III- V) representing three separate research manuscripts: Chapter IV and Chapter V, both are published in the Plant Science Journal. Detailed authors’ information and their contributions to each Chapter are mentioned in the “Connecting Text” section before each Chapter. Below is a general description of the thesis topics and the contributions of each author to the thesis.

Nancy Soni was the primary researcher for each Chapter. She conducted all the greenhouse experiments, laboratory experiments, analyzed all the data, wrote manuscripts and the thesis under the supervision of Dr. Ajjamada C. Kushalappa. Dr. Kushalappa provided continuous guidance, resources and funds to conduct the research. He had thoroughly edited the manuscripts and thesis and has given priceless suggestions throughout the research work. His contributions are the same for all the manuscripts. Dr. Raghavendra Gunnaiah, Assistant Professor at University of Horticultural Sciences, Bagalkot, Karnataka, India and Dr. Shivappa Hukkeri, Scientist-Cannabis Molecular Breeding at Destiny Bioscience, Saskatoon, Saskatchewan, Canada, provided expertise and insight on the QTL-Fhb1 sequencing project and data analysis. Mr. Achal Dhariwal, a Doctoral research fellow at the University of Oslo, Norway, helped in molecular docking and statistical analysis. Mr. Niranjan Hegde, Plant Science Department, McGill University, helped in greenhouse work and gene silencing experiment discussion. Mr. Bara Altartouri assisted in microscopy and providing images. Dr. Raj Duggavathi, Department of Animal Science, McGill University, Montreal, Quebec, Canada, provided lab access to perform qRT-PCR and tissue sectioning for histochemical study. Dr. Farhad Nazarian-Firouzabadi, Professor at Department of Agronomy and Plant Breeding, Lorestan University, Khorramabad, Iran, provided a protocol for gene expression data analysis.

Contributions to Knowledge

This thesis's Chapters describe original and novel findings on the identification and functional characterization of Fusarium head blight resistance gene, *TaLAC4* and *TaNAC032*, in conferring

resistance to FHB through cell wall reinforcement as the possible resistance mechanism predominant in wheat QTL-Fhb1.

Chapter III describes the original finding related to identifying five novel genes underlying QTL-Fhb1 based on a combined metabolo-genomics approach. Wheat NILs derived from the Sumai 3/Thatcher mapping population were inoculated with the pathogen (*Fg*) or mock. The rachis samples collected at 72 hpi were used to carry out metabolic profiling. The metabolic profiling of rachis data showed a significant accumulation of metabolites related to phenylpropanoids, flavonoids, fatty acids and terpenoids. These resistance-related metabolites may potentially act as constitutive and inducible defenses against the *F. graminearum* (*Fg*) attack. They can be further used as biomarkers following validation. Also, QTL-Fhb1 dissection based on a paired-end Illumina HiSeq™ 2500 platform identified 37 putative candidate genes. The annotated sequences of these genes were analyzed for synteny among chromosomes of related species such as *Oryza sativa*, *Sorghum bicolor*, and *Brachypodium distachyon*. These genes were narrowed down based on gene expression, SNP analysis, and metabolic profiling to identify potential FHB resistance candidates. The five novel candidates selected for FHB resistance are Cell Wall Invertase (CWIN), G-type lectin S-receptor-like serine/threonine-protein kinase (RKS1), NAC transcription factor 32-like, Glutamate synthase 1 (GLT1), and Laccase-4-like (LAC4). The polymorphism identified among these genes could be associated with the varied accumulation of resistance-related metabolites in the susceptible NIL. Following functional validation, these genes could further serve in breeding resistant wheat varieties.

Chapter IV represents the first study reporting the role of laccase in FHB resistance underlying wheat QTL-Fhb1. Gene expression analysis based on qRT-PCR in NILs differing at QTL-Fhb1 suggested induced expression of *TaLAC4* in resistant NIL (NIL-R) upon *F. graminearum* (*Fg*) inoculation. Multiple sequence alignment of *TaLAC4* gene sequences identified two significant substitutions, lysine to glutamate at position 250 (K250E) and histidine to aspartate at position 252 (H252D) in NIL-S. These mutations have been previously reported to affect DNA binding ability and dissociating ligand-receptor complex, respectively (Ris-Stalpers et al., 1991; Singh et al., 2013). *TaLAC4* function validated based on VIGS in NIL-R confirmed increased susceptibility to *Fg* infection based on disease severity analysis and fungal biomass quantification. Besides, the acid-soluble lignin test confirmed a 15 % higher amount of the total lignin content in NIL-R compared to silenced NIL-R. There was also an altered lignin distribution, which was based

on the phloroglucinol-HCL staining. Moreover, the metabolic profiling of *TaLAC4* silenced NIL-R revealed increased accumulation of monolignol derivatives such as coniferyl alcohol glucosides higher in abundance, suggests *TaLAC4* is necessary for the oxidative polymerization of monolignols to biosynthesize G lignin. This study opens the opportunity to explore other laccases or cell wall biosynthetic genes involving synergistically to confer a high level of resistance against FHB in wheat.

Chapter V reported the FHB resistance mechanism governed by the NAC transcription factor, *TaNAC032* underlying wheat QTL-Fhb1. For the first time, the study identified a transcription factor underlying QTL-Fhb1 conferring the FHB resistance due to its crucial role in lignin biosynthesis. The *in silico* promoter analysis identified RR metabolite biosynthetic genes containing secondary NAC binding elements (SNBE) to understand the primary transcriptional regulatory mechanism of secondary cell wall biosynthesis govern by *TaNAC032* in wheat QTL-Fhb1. The functional significance of the SNBE sites for the following genes: *TaCCR*, *TaCAD*, *TaLAC4*, and *TaMYB* were validated based on Arabidopsis as a search organism using GeneMANIA software (<http://www.genemania.org/>).

Further, functional validation of *TaNAC032* in NIL-R based on VIGS showed an increase in susceptibility to *F. graminearum* due to a significant increase in disease severity and fungal biomass. The silenced NIL-R also showed the decreased total lignin content, which was quantified based on the acid-soluble lignin test and the Weisner test. Eventually, the expression of downstream lignin-specific genes was also decreased in *TaNAC032* silenced NILs. This was also associated with the reduced abundances of significant metabolites related to monolignol derivatives, lignan glucosides and HCAAs. This study signifies the role of *TaNAC032* as a functional regulatory gene imparting resistance to FHB in wheat by regulating secondary cell wall biosynthetic genes due to cell wall reinforcement.

In general, the candidate genes in QTLs have been identified using NILs with susceptible backgrounds. In the studies presented here, we used NILs with a resistance background. Despite high resistance to FHB, the silenced gene rendered the NIL-R susceptible. Furthermore, in addition to Sumai 3 based NILs, the Agriculture and Agri-Food Canada (AAFC) also has developed NILs based on Nyubai. However, in this study, both the NIL-R and NIL-S were highly susceptible to FHB (Gunnaiah et al., 2012). Our study revealed that *TaNAC32* was mutated in both NILs. This confirmed that a molecular marker associated with FHB resistance though present in a genotype,

may not be associated with FHB resistance genes, questioning the use of molecular markers in breeding.

Furthermore, it is proved here that both of these genes should be functional in a cultivar to confer high resistance to the spread of FHB within spike; if any gene is non-functional, then there would be no type-II or rachis resistance. The two genes functionally validated in this study can be used to replace a mutated or non-functional gene in susceptible cultivars based on genome editing tools to enhance FHB resistance in *T. aestivum* and related species, provided the rest of the hierarchy of genes are functional.

CHAPTER I: INTRODUCTION

Wheat (*Triticum aestivum* L.), bread wheat, is an allohexaploid (AABBDD) with six sets of chromosomes that include two sets from three different species, $2n=6x=42$. The evolution of bread wheat results from two separate hybridization events. The initial hybridization occurred ten years ago between the two grass species *T. urartu* (the A-genome donor) and *T. speltooides* (the B genome donor). This new tetraploid species further hybridized with a diploid species, *T. tauschii* (the D genome donor), resulting in hexaploid wheat with 42 chromosomes, six complete genomes, each of 7 chromosomes (Marcussen et al., 2014). It is the largest grown crop, covering more than 240 million/ha globally (Curtis et al., 2009). It belongs to the Poaceae (formerly known as the *Gramineae*), which represents one of the largest families of flowering plants among 10,000 species and contributes up to 20 % of calories consumed worldwide due to the rich sources of starch and energy (CIMMYT, 2015). It constitutes essential components such as proteins, vitamins, dietary fiber, and phytochemicals beneficial for human health (Shewry and Hey, 2015). The annual global wheat production is 741 million tonnes in September 2016, with Canada ranking in sixth position with 27.6 million tonnes (FAO, 2016).

Over the last decade, an estimated consumption of 725 million tonnes increased wheat demand by 20 % compared to 598 million tonnes in 2006 (FAO, 2016). The production of major cereal crops, such as wheat and barley, has been continuously jeopardized due to various biotic and abiotic environmental stresses. Wheat is highly vulnerable to various pests, nematodes, diseases affecting head and grains (Black chaff, Common bunt, Ergot, Fusarium head blight, Loose smut, Sooty head molds, Septoria nodorum blotch a.k.a. Septoria glume blotch), diseases affecting leaves (Bacterial streak, Barley yellow dwarf, Leaf rust, Powdery mildew), and diseases affecting lower stems and roots (Cephalosporium stripe, Common root rot, Eyespot) (Duveiller et al., 2012). This leads to the extensive reduction of the crop quality and quantity. Fusarium head blight (FHB), also known as the wheat scab, is one of the most destructive wheat diseases caused by a fungal plant pathogen. Since 1991, FHB outbreaks across the eastern half of the United States have been common and widespread, affecting both yield and quality of wheat produced (Bai and Shaner, 1994; McMullen et al., 1997). Among several species causing FHB, the most prevalent ones include *Fusarium graminearum* Schwabe (teleomorph: *Gibberella zeae*), *Fusarium culmorum*, *Fusarium avenaceum* (teleomorph: *Gibberella avenaceum*) (Parry et al., 1995). In North America, *F. graminearum* Schwabe prevails over other species that can cause FHB (Atanasov, 1920;

Bergstrom et al., 1986; Parry et al., 1995; Sutton et al., 2007). During harvest, the light-weighted kernels and the fungus-infected wheat and barley head debris come into soil surface contact and become a vital site for the overwintering of the fungus. Further, hot and humid weather during crop growing season facilitate fungus development and spread by landing onto the kernels, glumes, or other head parts (Atanasov, 1920; Bergstrom et al., 1986; Ireta and Gilchrist, 1994; Parry et al., 1995; Sutton et al., 2007). In cereal crops such as wheat, the fungus macroconidia and ascospores germinate and penetrate through space between lemma and palea, colonize florets, and spread to other spikelets through the rachis leading to necrotic lesions, bleaching, and shriveling of kernels (Matny, 2015). *Fusarium* infection contaminates grains with mycotoxins (fungal secondary metabolites) such as deoxynivalenol (DON), nivalenol (NIV), and zearalenone (ZON), which weakens gluten strength, affecting the milling and baking qualities (Dexter et al., 1996; McMullen et al., 1997). Consumption of mycotoxin infected grains is hazardous to human and animal health, which causes cancers, immunosuppression, reproductive problems and abortion (Matny, 2015). Consequently, the Canadian Food Inspection Agency (CFIA) sets the limits of DON with >1 ppm ($\mu\text{g g}^{-1}$) for human consumption (McMullen et al., 1997).

Integrated FHB disease management strategies are mainly comprised of: (i) Cultural practices, (ii) Fungicides application, (iii) Biological control agents and, (iv) Plant host resistance. Cultural practices include proper crop rotation, good tillage practices, and implementation of phytosanitary measures such as collection and disposal of waste remains. Fungicides such as Caramba (BASF Corporation), Prosaro (Bayer CropScience), Proline (Bayer CropScience) belongs to the triazole class of fungicides. Triazole fungicides are triazole pesticides derivatives constituting the most important category of fungicides that have excellent protective, curative and eradicator power towards a broad spectrum of crop diseases. The fungicide group, demethylation inhibitors (DMI), which contain the triazole fungicides, are highly effective against many different fungal diseases, especially powdery mildews, rusts, and many leaf-spotting fungi (Mueller, 2006). The fungicides are most efficient for managing FHB if applied at an appropriate time interval (Bradley and McMullen, 2008). Also, biological control agents such as *Bacillus* and *Pseudomonas* and yeast belonging to *Rhodotorula*, *Sporobolomyces* and *Cryptococcus* genera were found effective in reducing the growth of *F. graminearum* (Palazzini et al., 2007). Unfortunately, they all are associated with several drawbacks: high cost, irregular efficacy, unpredictable nature of FHB outbreak and potential health risks (Stack, 2000; Buerstmayr et al., 2002; Xue et al., 2008).

Eventually, host plant resistance is considered the most efficient, economical, and eco-friendly approach to control the incidence of FHB and the accumulation of mycotoxin (Buerstmayr et al., 2002).

FHB resistance is quantitative and the severity dramatically varies with environmental conditions, making the selection of resistant genotypes very challenging (Bai and Shaner, 1994; Buerstmayr et al., 2002). The variation in FHB resistance among cultivars was first reported in the 19th century in the United States of America (Cummins, 1978). Three types of FHB resistance has been broadly categorized: (i) resistance to initial infection of spikelets (type-I), (ii) resistance to spread within the spike through rachis (type-II) and (iii) reduction of mycotoxin accumulation in grains (type-III) (Mesterhazy, 1995). Researchers from several different countries identified cultivars possessing different FHB resistance levels; however, only a few sources showed stable FHB resistance across environments. These have been used as the major sources of resistance in breeding programs (Yu et al., 2006). Among these, type II resistance is evaluated based on disease severity or the area under disease progress curve (AUDPC) over 15-20 days post-inoculation of a single pair of spikelets with a pre-adjusted spore concentration, thus reducing inoculum load variability. Whereas type I resistance is evaluated based on spray inoculation, which is comparatively more prone to experimental errors, leading to avoidance. The experimental errors have significantly been reduced by inoculating spikelets with known concentration of inoculum and measuring pathogen biomass in inoculated spikelets, under greenhouse conditions (Kumar et al., 2015).

More than a hundred quantitative trait loci (QTLs) for FHB resistance have been identified in wheat using Marker Assisted Selection (MAS) (Buerstmayr et al., 2012). The FHB resistance QTL, with major or minor effects, has been reported from all the 42 chromosomes of hexaploid wheat. Major QTL on chromosome 3B (QTL-Fhb1), 6B (QTL-Fhb2), and 2D exhibit type-II resistance, and chromosomes 5A (QTL-Fhb5) and 4B (QTL-Fhb4) confer type-I resistance. These QTLs were stable across different parental backgrounds and environments in several mapping populations (Buerstmayr et al., 2012). However, the resistance mechanisms underlying these QTL are yet unexplored. Thus, identifying genes underlying these QTLs and elucidating the mechanism associated is critical for transferring these genes into elite cultivars.

Among all the QTLs identified, the QTL-Fhb1 derived from Sumai-3 is the major QTL located on the 3BS chromosome arm, the largest of the wheat chromosome (Choulet et al., 2014).

The QTL-Fhb1 derived from Sumai-3 (resistant parent) and Thatcher (susceptible parent) cross explained 60 % of the phenotypic variation for rachis resistance (Cuthbert et al., 2006). Sumai-3 is a Chinese bread wheat cultivar that possesses a high level of rachis resistance. The QTL has been mapped as a Mendelian factor, spanning a region of 1.3 cM flanked by STS-80 and STS-142 markers. Different mapping populations have been used to fine-map QTL-Fhb1 conferring type II resistance to identify candidate genes involved in resistance (Cuthbert et al., 2006; Liu et al., 2008). Positional cloning of QTL-Fhb1 within a 261 kb region of the bacterial artificial chromosome (BAC) clones revealed seven novel genes. Four were used to develop transgenic lines but failed to confer resistance against FHB (Liu et al., 2008). Transcriptomics analysis of near-isogenic lines (NILs), generated by the process of repeated backcrossing carrying QTL-Fhb1, revealed increased transcript abundance of genes related to jasmonic acid, ethylene-related, ABC transporters, UDP-glucosyltransferases, WRKY transcription factors, PCD-related and xylanase inhibitors (Jia et al., 2009); glucanases, NBS-LRR, WRKY transcription factors and UDP-glucosyltransferases (Kugler et al., 2013); pathogen-related proteins, ABC transporter and jasmonic acid signaling related genes (Xiao et al., 2013), but none proved the FHB resistance mechanisms. A few genes have been identified as candidates and functionally validated, such as the pore-forming toxin gene (PFT) as the resistance gene and a histidine-rich calcium-binding protein (*TaHRC*) as the susceptible gene but the mechanisms of resistance has not been elucidated (Su et al., 2018; Li et al., 2019; Su et al., 2019).

Alternatively, functional analyses of these mapped QTL based on an integrated approach such as metabolomics combined with genomics are considered the most promising way to identify the molecular players involved in disease resistance (Kushalappa and Gunnaiah, 2013). Forward genetics is an approach (metabolomics, proteomics, transcriptomics and genomics) to identify the candidate gene for plant disease resistance. Whereas reverse genetics approach (e.g., virus-induced gene silencing (VIGS)) functionally characterizes the gene as the best approach to unveil the resistance mechanism in plants against biotic stress (Kushalappa and Gunnaiah, 2013).

Metabolomics is the comprehensive, non-biased, high throughput analysis of complex metabolite mixtures allowing the identification and quantification of every individual metabolite ideally. Metabolomics contributes to our understanding of the complex molecular interactions in biological systems, thus defining functional genomics methodology (Hall et al., 2002). They are the end products of cellular processes; their fold changes can be considered an individual's

phenotype to genetic or environmental changes (Fiehn, 2002). Metabolic profiling of wheat and barley spikelets inoculated with *F. graminearum* identified hundreds of metabolites, including monomers and polymers of phenylpropanoids, flavonoids, fatty acids, alkaloids and terpenes (Bollina et al., 2010; Kumaraswamy et al., 2011). Some of these metabolites were deposited to reinforce the cell wall, thus controlling the pathogen to initial infection or from rachis colonization (Gunnaiah et al., 2012). Metabolites have mapped in the metabolic pathways to identify the candidate genes such as *TaACT* in wheat QTL-2DL (Kage et al., 2017) and *HvWIN1* in barley (Kumar et al., 2016). Combined transcriptomics and metabolomics enabled the identification of resistant genes (R genes) such as *Ta4CL* in wheat QTL-Fhb2 (Dhokane et al., 2016) and *HvCERK1* in barley (Karre et al., 2017). Likewise, a combined metabolic-genomics study identified and functionally characterized the *TaACT* gene and *TaWRKY* transcription factor in QTL-2DL, imparting resistance against FHB (Kage et al., 2017; Kage et al., 2017). However, an association of RR metabolite with the gene is insufficient to understand the resistance mechanism; functional validation is still needed.

Among several available tools for functional validation, VIGS is a comparatively more efficient and fast technique to perform gene functional analyses in response to both biotic and abiotic stress (Senthil-Kumar et al., 2008; Cakir et al., 2010; Ramegowda et al., 2014). Upon functional validation, these candidate genes can be further used in breeding programs for crop improvement. Within this framework, the present study aimed at employing an integrated metabolo-genomic approach to identify and functionally characterize genetic determinants of FHB resistance underlying major QTL-Fhb1. The identified resistance genes can be further used in breeding resistant wheat varieties, thus improving wheat resistance against FHB.

1.1 OBJECTIVES AND HYPOTHESES

Hypotheses

1. Wheat near-isogenic lines (NILs), carrying resistance and susceptible alleles of the QTL- Fhb1, may vary in their gene sequence and gene expression upon *F. graminearum* inoculation.
2. Resistance gene(s) functional in resistant NIL biosynthesizes metabolites that are antimicrobial and/or reinforce cell walls to suppress the pathogen growth, thus the disease severity.
3. The mutated or non-functional gene(s) in susceptible NIL is inapt to synthesize these metabolite(s), or if they can, not significantly higher in abundance.
4. The silencing of the resistance gene(s) in the resistant NIL would compromise resistance against FHB.

Global Objective

The main objective of this research is to identify and functionally characterize the novel candidates associated with Fusarium head blight resistance in the wheat major QTL-Fhb1 by silencing them in resistant near-isogenic lines derived from a fixed resistant (Sumai 3*5/Thatcher) mapping population.

Specific Objectives

1. To identify the induced resistant gene(s) functional in wheat resistant NILs that are polymorphic in susceptible NILs based on QTL-Fhb1 sequencing.
2. To identify resistance-related induced metabolites in wheat near-isogenic lines accumulated higher in abundance to combat the infection by *Fusarium graminearum*.
3. To functionally validate the candidate gene(s) identified in wheat QTL-Fhb1 based on virus-induced gene silencing (VIGS) approach.
4. To confirm the silencing events based on disease severity assessment, fungal biomass quantification, metabolic profiling and lignin detection.

CHAPTER II: REVIEW OF LITERATURE

2.1 Fusarium head blight

2.1.1 Fusarium head blight epidemiology

Fusarium head blight (FHB) is one of the fatal diseases globally, affecting mainly wheat and barley (Leonard and Bushnell, 2003). The fungal species causing disease include *F. avenaceum*, *F. culmorum*, *F. poae* and *F. graminearum*. Among all, *F. graminearum* (*Gibberella zeae*) predominantly affects major cereal crops worldwide and is the primary causal agent of FHB (Bai et al., 2000). The disease was first discovered in England in 1884 and was known as “scab,” which later became “tombstone disease” due to the chalky, lifeless appearance of infected kernels (McMullen et al., 1997). The fungus is primarily known for producing mycotoxins such as deoxynivalenol, which has adverse effects on human and animal health. FHB is ranked as the ruinous plant disease by the USDA (United States Department of Agriculture). Since 1990, a loss of over 3 billion dollars due to FHB epidemics concerned all the wheat and barley farmers in the United States and Canada (Windels, 2000). Fungal species such as *F. graminearum* has more than one host such as oat, rye corn, rice, barley, and soybean, which significantly contribute towards infection by providing a source of inoculums. Several ascospores and asexual macroconidia, chlamydospores, and hyphal fragments serve as a primary and principle source of inoculums carried away by the wind to the site of infection (Perry, 1995; Bai and Shaner, 2004). As the optimum temperature for the pathogen growth and development is 25°C, any increase in the temperature increases fungal infection risk. Favorable environmental conditions such as hot and humid weather during the anthesis stage also subsidize infection incidence. The disease has caused immense losses in both the quality and quantity of the wheat grains to date.

2.1.2 Pathogen growth and colonization

The pathogen, *F. graminearum*, survives in the plant debris in the soil as infected mycelium or as ascocorps. Under favorable conditions (warm, wet, and humid), the ascocorps absorb water and forcibly release ascospores, the sexual stage (*Gibberella zeae*). These ascospores may travel a short distance through wind currents and land on susceptible wheat heads leading to infection (Leonard and Bushnell, 2003). The wheat anthesis stage is the primary stage of infection. The infection is mainly through the initial colonization of anthers or stomata. The extruded anthers

are colonized, and through that, it enters the spikelets. At anthesis time, they produce ascospores that germinate and penetrate through cracks between lemma and palea, enter into the spikelets through the stomata on the inner side and colonize the spikelet. From the infected spikelets, it spreads to neighboring spikelets within a spike through rachis. However, in general, it cannot colonize rachis in barley as they have high rachis resistance. The severity of infection depends on the stage of infection. For instance, there will be no development of kernels if the anthers get infected just after their emergence, which results in fungus colonization and florets destruction. If florets are infected a bit late, they will produce diseased kernels (shrunk, wrinkled, or tombstone in appearance) (Del Ponte et al., 2007). Furthermore, if kernels get colonized by the fungus during the late development stage, it might get contaminated with a mycotoxin. What is more disastrous is using infected seeds as a sowing material, which would serve as an inoculum source infecting seedlings.

The first symptoms of fusarium head blight can be visualized after the anthesis (flowering) stage, where diseased spikelets display premature bleaching. As the pathogens grow and spread, the infection symptoms may progress throughout the entire spike. Accumulation of light pink colored spores (sporodochia) may appear on the rachis and on individual spikelets under warm and moist environmental conditions, which is very favorable for the growth of *F. graminearum* (Bai and Shaner, 1996). Followed by this, blue-black spherical bodies known as perithecia (reproductive structures of fungus) may develop on the infected spikelet surface. Later, the fungus colonizes the entire spikelet and the developing grain. As a result, the infected kernels are found rough, shriveled, wrinkled, and grayish-brown colored (Del Ponte et al., 2007).

Relative humidity (>90 %) and moderate warm temperature (~ 15 – 30o C) are the best-suited conditions for the occurrence of FHB infection (Del Ponte et al., 2007). These conditions act as an inoculum during the anthesis stage to progress floret infection and grains colonization by fungus. Since the FHB disease cycle has limited timelines, such as sporulation, spore dispersal, and host infection, it is well suited to be examined by disease forecasting models. Disease forecasting models integrate factors like temperature, humidity, inoculum production, and plant development as forecasters regarding FHB severity (De Wolf et al., 2003).

2.1.3 Impacts of FHB in wheat production

FHB causes severe damage to wheat grains either directly or indirectly by contaminating grains with mycotoxins (Gilbert and Tekauz, 2011). Direct damage leads to a reduction in the yield

due to insufficient production of kernels through infected florets, which may get separated from the chaff during the threshing process, or kernels may not be produced at all. On the other hand, indirect damage contaminates grain with mycotoxins causes severe effects on human and animal health (Champeil et al., 2004). Mycotoxins are the chemicals produced by *Fusarium* species to defend themselves against other microorganisms or disrupt the plant's immune system. Deoxynivalenol (DON) is one of the major toxins produced by *F. graminearum* (Goswami and Kistler, 2004). DON, also known as vomitoxin, affects the digestive system of monogastric animals. It is known to disrupt cell function by interfering with protein synthesis. It adversely affects humans either through direct consumption of grains contaminated with DON or through the consumption of animals fed with contaminated grains, causing nausea, fever, vomiting, and headache (Pestka, 2008). DON contaminated grains also lead to feeding refusal by animals (McMullen et al., 1997). The USA and Eastern Canada have undergone losses of million metric tons in wheat yield for many years. During the 1990s, the Canadian province- Manitoba, suffered a high economic loss of USD 300 million, and Ontario and Quebec lost USD 200 million (Windels, 2000). Also, the loss of 7 million hectares of land due to FHB infection has been accounted for in China (Bai and Shaner, 2004). The primary concern for researchers is the DON levels in the FHB infected wheat. The DON level in infected human food was found very high (>20 ppm), in contrast to what is recommended (<1 ppm) by the Canadian Food Inspection Agency (CFIA). In this aspect, the FDA has set guidelines for DON levels allowable in livestock feed depending upon their tolerance levels (Schmale and Munkvold, 2009).

2.1.4 Management practices for FHB

Several management practices for FHB were used to reduce disease spread, including cultural, chemical, and biological approaches. Cultural practices include preparation of land, crop rotation with non-cereal crops, and water management during the anthesis stage to reduce disease prevalence (Champeil et al., 2004). Since primary inoculum is the major source of widespread disease, deep plowing practices, burying crop residues, early sowing of cultivars for a short duration helped to escape disease in some field areas (Champeil et al., 2004). Also, it has been found that a decrease in tillage and maize cropping leads to regional scab epidemics (McMullen et al., 1997; Buerstmayr et al., 2002; Bateman et al., 2007). Thus, proper removal of previous crop residues along with good tillage practices may be effective against FHB. Chemical controls include the application of fungicides; for instance, - foliar fungicides have been used against FHB during

the anthesis stage in some areas (McMullen et al., 1997; Mesterházy et al., 1999). However, these fungicides cannot provide complete resistance and are also associated with mycotoxin contamination. Also, fungicides are barely used in some areas because of their high cost, variability in the effectiveness, and FHB epidemics' inconsistency. However, small success has been achieved in commercial fungicides used for cereal seed treatment to control the occurrence of Fusarium seedling blight (Bradley and McMullen, 2008). Foliar fungicides have been found to reduce the FHB severity and DON mycotoxin levels up to 50-60 % during multi-state uniform fungicide trials (Bradley and McMullen, 2008). Different types of biocontrol agents like bacteria (*Bacillus spp.*, *Kluyvera cryocrescens*, *Paenibacillus fluorescens*, and *Pseudomonas fluorescens*), yeasts (*Cryptococcus spp* and *Sporobolomyces roseus*), and fungi (*Trichoderma harzianum* and *T. viren*) were found useful for controlling FHB (Bacon and Hinton, 2007). Biocontrol agents showed controlled FHB epidemics and also a reduction in the DON contamination. They are useful for protecting the spikelets post-flowering stage when no fungicides can be applied. However, against FHB, not only the regulatory issues, other scientific and technological barriers such as the establishment of appropriate screening methods, the development of appropriate formulation and application, as well as the design and use of tools for monitoring the biocontrol agents introduced into the agroecosystem is still challenging (Legrand et al., 2017). In contrast, host plant resistance is the most efficient, economical, and eco-friendly approach to control FHB incidence and its associated mycotoxin accumulation (Zhu et al., 2016). Thus, integrated management of FHB comprising biological control agents and plant host resistance offers a promising and additional strategy in managing FHB.

2.1.5 Types of FHB resistance

Though resistance against FHB is complicated due to the existing interactions among the genotypes, pathogens, and the environment, it has been broadly classified into three main types of resistance. The three types of resistance comprise a resistance to initial infection of spikelets (type I), resistance to spread of the infection within rachis (type II), and resistance to mycotoxin (type III) (Schroeder and Christensen, 1963; Miller et al., 1985). Evaluation of disease resistance based on spikelet resistance is inconsistent, and also variations in inoculums availability, spore deposition, and environment lead to experimental errors (Cuthbert et al., 2006; Buerstmayr et al., 2009). On the other hand, type II (rachis) resistance to Fusarium head blight is the resistance to the spread of symptoms from the infection. It is commonly measured by observing the progression

of blight throughout the spike from a single inoculated floret (point inoculation) to the neighboring spikelet through rachis (Shaner and Buechley, 2001). Rachis resistance confers both spikelet and rachis resistance and has been found stable in different genotypes across various populations (Cuthbert et al., 2006; Buerstmayr et al., 2009). Type III resistance exists in resistant cultivars carrying factors that prevent deoxynivalenol and other mycotoxins synthesis or promote its degradation (Miller et al., 1985). Wheat genotypes that showed partial or incomplete FHB resistance include Sumai-3, Wangshuibai, Ning 7840, and CItr 11028 derived from China, Nyubai, Shinchunaga, and Nobeokabouzu from Japan, Frontana and Encruzilhada from Brazil, Praa 8 and Novokrumka from Europe and Ernie and Freedom from Northern America (Bai and Shaner, 2004; Duan et al., 2014). Sumai-3 and its derivatives have exhibited high FHB resistance and hence have been used extensively in various breeding programs to identify resistance mechanisms (Yu et al., 2008).

2.2 Wheat crop breeding

2.2.1 Marker-assisted selection (MAS)

FHB resistance is quantitative and associated with low heritable traits that indicate that most of the variation in a trait is due to environmental factors and is not associated with genetic differences. Fusarium head blight is a low heritable trait, with most of the variations is due to environmental factors with little or no influence from the genetic differences (Buerstmayr et al., 2002; Bai and Shaner, 2004). This makes FHB phenotyping more challenging. Thus, molecular markers indicate the best tool for selecting the low heritable traits and mapping QTLs for resistance against FHB. As stated by Van Stanford et al., “Molecular markers technology provides tools needed for the identification, selection and combining favorable alleles through genotypic selection” (Van Sanford et al., 2001). Molecular markers have continuously been exploited in breeding programs for plant selection through marker-assisted selection (MAS), which has been developed to avoid the problems connected with conventional plant breeding to change the selection criteria from the selection of phenotypes towards the selection of genes, either directly or indirectly (Francia et al., 2005). With the availability of various molecular markers and genetic maps, MAS has become possible both for traits governed by major genes and quantitative trait loci (QTLs). However, the usefulness of molecular marker is associated with its capability to reveal polymorphism in the nucleotide sequence, allowing discrimination between different molecular

marker alleles. These polymorphisms can be identified using molecular marker techniques such as restriction fragment length polymorphisms (RFLP), amplified fragment length polymorphisms (AFLP), random amplified polymorphic sequences (RAPD), micro-satellite or simple sequence length polymorphisms (SSR), cleavable amplified poly-morphic sequences (CAPS), single-strand conformation polymorphisms (SSCP), single nucleotide polymorphisms (SNPs) (Mohan et al., 1997; Rafalski, 2002). Molecular markers have a gigantic future in agriculture research enabling the construction of linkage maps for multiple crop species. QTL (Quantitative trait locus) analyses use these linkage maps to identify chromosomal regions harboring genes that control single or multiple traits. Thus, molecular markers gave new directions to develop crops with improved characteristics (Jonah et al., 2011).

2.2.2. Quantitative trait locus (QTL) for FHB resistance

QTL or Quantitative trait locus analysis is a statistical process/method which connects two forms of information. This helps to describe the genetic basis of the variations within complex traits. QTL analysis allows researchers in fields as diverse as agriculture, evolution, and medicine to link certain complex phenotypes to specific regions of chromosomes. This process aims to identify the action, interaction, number, and precise location of these regions.

Molecular markers have been used to identify QTL in different FHB resistance sources such as Sumai-3, Ernie, Freedom, Truman, Wuhan-1, W14, Frontana, Wangshuibai, Ning 7840, and CJ 9306. More than 100 QTL have been identified, but only a few were stable across the environment and locations (Yu et al., 2008). the 3BS chromosome of Sumai-3 and its derivatives harboring *QTL-Fhb1* is the most widely used QTL for FHB resistance (Waldron et al., 1999; Rudd et al., 2001). It has been found as an effective and stable source of FHB resistance across different genetic backgrounds (Bai and Shaner, 2004). Apart from this, QTLs were also mapped on chromosome 5AS and 6BS using Sumai-3 and its derivatives (Stack, 2000; Buerstmayr et al., 2002; Yu et al., 2006). A significant achievement was made by developing other resistance cultivars such as W14 and CJ9306 and their derivatives VA01W476 using resistant sources such as Sumai-3, Wangshuibai, Ning-7840, and Frontana (Jiang and Ward, 2006). The FHB resistance in these cultivars was believed to be better than Sumai-3 and also vary in superior agronomic characteristics (Jiang et al., 2007). Also, *QFhs.nau-2DL* derived from CJ9306 was identified, contributing 20 % towards variation in DON accumulation and 15.5 % towards type-II resistance

(Jiang et al., 2007). *QTL-2DL* derived from Wangshuibai was also detected, accounting for an 11 % variation in FHB resistance.

Likewise, QTLs derived from Wangshuibai were mapped on chromosome 4B, 5A, and 5B. Furthermore, various QTLs were derived from Ernie and mapped on chromosomes 2B, 3B, 4BL, and 5A, suggesting 43.3 % of FHB severity variation (Liu et al., 2007). FHB resistance QTL on chromosome 2DL and 4BS derived from Wuhan1 (Chinese cultivar) were also identified using double haploid lines through mapping study (Somers et al., 2003). Since various efforts have been made to identify QTL from different resistance sources, the dissection of QTL will enable identifying the underlying gene(s) and gene mechanisms (Bradley and McMullen, 2008).

2.3 Wheat chromosome 3B and QTL-Fhb1

In the practice of sequencing a complete hexaploid wheat genome (17Gbp), an effort was made by IWGSC to retrieve the physical mapping and reference sequence of all the 21 wheat chromosomes. Among the entire wheat chromosome, 3B is the largest chromosome in size (~1Gbp). According to the various studies conducted, the first chromosome harboring a complete BAC (Bacterial Artificial Chromosome) library and a physical map (Šafář et al., 2004; Paux et al., 2008). BAC (Bacterial artificial chromosome) library is the large “DNA insert” library of choice. Furthermore, it is also a crucial tool specifically for map-based cloning, molecular cytogenetics, physical mapping, comparative genomics, and genome sequencing. These are DNA fragments of some particular (known) sizes that can be used to help identify the fragments of DNA of a particular size. This makes sure that the BAC library is accurately made up of DNA fragments that too of a particular size range. These DNA fragments are inserted into a BAC vector using an enzyme called ligase to join the two bits of DNA together.

QTL-Fhb1 is the major QTL located on the 3BS chromosome derived from Sumai-3, a Chinese cultivar (Cuthbert et al., 2006). It was identified and designated as *Qfhs.ndsu-3BS* and mapped by restriction fragment length polymorphism (RFLP) analysis (Waldron et al., 1999). Mapping populations with resistant (Sumai-3) and susceptible (Thatcher) genetic background were used to isolate and mapped Fhb1 on 3BS chromosomes within the 1.27-cM interval (S/T) (Cuthbert et al., 2006). Two microsatellite markers, Xgwm533 and Xgwm493, were used to flank *Qfhs.ndsu-3BS* on the 3BS chromosome (Anderson et al., 2001). Sequence-tagged sites (STS) markers developed from wheat expressed sequence tags (ESTs) were used to increase the marker density near *Qfhs.ndsu-3BS* in order to facilitate fine mapping (Liu and Anderson, 2003). This QTL has

been verified in several mapping populations. It lies in the deletion bin 3BS 0.78–0.87, which is a position on the genetic map with a unique segregation pattern and is separated from adjacent bins by a single recombination event (Bai and Shaner, 1996; Buerstmayr et al., 2002; Zhou et al., 2002; Liu and Anderson, 2003). QTL-Fhb1 has been proved to impart rachis resistance against FHB, thus is of significant importance (Bai and Shaner, 1996; Waldron et al., 1999; Anderson et al., 2001; Yang et al., 2003).

2.3.1 Gene discovery in QTL-Fhb1

Several studies were carried out, expediting the identification of genes responsible for FHB resistance. For instance, map-based cloning led to identifying seven putative candidate genes in QTL-Fhb1 and functionally validated *UMN10* as a diagnostic marker (Liu et al., 2008). Diagnostic markers enable efficient and quick characterization and screening of germplasm for allelic diversity with accuracy since they are not subjected to recombination. This avoids false selection or loss of information in marker-assisted breeding (Ogbonnaya et al., 2001; Avila et al., 2007; Nadeem et al., 2018). Transcriptomics analysis of NILS carrying QTL-Fhb1 identified increased transcript abundance of genes related to jasmonic acid, ethylene-related, ABC transporters, UDP-glycosyltransferases, WRKY transcriptional factors, PCD-related, and xylanase inhibitors but not functionally validated (Jia et al., 2009). Furthermore, an integrated metabolic-proteomic approach was applied, which led to identifying metabolites related to HCAAs, phenolic glycosides, and flavonoids (Gunnaiyah et al., 2012). An effort was made by Kugler et al. to carry out RNA-Seq analysis using NILs, which led to the identification of genes such as glucanases, NBS-LRR, WRKY transcription factors, and UDP-glycosyltransferases. Although unable to prove resistance function (Kugler et al., 2013). Likewise, RNA-Seq, which uses next-generation sequencing to analyze the continuously changing cellular transcriptome, identified pathogen-related proteins, ABC transporter, and jasmonic acid signaling-related genes but were not functionally validated (Xiao et al., 2013). To improve FHB resistance in wheat NILs containing the contrasting alleles at QTL-Fhb1 derived from Sumai-3 and Stoa (susceptible), fine mapped to 0.08cm, a pore-forming toxin gene (PFT) was identified. Silencing the PFT gene in NIL-R led to a severely bleached spike (Rawat et al., 2016). However, this gene failed to confirm FHB resistance in Wangshubai and Sumai-3 (Jia et al., 2018). RNA-seq analysis of 1Mb genomic contig harboring Fhb1 from the Sumai-3 derivative CM-82036 identified 28 genes, including a GDSL lipase gene, as a potential candidate based on high expression in NIL-R (Schweiger et al., 2016). In Arabidopsis and wheat,

GDSL lipase has been reported to modulate system immunity by exploiting the ethylene (ET) signaling pathway (Ling, 2008; Kwon et al., 2009). Recently, a histidine-rich calcium-binding protein (*TaHRC*) was identified with a large deletion in the start codon region of its susceptible allele and functionally validated to confer FHB resistance by preventing *F. graminearum* spread (Su et al., 2018; Li et al., 2019; Su et al., 2019). So far, GDSL, PFT, and HRC genes are considered as a genetic component of QTL-Fhb1 and a key determinant for FHB resistance in wheat, but the mechanism of resistance is still at large.

2.4 Forward genetics approach to identify novel candidates in FHB resistance

2.4.1 QTL-sequencing

Quantitative trait locus (QTL)-Seq is a method that combines bulked segregant analysis (BSA) and high-throughput whole-genome re-sequencing to detect the major locus of a certain quantitative trait in a segregating population. However, identifying the gene(s) and gene mechanisms to impart resistance against FHB requires a comprehensive dissection of QTL associated with important agronomic quantitative traits. The advancement in high-throughput next-generation sequencing technologies has smoothed the path to attain QTL-sequencing. Various crops have been studied for investigating genes underlying major QTL by adopting a QTL-sequencing strategy. In brassica, a fine mapped QTL region harboring genes responsible for seed glucosinolate contents such as *GSL-Elong*, *Myb28*, *GSL-ALK*, and *GSL-PRO* were studied for underlying genetic mechanisms (Bisht et al., 2009). In radish roots, *GSL-QTL-2* regions were analyzed for the SNP markers corresponds to candidate genes such as *RsMAM3*, *RsIPMDM1*, and *RsBCAT4* responsible for the biosynthesis of 4-methylthio-3-butenyl glucosinolate (4MTB-GSL) (Zou et al., 2013). In rice, QTL-sequencing was used to reveal gene(s) or QTLs linked with blast resistance, thus conveying resistance against *Magnaporthe oryzae*, a fungal pathogen in rice cultivar (Takagi et al., 2013). In cucumber, a candidate gene *Ef1.1* underlying a major QTL controlling early flowering on chromosome 1 has been identified successfully employing QTL-sequencing based on NGS technology (Lu et al., 2014). A study was performed to identify potential candidate genes underlying major Chickpea QTL associated with 100-seed weight using NGS-based whole genome QTL-sequencing integrated with QTL mapping followed by differential expression profiling. This study revealed six protein-coding putative candidate genes, where COP9 signalosome complex subunit 8 (*CSN8*) served as a potential candidate having a role in enhancing

seed weight and yield (Das et al., 2015). In the recent past, SNP markers and leaf rust resistance locus, Lr19 underlying QTL (*Qfhs-pur-7EL*) were identified against fungal pathogens, *F. graminearum*, and *P. triticina* Eriks using genotyping-by-sequencing (GBS) (Xiao et al., 2016).

In the light of above-mentioned alluring studies, sequencing wheat major QTL-Fhb1 based on flanking marker sequences will pave the way towards discovering genes and their role in FHB resistance. A flanking marker is an identifiable region, that is polymorphism, located near a gene that can be used in linkage studies to track the gene's coinheritance in question.

2.4.2 Metabolomics

Metabolomics generates a profile of small molecules derived from cellular metabolism through complex networks of biochemical reactions, thereby providing insights into multiple aspects of cellular physiology. Advancements in technology have paved the way to the rapid and increasingly expansive data acquisition with samples as small as single cells. However, substantial challenges in the field remain (Liu and Locasale, 2017).

Metabolomics is defined as a systematic identification and quantitation of all metabolites in an organism or biological sample under specified conditions (Shulaev, 2006). Metabolites being closer to phenotype help answer several questions related to the plant phenotypes and provide the missing link between the genotype and the phenotype (Fiehn, 2002; Hall et al., 2002; Okazaki and Saito, 2012). Metabolomics investigates the activity and status of cellular and organismal metabolism on a global or network scale to delineate the endpoints of physiology and pathophysiology. It involves measuring small-molecule compounds, including endogenous and exogenous molecules, that are the products and substrates of chemical reactions within biological systems. A metabolomics experiment directly reflects the metabolic network activity that leads to the production of these metabolites and yields essential information about the system's underlying biological status in question (Jang et al., 2018). However, the fundamental chemical structure's difference impedes unraveling the biological questions to the level of other omics technologies like genomics and proteomics, thus requiring future advancements (Okazaki and Saito, 2012). Even though metabolomics has been widely used as a tool for functional genomics, discover biomarkers, safety assessment of genetically modified crops, QTL analysis, stress resistance (abiotic and biotic) and trait improvement in plants (Soga et al., 2006; Urano et al., 2009; Ward et al., 2010; Gunnaiah et al., 2012; Yogendra et al., 2014; Yogendra et al., 2017).

2.4.2.1 Metabolite extraction and analytical platforms

Accurate determination of intracellular metabolite levels requires well-validated procedures for sampling and sample treatment. Several methods exist for metabolite extraction, but the literature is contradictory regarding the adequacy and performance of each technique. A metabolome consists of a vast array of compounds; hence the fully integrated strategy for metabolite extraction, optimal separation, detection, identification, and data analysis will affect the final output and advancement, further dependent on analytical and computational developments (Hall et al., 2002). The metabolite extraction is the primary step in metabolic profiling; thus, a comprehensive approach should be used to quench maximum metabolites. Likely, using one single solvent cannot extract all the metabolites; therefore, one which gives maximum extraction must be used (Shulaev et al., 2008; Gunnaiah, 2013). Besides, the polarity of the analytes in consideration and the analytical platform also contribute significantly to metabolite extraction. Among several concentrations of methanol and chloroform tried and tested, it was found that 70% to 75% methanol (v/v) is the most efficient in extracting a wide range of secondary metabolites from various plants and tissues (De Vos et al., 2007).

The analytical techniques that are most often used for metabolite profiling include NMR, gas chromatography-mass spectrometry (GC-MS), liquid chromatography-mass spectrometry (LC-MS), and capillary electrophoresis-mass spectrometry (CE-MS) to gain a broad perspective of the metabolome of a tissue (Shulaev, 2006). GC combined with MS-based metabolite profiling represents a highly sensitive, reliable, robust approach but is limited to volatile compounds and requires derivatization (Lisec et al., 2006). It also has the advantage of large commercial and public libraries being available (Schauer et al., 2005). GC combined with the time of flight (TOF)-MS was the mainstream method, and later GC-MS was routinely used (Fiehn et al., 2000; Lisec et al., 2006). GC-MS-based metabolomics technique has broad applications in identifying and quantifying primary plant metabolites primarily involved in natural growth, reproduction, and development and generally perform a physiological function within the organism. These include amino acids, sugars, sugar alcohols, organic acids, and polyamines, thus focusing exclusively on primary metabolic pathways (Wang et al., 2015). CE-MS additionally fills the comparable need like GC-MS yet isn't mainstream and only sometimes utilized. It gives enormous scope quantitative information to vast loads of metabolites like GC-TOF or MS (Vinaixa et al., 2016).

LC-MS, then again, is the most favored method for the investigation of plant secondary metabolites. The bit of leeway is that no derivatization is required. It holds a large sample capacity; however, it's slow compared to other techniques (De Vos et al., 2007). LC, in combination with a soft ionization strategy, can be more proficient. Electrospray ionization (ESI) or atmospheric pressure chemical ionization (APCI) results in a positive or negative mode ionization. The LC-MS approach helps recognize and measure numerous semi-polar compounds such as phenolic acids, phenylpropanoids, flavonoids, alkaloids, glycosylates, saponins and others (De Vos et al., 2007). In response to *F. graminearum* infection, several resistance-related metabolites in barley and wheat using LC-MS have been accounted (Bollina et al., 2010; Bollina et al., 2011; Kumaraswamy et al., 2011).

Nuclear magnetic resonance (NMR) spectroscopy has also come to the fore in plant metabolomics as the choice method for natural product structure determination (Ward et al., 2007). NMR provides another non-destructive, non-biased, highly quantitative platform, doesn't require derivatization or separation, can determine the atomic state of compounds and enables identification of complex unidentified compounds (Okazaki and Saito, 2012). However, the drawback persists with low sensitivity, which reduces NMR utilization over Mass spectrometry (De Vos et al., 2007). Other direct injection approaches such as Fourier transform- ion cyclotron resonance mass spectrometry (FTMS) and TOF-MS has been a platform of choice due to high sensitivity and resolution, thus have been used for metabolite fingerprinting without separation. FTMS has an advantage over other analytical platforms due to its ability to detect compounds before separation and provide accurate chemical formulae of the detected peaks, which helps metabolite annotations (Okazaki and Saito, 2012).

Nonetheless, direct conveyance frameworks may expand the adduct development, and it needs an identification framework for sub-atomic isomers (De Vos et al., 2007). Matrix-assisted laser desorption/ionization (MALDI) imaging has likewise been utilized to distinguish plant metabolites yet with restricted applications (Kaspar et al., 2011). Additionally, platforms like stable isotope- enabled mass spectrometry have opened new entryways for plant metabolomics misused and have been favorable in improving the metabolite annotation and identifying associated pathways (Zhao et al., 2020).

2.4.2.2 Computational framework and advancement of metabolomics

Several tools are available for data processing, which is a critical step in large scale, untargeted metabolomics. The processing of LC-MS data depends upon the use and the and large scale, untargeted metabolomics. The drawback remains associated with a very few secondary metabolites have been identified in plant species compared to the primary metabolites (Kushalappa and Gunnaiah, 2013). However, data processing developments in the past years have made data processing holistic, unbiased and made it simple than before. Software packages available for mass peak detection and alignment includes XCMS (Smith et al., 2006), XCMS² (Benton et al., 2008), MetAlign (Lommen and Kools, 2012), MZmine (Katajamaa et al., 2006; Pluskal et al., 2010), Markerlynx and others. These packages consist of four necessary steps: deconvolution, grouping, alignment across samples and gap filling. Based on mass identified and retention time, analytical information in the profile is transformed into coordinates followed by alignment (De Vos et al., 2007). Often, multiple peaks for the same compound are identified as the output of these software packages, including adducts, isotopes, and dimers. The annotation/identification of the metabolites is made using the accurate mass, fragmentation pattern and number of carbons based on isotope ratio (Kushalappa and Gunnaiah, 2013). The accurate mass of compounds can be referenced with the masses of the compounds available in public or commercially available libraries and databases. Likewise, the fragmentation patterns of compounds can be matched with the databases like KEGG, METLIN, Lipid Maps, PlantCyc, MetaCyc, MASS BANK, KNAsSAcK and others. The fragmentation patterns can also be confirmed using ChemDraw, ChemSketch or other chemical drawing software for compounds and standards for the respective compound (De Vos et al., 2007; Kushalappa and Gunnaiah, 2013). Metabolite identification can also be performed by knowing the number of carbon atoms present in the molecular based on isotope ratio (Kushalappa and Gunnaiah, 2013).

2.5 Reverse genetics approach for functional genomics

2.5.1 Virus-induced gene silencing (VIGS)

Virus-induced gene silencing (VIGS) is one of the reverse genetics tools for analyzing gene function that uses viral vectors carrying a target gene fragment to produce dsRNA, which triggers RNA-mediated gene silencing. In plants, virus-induced gene silencing (VIGS) has broad applications in both forward and reverse genetics and is an effective means for the functional

annotation of genes. Functional validation of genes in cereal crops such as wheat is very challenging due to its big and complex genome. For instance, functional analysis of genes has been efficiently carried out in model crops such as Arabidopsis and rice using T-DNA knockout libraries and T-DNA activation (Weigel et al., 2000). However, none of these techniques can be exploited for gene functional validation in wheat due to very low transformation efficiency. Also, wheat being polyploid is not suited for gene functional validation through the loss of function mutations because of homologous genes (Cakir et al., 2010). Thus, Virus-induced gene silencing has proved to be an asset in genetics for carrying out gene functional analysis.

VIGS was first used to describe the phenomenon of recovery from virus infection (Van Loon and Van Kammen, 1970). RNA-mediated post-transcriptional gene silencing-based defense response against pathogens carried out by VIGS is a host's natural mechanism (Ratcliff et al., 1997; Robertson, 2004). It uses viral vectors carrying a target gene fragment to produce dsRNA, which triggers RNA-mediated gene silencing. So far, various viral vectors for carrying gene silencing in different crop plants have been used, which includes barley stripe mosaic virus (BSMV), tomato mosaic virus (TMV), potato virus X (PVX), and tobacco rattle virus (TRV) (Kang et al., 2013; Manmathan et al., 2013). However, the extensive use of BSMV vectors has been observed in crops such as wheat and barley (Tai et al., 2005). For the first time, Ma et al. (2012) carried out virus-induced gene silencing in spikes or grains of monocotyledonous species using the Barley stripe mosaic virus (BSMV)-based vector. PDS encoding phytoene desaturase was used as a marker gene for checking the feasibility of BSMV used for gene silencing in grains, followed by silencing the gene of interest (Ma et al., 2012). VIGS is considered the best technique to study the gene function in plant development, biotic and abiotic stress resistance (Robertson, 2004; Burch-Smith et al., 2006; Senthil-Kumar et al., 2008; Ramegowda et al., 2014).

This approach was successfully employed in revealing gene functions of Lr21, Lr10 (resistance to leaf rust), pm3b, Pm21 (powdery mildew resistance loci) in wheat (Scofield et al., 2005; Cao et al., 2011; Kang et al., 2013; Manmathan et al., 2013). The transcription factor (WKRY53) and phenylalanine ammonia-lyase (PAL) were identified as having significant roles in aphid resistance based on VIGS in wheat (Van Eck et al., 2010). The role of gene encoding high molecular weight glutenin subunit 1Bx14 was functionally validated by silencing (Ma et al., 2012). Mlo gene was silenced in *Triticum aestivum* for the resistance against powdery mildew (Várallyay et al., 2012). Silencing of two genes, *TaEral* and *TaSall*, which enhances drought tolerance, was

achieved by exploiting the VIGS approach (Manmathan et al., 2013). BSMV-VIGS system was successfully used to study wheat genes involved in *Z. tritici*-wheat leaf interactions against *Septoria tritici* leaf blotch (STB) disease of wheat (Lee et al., 2015).

CONNECTING STATEMENT FOR CHAPTER III

As discussed previously in Chapter II, the most promising approach for FHB resistance is to develop and cultivate resistant varieties. Wheat QTL-Fhb1 is the major effect QTL for FHB resistance, mainly associated with type II resistance (resistance to spread of the pathogen within the spike through rachis). Several genes were identified and functionally validated for their resistance effects, yet the resistance mechanism is not entirely understood. The microarray-based analysis revealed that the FHB resistance mechanism is organ-specific. After glume, the rachis is considered the second most responsive organ when exposed to the macroconidia of *F. graminearum* (Golkari et al., 2007). Thus, the structural and biochemical composition of rachis varies in resistant and susceptible NILs, which plays a critical role in restricting pathogen advancement (Miller et al., 2011; Lahlali et al., 2015). We hypothesized that NILs carrying resistance and susceptible alleles of the QTL- Fhb1 might vary in their gene sequence and gene expression upon *F. graminearum*. We also hypothesized that if the resistance gene is functional in resistant NIL, it may biosynthesize metabolites that are antimicrobial and/or reinforce cell walls to control the pathogen and impart rachis resistance. In the present study, candidate genes involved in rachis resistance underlying wheat major QTL-Fhb1 based on metabolic profiling and dissecting wheat fine mapped QTL-Fhb1 using paired-end Illumina HiSeq™ 2500 platform were identified. The functional characterization of selected potential genes was conducted and reported in the following studies.

Nancy Soni wrote the first draft of the manuscript. She conceived the experimental design and performed most of the experiments. Dr. Raghavendra Gunnaiah and Dr. Shivappa Hukkeri, former Ph.D. students in Dr. Kushalappa's lab, helped with metabolomics analysis and synteny mapping, respectively. Dr. Kushalappa has been actively involved in designing each experiment's strategies, corrected several drafts of the manuscript and provided full funding to carry out the work performed in this Chapter.

CHAPTER III

Combined metabolo-genomics approach-based identification of genetic determinants of Fusarium head blight resistance in wheat QTL-Fhb1

Nancy Soni¹, Raghavendra Gunnaiah^{1,2}, Shivappa Hukkeri^{1,3}, and Ajjamada C. Kushalappa¹

¹ Plant Science Department, McGill University, Ste.-Anne-de-Bellevue, Quebec, Canada; ² University of Horticultural Science, Bagalkot, Karnataka, India; ³ University of Saskatchewan, Saskatoon, SK, Canada

***Corresponding author:**

Dr. Ajjamada C. Kushalappa

Professor, McGill University

Ste. Anne-de-Bellevue, QC, Canada H9X3V9

Tel: 1(514-709-5874) Email: ajjamada.kushalappa@mcgill.ca

Keywords: Fusarium head blight, wheat NILs; QTL-Sequencing; SNP analysis; semi-quantitative PCR; metabolomics.

3.1 Abstract

Fusarium head blight (FHB) is one of the most damaging diseases of wheat worldwide. QTL-Fhb1 is a prominent FHB resistance locus of wheat successfully introgressed in wheat breeding programs. It confers significantly high resistance to the causal pathogen *Fusarium graminearum* (*Fg*) and mycotoxin deoxynivalenol. However, mechanisms of resistance are still elusive. In this study, a prospective resistance mechanism has been elucidated based on a combined metabolomics approach. Semi-targeted metabolomics of rachis sample, following mock and *Fg* inoculation, identified a total of 111 significant metabolites, classified further into resistance-related constitutive (RRC) and resistance-related induced (RRI) metabolites. Illumina HiSeq next-generation DNA sequencing of the NILs with resistant and susceptible allele identified 37 putative candidate genes. The differences in gene expression profiles between near-isogenic lines segregating for Fhb1 inoculated with *Fg* or treated with mock were investigated based on semi-quantitative PCR. Among several genes identified, the pathogen-induced *TaNAC32*, *TaLAC4*, *TaCwInv*, *TaLECRK1*, and *TaGST1* in the NIL-R were found to be polymorphic in the NIL-S, suggests their potential role in FHB resistance. The list of candidate genes, SNP variant analysis and metabolic profiling represents a valuable resource for breeding and future studies aiming to functionally validate role of these genes for *Fg* and deoxynivalenol resistance.

Significance and Impact of the Study: This study identifies novel candidate genes for FHB resistance in wheat major QTL-Fhb1 based on a combined metabolo-genomic approach. These genes can be functionally validated in NILs or wheat cultivar for their role in FHB resistance.

3.2 Introduction

Fusarium head blight caused by *Fusarium spp.*, especially *Fusarium graminearum* (*Fg*), is one of the most devastating wheat diseases (Bai and Shaner, 2004; Buerstmayr et al., 2009). FHB epidemics lead to substantial economic losses due to reduced yield and quality of the grain, mainly due to mycotoxin contamination. DON-contaminated wheat grains are harmful to animals and humans (Jiang et al., 2007; Gauthier et al., 2015). Consequently, the regulatory agencies in Canada and other countries have set the upper limits of DON level in wheat grain at 1ppm for human consumption and at 5ppm for animal feeds (Ferrigo et al., 2016). The current FHB management practices based on cultural practices and fungicides are inadequate to achieve these limits.

Genetic improvement of wheat is the most effective strategy to manage FHB (Bai and Shaner, 2004; Dean et al., 2012). Mainly three types of FHB resistance have been used in breeding programs, such as resistance against initial infection of spikelets (Type I), pathogen spread within the spike (Type II), and mycotoxin degradation (Type III) (David Miller and Arnison, 1986). More than 250 quantitative trait loci (QTL) for FHB resistance were identified in all the 21 chromosomes, of which 50 were considered unique as diversely present in wheat populations (Liu et al., 2009). Among these, significant QTL-Fhb1 (syn. Qfhs.ndsu.3BS, Fhb1) localized on the 3BS chromosome, accounts for 60 % FHB resistance under various genetic backgrounds and environments and considered as the most reliable (Anderson et al., 2001; Buerstmayr et al., 2002; Basnet et al., 2012). Therefore, this QTL has been studied extensively to uncover the role in type II FHB resistance and the underlying mechanisms.

Sumai-3 derived QTL-Fhb1 was first identified in several mapping populations and fine mapped to a 1.2 cM interval between sts3B-189 and sts3B-206 from the original SSR markers, gwm493 and gwm533 (Bai et al., 1999; Waldron et al., 1999; Anderson et al., 2001; Buerstmayr et al., 2002; Liu et al., 2008). The dissection of host responses to DON led to the identification of genes such as DON-glucosyltransferases to combat the toxin by converting DON into DON-3-O-glucoside (D3G) in double haploid lines (Lemmens et al., 2005; Sharma et al., 2018). Likewise, transcriptomics of Sumai3 and two susceptible NILs, inoculated with *Fg*, revealed genes encoding β -1,3-glucanase (PR-2), wheatwaxins (PR-4) and thaumatin-like proteins (PR-5) (Golkari et al., 2009). RNA-sequencing based differential gene expression analyses in NILs with contrasting QTL-Fhb1 identified glucanases, nucleotide-binding site-leucine-rich repeat (NBS-LRR), WRKY transcription factors, and UDP-glucosyltransferases as candidate genes (Kugler et al., 2013;

Hofstad et al., 2016). A gene encoding chimeric lectin-containing two agglutinin domains and an ETX/MTX2 domain involved in carbohydrate binding and pore-forming named PFT (pore-forming toxin-like) was identified as the candidate gene in QTL-Fhb1 from Sumai 3 (Rawat et al., 2016). However, this gene failed to confirm FHB resistance in Wangshubai and Sumai-3 (Jia et al., 2018). RNA-seq analysis of 1Mb genomic contig harboring QTL-Fhb1 from the Sumai-3 derivative CM-82036 identified 28 genes, including a GDSL lipase gene, as a potential candidate based on high expression in NIL-R (Schweiger et al., 2016). In Arabidopsis and wheat, GDSL lipase has been reported to modulate system immunity by exploiting the ethylene (ET) signaling pathway (Ling, 2008; Kwon et al., 2009). In the recent past, a histidine-rich calcium-binding protein (*TaHRC*) was identified as a susceptible gene conferring resistance to FHB based on a large deletion in the start codon region of its susceptible allele (Bai et al., 2018; Su et al., 2018; Su et al., 2019). Later, it was claimed that the deletion led to the expression of a new protein that confers resistance to FHB (Li et al., 2019). Also, previously a candidate for FHB resistance known as wheat gene WFhb1-1 was identified, which has been recently cloned as a key functional component of Qfhb1 with potential antifungal function in wheat (Paudel et al., 2020). Therefore, the race for the identification of the FHB resistance genic component is still going on.

Systems biology approach integrating with other multiple ‘omic’ platforms emerging as an essential platform to identify novel biological pathways and understanding the disease resistance mechanisms (Shah and Newgard, 2015). Metabolites being closer to the phenotype are considered to explain the mechanisms of FHB resistance. Previously, a semi-comprehensive metabolomic analysis revealed high fold change increase in abundance of hydroxycinnamic acid amides (HCAAs) and fatty acid metabolites in response to *Fg* in wheat NILs and identified *TaACT* and *TaWRKY70* as a candidate gene for FHB resistance (Kage et al., 2017; Kage et al., 2017). Furthermore, an integrated metabolic-RNA sequencing has identified *Ta4CL3* in wheat and *HvCERK1*, *HvWRKY23*, and *HvWIN1* in barley as R genes (Kumar et al., 2016; Karre et al., 2017; Karre et al., 2019). Thus, it was conceptualized that plants’ resistance against pathogens is mainly due to hierarchies of genes, including regulatory and biosynthetic genes that eventually produced RR metabolites and proteins that suppress pathogen progress in plants (Kushalappa et al., 2016). The present study uses a functional genomics approach, which includes genomics and metabolomics, to discover the novel genes and detect novel pathways of the metabolic network. This study will accelerate our understanding of genes that might be responsive for FHB resistance

in wheat and the mechanism of secondary metabolism involved in resistance. These genes can be further considered for functional validation, followed by their employment in breeding practices or improving cultivars based on genome editing approaches.

3.3 Materials and methods

3.3.1 Plant production and experimental design

Wheat NILs carrying resistant and susceptible QTL-Fhb1 were derived from a cross (Sumai 3*5/Thatcher) (S/T) where Sumai3 is FHB resistant Chinese spring wheat cultivar, and Thatcher is a susceptible wheat cultivar. The QTL-Fhb1 was successfully fine mapped within a 1.27-cM interval in the S/T population on chromosome 3BS (Cuthbert et al., 2006). The experiment was conducted in a randomized complete block design (RCBD) with two genotypes (resistant and susceptible NILs) provided by Dr. S. Fox, AAFC, Winnipeg, Canada), two inoculations (mock and pathogen = *Fg* isolate (155.SLS, obtained from Dr. S. Rioux, CÉROM, Quebec) and five biological replications over time. Each experimental unit consisting of nine plants, three plants in each of three pots. The plants were maintained in the greenhouse precisely as suggested by Kage et al. (Kage et al., 2017).

3.3.2 Pathogen production and inoculation

The *Fg* isolate was grown on potato dextrose agar for 4-5 days at 26 °C and further sub-cultured on Rye B agar media, with UV exposure for three days, for sporulation. Macroconidia were harvested from seven-day-old cultures, and the spore count was adjusted to 10⁵ macroconidia ml⁻¹ using a hemocytometer (American Scientific Products, USA) (Chamarthi et al., 2019). In the mid-region of the spike, three alternate pairs of spikelets at 50 % anthesis (GS 65) were point inoculated with 10 µL of either macro conidial suspension or mock solution using a syringe with Leuer lock (GASTIGHT 1750 DAD, Reno, USA). At least ten spikes per replication were selected from three pots containing three plants. Inoculated plants were covered with transparent plastic bags sprayed inside with water to maintain high humidity. The bags were removed 48 h post-inoculation (hpi) (Kage et al., 2017).

3.3.3 Disease severity assessment

The number of spikelets diseased was recorded at 3-day intervals for 15 days. From the data collected, the proportion of spikelets diseased (PSD = number of spikelets diseased/total number

of spikelets in a spike) and area under the disease progress curve (AUDPC) were calculated. A Student *t*-test was used to compare the AUDPC variations between NILs (Gunnaiah, 2013).

3.3.4 Sample collection, metabolite extraction, and Liquid chromatography-mass spectrometry (LC-MS) analysis

For metabolomics, ten spikes with three alternate pairs of spikelets, pathogen or mock-inoculated, per replication, harvested at 72 hpi, with a total of 60 spikes, were used. The spike region beyond the inoculated spikes was discarded. The rachis and spikelets were separated from the remaining, frozen in liquid nitrogen, and stored in separate vials at -80 degrees Celsius until further use. The metabolites extraction was performed as suggested by De Vos et al. (2007) with some modifications (De Vos et al., 2007). One hundred milligrams (100mg) of the powdered rachis sample were placed in a 1.5-ml microcentrifuge tube washed with methanol and precooled with liquid nitrogen. 350ul of 60% cold methanol was added and vortexed, and samples were sonicated at 25 degrees Celsius for 15 minutes. Followed by this, 350ul of 100% methanol in the same samples was added and vortexed. After 10 minutes of incubation in the cold room, samples were sonicated at 40 kHz for 15 mins in a water bath set at room temperature. Afterward, sample extracts were centrifuged for 10 min at 20 000 g at room temperature, and the supernatant was collected. The supernatant was filtered through a 0.22-mm Poly(vinylidene fluoride) (PVDF) membrane filter (Millipore Corporation, Bedford, MA, USA) and finally centrifuged at 2520 g for 10 min. An aliquot of 100ul of the filtrate was used for metabolite analysis using liquid chromatography coupled with high-resolution hybrid mass spectrometers (LC-ESI-LTQ-Orbitrap, Thermo Fisher, Waltham, MA) (Bollina et al., 2010; Gunnaiah et al., 2012).

3.3.4.1 LC-MS data processing, statistical analysis and metabolites identification

The Xcalibur raw files obtained from LC-HRMS output were converted into an mzXML format using MSConverterGUI. The MS data on abundance was processed using an interactive LC-MS data processing software, mzMine2 (Pluskal et al., 2010). Publicly available databases such as PlantCyc, KEGG, LIPID MAPS, and METLIN were used to identify metabolites. Metabolites were further confirmed based on MS/MS fragmentation patterns in MASSBANK, METLIN, and in silico fragmentation, as described previously (Gunnaiah et al., 2012). Following normalization, peak abundances were subjected to one-way analysis of variance (ANOVA) performed using Metaboanalyst v 3.0 (Xia and Wishart, 2011). An adjusted *p*-value (FDR) cutoff of $P < 0.05$ and $P <$

0.01, followed by Fisher's LSD post hoc test, was used to identify significant peaks across all the samples and treatments. Subsequently, the fold change (FC) in abundances of peaks were calculated for RR metabolites: resistance-related constitutive ($RRC = RM/SM > 1.0$) and resistance-related induced ($RRI = (RP/RM > 1.0)/(SP/SM > 1.0)$) metabolites; where R is resistant, S is susceptible, P is a pathogen and M is mock (Bollina et al., 2010; Gunnaiah et al., 2012).

3.3.4 QTL-Fhb1 sequencing

The seedlings of wheat NILs, with resistant and susceptible QTL-Fhb1, were grown and maintained in the greenhouse. The leaves were harvested, DNA extracted using QIAGEN mini kit, and verified for the quality to construct the genomic DNA library. The probes for the target QTL-Fhb1 region fine mapped on chromosome 3BS within a 1.27-cM interval (S/T) using flanking markers XSTS3B-138 and XSTS3B-142 were designed by Roche Nimblegen. The paired-end Illumina HiSeq™ 2500 platform at genome Quebec, McGill University, was used to capture the QTL-Fhb1 region.

3.3.4.1 Bioinformatics analysis and *In-silico* annotation of a gene identified

Bioinformatic analysis using QTL-Fhb1 raw reads were performed by the Genotypic Technology Pvt Ltd, Bangalore, India (<https://www.genotypic.co.in/>). The raw reads were processed by a Genotypic proprietary tool for adapters and low-quality bases trimming towards 3'-end. The processed reads were aligned to the reference sequence using the Bowtie2 program (Langmead and Salzberg, 2012). The consensus sequence was generated from the aligned reads using the Genotypic proprietary tool and annotated using the Augustus program (Stanke et al., 2008). Further, GO enrichment analysis was implemented using the agriGO 2.0 (<http://systemsbiology.cau.edu.cn/agriGOv2/index.php>). Enriched GO terms were analyzed based on the REVIGO program to remove redundant GO terms and to reflect the similarity of given terms by semantic space (<http://revigo.irb.hr/>) (Xiong et al., 2017). The top biological process category GO REVIGO was used to analyze the terms with the lowest p values for enrichment.

3.3.4.2 Comparative mapping

Markers XSTS3B-138 and XSTS3B-142 flanking the fine mapped QTL-Fhb1 region were used to construct a physical map harboring all the putative candidate genes identified. Putatively identified genes localized within the fine mapped intervals in a high-density genetic linkage map

were searched for the genomic synteny, which is widely used in studying complex genomes and possibly function of genes in closely related species such as *Oryza sativa*, *Sorghum bicolor*, and *Brachypodium distachyon* using MapChart software version 2.1 (Voorrips, 2002).

3.3.4.3 First-strand cDNA synthesis and semi-quantitative PCR analysis

The rachis samples collected at 48 hpi for gene expression analysis were used for total RNA isolation using the RNeasy plant mini kit (Qiagen Inc.). Purified total RNA (~1–2 µg) was used to synthesize cDNA using the iScript cDNA synthesis kit (BioRad, ON, Canada) for the relative quantification of transcript expression. Taking the standardized cDNA concentration for each sample, semi-quantitative PCR was performed using GoTaq® Green Master Mix (Promega, USA) in a T100™ Thermal Cycler (BioRad, Canada) using gene-specific primers. To ensure no false-positive PCR fragments were generated and to discriminate wheat genomes, the primer sets were designed spanning the 3'UTR region (the most divergent region) using primer3 software enlisted in the table (Table 3.3). For PCR, an initial denaturation step of 5 min at 94°C was followed by 30 cycles of 30 sec 94°C, 40 sec 55°C, 1 min 72°C and end step 5 min 72°C. *TaActin* gene was used as an endogenous reference for adjusting the relative transcript level. The experiment was performed with three biological and technical replicates for each treatment. All the agarose gel images saved were processed further for digital image analysis using ImageJ software version 1.4.3u. The Wilcoxon rank-sum test method based statistical analysis determined the level of significant difference at $p < 0.05$. The data obtained as “area,” representing the PCR band density, were used to prepare a Heat map using R package gplots. Clustering established using the complete package and pairwise Euclidean distances testing hclust (hierarchical cluster) function in R. The data were analyzed for statistical significance based on the Student *t-test*.

3.3.4.4 Single nucleotide polymorphism (SNP) analysis

The line-specific marker identification was carried out to explore genetic variants such as SNPs and InDels. Full-length genomic sequences of all the genes were mapped for variant searches in both the NILs to identify potential FHB resistance candidates. Further, the effect of genomic variants at the protein level was identified based on multiple sequence alignment of amino acid sequences of resistant and susceptible NIL using MultAlin software (Corpet, 1988).

3.4 Results

3.4.1 Resistant NIL had reduced disease severity

Wheat spikes showing blackish-brown discoloration along with necrotic lesions or bleaching symptoms were considered as diseased. The FHB symptoms in NIL-R were restricted only to a pair of spikelets inoculated, with no further spread, suggesting that the pathogen colonized only the spikelets inoculated and did not spread further until 15 dpi. On the contrary, in NIL-S, the complete spike showed diseased symptoms, spreading from the point of inoculation to top and bottom ends at 15 dpi (Fig. 3.1a). The proportion of spikelets diseased (PSD) was significantly higher in NIL-S (2.88) as compared to NIL-R (0.37) (Fig. 3.1b).

3.4.2 Resistant-related (RR) metabolites in response to *Fg* infection in wheat NILs

A total of 111 significant metabolites common to all the five replicates, excluding adducts and isotopes, among which 25 were annotated as RR metabolites, classified further as resistance-related constitutive (RRC) and resistance-related induced (RRI) metabolites (Table 3.1). These metabolites were further confirmed based on fragmentation patterns (Supp. Table 3.1). Mapping these metabolites to the metabolic pathways identified RRI metabolites belong to phenylpropanoid pathway, fatty acids, terpenoids, and primary metabolism. For instance, Phenylpropanoids (monolignols, lignans, lignan glucosides, flavonoids): coniferyl ferulate (FC= 5.64), podorhizol beta-D-glucoside (FC= 5.15), sinapyl alcohol (FC= 4.4), 4- coumaric acid (FC= 3.35), p-coumaroyl diketide (FC= 2.09), sinapic acid methyl ester (FC= 2.99), isorhamnetin 3-(6"-malonylglucoside) (FC= 2.53) and a lignan, clesitanthin A (FC= 3.59); Lipid biosynthesis (fatty acids): PA(17:1(9Z)/0:0);1-(9Z-heptadecenoyl)-sn-glycero-3-phosphate (FC= 2.11), 3-hydroxybut-2-enoic acid (FC= 3.20) and PI(18:4(6Z,9Z,12Z,15Z)/0:0) (FC= 2.10); *Alkaloids*: emetamine, an isoquinoline alkaloid (FC= 2.27); *Others*: succinate (FC=3.51) and 6-Hydroxymelatonin (FC= 2.50) involved in glutamate and tryptophan metabolism respectively were identified in wheat NILs with more than two-fold change abundance.

3.4.3 Genes identified in QTL-Fhb1

Dissection of fine mapped QTL-Fhb1 tightly linked with STS markers (XSTS 142 and XSTS 80) was carried out through the paired-end Illumina HiSeq™ 2500 platform. The raw data obtained was further processed through bioinformatics analysis to identify candidate genes responsible for

FHB resistance. Mapping of raw reads around 77-86 % to the wheat Chinese spring reference genome led to identifying novel genes present in both the NILs carrying the resistant and susceptible allele. In total, 98 genes identified, which were common in both the NILs and the high number, could be attributed to the large and complex wheat genome. Out of 98 genes, only 37 were coding genes based on consensus sequence prediction employing the Augustus model (Table 3.2). The sequenced amplicons were annotated further using FGeneSH, and Blast2Go and the non-annotated sequence in the Augustus model were annotated using BLAST programmed with Wheat EST sequence. Following that, the predicted genes were undergone a homology search using BLAST against *Arabidopsis thaliana*, *Sorghum bicolor*, *Brachypodium distachyon*, and *Oryza sativa*.

3.4.4 GO enrichment analyses revealed over-represented GO term(s)

The putative candidate genes were further classified based on GO enrichment analyses (Supp. Table 3.2). Biological processes such as glutamate, mRNA, carbohydrate, cellular, cellular catabolic, multi-organism, and response to oxidative stress were significantly enriched (Fig. 3.2a). The enriched molecular functions were mainly related to iron ion binding, hydrolase activity, carbon-carbon lyase activity, catalytic activity, protein serine/threonine kinase activity, and oxidoreductase activity and iron-sulfur cluster binding (Fig. 3.2b).

3.4.5 Gene synteny among relative species

The genomic synteny analysis among related species provided new insights into the significance of the fine mapped QTL-Fhb1 and the underlying genes within it. The linkage map was built using physical distance among the annotated genes between the flanking markers (XSTS3B-138, XSTS3B-142) to show gene order and the relative distances of the genes on the 3BS chromosome (Fig. 3.3a). The orthologous genes on different chromosomes in the related species such as *Oryza sativa*, *Sorghum bicolor*, and *Brachypodium distachyon* and wheat genome displayed significant synteny to the predicted candidate genes on the 3BS chromosome (Fig. 3.3b).

3.4.6 Gene expression profiling post-Fg infection

Gene expression analysis of all 37 genes in four different samples (RP, RM, SP, and SM, based on two genotypes and two inoculations) revealed varying levels of expression patterns in both the NILs (Fig. 3.4). Gene #3 (glycosyltransferase HGA-like), gene #9 (cell wall invertase), gene #16

(G-type lectin S-receptor-like serine/threonine-protein kinase (RKS1), LECRK1), gene #17 (NAC transcription factor 32-like), gene #19 (calmodulin *TaCaM2-2*), gene #25 (glutamate synthase1), gene #33 (laccase-4-like) and gene #36 (two-component response regulator ORR25-like) were significantly expressed in NIL-R upon *Fg* inoculation (RP). These were mainly involved in lignin biosynthesis, response to oxidative stress, glutamate metabolic process, and transcriptional regulation. This further suggests their potential role in plant defense upon *Fg* inoculation in NIL-R. Likewise, 13 genes were identified as resistance-related constitutive (RRC) genes, mainly involved in primary metabolism (Fig. 3.4; Table 3.2). Only one gene encodes for Executer 2 protein was strongly expressed in SM with an unknown biological process. Likewise, gene #2 (Sarcoplasmic reticulum histidine-rich calcium-binding protein), gene #7 (phosphatidylserine synthase), gene #13 (putative disease resistance protein RGA3), and gene #26 (1,3 beta-glucan synthase) displayed increased expression in SP, implying a possible role in susceptibility to FHB, though need functional validation.

3.4.7 Genetic variants among NILs

Among 37 putatively identified genes, 12 genes were identified with several SNPs in NIL-S compared to NIL-R (Table 3.4). These SNPs also corresponds to several mutations at the protein level, leading to functional consequences of genetic variation (Fig. 3.5). These include gene #8 (fructose-bisphosphate aldolase 1), gene #9 (cell wall invertase), gene #12 (ubiquitin-conjugating enzyme E2), gene #16 (LECRK1), gene #17 (NAC transcription factor 32-like), gene #25 (glutamate synthase 1), gene #26 (1,3beta-glucan synthase), gene #28 (potassium channel KAT3-like), gene #31 (β -glucosidase BoGH3B-like), gene #32 (scarecrow-like protein 9), gene #2 (HRC) and gene #33 (laccase-4-like) (Table 3.4). These genes were mostly responsive to oxidative stress, regulation of transcription, and carbohydrate metabolic processes providing insights into the potential genomic targets contributing to disease resistance.

3.4.8 Prioritization of Candidate Genes

An integrated approach of QTL sequencing and metabolomics unfolded the unique candidate genes involved in FHB resistance and provide insights into the FHB resistance mechanism, the pathways upregulated, and the biosynthetic gene(s) involved in biosynthesizing these RR metabolites. This study was mainly aimed at the identification of candidate genes in NIL-R responsive to *Fg* infection. The workflow diagram of the conjoint approach to identify potential

candidates is shown (Fig. 3.6). Metabolomics and QTL-Fhb1 sequencing, including differential gene expression analyses, and SNP variant analysis data, suggested some promising candidate genes: laccase-4-like, cell wall invertase, G-type lectin S-receptor-like serine/threonine-protein kinase, NAC transcription factor 32-like and glutamate synthase 1, which may impart a high level of FHB resistance in wheat. However, future study is needed to further validate these genes(s) in wheat NILs and related species in response to FHB infection to confirm their resistance role.

3.5 Discussion

The present study revealed few potential molecular players determining the level of FHB resistance between the two wheat NILs, unraveling the genetic architecture through an integrated approach of metabolomics and genomics. Previously, QTL-Fhb1, covering ~1 Mb interval between molecular markers sts3B-32 and sts3B-206 derived from a cross of CM-82036 (highly resistant donor cv.) and Remus (highly susceptible cultivar) using CM-82036 as the recurrent parent, identified 28 genes based on RNA-seq study (Buerstmayr et al., 2002; Schweiger et al., 2016). In this study, a fine mapped QTL-Fhb1 derived from Sumai-3 and Thatcher was re-sequenced using flanking markers, XSTS-3B 80 and XSTS-3B 142 covering 1.27 cM to identify FHB responsive candidate gene(s) (Cuthbert et al., 2006). Among 37 putative candidates identified in this study, genes #5, gene #10, gene #14, gene #18, gene #20, gene #21, gene #27, gene #29, gene #30, gene #34, and gene #37 were excluded as no significant differential expression was observed among NILs. Although several related genes or gene families have already been identified through the omics approach in response to *Fg* infection in wheat, only a few were functionally validated based on RNAi silencing, overexpression, CRISPR mutants, and haplotype association analysis.

However, resistance in wheat against FHB is quantitative, involving additive effects of several governing the resistance, yet the underlying resistance mechanisms are still unknown. Thus, based on metabolomics analysis, gene expression profiling of putative candidate genes in resistant NIL post-*Fg* infection and SNP analysis, we have listed and discussed potential candidates for FHB resistance. These candidates possess either a direct or indirect association to FHB resistance by modulating other regulatory genes or enzymes in the background of NILs varying in QTL-Fhb1.

3.5.1 Functional genomic analysis of constitutive and inducible defense responses to *Fg* infection in wheat NILs with contrasting FHB resistance

In response to pathogen attack, plants adopt both constitutive and induced defenses. The trade-off between the two leads to defense diversity, where constitutive defense serves as the first place of defense through numerous plant toxins and induced defense response mediated by hypersensitive response minimizes the infectious period (Lam et al., 2001; Wittstock and Gershenson, 2002; Boots and Best, 2018). Furthermore, the most substantial cost incurred in the case of induced defense responses in response to infections, constitutive defense response, must be paid even in the absence of disease (Boots and Best, 2018). The major resistant effect of QTL-Fhb1 can be explained based upon genetic changes that occur in a genotype, such as induction and constitutive expression of the gene, genetic mutation, or genotype-specific expression of the gene in either resistant or susceptible phenotype (Xie et al., 2007; Schweiger et al., 2016). This study has identified 37 putative candidate genes which are engaged in different biological and molecular function. Genes explicitly engaged in defense response against pathogen attack (*Fg*), concluded as potential resistant gene(s), and further discussed.

3.5.2 Novel candidates for FHB resistance

3.5.2.1 Glutamate metabolic process

Gene expression analysis affirmed significantly induced expression of gene #25 in resistant NIL upon *Fg* inoculation (RP) compared to NIL-S (Figure 3.4). GLT1 catalyzes biosynthesis of L-glutamate, which further catalyzed by glutamate decarboxylase to form gamma-aminobutyrate (GABA). Subsequently, GABA gets converted to succinate, an essential component of the Citrate cycle (TCA cycle). In this study, gene #4 was identified with constitutive expression with no SNPs detected, thus eliminated as a candidate. Gene #25 consists of various substitutions in susceptible NIL based on SNP analysis (Table 3.4; Fig. 3.5). GO enrichment analysis unveiled glutamate metabolism as one of the most significantly enriched biological processes in our study (Fig. 3.2a). A study reported a concurrent over-activation of the cytosolic glutamine synthetase and the GABA against *B. cinerea* in tomato by suppressing pathogen-induced senescence, thus dominating anti-cell-death defense mechanism which constructs an effective defense response against necrotrophic pathogens (Seifi et al., 2013). Therefore, Gene #25 is considered a potential candidate gene for functional validation for conferring FHB resistance in wheat.

3.5.2.2 Response to oxidative stress/ Oxidation-Reduction

Gene #33 (Laccase) encodes for an unnamed protein product was identified with comparatively high transcript abundance in resistant NIL upon *Fg* inoculation (RP) as compared to NIL-S (Fig. 3.4). GO enrichment analysis represented oxidation-reduction as a significantly enriched molecular function (Figure 3.3b). Plant laccases catalyze monolignols' oxidation into the primary lignification stage and process lignin polymerization in the xylem (Hoopes and Dean, 2004). In QTL-Fhb2, an integrated metabolo-transcriptomics study also reported secondary cell wall lignification related genes, including laccase as a candidate gene in response to *Fg* in wheat RILs (Dhokane et al., 2016). A transcriptome-based study of two major QTLs, QTL-Fhb5 and QTL-Fhb1, identified laccase protein as one of the potential FHB associated candidates (Schweiger et al., 2013). In barley, GO enrichment analysis of DEGs revealed oxidoreductases, including laccases, as one among the highly enriched group after 96 hpi of *Fg* (Huang et al., 2016). Apart from having a role in lignin polymerization, overexpression of laccase (*GhLac1*) in cotton (*Gossypium spp.*) was identified with enhanced resistance to the fungal pathogen *Verticillium dahliae* and the insect pests cotton bollworm (*Helicoverpa armigera*) and cotton aphid (*Aphis gossypii*) (Hu et al., 2018). In Arabidopsis, lac11, lac4, lac17 triple mutant showed no major effect on the peroxidase transcript activity, suggesting laccase is independent of peroxidase activity for monolignol polymerization during vascular bundle development (Zhao et al., 2013). Further, Gene #33 was identified with two significant substitutions, lysine to glutamate (K250E) and histidine to aspartate (H252D) (Fig. 3.5).

Moreover, untargeted metabolomics analysis revealed the accumulation of coniferyl ferulate (FC= 5.64) and sinapyl alcohol (FC= 4.4) belonging to phenylpropanoids with high fold change difference (Table 3.1). Oxidative polymerization of two primary monomers, coniferyl alcohol and sinapyl alcohol, leads to lignin polymerization (Zhao et al., 2013). Thus, based on gene expression, SNP variant analysis, and associated RR metabolite, gene #33 is considered a high potential candidate for FHB resistance.

3.5.2.3 Carbohydrate metabolic process

Gene #9 (Cell wall invertase (Cw-Inv)), also known as beta-fructofuranosidase, was identified with a serine to alanine substitution (S497A) based on amino acid sequence comparison between NILs (Fig. 3.5). This mutation prevents potential phosphorylation events that play critical

roles in the plant immune response (Bauer et al., 2003). During plant-pathogen interaction, cell wall invertases have been reported to be crucial for proper sucrose and carbohydrate partitioning and signaling to trigger defense responses (Tauzin and Giardina, 2014). Thus, serine substitution to alanine in NIL-S may impede sugar partitioning and signaling events during *Fg* infection. Concurrently, strongly induced expression in resistant NIL compared to susceptible NIL upon *Fg* inoculation was observed based on gene expression study (Fig. 3.4). In *A. thaliana*, repressed callose deposition was observed upon an increase in exogenous sucrose concentrations, suggesting hexose cleavage products of sucrose in cell wall reinforcement to restrict pathogen invasion (Luna et al., 2010). Similar plant invertases have been reported in wheat in response to powdery mildew infection (Sutton et al., 2007). RNA sequencing analysis of four wheat genotypes (Nyubai, Wuhan 1, HC374, and Shaw) revealed much higher upregulation of beta- fructofuranosidases in HC374 at 4 dpi of *Fg* (Pan et al., 2018). Gene #31 (Beta-glucosidase BoGH3B-like) belongs to glycoside hydrolase family three protein. Broadly GH family mainly comprises β -glucosidases induced in the response of biotic and abiotic stresses and therefore required for plant development. These β -glucosidases, though found in several organisms but perform distinct functions. For instance, these glucosidases are associated with cell wall catabolism, signaling, lignification, defense, symbiosis, and secondary metabolism in plants (Opassiri et al., 2006; Calderan-Rodrigues et al., 2018). Gene #8 and gene #31 both were constitutively expressed in NIL-R (RM), although they were not expressed upon *Fg* and NIL-S. In contrast, gene #9, based on SNP calling and induced gene expression upon *Fg* inoculation, can be considered for functional validation as a significant candidate for FHB resistance.

3.5.2.4 Receptor-like kinases

Gene #16 (G-type lectin S-receptor-like serine/threonine-protein kinase (RKS1)), also known as LECRK1, displays strong induced expression in resistant NIL post-*Fg* inoculation (RP) (Fig. 3.4). Interestingly, a deletion of 15 amino acids (D367-K381) was spotted in NIL-R compared to NIL-S, comprised of plant PAN/APPLE-like domain and functions in mediating protein-protein or protein-carbohydrate interactions (Fig. 3.5). Cell surface localized lectin receptor kinases function in priming pattern-triggered immunity and mediating downstream signaling events (Jones and Dangl, 2006; Lacombe et al., 2010). An orthologous gene, Bph3 gene encoding plasma membrane-localized lectin receptor kinases, confer broad-spectrum disease resistance against brown planthopper and white back planthopper (Liu et al., 2014). In response to

Fg infection in wheat, several similar lectin receptor kinases were also identified upregulated (Dhokane et al., 2016; Pan et al., 2018). Multiple genomic SNPs and high transcript abundance in NIL-R make gene #16 more intriguing to study FHB resistance further. Besides, Gene #11 (Rust resistance kinase Lr10) Gene#22 (Acetyl-CoA carboxylase (Acc-1)) involved in protein serine/threonine kinase activity. Lr genes are involved in defense against rust disease such as *Puccinia triticina* in bread wheat (*Triticum aestivum* L.) (Krattinger et al., 2009; Manickavelu et al., 2010). However, these genes were constitutively expressed in resistant NIL (RM), whereas not expressed significantly in NIL-S.

3.5.2.5 Regulation of transcription

Gene #17 encodes for NAC domain-containing protein (*TaNAC032*) was identified as an induced R gene in NIL-R post-*Fg* infection (Fig. 3.4). The deletion of 121 nucleotides in NIL-S corresponds to the deletion of 41 amino acids (N62-R102) resulted in the deletion of conserved NAC domain in NAC transcription factor 32, apart from various other SNPs compared to NIL-R (Table 3.4; Fig. 3.5). Secondary wall NACs (SWNS) is the group of closely related NAC TFs that function as master switches either directly by modifying the cell wall and facilitating programmed cell death (PCD) or indirectly by binding to 19 bp secondary wall NAC binding element (SNBE) sequences. Thus, it activates the expression of downstream transcription factors and genes involved in lignin or secondary cell wall biosynthesis (Mitsuda et al., 2005; Yamaguchi et al., 2011; Zhang et al., 2018). Although no direct involvement of NAC32 in response to biotic stress is evident, other NAC TF such as *TaNACL-D1* was identified as a candidate against FHB infection and DON in wheat (Perochon et al., 2019). Over-expression of NAC leads to increased lignin deposition in *Arabidopsis* (Zhong et al., 2006). In our study, untargeted metabolomics analysis unveiled a higher accumulation of various free phenylpropanoids, lignans and phenolic glycosides with high fold change. These are mainly involved in reinforcing secondary cell walls suggesting gene #17 in regulating other regulatory factors or lignin-specific genes in response to pathogen attack. Thus, gene #17 represents one of the potential candidates for FHB resistance.

Also, Gene #32 (Scarecrow-like protein 9) encodes for GRAS family protein such as *A. thaliana* protein SCARECROW, a transcription factor required for quiescent center cells specification and maintenance of surrounding stem cells, and the asymmetric cell division involved in radial pattern formation in roots (Pysh et al., 1999). An *A. thaliana* SCARECROW-like 14 (SCL14 is involved in the detoxification of plants challenged with harmful endogenous

metabolites, particularly, Xenobiotics (Fode et al., 2008). Also, In response to *Pseudomonas syringae* pv. tomato infection in tomato, GRAS family of transcriptional regulators, plays a crucial role in resistance (Mayrose et al., 2006). Another gene related to transcription regulation, Gene #36 (Two-component response regulator ORR25-like), is a transcriptional activator that binds specific DNA sequences. This gene encodes for Myb-related protein-containing REC and myb_SHAQKYF domain-containing protein. Myb transcription factors are majorly involved in biotic and abiotic stresses, development, differentiation, metabolism, and defense response (Ambawat et al., 2013). For instance, *AtMYB30* is engaged in response to pathogen attack by activating hypersensitive cell death program (Li et al., 2009), while, *AtMYB108* is involved in both biotic and abiotic stress responses (Mengiste et al., 2003). Expression analyses revealed a high expression of this gene in resistant NIL upon *Fg* inoculation, hinting as a potential candidate, although no SNPs were detected based on SNP variant analysis.

3.5.3 Metabolic profiling provided key insights to metabolic pathways actively participating in pathogen invasion

Plant/pathogen interaction outcome depends on a complex cascade of recognition, attack, and defense reactions at the plant/microbe interface. Initially, early defense response events occur at the host's genetic level, such as ion fluxes across the plasma membrane, cascades of phosphorylations and dephosphorylations, and production of reactive oxygen species (Dixon and Paiva, 1995). Later, these events are continued globally by metabolic modifications that include: (a) stimulation of the phenylpropanoid and fatty acid pathways, (b) production of defense-specific chemical messengers such as salicylic acid (SA) or jasmonates, and (c) accumulation of components with antimicrobial activities such as phytoalexins and pathogenesis-related (PR) proteins (Somssich and Hahlbrock, 1998). In our study, NILs with contrasting allele subjected to non-targeted metabolic profiling identified several resistant related significant metabolites underlying different metabolic pathways such as phenylpropanoids, fatty acids, terpenoids, and flavonoids. Phenylpropanoid-related metabolites, including monolignols, lignans, lignan glucosides and flavonoids, were identified as RRI metabolites higher in abundance. For instance, coniferyl ferulate, p-coumaroyldiketide, sinapyl-alcohol, sinapic acid methyl ester, cleistanthin A and isorhamnetin 3-(6"-malonylglucoside) were identified with high fold change (Table 3.1). As plant cell wall is a mechanical barrier to the pathogen progression, lignin deposition leads to the reinforced cell wall, which is more resistant to fungal cell wall degrading enzymes and limits

diffusion of mycotoxins produced by a pathogen (Siranidou et al., 2002; Sattler and Funnell-Harris, 2013; Gunnaiah and Kushalappa, 2014). Lignans also exhibit antifungal properties against several pathogenic fungi by playing a role as antifungal phytoalexin (Cho et al., 2007).

Transcriptomics-based studies have indicated the induction of expression of several genes involved in flavonoids synthesis in response to wheat upon *Fg* inoculation (Ravensdale et al., 2014). Flavonoids function in plant defense mechanism through mechanisms: exhibiting antioxidant properties, reinforcement of plant structure, thus act as a physical barrier against fungal infection, inhibition of plant cell wall degrading enzymes secreted by fungal pathogens and ability to restrain mycelium hyphae elongation by inhibiting fungal spore development (Treutter, 2005; Venturini et al., 2015) This is also coinciding with the previous metabolomics approaches led to the identification of several RR metabolites belonging mainly to phenylpropanoid pathway particularly hydroxycinnamic acids (HCAAs) such as N-caffeoylputrescine, feruloyl-2-hydroxyputrescine, coumaroylagmatine, and coumaroyl-putrescine, in response to *Fg* infection in wheat NILs and RILs (Gunnaiah and Kushalappa, 2014; Dhokane et al., 2016; Kage et al., 2017). The phenylpropanoid pathway and its related metabolites are crucial for plant defense response to pathogen attack.

Further, aromatic amino acids such as phenylalanine, tyrosine, and tryptophan act as a precursor for a wide range of metabolites involved in resistance to DON-producing fusarium species, thus play an essential role in plant defense against biotic stress (Tzin and Galili, 2010). Wherein tryptophan catabolism leads to the generation of indole-3-acetic acid (auxin), glucosinolates, and terpenoids. Like, 6-Hydroxymelatonin (FC= 2.50) (Table 3.1) in tryptophan metabolism has extensively studied in plants under stress conditions such as heat, cold, salt, drought, heavy metal pathogen attack. In response to pathogen attack, it activates other stress-relevant hormones, like salicylic acid, ethylene, and jasmonic acid (Yu et al., 2018).

In plants, fatty acids and their derivatives are essential for basal immunity and gene-mediated resistance response. Also, to play a role in the induction of systemic acquired resistance and role in plant defense signaling pathway, they carry antimicrobial effect to limit the fungal pathogen growth, including *Fg*. Also, fatty acids were supposed to modulate ROS production and establish a physical barrier to combat pathogens through cuticle formation (Kumaraswamy et al., 2011, Walters et al., 2004). RRI metabolite identified as 3-hydroxybut-2-enoic acid, PA(17:1(9Z)/0:0);1-(9Z-heptadecenoyl)-sn-glycero-3-phosphate and

PI(18:4(6Z,9Z,12Z,15Z)/0:0) (Table 3.1) involved in fatty acid biosynthesis, which are involved in early detection of pathogens. In response to various stresses, the levels of free fatty acids increase to play a major role in establishing a plant-microbe relationship (Walley et al., 2013).

Terpenoids derived via the mevalonate and methylerythritol 4-phosphate pathways in plant cells constitute the largest and most diverse plant secondary metabolites. Based on metabolomics studies, terpenoids as biochemical defense compounds both constitutive and induced against *Fg* in wheat and barley are evident about their essential role in plant-pathogen interactions (Gunnaiyah et al., 2012; Kumaraswamy et al., 2012; Petti et al., 2012). This study identified Laurenobiolide (FC= 1.54) (Table 1), a phytochemical compound belonging to terpenoids. Interestingly, in this study, Emetamine (FC= 2.27) (Table 3.1) as RRC metabolite involved in isoquinoline alkaloid biosynthesis belongs to tropane alkaloid was identified. Alkaloids play an essential role in both biotic and abiotic stresses, thus contributes to plant innate immunity (Piasecka et al., 2015). This clearly illustrates the involvement of secondary metabolites derived from five biosynthetic routes, namely the phenylpropanoid, terpenoid, flavonoids and fatty acids metabolic pathways in FHB resistance. However, further detailed analysis of these compounds by isolating individual or group of metabolites and identifying individual compounds based on standards could confirm these metabolites' presence in wheat.

Among primary metabolism, we have identified Succinate (FC= 3.51) (Table 3.1), a GABA metabolite involved in alanine, aspartate, and glutamate metabolism pathways. An outbreak of stresses such as pathogen attack, heat shock, low temperature, acidification, oxygen deficiency, mechanical stimulation, and drought leads to the accumulation of GABA in higher plants (Bouche et al., 2004; Bown et al., 2006). Omics based approach revealed the role of glutamate metabolism in response to *Fg* infection to be associated with GABA and GABA-shunt (production mechanism bypassing two steps in tricarboxylic acid (TCA) cycle and producing GABA from glutamate), however more functional specifications are needed (Seifi et al., 2013; Chen et al., 2018; Eldakak et al., 2018).

In conclusion, this study used the metabolo-genomics approach to identify genetic determinants of FHB resistance in the major QTL-Fhb1, which facilitated identifying a few potential candidate genes in wheat NILs varying in QTL-Fhb1. However, these genes are not independent; instead, they are part of metabolic pathways and can confer FHB resistance only in association with the gene hierarchy in NIL backgrounds to biosynthesize each metabolite. The genes involved in the

biosynthesis of conjugated metabolites, especially those related to lignin in the phenylpropanoid pathway, which reinforces the cell walls are the major players. For these downstream genes to express, they should be associated with the rest of the gene hierarchy: receptors, signal transduction, signaling, and regulatory genes. Thus, the genes identified in this study should be considered further for functional analysis, which may help to interpret more clearly their role in FHB resistance. Following validation of resistance functions in commercial wheat cultivars and editing them to make them functional can enhance FHB resistance.

3.6 Author contribution statement

NS wrote the manuscript and analyzed QTL-Fhb1 gene sequencing data, metabolomics data, and generation of all figures and tables. Also, conducted and analyzed semi-quantitative PCR experiment; RG, conducted disease severity, metabolite sample preparation, and LC-HRMS analysis; RG, SH initiated QTL-Fhb1 sequencing project and guided through the study; SH helped in developing synteny map and discussing manuscript; ACK*, conceived the idea, aided in designing the experiments and edited the manuscript. All authors read and approved the manuscript.

3.7 Compliance with ethical standards

The authors declare that the experiments comply with the McGill Environment, Health and Safety guidelines and the current laws of Canada.

3.8 Conflict of interest

The authors declare no conflict of interest.

3.9 Acknowledgments

This work was funded by the Natural Sciences and Engineering Research Council of Canada (NSERC), McGill Sustainability Systems Initiative (MSSI) and Ministère de l'Agriculture, des Pêcheries et de l'Alimentation du Québec (MAPAQ), Québec, Canada. We thank Dr. S. Fox, AAFC, Winnipeg, Canada for providing wheat NILs and Dr. R. H. Proctor, USA for providing *Fg* isolate (GZ-3639). We thank Mr. Yves Dion, Centre de recherche sur les grains (CÉROM), Canada, for his guidance and support. We also acknowledge Mr. Achal Dhariwal, University of Oslo, Norway for assisting in bioinformatics analysis and other anonymous reviewers for their valuable comments and suggestions for improving the manuscript.

REFERENCES

- Ambawat S, Sharma P, Yadav NR, Yadav RC** (2013) MYB transcription factor genes as regulators for plant responses: an overview. *Physiology and molecular biology of plants : an international journal of functional plant biology* **19**: 307-321
- Anderson JA, Stack RW, Liu S, Waldron BL, Fjeld AD, Coyne C, Moreno-Sevilla B, Fetch JM, Song QJ, Cregan PB, Frohberg RC** (2001) DNA markers for Fusarium head blight resistance QTLs in two wheat populations. *Theoretical and Applied Genetics* **102**: 1164-1168
- Bai G, Kolb FL, Shaner G, Domier LL** (1999) Amplified fragment length polymorphism markers linked to a major quantitative trait locus controlling scab resistance in wheat. *Phytopathology* **89**: 343-348
- Bai G, Shaner G** (2004) Management and resistance in wheat and barley to fusarium head blight. *Annual Review of Phytopathology* **42**: 135-161
- Bai G, Su Z, Cai J** (2018) Wheat resistance to Fusarium head blight. *Canadian Journal of Plant Pathology* **40**: 336-346
- Basnet BR, Glover KD, Ibrahim AMH, Yen Y, Chao S** (2012) A QTL on chromosome 2DS of 'Sumai 3' increases susceptibility to Fusarium head blight in wheat. *Euphytica* **186**: 91-101
- Bauer PM, Fulton D, Boo YC, Sorescu GP, Kemp BE, Jo H, Sessa WC** (2003) Compensatory phosphorylation and protein-protein interactions revealed by loss of function and gain of function mutants of multiple serine phosphorylation sites in endothelial nitric-oxide synthase. *J Biol Chem* **278**: 14841-14849
- Bollina V, Kumaraswamy GK, Kushalappa AC, Choo TM, Dion Y, Rioux S, Faubert D, Hamzehzarghani H** (2010) Mass spectrometry-based metabolomics application to identify quantitative resistance-related metabolites in barley against Fusarium head blight. *Mol Plant Pathol* **11**: 769-782
- Boots M, Best A** (2018) The evolution of constitutive and induced defences to infectious disease. *Proceedings of the Royal Society B: Biological Sciences* **285**: 20180658
- Bouche N, Fait A, Zik M, Fromm H** (2004) The root-specific glutamate decarboxylase (GAD1) is essential for sustaining GABA levels in Arabidopsis. *Plant Mol Biol* **55**: 315-325
- Bown AW, Macgregor KB, Shelp BJ** (2006) Gamma-aminobutyrate: defense against invertebrate pests? *Trends Plant Sci* **11**: 424-427
- Buerstmayr H, Ban T, Anderson JA** (2009) QTL mapping and marker-assisted selection for Fusarium head blight resistance in wheat: a review. *Plant Breeding* **128**: 1-26
- Buerstmayr H, Lemmens M, Hartl L, Doldi L, Steiner B, Stierschneider M, Ruckebauer P** (2002) Molecular mapping of QTLs for Fusarium head blight resistance in spring wheat. I. Resistance to fungal spread (Type II resistance). *Theor Appl Genet* **104**: 84-91
- Calderan-Rodrigues MJ, Fonseca JG, Clemente HS, Labate CA, Jamet E** (2018) Glycoside hydrolases in plant cell wall proteomes: Predicting functions that could be relevant for improving biomass transformation processes. *Advances in Biofuels and Bioenergy* **1**: 165-182

- Chamarthi S, Kumar K, Gunnaiah R, Kushalappa A, Dion Y, Choo T** (2019) Identification of fusarium head blight resistance related metabolites specific to doubled-haploid lines in barley. *European Journal of Plant Pathology* **138**: 67-78
- Chen F, Liu C, Zhang J, Lei H, Li H-P, Liao Y-C, Tang H** (2018) Combined metabonomic and quantitative rt-pcr analyses revealed metabolic reprogramming associated with fusarium graminearum resistance in transgenic arabidopsis thaliana. *Frontiers in Plant Science* **8**
- Cho HY, Lee-Parsons CW, Yoon SY, Rhee HS, Park JM** (2007) Enhanced benzophenanthridine alkaloid production and protein expression with combined elicitor in *Eschscholtzia californica* suspension cultures. *Biotechnol Lett* **29**: 2001-2005
- Corpet F** (1988) Multiple sequence alignment with hierarchical clustering. *Nucleic acids research* **16**: 10881-10890
- Cuthbert PA, Somers DJ, Thomas J, Cloutier S, Brule-Babel A** (2006) Fine mapping Fhb1, a major gene controlling fusarium head blight resistance in bread wheat (*Triticum aestivum* L.). *Theor Appl Genet* **112**: 1465-1472
- David Miller J, Arnison PG** (1986) Degradation of deoxynivalenol by suspension cultures of the fusarium head blight resistant wheat cultivar Frontana. *Canadian Journal of Plant Pathology* **8**: 147-150
- De Vos RC, Moco S, Lommen A, Keurentjes JJ, Bino RJ, Hall RD** (2007) Untargeted large-scale plant metabolomics using liquid chromatography coupled to mass spectrometry. *Nature protocols* **2**: 778
- Dean R, Van Kan JA, Pretorius ZA, Hammond-Kosack KE, Di Pietro A, Spanu PD, Rudd JJ, Dickman M, Kahmann R, Ellis J, Foster GD** (2012) The Top 10 fungal pathogens in molecular plant pathology. *Mol Plant Pathol* **13**: 414-430
- Dhokane D, Karre S, Kushalappa AC, McCartney C** (2016) Integrated metabolo-transcriptomics reveals fusarium head blight candidate resistance genes in wheat qtl-fhb2. *PloS one* **11**: e0155851-e0155851
- Dixon RA, Paiva NL** (1995) Stress-induced phenylpropanoid metabolism. *The Plant cell* **7**: 1085-1097
- Eldakak M, Das A, Zhuang Y, Rohila JS, Glover K, Yen Y** (2018) A quantitative proteomics view on the function of qfhb1, a major qtl for fusarium head blight resistance in wheat. *Pathogens* **7**: 58
- Ferrigo D, Raiola A, Causin R** (2016) Fusarium toxins in cereals: Occurrence, legislation, factors promoting the appearance and their management. *Molecules* **21**
- Fode B, Siensen T, Thurow C, Weigel R, Gatz C** (2008) The Arabidopsis GRAS protein SCL14 interacts with class II TGA transcription factors and is essential for the activation of stress-inducible promoters. *The Plant cell* **20**: 3122-3135
- Gauthier L, Atanasova-Penichon V, Chereau S, Richard-Forget F** (2015) Metabolomics to decipher the chemical defense of cereals against fusarium graminearum and deoxynivalenol accumulation. *Int J Mol Sci* **16**: 24839-24872
- Golkari S, Gilbert J, Ban T, Procnier JD** (2009) QTL-specific microarray gene expression analysis of wheat resistance to Fusarium head blight in Sumai-3 and two susceptible NILs. *Genome* **52**: 409-418
- Gunnaiah R** (2013) Functional characterization of wheat fusarium head blight resistance qtl (fhb1) based on non-targeted metabolomics and proteomics. *McGill University*

- Gunnaiah R, Kushalappa AC** (2014) Metabolomics deciphers the host resistance mechanisms in wheat cultivar Sumai-3, against trichothecene producing and non-producing isolates of *Fusarium graminearum*. *Plant Physiol Biochem* **83**: 40-50
- Gunnaiah R, Kushalappa AC, Duggavathi R, Fox S, Somers DJ** (2012) Integrated Metabolo-Proteomic Approach to Decipher the Mechanisms by Which Wheat QTL (Fhb1) Contributes to Resistance against *Fusarium graminearum*. *PLOS ONE* **7**: e40695
- Hofstad AN, Nussbaumer T, Akhunov E, Shin S, Kugler KG, Kistler HC, Mayer KFX, Muehlbauer GJ** (2016) Examining the Transcriptional Response in Wheat Fhb1 Near-Isogenic Lines to *Fusarium graminearum* Infection and Deoxynivalenol Treatment. *The Plant Genome* **9**
- Hoopes JT, Dean JF** (2004) Ferroxidase activity in a laccase-like multicopper oxidase from *Liriodendron tulipifera*. *Plant Physiol Biochem* **42**: 27-33
- Hu Q, Min L, Yang X, Jin S, Zhang L, Li Y, Ma Y, Qi X, Li D, Liu H, Lindsey K, Zhu L, Zhang X** (2018) Laccase GhLac1 Modulates Broad-Spectrum Biotic Stress Tolerance via Manipulating Phenylpropanoid Pathway and Jasmonic Acid Synthesis. *Plant Physiology* **176**: 1808-1823
- Huang L, Liu Y, Liu X, Ban L, Wang Y, Li M, Lu F** (2016) Functional expression of *Trametes versicolor* thermotolerant laccase variant in *Pichia pastoris*. *Biotechnology & Biotechnological Equipment* **30**: 261-269
- Jia H, Zhou J, Xue S, Li G, Yan H, Ran C, Zhang Y, Shi J, Jia L, Wang X, Luo J, Ma Z** (2018) A journey to understand wheat *Fusarium* head blight resistance in the Chinese wheat landrace Wangshuibai. *The Crop Journal* **6**: 48-59
- Jiang G-L, Shi J, Ward RW** (2007) QTL analysis of resistance to *Fusarium* head blight in the novel wheat germplasm CJ 9306. I. Resistance to fungal spread. *Theoretical and Applied Genetics* **116**: 3-13
- Jones JD, Dangl JL** (2006) The plant immune system. *Nature* **444**: 323-329
- Kage U, Karre S, Kushalappa AC, McCartney C** (2017) Identification and characterization of a *Fusarium* head blight resistance gene TaACT in wheat QTL-2DL. *Plant Biotechnology Journal* **15**: 447-457
- Kage U, Yogendra KN, Kushalappa AC** (2017) TaWRKY70 transcription factor in wheat QTL-2DL regulates downstream metabolite biosynthetic genes to resist *Fusarium graminearum* infection spread within spike. *Scientific Reports* **7**: 42596
- Karre S, Kumar A, Dhokane D, Kushalappa AC** (2017) Metabolo-transcriptome profiling of barley reveals induction of chitin elicitor receptor kinase gene (HvCERK1) conferring resistance against *Fusarium graminearum*. *Plant Mol Biol* **93**: 247-267
- Karre S, Kumar A, Yogendra K, Kage U, Kushalappa A, Charron J-B** (2019) HvWRKY23 regulates flavonoid glycoside and hydroxycinnamic acid amide biosynthetic genes in barley to combat *Fusarium* head blight. *Plant Molecular Biology* **100**: 591-605
- Krattinger SG, Lagudah ES, Spielmeier W, Singh RP, Huerta-Espino J, McFadden H, Bossolini E, Selter LL, Keller B** (2009) A putative ABC transporter confers durable resistance to multiple fungal pathogens in wheat. *Science* **323**: 1360-1363

- Kugler KG, Siegwart G, Nussbaumer T, Ametz C, Spannagl M, Steiner B, Lemmens M, Mayer KF, Buerstmayr H, Schweiger W** (2013) Quantitative trait loci-dependent analysis of a gene co-expression network associated with Fusarium head blight resistance in bread wheat (*Triticum aestivum*L.). *BMC Genomics* **14**: 728
- Kumar A, Yogendra KN, Karre S, Kushalappa AC, Dion Y, Choo TM** (2016) WAX INDUCER1 (HvWIN1) transcription factor regulates free fatty acid biosynthetic genes to reinforce cuticle to resist Fusarium head blight in barley spikelets. *Journal of experimental botany* **67**: 4127-4139
- Kumaraswamy GK, Kushalappa AC, Choo TM, Dion Y, Rioux S** (2012) Differential metabolic response of barley genotypes, varying in resistance, to trichothecene-producing and -nonproducing (tri5-) isolates of *Fusarium graminearum*. *Plant Pathology* **61**: 509-521
- Kushalappa AC, Yogendra KN, Karre S** (2016) Plant innate immune response: Qualitative and quantitative resistance. *Critical Reviews in Plant Sciences* **35**: 38-55
- Kwon SJ, Jin HC, Lee S, Nam MH, Chung JH, Kwon SI, Ryu CM, Park OK** (2009) GDSL lipase-like 1 regulates systemic resistance associated with ethylene signaling in *Arabidopsis*. *Plant J* **58**: 235-245
- Lacombe S, Rougon-Cardoso A, Sherwood E, Peeters N, Dahlbeck D, van Esse HP, Smoker M, Rallapalli G, Thomma BP, Staskawicz B, Jones JD, Zipfel C** (2010) Interfamily transfer of a plant pattern-recognition receptor confers broad-spectrum bacterial resistance. *Nat Biotechnol* **28**: 365-369
- Lam E, Kato N, Lawton M** (2001) Programmed cell death, mitochondria and the plant hypersensitive response. *Nature* **411**: 848-853
- Langmead B, Salzberg SL** (2012) Fast gapped-read alignment with Bowtie 2. *Nat Methods* **9**: 357-359
- Lemmens M, Scholz U, Berthiller F, Dall'Asta C, Koutnik A, Schuhmacher R, Adam G, Buerstmayr H, Mesterhazy A, Krska R, Ruckebauer P** (2005) The ability to detoxify the mycotoxin deoxynivalenol colocalizes with a major quantitative trait locus for Fusarium head blight resistance in wheat. *Mol Plant Microbe Interact* **18**: 1318-1324
- Li G, Zhou J, Jia H, Gao Z, Fan M, Luo Y, Zhao P, Xue S, Li N, Yuan Y, Ma S, Kong Z, Jia L, An X, Jiang G, Liu W, Cao W, Zhang R, Fan J, Xu X, Liu Y, Kong Q, Zheng S, Wang Y, Qin B, Cao S, Ding Y, Shi J, Yan H, Wang X, Ran C, Ma Z** (2019) Mutation of a histidine-rich calcium-binding-protein gene in wheat confers resistance to Fusarium head blight. *Nature Genetics* **51**: 1106-1112
- Li L, Yu X, Thompson A, Guo M, Yoshida S, Asami T, Chory J, Yin Y** (2009) *Arabidopsis* MYB30 is a direct target of BES1 and cooperates with BES1 to regulate brassinosteroid-induced gene expression. *Plant J* **58**: 275-286
- Ling H** (2008) Sequence analysis of GDSL lipase gene family in *Arabidopsis thaliana*. *Pak J Biol Sci* **11**: 763-767
- Liu S, Hall MD, Griffey CA, McKendry AL** (2009) Meta-analysis of qtl associated with fusarium head blight resistance in wheat. *Crop Science* **49**: 1955-1968
- Liu S, Pumphrey M, Gill B, Trick H, Zhang J, Dolezel J, Chalhoub B, Anderson J** (2008) Toward positional cloning of Fhb1 , a major QTL for Fusarium head blight resistance in wheat. *Cereal Research Communications* **36**: 195-201

- Liu Y, Wu H, Chen H, Liu Y, He J, Kang H, Sun Z, Pan G, Wang Q, Hu J, Zhou F, Zhou K, Zheng X, Ren Y, Chen L, Wang Y, Zhao Z, Lin Q, Wu F, Zhang X, Guo X, Cheng X, Jiang L, Wu C, Wang H, Wan J** (2014) A gene cluster encoding lectin receptor kinases confers broad-spectrum and durable insect resistance in rice. *Nature Biotechnology* **33**: 301
- Luna E, Pastor V, Robert J, Flors V, Mauch-Mani B, Ton J** (2010) Callose deposition: A multifaceted plant defense response. *Molecular Plant-Microbe Interactions* **24**: 183-193
- Manickavelu A, Kawaura K, Oishi K, Shin-I T, Kohara Y, Yahiaoui N, Keller B, Suzuki A, Yano K, Ogihara Y** (2010) Comparative gene expression analysis of susceptible and resistant near-isogenic lines in common wheat infected by *Puccinia triticina*. *DNA research : an international journal for rapid publication of reports on genes and genomes* **17**: 211-222
- Mayrose M, Ekengren SK, Melech-Bonfil S, Martin GB, Sessa G** (2006) A novel link between tomato GRAS genes, plant disease resistance and mechanical stress response. *Mol Plant Pathol* **7**: 593-604
- Mengiste T, Chen X, Salmeron J, Dietrich R** (2003) The BOTRYTIS SUSCEPTIBLE1 gene encodes an R2R3MYB transcription factor protein that is required for biotic and abiotic stress responses in *Arabidopsis*. *The Plant cell* **15**: 2551-2565
- Mitsuda N, Seki M, Shinozaki K, Ohme-Takagi M** (2005) The NAC Transcription Factors NST1 and NST2 of *Arabidopsis*; Regulate Secondary Wall Thickenings and Are Required for Anther Dehiscence. *The Plant Cell* **17**: 2993
- Opassiri R, Pomthong B, Onkoksoong T, Akiyama T, Esen A, Ketudat Cairns JR** (2006) Analysis of rice glycosyl hydrolase family 1 and expression of Os4bglu12 beta-glucosidase. *BMC Plant Biol* **6**: 33
- Pan Y, Liu Z, Rocheleau H, Fauteux F, Wang Y, McCartney C, Ouellet T** (2018) Transcriptome dynamics associated with resistance and susceptibility against fusarium head blight in four wheat genotypes. *BMC Genomics* **19**: 642
- Paudel B, Zhuang Y, Galla A, Dahal S, Qiu Y, Ma A, Raihan T, Yen Y** (2020) WFhb1-1 plays an important role in resistance against *Fusarium* head blight in wheat. *Scientific reports* **10**: 1-15
- Perochon A, Kahla A, Vranic M, Jia J, Malla KB, Craze M, Wallington E, Doohan FM** (2019) A wheat NAC interacts with an orphan protein and enhances resistance to *Fusarium* head blight disease. *Plant Biotechnol J*
- Petti C, Reiber K, Ali SS, Berney M, Doohan FM** (2012) Auxin as a player in the biocontrol of *Fusarium* head blight disease of barley and its potential as a disease control agent. *BMC plant biology* **12**: 224
- Piasecka A, Jedrzejczak-Rey N, Bednarek P** (2015) Secondary metabolites in plant innate immunity: conserved function of divergent chemicals. *New Phytol* **206**: 948-964
- Pluskal T, Castillo S, Villar-Briones A, Orešič M** (2010) MZmine 2: Modular framework for processing, visualizing, and analyzing mass spectrometry-based molecular profile data. *BMC Bioinformatics* **11**: 395
- Pysh LD, Wysocka-Diller JW, Camilleri C, Bouchez D, Benfey PN** (1999) The GRAS gene family in *Arabidopsis*: sequence characterization and basic expression analysis of the SCARECROW-LIKE genes. *Plant J* **18**: 111-119

- Ravensdale M, Rocheleau H, Wang L, Nasmith C, Ouellet T, Subramaniam R** (2014) Components of priming-induced resistance to *Fusarium* head blight in wheat revealed by two distinct mutants of *Fusarium graminearum*. *Molecular Plant Pathology* **15**: 948-956
- Rawat N, Pumphrey MO, Liu S, Zhang X, Tiwari VK, Ando K, Trick HN, Bockus WW, Akhunov E, Anderson JA, Gill BS** (2016) Wheat *Fhb1* encodes a chimeric lectin with agglutinin domains and a pore-forming toxin-like domain conferring resistance to *Fusarium* head blight. *Nat Genet* **48**: 1576-1580
- Sattler S, Funnell-Harris D** (2013) Modifying lignin to improve bioenergy feedstocks: strengthening the barrier against pathogens?†. *Frontiers in Plant Science* **4**: 70
- Schweiger W, Steiner B, Ametz C, Siegwart G, Wiesenberger G, Berthiller F, Lemmens M, Jia H, Adam G, Muehlbauer GJ, Kreil DP, Buerstmayr H** (2013) Transcriptomic characterization of two major *Fusarium* resistance quantitative trait loci (QTLs), *Fhb1* and *Qfhs.ifa-5A*, identifies novel candidate genes. *Molecular Plant Pathology* **14**: 772-785
- Schweiger W, Steiner B, Vautrin S, Nussbaumer T, Siegwart G, Zamini M, Jungreithmeier F, Gratl V, Lemmens M, Mayer KFX, Bérghès H, Adam G, Buerstmayr H** (2016) Suppressed recombination and unique candidate genes in the divergent haplotype encoding *Fhb1*, a major *Fusarium* head blight resistance locus in wheat. *Theoretical and Applied Genetics* **129**: 1607-1623
- Seifi HS, Van Bockhaven J, Angenon G, Hofte M** (2013) Glutamate metabolism in plant disease and defense: friend or foe? *Mol Plant Microbe Interact* **26**: 475-485
- Shah SH, Newgard CB** (2015) Integrated metabolomics and genomics: systems approaches to biomarkers and mechanisms of cardiovascular disease. *Circulation. Cardiovascular genetics* **8**: 410-419
- Sharma P, Gangola MP, Huang C, Kutcher HR, Ganeshan S, Chibbar RN** (2018) Single nucleotide polymorphisms in b-genome specific udp-glucosyl transferases associated with *Fusarium* head blight resistance and reduced deoxynivalenol accumulation in wheat grain. *Phytopathology* **108**: 124-132
- Siranidou E, Kang Z, Buchenauer H** (2002) Studies on symptom development, phenolic compounds and morphological defence responses in wheat cultivars differing in resistance to *Fusarium* head blight. *Journal of Phytopathology* **150**: 200-208
- Somssich IE, Hahlbrock K** (1998) Pathogen defence in plants — a paradigm of biological complexity. *Trends in Plant Science* **3**: 86-90
- Stanke M, Diekhans M, Baertsch R, Haussler D** (2008) Using native and syntenically mapped cDNA alignments to improve de novo gene finding. *Bioinformatics* **24**: 637-644
- Su Z, Bernardo A, Tian B, Chen H, Wang S, Ma H, Cai S, Liu D, Zhang D, Li T, Trick H, St. Amand P, Yu J, Zhang Z, Bai G** (2019) A deletion mutation in *TaHRC* confers *Fhb1* resistance to *Fusarium* head blight in wheat. *Nature Genetics* **51**: 1099-1105
- Su Z, Jin S, Zhang D, Bai G** (2018) Development and validation of diagnostic markers for *Fhb1* region, a major QTL for *Fusarium* head blight resistance in wheat. *Theor Appl Genet* **131**: 2371-2380
- Sutton PN, Gilbert MJ, Williams LE, Hall J** (2007) Powdery mildew infection of wheat leaves changes host solute transport and invertase activity. *Physiologia Plantarum* **129**: 787-795

- Tauzin AS, Giardina T** (2014) Sucrose and invertases, a part of the plant defense response to the biotic stresses. *Frontiers in plant science* **5**: 293
- Treutter D** (2005) Significance of flavonoids in plant resistance and enhancement of their biosynthesis. *Plant Biol (Stuttg)* **7**: 581-591
- Tzin V, Galili G** (2010) The biosynthetic pathways for shikimate and aromatic amino acids in arabidopsis thaliana. *Arabidopsis Book* **8**: e0132
- Venturini G, Toffolatti SL, Assante G, Babazadeh L, Campia P, Fasoli E, Salomoni D, Vercesi A** (2015) The influence of flavonoids in maize pericarp on fusarium ear rot symptoms and fumonisin accumulation under field conditions. *Plant Pathology* **64**: 671-679
- Voorrips RE** (2002) Mapchart: Software for the graphical presentation of linkage maps and qtls. *Journal of Heredity* **93**: 77-78
- Waldron BL, Moreno-Sevilla B, Anderson JA, Stack RW, Frohberg RC** (1999) RFLP mapping of QTL for Fusarium head blight resistance in wheat. *Crop Science* **39**: 805-811
- Walley JW, Kliebenstein DJ, Bostock RM, Dehesh K** (2013) Fatty acids and early detection of pathogens. *Current Opinion in Plant Biology* **16**: 520-526
- Wittstock U, Gershenzon J** (2002) Constitutive plant toxins and their role in defense against herbivores and pathogens. *Current opinion in plant biology* **5**: 300-307
- Xia J, Wishart DS** (2011) Metabolomic data processing, analysis, and interpretation using MetaboAnalyst. *Curr Protoc Bioinformatics* **Chapter 14**: Unit 14.10
- Xie GQ, Zhang MC, Chakraborty S, Liu CJ** (2007) The effect of 3BS locus of Sumai 3 on Fusarium head blight resistance in Australian wheats. *Australian Journal of Experimental Agriculture* **47**: 603-607
- Xiong H, Guo H, Xie Y, Zhao L, Gu J, Zhao S, Li J, Liu L** (2017) RNAseq analysis reveals pathways and candidate genes associated with salinity tolerance in a spaceflight-induced wheat mutant. *Scientific Reports* **7**: 2731
- Yamaguchi M, Mitsuda N, Ohtani M, Ohme-Takagi M, Kato K, Demura T** (2011) VASCULAR-RELATED NAC-DOMAIN7 directly regulates the expression of a broad range of genes for xylem vessel formation. *Plant J* **66**: 579-590
- Yu Y, Lv Y, Shi Y, Li T, Chen Y, Zhao D, Zhao Z** (2018) The role of phyto-melatonin and related metabolites in response to stress. *Molecules* **23**: 1887
- Zhang J, Xie M, Tuskan GA, Muchero W, Chen J-G** (2018) Recent advances in the transcriptional regulation of secondary cell wall biosynthesis in the woody plants. *Frontiers in Plant Science* **9**
- Zhao Q, Nakashima J, Chen F, Yin Y, Fu C, Yun J, Shao H, Wang X, Wang ZY, Dixon RA** (2013) Laccase is necessary and nonredundant with peroxidase for lignin polymerization during vascular development in Arabidopsis. *Plant Cell* **25**: 3976-3987
- Zhong R, Demura T, Ye ZH** (2006) SND1, a NAC domain transcription factor, is a key regulator of secondary wall synthesis in fibers of Arabidopsis. *Plant Cell* **18**: 3158-3170

Table 3.1 Resistance related induced (RRI) and resistance related constitutive (RRC) metabolites putatively identified upon *Fg* and mock inoculation in NILs rachis with resistant and susceptible QTL-Fhb1.

Sr. No.	Observed Mass (Da) ^a	Metabolite	Fold change	RR classification
Phenylpropanoids : Monolignols, Lignans, Lignan glucosides and flavonoids				
1	357.1359	Coniferyl ferulate	5.64***	RRI
2	579.2111	Podorhizol beta-D-glucoside	5.15**	RRI
3	210.0891	Sinapyl-alcohol	4.4**	RRI
4	540.1623	Cleistanthin A	3.59*	RRI
5	164.0473	4-coumaric acid	3.35***	RRI
6	238.0840	Sinapic acid methyl ester	2.99*	RRI
7	564.1068	Isorhamnetin 3-(6"-malonylglucoside)	2.53	RRI
8	206.0579	p-coumaroyldiketide	2.09*	RRI
9	356.1104	1-O-Feruloyl-beta-D-glucose	1.99**	RRI
10	654.1786	Iristectorigenin A 7-O-gentiobioside	1.94	RRI
11	372.1203	(+)-sesamolol	1.81***	RRI
12	580.2147	(+)-Syringaresinol O- β -D-glucoside	1.75	RRI
13	342.0970	Caffeic acid 3-glucoside	1.64*	RRI
14	726.2354	Naringenin 7-O-(2",6"-di-O-alpha-rhamnopyranosyl)-beta-glucopyranoside	1.55	RRI
15	520.1936	(-)-Pinoresinol glucoside	1.53**	RRI
16	414.1277	(-)-Podophyllotoxin	1.5*	RRI
Lipid biosynthesis				

^a Observed Mass: To the observed mass one H mass was added because the LC/MS analysis was done in negative ionization mode.

17	103.0409	3-hydroxybut-2-enoic acid	3.20	RRI
18	440.2766	PA(17:1(9Z)/0:0);1-(9Z-heptadecenoyl)-sn-glycero-3-phosphate	2.11*	RRI
19	592.2638	PI(18:4(6Z,9Z,12Z,15Z)/0:0)	2.10*	RRC
Terpenoids and alkaloids				
20	476.2724	Emetamine	2.27**	RRC
21	291.1624	Laurenobiolide	1.54**	RRI
22	522.2091	Isobrucein A	1.52*	RRI
23	376.1361	Loganate	1.49*	RRI
24	376.1516	Ailanthone	1.44**	RRI
Other metabolites (Glutamate metabolism, Tryptophan metabolism, Phenolic compounds)				
25	118.0239	Succinate	3.51***	RRC
26	249.1202	6-Hydroxymelatonin	2.50**	RRI
27	162.0571	Quinoline-3,4-diol	1.61**	RRI

Significance (Students *t*-test): * $P < 0.05$, ** $P < 0.01$, *** $P < 0.001$

Detailed compound identification is presented in Supp. Table 3.1. Fold change (FC) was calculated based on relative intensity of metabolites: RRC = RM/SM>1.0; RRI = (RP/RM>1.0)/(SP/SM>1.0), where RM = Resistant Mock; SM = Susceptible Mock; RP = Resistant Pathogen; RM = Resistant Mock. Note: ** significant at $P < 0.01$; *significant at $P < 0.05$; the significance of RRI was based on RP>RM and SP>SM.

Table 3.2 Genes located in the QTL-Fhb1 region derived from Sumai 3*5/Thatcher population flanking between markers XSTS3B-138 and XSTS3B-142.

Gene No. ^b	Wheat Ensembl ID	Genomic location	GenBank ID	Final Annotation ^c	Coverage (%)	E-value
#1	TraesCS3B02G000200	3B:218045-222328	AK455950.1	EXECUTER 2	0.97	0
#2	TraesCS3B02G019900	3B:8526623-8529426	CBH32655.1	Sarcoplasmic reticulum histidine-rich calcium-binding protein	0.9579	3E-157
#3	TraesCS3B02G022000	3B:9404342-9408751	AJ867398.1	Glycosyltransferase, HGA-like	0.94	0
#4	TraesCS3B02G022900	3B:9913916-9917749	FN564434.1	Glutamate decarboxylase	0.99	6E-115
#5	TraesCS3B02G023200	3B:9931500-9939414	FN564434.1	Polygalacturonase 3	0.98	0
#6	TraesCS3B02G023400	3B:10045662-10048767	FN564434.1	F-box like domain superfamily containing protein	0.97	0
#7	TraesCS3B02G024600	3B:10627150-10632531	FN564434.1	Phosphatidylserine synthase	1	1E-104
#8	TraesCS3B02G025200	3B:10953564-10957184	KY930446.1	Fructose-bisphosphate aldolase 1	1	3E-141
#9	TraesCS3B02G028500	3B:12302917-12305457	AF030420.1	Cell wall invertase	0.85	2E-151

^b Gene no. depict relative positions in the direction of markers STS3B-138 and STS3B-142.

^c Annotations were made based WheatEnsembl database and BlastN against *Triticum aestivum*.

#10	TraesCS3B02G030000	3B:13814087-13817475	AK447232.1	Uncharacterized protein	0.8	3E-108
#11	TraesCS3B02G030500	3B:13961374-13964727	U51330.1	Rust resistance kinase Lr10	0.85	0
#12	TraesCS3B02G034500	3B:16449576-16455782	AK335700.1	Ubiquitin-conjugating enzyme E2 conversed domain	0.98	0
#13	TraesCS3B02G084100	3B:52916105-52923537	MG560142.1	Putative disease resistance protein RGA3	0.83	2E-164
#14	TraesCS3B02G126200	3B:102594018-102599840	KY461076.1	NAC domain-containing protein 75	0.95	5E-62
#15	TraesCS3B02G126700	3B:103243031-103246106	AK334701.1	G-patch domain containing protein	0.98	0
#16	TraesCS3B02G175500	3B:177086624-177088975	AK452408.1	G-type lectin S-receptor-like serine/threonine-protein kinase (RKS1), LECRK1	0.97	0
#17	TraesCS3B02G194000	3B:214284139-214285430	AK455477.1	NAC transcription factor 32-like	0.81	3E-23
#18	TraesCS3B02G202200	3B:236195446-236197956	MG560141.1	Purple acid phosphatase	0.94	0
#19	TraesCS3B02G219900	3B:266563760-266567261	MG560141.1	Calmodulin TaCaM2-2	0.92	0
#20	TraesCS3B02G256300	3B:413958242-413960680	AK455595.1	Cytochrome P450 72A14-like	0.98	0
#21	TraesCS3B02G272100	3B:437908829-437915002	MG560141.1	Peroxidase 19-like	0.95	1E-135
#22	TraesCS3B02G273000	3B:439463486-439466300	EU660902.1	Acetyl-CoA carboxylase (Acc-1)	0.91	0

#23	TraesCS3B02G275700	3B:445592555-445595475	MG560141.1	Violaxanthin de-epoxidase (VDE) domain containing protein	0.91	7E-65
#24	TraesCS3B02G297300	3B:476944285-476946311	AK448685.1	WD40 repeat domain containing protein	0.99	0
#25	TraesCS3B02G299800	3B:481595302-481606660	FN564429.1	Glutamate synthase 1 (GLT1)	0.98	1E-130
#26	TraesCS3B02G327500	3B:528138893-528147684	DQ086483.1	1,3-beta-glucan synthase	0.98	0
#27	TraesCS3B02G327600	3B:528172449-528177761	FJ436983.1	DUF1421 domain containing protein	0.92	0
#28	TraesCS3B02G328800	3B:531210808-531213439	HF541871.1	Potassium channel KAT3-like	0.91	0
#29	TraesCS3B02G331400	3B:536433922-536438211	FJ830847.1	Heat shock protein 70	0.97	0
#30	TraesCS3B02G333100	3B:539559841-539561616	HM236489.1	UDP-arabinopyranose mutase 1-like	0.85	2E-120
#31	TraesCS3B02G341500	3B:548046061-548050821	AK455728.1	Beta-glucosidase BoGH3B-like	0.98	0
#32	TraesCS3B02G392600	3B:618148246-618151575	MG560140.1	Scarecrow-like protein 9	0.87	6E-152
#33	TraesCS3B02G392700	3B:618154243-618157461	AK331516.1	Laccase-4-like	0.99	0
#34	TraesCS3B02G425700	3B:663573757-663574893	HE996279.1	Protein PELOTA 1-like	0.97	0
#35	TraesCS3B02G497800	3B:741463238-741466391	HQ702206.1	NB-ARC domain-containing protein	0.93	0

#36	TraesCS3B02G517000	3B:760051120- 760055994	FN564434.1	Two-component response regulator ORR25-like	0.94	0
#37	TraesCS3B02G566400	3B:798408352- 798408783	FN564426.1	SKP1-like protein	0.95	3E-107

Table 3.3 List of primers used in the gene expression study.

Designate d Gene no.	Gene/Primer Name	Forward primer (5'-3')	Reverse primer (5'-3')
gene # 1	EXECUTER 2	AAACATGGCATTGTTGTTCC	GGTCTCGCCCGACATATCTA
gene #2	Sarcoplasmic reticulum histidine-rich calcium-binding protein	ACTCTGTGACGGCAATGTTT	AGAGCCGGAGACAGTAACAT
gene # 3	Glycosyltransferase, HGA-like	GTGAGGGATGACGACACAGA	CCATAAAATGCCCCGAATC
gene #4	Glutamate decarboxylase	TGGCCGTGCTTTGTTTTAAC	GCTCTTGACAGTTCACATACG
gene # 5	Polygalacturonase 3	TGGGGTGAAGCTAATGTGGT	ACATCTGCAATCGCTCTAACC
gene # 6	F-box like domain superfamily containing protein	GGGCCCTGCCAGTTGTAATTT	TTGAAATGCACAGATCAGCA
gene # 7	Phosphatidylserine synthase	GCCACACCATTCTTTTCTC	ACCGATCAATGGCCTACTG
gene # 8	Fructose-bisphosphate aldolase 1	TTCGGCCTATACCCCTAGAA	TACTTCGCAAAAACGCAACA
gene # 9	Cell wall invertase	CACGGAAACATGGGAATGAAT	GGGACATAAACTGATCTGCAA
gene # 10	Uncharacterized protein	CCGTACATGGTTTGGTTGAG	TGCATCCAGAGGTTATTGGA
gene # 11	Rust resistance kinase Lr10	CCGTCAGGCAGGTACATATT	TCAGGTGGTAATAGAGTGGAA
gene # 12	Ubiquitin-conjugating enzyme E2 conversed domain	AAGCTTTGTGGGTTTGTGTT	CTGCATCTCTACCCTTGGAAAT
gene # 13	Putative disease resistance protein RGA3	GCCGTATTCTTCCTGTACA	AGCAAGTAAGTGGAAAGTGGAT
gene # 14	NAC domain-containing protein 75	CAAATGTGTCTTGCGAGCAT	ACCGAGTTCATGTTGAAATG
gene # 15	G-patch domain containing protein	CAAATGTGTCTTGCGAGCAT	ACCGAGTTCATGTTGAAATG

gene # 16	G-type lectin S-receptor-like serine/threonine-protein kinase (RKS1), LECRK1	AGTCACTTGTTGCTGAGTTG	TTGCTCATTCCGTAGAGAGTT
gene # 17	NAC transcription factor 32-like	TCGACCAGTGTGAGTAGAGT	GAAGCTGCACTGATTGAGAA
gene # 18	Purple acid phosphatase	TTGTGATCGAAGCCAACTCT	GCCTTTCATGCTACCTCACA
gene # 19	Calmodulin TaCaM2-2	CGACCTGTCTGGGTAAGTT	CCCAGTTTCAGGATCAAATG
gene # 20	Cytochrome P450 72A14-like	ATCTTGCTTTCGGCTTTG	CCCAGTTTCAGGATCAAATGA
gene # 21	Peroxidase 19-like	TCCCTTACAGTGCCTTCAA	TGCAATCGGATCCTACCATT
gene # 22	Acetyl-CoA carboxylase (Acc-1)	GGCATTTTACCAGAAGCATGA	CAGAAGGTATACACTGCATAG AA
gene # 23	Violaxanthin de-epoxidase (VDE) domain containing protein	GGGCAATTCTTTTCCCAACT	AACGTCGACCTCCCAATTAC
gene # 24	WD40 repeat domain containing protein	TGGTAAAACGGCTGTGGTAT	GCGGCTAAGACACAGATAGT
gene # 25	Glutamate synthase 1 (GLT1)	TTGGGCTCAATAGGGAAAGA	CCAACAAACAATAGCCAACCA
gene # 26	1,3-beta-glucan synthase	TGGCGATTTATGCATTGAGT	ATCAGAACTCACGGGTAAGC
gene # 27	DUF1421 domain containing protein	TGCCGTCTATTGATTCTGTCC	TCACCGTAATCCAGTTGTGC
gene # 28	Potassium channel KAT3-like	CAAAATGATCTGGGGACTGG	CGGGGTCTTGGACACTTAAA
gene # 29	Heat shock protein 70	AGGGATCTTGTTGGCTGTAA	ACGCTAGTTCAACCAAGTCA
gene # 30	UDP-arabinopyranose mutase 1-like	ATACCGGTTTCTTCAGTTCGT	ACGGCAGCTAATGTTTTGTAG
gene # 31	Beta-glucosidase BoGH3B-like	TTCACCGCTAATCTGCTCTT	CAGGGAACAATGTCCATGTG
gene # 32	Scarecrow-like protein 9	TTAGCATTTTTGGTGGAGCA	CAACCAAGCAAATGAAAAAGG
gene # 33	Laccase-4-like	GTTTAATTTGCGCCCCTCAT	ACGGGCTAAACACACTACAA
gene # 34	Protein PELOTA 1-like	CACTTATTTCTGTTATACCAAG CA	CACCACATGCTAGCAATTCT
gene # 35	NB-ARC domain-containing protein	GTTGTCCAGCTTTGGAGGAA	TGCATCGTCTTTTCAACTCC
gene # 36	Two-component response regulator ORR25-like	GGGGCTCTTTAAGGCAATA	TGCAGAACACGTCAATTCTCA
gene # 37	SKP1-like protein	TTTTCACTGGACTCTGTGACG	GCAGAGCCGGAGACAGTAAC

Table 3.4 List of candidates possessing multiple genomic variants based on SNP variant analysis.

3BSTR_Predicted_Genes	Position	3BSTR	3BSTS_Variant_Base	Position	3BSTR	3BSTS_Variant_Base	Position	3BSTR	3BSTS_Variant_Base
Gene #8	2423	G	A	2720	G	A	3029	T	G
	2441	T	C	2733	G	A	3077	T	C
	2611	G	A	2746	T	C	3999	A	C
	2617	T	C	2757	A	C	4029	C	T
	2646	G	T	2849	A	G	4035	G	T
	2673	C	T	2987	T	G			
	2361	T	G						
Gene #12	1048	A	G	1544	A	G	439	G	A
	1051	G	A	1546	A	G	499	G	A
	1096	G	C	1615	A	G	177	T	C
	1139	T	C	1625	G	A	2218	T	C
	1204	G	A	1637	G	A	2239	G	A
	1387	G	A	1266	C	T	381	T	C
	1017	A	G	1516	AGTA CGTA	AGTA	1326	T	C
Gene #16	1083	A	G	447	G	A	1350	C	T
	1119	G	A	486	A	T	1404	G	A
	1122	G	C	596	G	C	804	C	T
	839	G	A						
	6706	A	G	7276	C	T	7885	G	A
Gene #25	6792	A	G	7385	CT	CTCTT	7938	G	C
	6821	ATT	AT	7412	T	C	8014	C	T

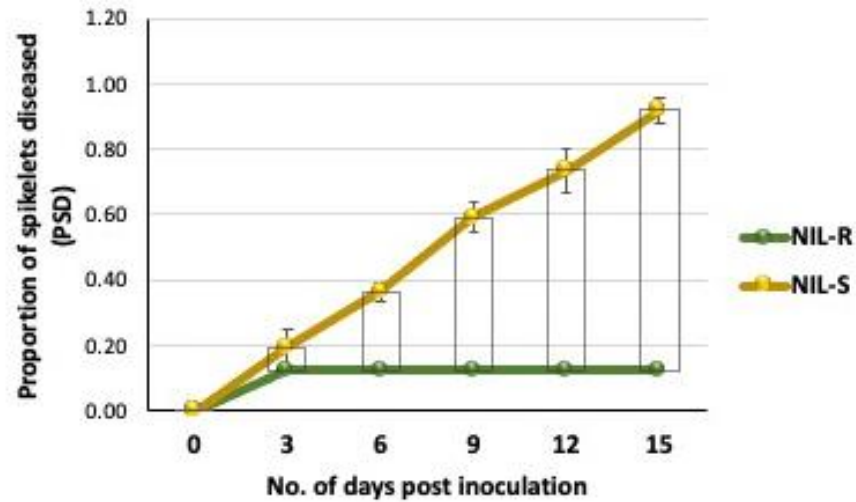
	6879	TCCC	TC	7419	C	T	8030	C	T
	6893	GCTCTCTCTCTCTCTCTCT,G CTCTCTCTCTCTCTCT	GCTCTCTCTCTCT CTCTCTCTCT	7559	G	A	8037	ACTC CTC	ACTC
	8133	C	T	8153	C	T	8225	T	C
Gene #28	2010	GTGGAGT	G	2740	C	A	2449	T	C
	2111	G	C	2231	C	T	2453	A	C
	2120	C	T	2237	G	A	2462	A	C
	2149	A	G	2270	A	G	2469	G	A
	2156	T	A	2316	C	T	2472	C	T
	2163	A	G	2348	G	A	2485	C	T
	2387	CAAAAA	CAAAA						
Gene #31	3154	A	AG	3681	A	G	4137	A	C
	3152	A	G	3708	A	G	4173	G	A
	3209	A	T	3718	A	C	4213	C	T
	3296	C	T	3727	T	C	4218	CTT	CT
	3375	G	A	3745	C	T	4219	TTAC	T
	3399	G	A	4038	T	C	4249	G	T
	3446	A	G	4049	A	G	4276	T	C
	3477	G	C	4067	T	C	4446	G	A
	3561	G	A	4072	C	A	4452	T,A	G
	3642	G	A	4131	G	A	4469	G	C
Gene #32	1005	C	T	1287	T	C	1827	C	A
	1047	C	T	1340	T	C	1899	G	A
	1062	T,C	G	1461	C	T	1903	G	C
	1086	C	T	1504	A	C	1928	C	A
	1122	T	A	1602	T	C	1956	G	A

	1134	C	T	1680	C	T	1999	A	G
	1173	C	G	1740	T	C	2061	T	C
	1182	G	C	1797	A	G	2067	ATCC T	AT
Gene #33	2315	A	G	2320	G	C	2321	C	G
Gene #17	464	A		1245	T	C			
Gene #26	1158	A	G	1512	G	T	2394	G	A
	1170	C	T	1557	G	A	2601	A	C
	1209	A	G	1659	G	A	2691	T	C
	1242	G	A	1851	A	G	2763	A	G
	1266	T	C	1956	A	C	2842	A	G
	1269	A	G	2107	G	T	2907	G	C
	1329	G	C	2214	A	G	2929	A	C
	1344	G	A	2252	A	C	3003	T	C
	1362	T	C	2335	A	G	3072	T	C
	1374	A	G	2354	G	A	3134	TGCA	T

Figure 3.1 Phenotyping of NILs differing at QTL-Fhb1. (a) NILs varying in FHB resistance following inoculation of one pair of spikelets in the mid-region of spike with *F. graminearum* (*Fg*) spore suspension, at 12 dpi. The rachis in NIL-R shows only necrotic spots or diseased symptoms limited to the inoculated spikelet, while in S-RIL the complete spike showed bleaching and diseased symptoms at 12 dpi; (b) Disease severity analysis in NILs, based on visual observations of proportion of spikelets diseased (PSD).



(a)



(b)

Figure 3.2 Gene ontology (GO) term enrichment analysis. The GO annotation results were based on 37 putative candidate genes identified based on a paired-end Illumina HiSeq™ 2500 platform. The top eight GO terms enriched in genes identified in QTL-Fhb1 are based on the lowest over-represented p values. Circles in closer proximity have GO terms that are more closely related. The size of the circle indicates the number of related genes involved in the same: (a) biological process and ;(b) molecular functions. The color of the circle depicts the statistical significance of the enriched GO terms based on the over-represented p-value.

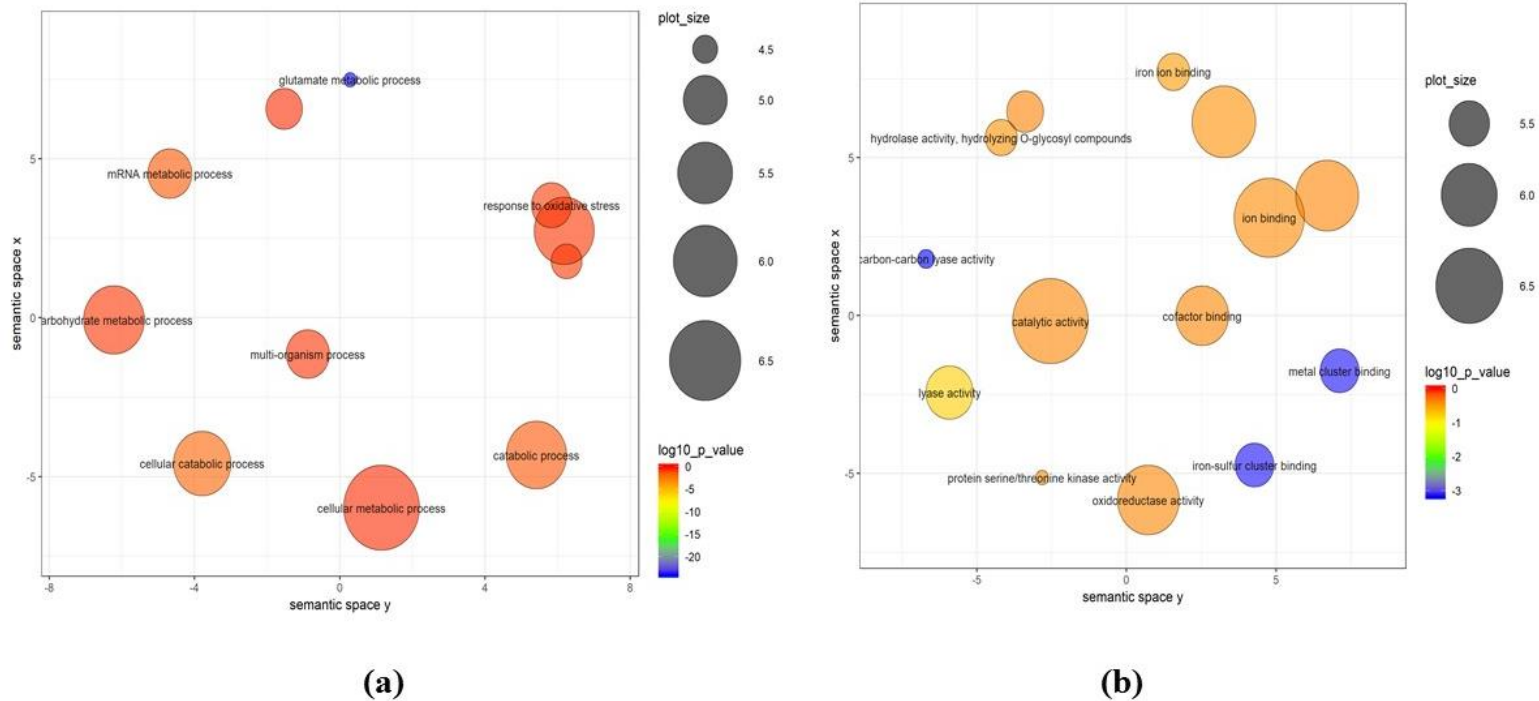
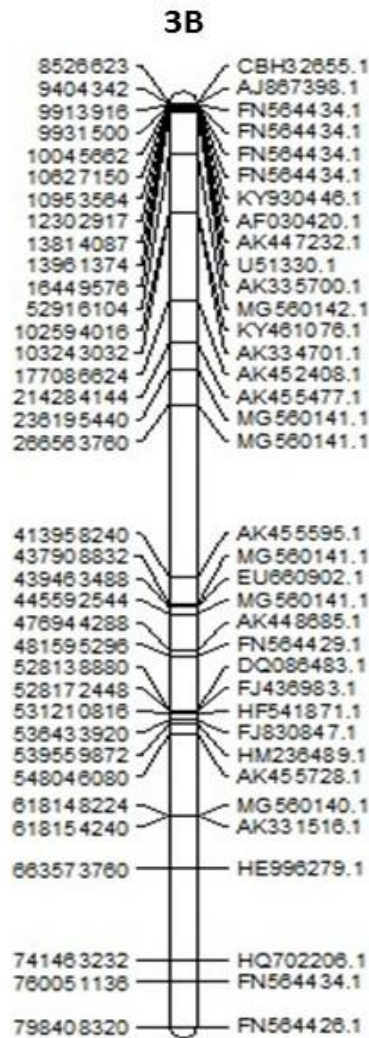
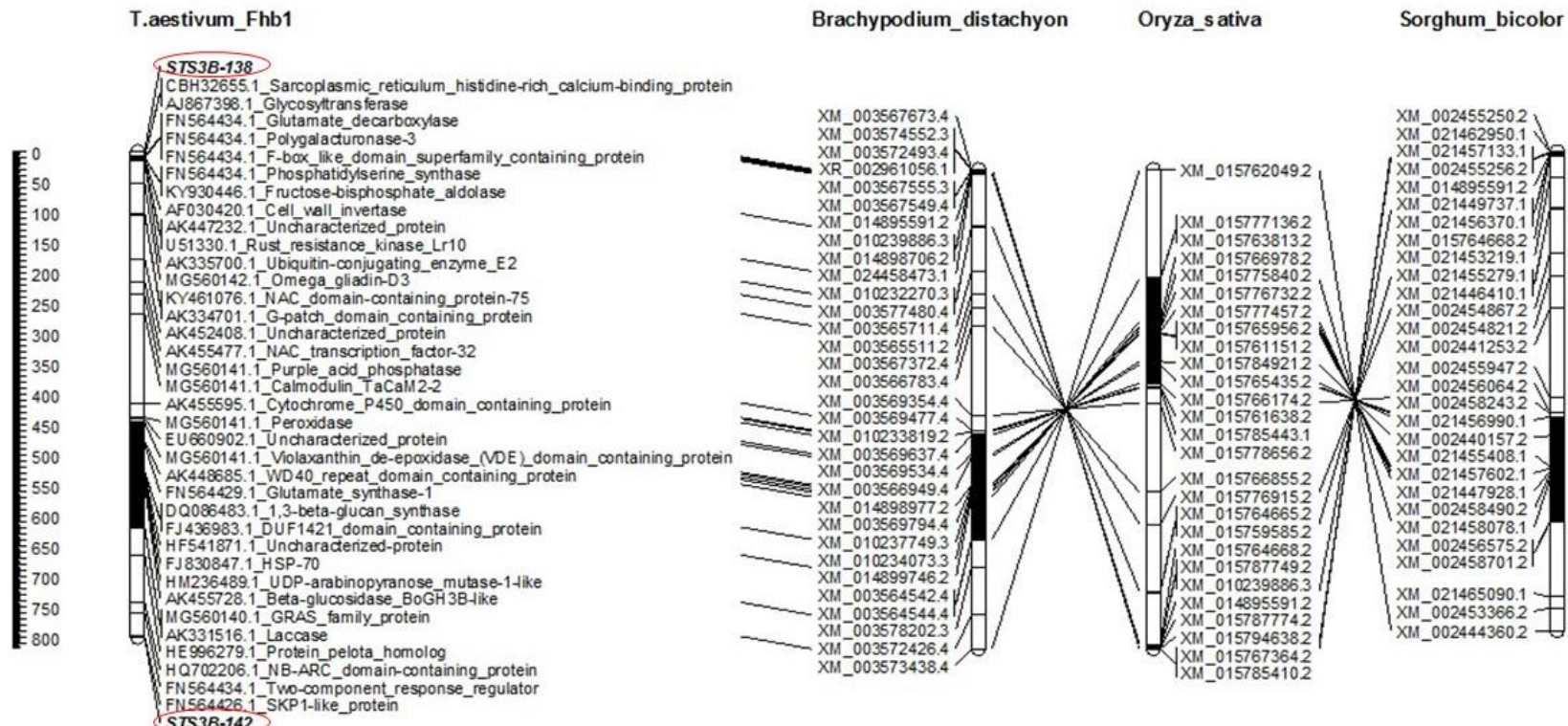


Figure 3.3 Comparative mapping of chromosome 3B linkage map with the corresponding 3B physical bin map and novel genes underlying QTL-Fhb1 between XSTS3B-138 and XSTS3B-142 flanking markers. (a) The linkage map displays gene order and the relative distances of the genes on the 3BS chromosome flanking between STS3B-138 and STS3B-142 markers; (b) The orthologous genes on different chromosomes in the related species such as *Oryza sativa*, *Sorghum bicolor*, and *Brachypodium distachyon*. Left side for genetic map=linkage distance (cM); Left side for gene predicted= NCBI IDs.



(a)



(b)

Figure 3.4 Heatmap of differentially expressed genes. The expression levels of putative candidate genes are represented in resistant NILs and susceptible NILs, both in mock and pathogen inoculated samples. The rows represent putative candidate genes, whereas columns depict different treatment groups. The two dendrograms are shown at the top and left sides.

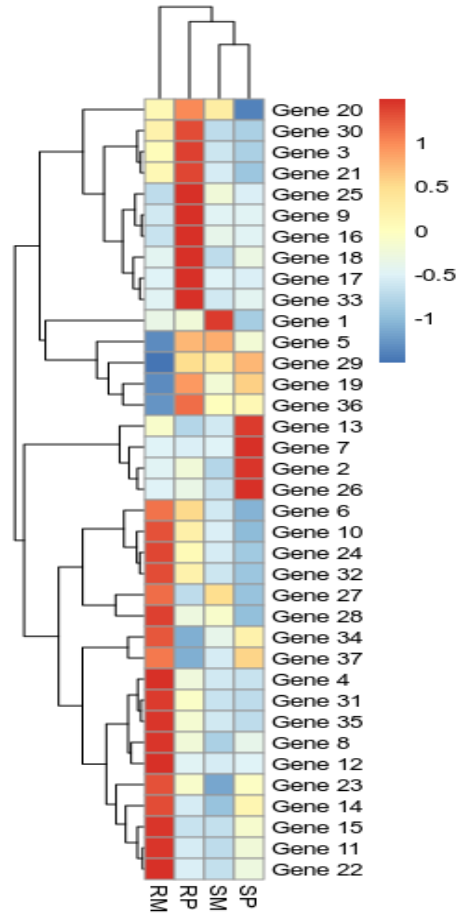
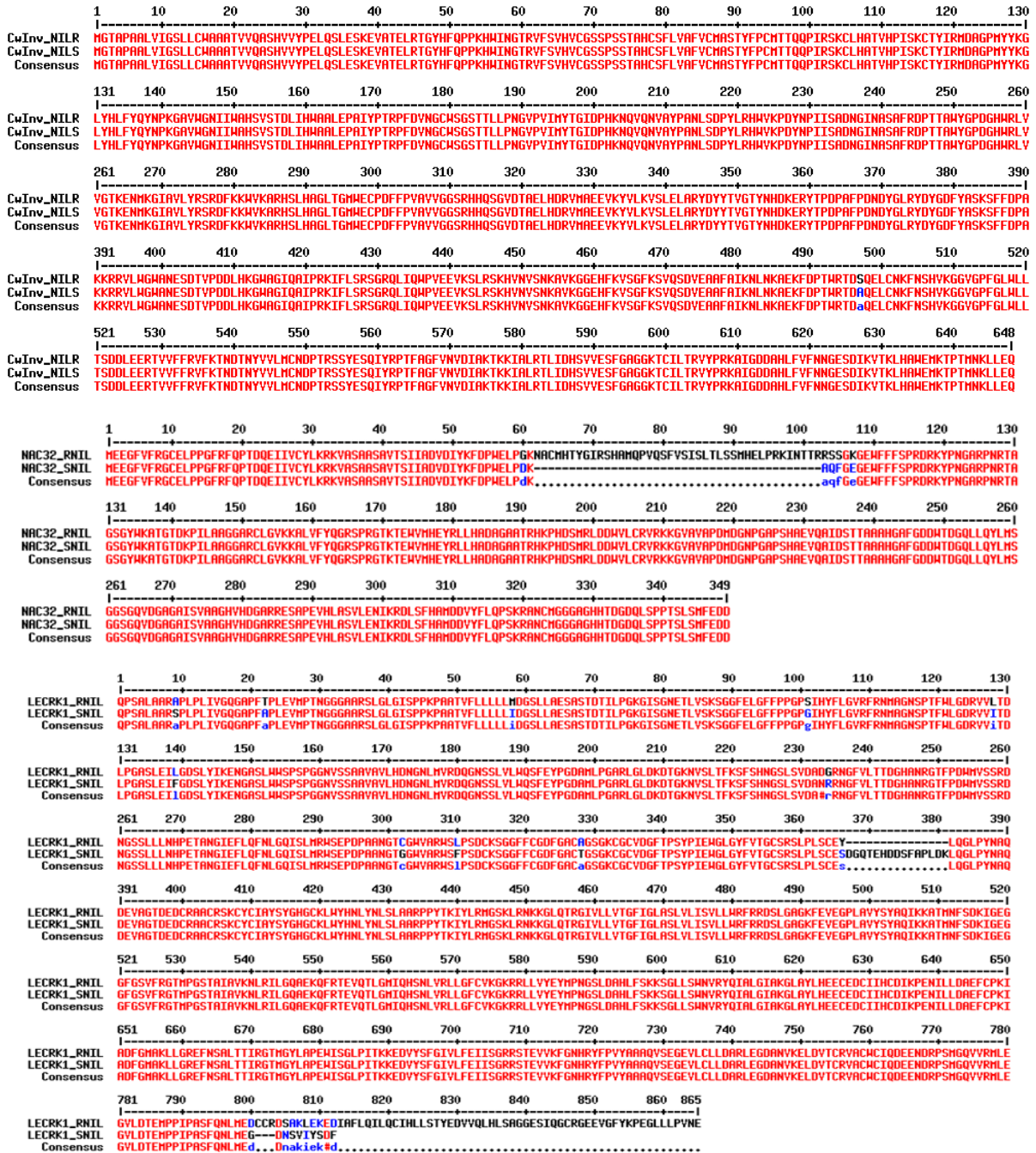


Figure 3.5 MultAlin software based amino acid sequence alignment of resistant and susceptible NIL. CwInv, NAC32-like, LECRK1, Laccase-4-like, *TaHRC*, FBA1, Ubiquitin, KAT3, and SCL9 were identified with multiple allelic variations at the protein level.



1 10 20 30 40 50 60 70 80 90 100 110 120 130
Ubiquitin_RNII
Ubiquitin_SNIIL
Consensus
MENLPHVPSAIEKKNQNETSDADAGEPEEYADVFYVREDDVYSLKSNKARGLVMEVAGEYDSEGSITDDESDRENERKSRHKTENVYVGGDANANRSHGDDVVESSQLPDKVKRVLIDGTEHTEDIDS
MENLPHVPSAIEKKNQNETSDADAGEPEEYADVFYVREDDVYSLKSNKARGLVMEVAGEYDSEGSITDDESDRENERKSRHKTENVYVGGDANANRSHGDDVVESSQLPDKVKRVLIDGTEHTEDIDS
MENLPHVPSAIEKKNQNETSDADAGEPEEYADVFYVREDDVYSLKSNKARGLVMEVAGEYDSEGSITDDESDRENERKSRHKTENVYVGGDANANRSHGDDVVESSQLPDKVKRVLIDGTEHTEDIDS

131 140 150 160 170 180 190 200 210 220 230 240 250 260
Ubiquitin_RNII
Ubiquitin_SNIIL
Consensus
VYVYVORTFLHGDHVASSDPTGQMGLVADVSLAYDLQGAHGEHIKGVSAKDLRRITREFNVGDYVYVSGLALGRVDEVFQNVSVLFDGGSVCKVSRADPRLRLASGPHHPDITACFPYVGGVYKRVSSVYK
VYVYVORTFLHGDHVASSDPTGQMGLVADVSLAYDLQGAHGEHIKGVSAKDLRRITREFNVGDYVYVSGLALGRVDEVFQNVSVLFDGGSVCKVSRADPRLRLASGPHHPDITACFPYVGGVYKRVSSVYK
VYVYVORTFLHGDHVASSDPTGQMGLVADVSLAYDLQGAHGEHIKGVSAKDLRRITREFNVGDYVYVSGLALGRVDEVFQNVSVLFDGGSVCKVSRADPRLRLASGPHHPDITACFPYVGGVYKRVSSVYK

261 270 280 290 300 310 320 330 340 350 360 370 380 390
Ubiquitin_RNII
Ubiquitin_SNIIL
Consensus
TSRHLHGAKASRLERATYTKVETRAAYIYVHIASAHCGTNDQSVPEEQNKDILLSCFSYASHQLAECHPOPHITSSCANDALMECSKMKELNSEQADVPESAVDVAEQAGQNTKTQVNPLEKHGDSLA
TSRHLHGAKASRLERATYTKVETRAAYIYVHIASAHCGTNDQSVPEEQNKDILLSCFSYASHQLAECHPOPHITSSCANDALMECSKMKELNSEQADVPESAVDVAEQAGQNTKTQVNPLEKHGDSLA
TSRHLHGAKASRLERATYTKVETRAAYIYVHIASAHCGTNDQSVPEEQNKDILLSCFSYASHQLAECHPOPHITSSCANDALMECSKMKELNSEQADVPESAVDVAEQAGQNTKTQVNPLEKHGDSLA

391 400 410 420 430 440 450 460 470 480 490 500 510 520
Ubiquitin_RNII
Ubiquitin_SNIIL
Consensus
DRSNHSDGMDTCVHKDSESGASVSLPKEGVHDHATYRKKIRKVFYRKKRKRKRDESFESALLISDITYTKVDVLDQGRKECGVSSLSLIPITQTPMDHEFFPEQYRVEKYSDDVDQPSERRVGLVRSY
DRSNHSDGMDTCVHKDSESGASVSLPKEGVHDHATYRKKIRKVFYRKKRKRKRDESFESALLISDITYTKVDVLDQGRKECGVSSLSLIPITQTPMDHEFFPEQYRVEKYSDDVDQPSERRVGLVRSY
DRSNHSDGMDTCVHKDSESGASVSLPKEGVHDHATYRKKIRKVFYRKKRKRKRDESFESALLISDITYTKVDVLDQGRKECGVSSLSLIPITQTPMDHEFFPEQYRVEKYSDDVDQPSERRVGLVRSY

521 530 540 550 560 570 580 590 600 610 620 630 640 650
Ubiquitin_RNII
Ubiquitin_SNIIL
Consensus
NKKRTVSVSHKSSSLHAEQPREIECTEVYSAYELDGHDPDYCYGVVYVRLPSVSHPESSNGGNTHELKKNVDESEARSASNAVPPDVAEEQLSQKESSEVTHLSVGVNIVFGQDGEIEVTHGDS
NKKRTVSVSHKSSSLHAEQPREIECTEVYSAYELDGHDPDYCYGVVYVRLPSVSHPESSNGGNTHELKKNVDESEARSASNAVPPDVAEEQLSQKESSEVTHLSVGVNIVFGQDGEIEVTHGDS
NKKRTVSVSHKSSSLHAEQPREIECTEVYSAYELDGHDPDYCYGVVYVRLPSVSHPESSNGGNTHELKKNVDESEARSASNAVPPDVAEEQLSQKESSEVTHLSVGVNIVFGQDGEIEVTHGDS

651 660 670 680 690 700 710 720 730 740 750 760 770 780
Ubiquitin_RNII
Ubiquitin_SNIIL
Consensus
VSKYVGHPIYVYVREDDGGSIDGAPSDAGSMEYVDNEMDLDDPANDLQNAVQNSIEHENGFSNQDETSVSGSPLSVAFGFVTRLASEIFARGKKHLGDSMDAHEVESQSQNEVSESGDDTKN
VSKYVGHPIYVYVREDDGGSIDGAPSDAGSMEYVDNEMDLDDPANDLQNAVQNSIEHENGFSNQDETSVSGSPLSVAFGFVTRLASEIFARGKKHLGDSMDAHEVESQSQNEVSESGDDTKN
VSKYVGHPIYVYVREDDGGSIDGAPSDAGSMEYVDNEMDLDDPANDLQNAVQNSIEHENGFSNQDETSVSGSPLSVAFGFVTRLASEIFARGKKHLGDSMDAHEVESQSQNEVSESGDDTKN

781 790 800 810 820 830 840 850 860 870 880 890 900 910
Ubiquitin_RNII
Ubiquitin_SNIIL
Consensus
EDENRHSSESTVYTTNDSNAEKSVYVHADEPADSCLKHFQVLCQPPDHYLELNIAGTGGKRVKVKYQOEHGILEKNDPDIYVYVFEEDRMLNRVYIGASGTPYQDGLFFDFVLPPEFPQAPP
EDENRHSSESTVYTTNDSNAEKSVYVHADEPADSCLKHFQVLCQPPDHYLELNIAGTGGKRVKVKYQOEHGILEKNDPDIYVYVFEEDRMLNRVYIGASGTPYQDGLFFDFVLPPEFPQAPP
EDENRHSSESTVYTTNDSNAEKSVYVHADEPADSCLKHFQVLCQPPDHYLELNIAGTGGKRVKVKYQOEHGILEKNDPDIYVYVFEEDRMLNRVYIGASGTPYQDGLFFDFVLPPEFPQAPP

911 920 930 940 950 960 970 980 990 1000 1010 1020 1030 1040
Ubiquitin_RNII
Ubiquitin_SNIIL
Consensus
AYYHSGGLRVNPNLYVDGKGLVLEKPYFNEAGYEKQVGTVEGEKALPYNENTYLLSVKSHLYLRRPPHNFEDVKSFKCKRGHYLILKACEAYLQGVAVVGLNDACPPDTDTKEYSCSHGFKLALGK
AYYHSGGLRVNPNLYVDGKGLVLEKPYFNEAGYEKQVGTVEGEKALPYNENTYLLSVKSHLYLRRPPHNFEDVKSFKCKRGHYLILKACEAYLQGVAVVGLNDACPPDTDTKEYSCSHGFKLALGK
AYYHSGGLRVNPNLYVDGKGLVLEKPYFNEAGYEKQVGTVEGEKALPYNENTYLLSVKSHLYLRRPPHNFEDVKSFKCKRGHYLILKACEAYLQGVAVVGLNDACPPDTDTKEYSCSHGFKLALGK

1041 1050 1060 1071
Ubiquitin_RNII
Ubiquitin_SNIIL
Consensus
ILPRLITALKDIGDCSQEHLGKETAQES
ILPRLITALKDIGDCSQEHLGKETAQES
ILPRLITALKDIGDCSQEHLGKETAQES

1 10 20 30 40 50 60 70 80 90 100 110 120 130
SCL9_RNII
SCL9_SNIIL
Consensus
TAQAPALVHEHARPAVPSLSLLPYRRAQSPGQTHYRNFHGAPRAPSVMHSIHVRRPTISAPPVAGHPLRVSSPGRWTERTTQGHARVGYDTSADSPGRRRARAPIPRLSKTAPRLHFPFFILPL
TAQAPALVHEHARPAVPSLSLLPYRRAQSPGQTHYRNFHGAPRAPSVMHSIHVRRPTISAPPVAGHPLRVSSPGRWTERTTQGHARVGYDTSADSPGRRRARAPIPRLSKTAPRLHFPFFILPL
TAQAPALVHEHARPAVPSLSLLPYRRAQSPGQTHYRNFHGAPRAPSVMHSIHVRRPTISAPPVAGHPLRVSSPGRWTERTTQGHARVGYDTSADSPGRRRARAPIPRLSKTAPRLHFPFFILPL

131 140 150 160 170 180 190 200 210 220 230 240 250 260
SCL9_RNII
SCL9_SNIIL
Consensus
LALPKLGHPPPLSPLPPLSGPLRYAPSELVGPVRYLTPRGRLEYLSALITATLCHLGGGGGGVSHVNDRALHDSGLPGLGKLPITYQIPDVFTRAEELSLLLFPDGDADAYLARAAPPPLPSP
LALPKLGHPPPLSPLPPLSGPLRYAPSELVGPVRYLTPRGRLEYLSALITATLCHLGGGGGGVSHVNDRALHDSGLPGLGKLPITYQIPDVFTRAEELSLLLFPDGDADAYLARAAPPPLPSP
LALPKLGHPPPLSPLPPLSGPLRYAPSELVGPVRYLTPRGRLEYLSALITATLCHLGGGGGGVSHVNDRALHDSGLPGLGKLPITYQIPDVFTRAEELSLLLFPDGDADAYLARAAPPPLPSP

261 270 280 290 300 310 320 330 340 350 360 370 380 390
SCL9_RNII
SCL9_SNIIL
Consensus
ASASGSSPPDRALVSSPARRAARAGQAQPDSEVSDIYLGYINRMLHREIDIEKFDHYPHQALILRAEKPFLEILADQPPCSGGSTVESPDGSSATINSFNSLATCNCAPSSGGLRAMQAPPALEFPT
ASASGSSPPDRALVSSPARRAARAGQAQPDSEVSDIYLGYINRMLHREIDIEKFDHYPHQALILRAEKPFLEILADQPPCSGGSTVESPDGSSATINSFNSLATCNCAPSSGGLRAMQAPPALEFPT
ASASGSSPPDRALVSSPARRAARAGQAQPDSEVSDIYLGYINRMLHREIDIEKFDHYPHQALILRAEKPFLEILADQPPCSGGSTVESPDGSSATINSFNSLATCNCAPSSGGLRAMQAPPALEFPT

391 400 410 420 430 440 450 460 470 480 490 500 510 520
SCL9_RNII
SCL9_SNIIL
Consensus
REFLQPPQFYQDLIPESCVYVAGGAPYDAHEFNPLDRLSQSSSFASNGSSVAFSEGFEPNLSTGRGVDPDGLSDYVLSQQAARSRGFEESGRFLPQESKLVLDVON
REFLQPPQFYQDLIPESCVYVAGGAPYDAHEFNPLDRLSQSSSFASNGSSVAFSEGFEPNLSTGRGVDPDGLSDYVLSQQAARSRGFEESGRFLPQESKLVLDVON
REFLQPPQFYQDLIPESCVYVAGGAPYDAHEFNPLDRLSQSSSFASNGSSVAFSEGFEPNLSTGRGVDPDGLSDYVLSQQAARSRGFEESGRFLPQESKLVLDVON

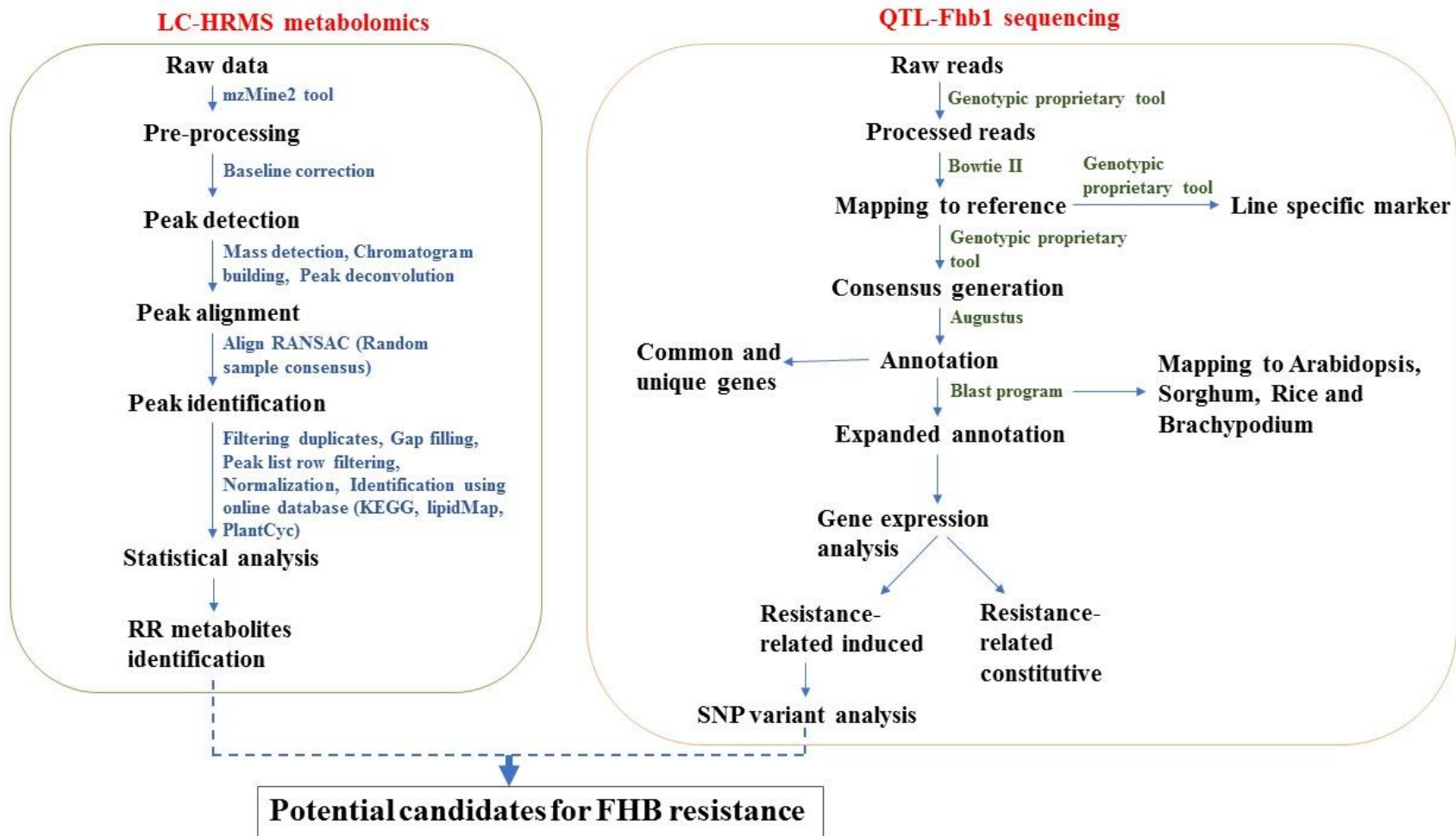
521 530 540 550 560 570 580 590 600 610 620 630 640 650
SCL9_RNII
SCL9_SNIIL
Consensus
KADREVAIHRGKHFYGOOLDADAEVRCCKHSAPVVDVHLVREHMOKHDVRAQSGGAGKGGSGKGRGKQVQPKKVEVDLETLIHFAQSVSIDDRRSATOLLKQI
KADREVAIHRGKHFYGOOLDADAEVRCCKHSAPVVDVHLVREHMOKHDVRAQSGGAGKGGSGKGRGKQVQPKKVEVDLETLIHFAQSVSIDDRRSATOLLKQI
KADREVAIHRGKHFYGOOLDADAEVRCCKHSAPVVDVHLVREHMOKHDVRAQSGGAGKGGSGKGRGKQVQPKKVEVDLETLIHFAQSVSIDDRRSATOLLKQI

651 660 670 680 690 700 710 720 730 740 750 760 770 780
SCL9_RNII
SCL9_SNIIL
Consensus
RQHASANGDGDRLAHCFANGLERLARGNSQIYKLTISRFACADILKAYQLVLRACPFKIKSHYFANQITNHAVEKAKKYNIVDFGVYVGFQWPLIQRLSKRPGGPELRIITAITDPPGFPRAERI
RQHASANGDGDRLAHCFANGLERLARGNSQIYKLTISRFACADILKAYQLVLRACPFKIKSHYFANQITNHAVEKAKKYNIVDFGVYVGFQWPLIQRLSKRPGGPELRIITAITDPPGFPRAERI
RQHASANGDGDRLAHCFANGLERLARGNSQIYKLTISRFACADILKAYQLVLRACPFKIKSHYFANQITNHAVEKAKKYNIVDFGVYVGFQWPLIQRLSKRPGGPELRIITAITDPPGFPRAERI

781 790 800 810 820 830 840 850 860 870 880 890 900 910
SCL9_RNII
SCL9_SNIIL
Consensus
EEIGRYLSDYATQTKVFPFKYHGISQFEAVRVEDLHIEKDEILLVNSHFRFKTLHDESVVAFSPRNMYLNTIRKHKPHVFIHGVYNGSYNAPFFVSRFREALFQSAHFHLEANIIPRONEERLLIESTI
EEIGRYLSDYATQTKVFPFKYHGISQFEAVRVEDLHIEKDEILLVNSHFRFKTLHDESVVAFSPRNMYLNTIRKHKPHVFIHGVYNGSYNAPFFVSRFREALFQSAHFHLEANIIPRONEERLLIESTI
EEIGRYLSDYATQTKVFPFKYHGISQFEAVRVEDLHIEKDEILLVNSHFRFKTLHDESVVAFSPRNMYLNTIRKHKPHVFIHGVYNGSYNAPFFVSRFREALFQSAHFHLEANIIPRONEERLLIESTI

911 920 930 940 950 960 970 980 990 999
SCL9_RNII
SCL9_SNIIL
Consensus
FSREAINVISCEGHERMERPEYTKQAVRNQARAFKQLPLDQETAKRAREKVKCYHKNFIIIDENGGALLGKHKGRILYALSTKANPQF
FSREAINVISCEGHERMERPEYTKQAVRNQARAFKQLPLDQETAKRAREKVKCYHKNFIIIDENGGALLGKHKGRILYALSTKANPQF
FSREAINVISCEGHERMERPEYTKQAVRNQARAFKQLPLDQETAKRAREKVKCYHKNFIIIDENGGALLGKHKGRILYALSTKANPQF

Figure 3.6 The workflow of combined metabolo-genomics approach to identify potential FHB resistance genes in wheat NILs.



CONNECTING STATEMENT FOR CHAPTER IV

In the previous Chapter III, we have identified five novel candidates for FHB resistance based on a combined metabolo-genomics approach. These include cell wall invertase, G-type lectin S-receptor-like serine/threonine-protein kinase (RKS1), NAC transcription factor 32-like, glutamate synthase 1, and laccase-4-like. As hypothesized, these genes were associated with differential accumulation of RR metabolites, gene sequence and gene expression. Lignification is a common defense mode against pathogens during plant-microbe interactions (Vance et al., 1980; Bhuiyan et al., 2009). It makes plant cell walls more resistant to the mechanical pressure exerted by the fungal pathogen and water, which lessens the effect of cell wall degrading enzymes from the pathogen (Vance et al., 1980; Nicholson and Hammerschmidt, 1992; Bhuiyan et al., 2009). Various resistant varieties have shown the accumulation of lignin and lignin-like phenolic compounds as defense responses (Lahlali et al., 2016). Based on high fold-change induction of RR metabolites mainly related to phenylpropanoids and mapping back these RR metabolites to the metabolic pathway, identified laccase-4-like as the potential candidate. Therefore, we prioritized the *TaLAC4* gene to study further in response to *F. graminearum* in wheat NILs. We hypothesized that the silencing of *TaLAC4* in resistant NIL would compromise resistance against FHB. Sequence analysis, gene expression and functional characterization of the *TaLAC4* gene were conducted and reported in the following study.

Nancy Soni wrote the first draft of the manuscript, and she conceived the experimental design, performed all the laboratory and greenhouse experiments. Mr. Niranjan Hegde provided valuable suggestions related to the gene silencing experiment and assisted in greenhouse work. Mr. Achal Dhariwal, a pre-doctoral fellow at the University of Oslo, Norway, helped in molecular docking and statistical analysis. Dr. Kushalappa conceived the idea, aided in designing the experiments and edited the drafts of the manuscript.

CHAPTER IV

Role of laccase gene in wheat NILs differing at QTL-Fhb1 for resistance against Fusarium head blight

Nancy Soni¹, Niranjan Hegde¹, Achal Dhariwal², and Ajjamada C. Kushalappa¹

¹Plant Science Department, McGill University, Ste.-Anne-de-Bellevue, Quebec, Canada;

²University of Oslo, Norway

***Corresponding author:**

Dr. Ajjamada C. Kushalappa

Professor, McGill University

Ste. Anne-de-Bellevue, QC, Canada H9X3V9

Tel: 1(514-709-5874) Email: ajjamada.kushalappa@mcgill.ca

Reprinted with permission from Elsevier:

Soni N, Hegde N, Dhariwal A, Kushalappa AC, 2020. Role of laccase gene in wheat NILs differing at QTL-Fhb1 for resistance against Fusarium head blight. *Plant Science* **298**, 110574.

<https://doi.org/10.1016/j.plantsci.2020.110574>

4.1 Abstract

Fusarium head blight (FHB), caused mainly by *Fusarium graminearum* (*Fg*), is one of the most severe diseases of wheat. It affects grain yield and quality due to mycotoxin contamination, which is harmful for both human and livestock consumption. Cell wall lignification, following pathogen invasion, is one of the innate defense responses. Plant laccases are known to lignify the secondary cell walls. A metabolo-genomics study identified laccase as one of the candidate genes in QTL-Fhb1 of wheat NILs derived from Sumai 3*5/Thatcher cross. Based on phylogenetics, it was named as *TaLAC4*. Real-time qPCR revealed a strongly induced expression of *TaLAC4* in NIL-R. The VIGS based transient silencing of *TaLAC4* in NIL-R resulted in an increased susceptibility leading to *Fg* spread within the entire spike in 15 dpi, contrasting to non-silenced where the infection was limited to inoculated spikelets. Histopathology revealed thickened cell walls, mainly due to G-lignin, in non-silenced NIL-R, relative to silenced, in conjunction with higher total lignin content. Metabolic profiling of *TaLAC4* silenced NILs identified the accumulation of several precursor metabolites higher in abundances upstream *TaLAC4*. These results confirm that the resistance function of *TaLAC4* in NIL-R is due to pathogen-induced lignification of secondary cell walls in the rachis.

4.2 Introduction

Fusarium head blight (FHB), mainly caused by *F. graminearum* (*Fg*), is globally a devastating disease affecting wheat, barley, corn, and other small grain crops. FHB epidemics lead to significant loss of grain yield and quality due to mycotoxins contamination (McMullen et al., 1997; McMullen et al., 2012). Wheat continues being the essential source of food grain for humans, growing on the land area more than any other commercial crop, with approximately 700 billion tonnes global production and 46.8 billion US\$ of total export value (FAO, 2019). Enhancing plant immunity based on an understanding of plant-pathogen interaction provides a promising and environmentally friendly approach to reducing losses caused by FHB (Lacombe et al., 2010). In wheat, the QTL-Fhb1 (syn *Qfhs.ndsu-3BS*) derived from Chinese cultivar Sumai 3, is one amongst the major effect QTLs conferring moderately high levels of FHB resistance (Anderson et al., 2001; Jin et al., 2013). Several FHB resistance genes, such as GDSL, PFT and HRC have been identified and functionally validated as a genic component of QTL-Fhb1, but the resistance mechanisms are still elusive (Rawat et al., 2016; Su et al., 2018; Li et al., 2019; Su et al., 2019). FHB resistance,

however, is controlled by hierarchies of genes, and transfer of a single gene may not confer resistance (Kushalappa et al., 2016).

Plants have multilayered defense responses against microbial pathogen attack. For instance, to restrict pathogen entry into the cell, plants undergo reinforcement of preformed physical and physiological barriers (Chisholm et al., 2006; Jones and Dangl, 2006). Also, plasma membrane-bound and intracellular immune receptors commence defense responses either directly by physical interactions with pathogen-derived immunogens or indirectly by following modifications acquired by host plants upon pathogen invasion (Jones and Dangl, 2006; Kourelis and van der Hoorn, 2018). Besides, other antimicrobial compounds suppress pathogenicity by detoxifying or inhibiting virulence factors activity (Kitajima and Sato, 1999; Thomma et al., 2002; Ahuja et al., 2012). As plant cell wall is a mechanical barrier to the pathogen progression, lignin deposition via phenylpropanoid metabolism leads to the reinforced cell wall, which is more resistant to fungal cell wall degrading enzymes and limits diffusion of mycotoxins produced by a pathogen (Gunnaiah et al., 2012; Sattler and Funnell-Harris, 2013).

In plants, phenylpropanoid metabolism is the crucial secondary metabolic pathway involved in defense responses against both biotic and abiotic stresses (La Camera et al., 2004). Lignin biosynthesis via the phenylpropanoid pathway involves polymerization of monolignols forming sinapyl alcohol lead syringyl units, coniferyl alcohol lead guaiacyl units, and p-coumaric acid lead hydroxyphenol units. They reinforce cell wall by providing mechanical strength which further act as a physical barrier for pathogen colonization (Bonello and Blodgett, 2003; Fraser and Chapple, 2011). In response to pathogen ingress, lignin deposition limits the diffusion of toxins and enzymes produced by pathogen, limiting water and nutrient supply to the pathogen (Naoumkina et al., 2010; Mottiar et al., 2016). Thus, plant immune responses as defense-induced lignification against various pathogens represent basal defense mechanisms and employed for the activated immune response as a biochemical marker (Baayen, 1988; Menden et al., 2007; Bhuiyan et al., 2009; Adams-Phillips et al., 2010; Kishi-Kaboshi et al., 2010)

Laccase (p-diphenol: dioxygen oxidoreductase, EC.1.10.3.2; LAC) mainly involved in catalyzing one-electron oxidation of substrates such as phenols and derivatives and four-electron reduction of dioxygen to water (Mot and Silaghi-Dumitrescu, 2012). Due to its ability to oxidize various substrates, LACs have been exploited in the industrial processes (Foorootanfar and Faramarzi, 2015). In the recent past, several advancements have been made on the role of plant

LACs in lignin biosynthesis (Liang et al., 2006; Berthet et al., 2011; Cesarino et al., 2013; Zhao et al., 2013). In Arabidopsis, the knocking down of LAC4 and LAC17 resulted in xylem disruption and the detection of the soluble constituents (Berthet et al., 2011). Further, knockout mutants of *AtLAC4*, *AtLAC17* and *AtLAC11* were identified with several physiological changes, including growth inhibition, narrowed stems, and lack of lignified vascular bundles. Thus, apart from other laccases, *AtLAC11* also indicates its role in lignin polymerization (Zhao et al., 2013). In cotton, over-expression of *GhLAC1* led to increased lignification, resulting in enhanced tolerance to the fungal pathogen *Verticillium dahlia*, the insect pests cotton bollworm (*Helicoverpa armigera*) and the cotton aphid (*Aphis gossypii*) (Hu et al., 2018). Also, over-expression of *GhLAC15* was found to be associated with increased cell wall lignification, total lignin content, and G monolignol subunit and G/S ratio, contributing towards improved resistance against *Verticillium* wilt infection in Arabidopsis (Zhang et al., 2019).

In this study, we report the mechanisms of the *TaLAC4* gene, identified in the wheat major QTL-Fhb1, based on virus-induced silencing of *TaLAC4* in NIL-R. The disease severity and pathogen biomass were significantly increased when *TaLAC4* was silenced in NIL-R, as compared to non-silenced. The total lignin was higher in *TaLAC4* non-silenced than in silenced NIL-R, following pathogen inoculation. The histopathology revealed more thickened cell walls in *TaLAC4* non-silenced NIL-R compared to silenced NIL. These explained the resistance mechanisms of *TaLAC4*. The metabolic profiling of *TaLAC4* silenced NIL-R, following pathogen inoculation, revealed accumulation of several metabolites higher in abundances upstream of *TaLAC4*, relative to mock inoculation, such as monolignol derivatives like coniferyl alcohol glucosides, coumarins, fatty acids, flavonoids, HCCAs, and phenylpropanoids. Whereas no metabolites significantly increased in non-silenced NIL-R.

4.3 Materials and methods

4.3.1 Plant production and experimental design

NILs (near-isogenic lines) used in this study were derived from a cross of Sumai3*5/Thatcher (S/T), where Sumai3*5 is a resistant Chinese spring wheat cultivar, and thatcher is susceptible wheat cultivar to FHB (Cuthbert et al., 2006). The QTL-Fhb1 was successfully fine mapped within a 1.27-cM interval in S/T population on chromosome 3BS. The NILs were differing in an effective allele at the QTL-FHB1, such as FHB susceptible and resistant alleles, were obtained from Dr. S.

Fox, AAFC, Winnipeg, Canada. The experiment was laid out in a randomized complete block design (RCBD) with two genotypes (resistant and susceptible NILs), two treatments (pathogen and mock), and five biological replications over time, with each experimental unit consisting of nine plants, three plants in each pot. The plants were grown in greenhouse conditions maintained at 23 ± 2 °C temperature, daylight of 16 h, and relative humidity of 70 ± 10 % throughout the growing period. A compound slow-releasing fertilizer 14:14:14 (NPK) and 0.03 % of trace elements were applied at the rate of 5 g per pot once in every 15 days to each pot (Kage et al., 2017).

4.3.2 Pathogen production and inoculation

The *Fg* isolate (155.SLS, obtained from Dr. S. Rioux, CÉROM, Quebec) was grown on potato dextrose agar for four to five days at 26 °C and further sub-cultured on Rye B agar media, with UV exposure for three days, for sporulation. Macroconidia were harvested from seven-day-old cultures, and the spore count was adjusted to 10^5 macroconidia ml⁻¹ using a hemocytometer (American Scientific Products, USA) (Chamarthi et al., 2019). Three alternate pairs of spikelets, in the mid-region of the spike, were point inoculated with ten µl of either macro conidial suspension (P) or mock-solution (M) using a syringe with Leuer lock (GASTIGHT 1750 DAD, Reno, USA), at 50 % anthesis stage. At least ten spikes per replication were inoculated from three pots containing three plants. Inoculated plants were covered with transparent plastic bags sprayed with water to maintain high moisture. The bags were removed 48 h post-inoculation (hpi) (Kage et al., 2017; Kage et al., 2017).

4.3.3 Candidate gene identification in QTL-Fhb1

A paired-end Illumina HiSeq™ 2500 platform was used to capture the QTL-Fhb1 region flanking between two SSR markers, XSTS3B-138, and XSTS3B-142 (Cuthbert et al., 2006). The raw reads obtained were annotated using wheat reference-based analysis. The annotated sequences were analyzed for synteny among chromosomes of related species such as *Oryza sativa*, *Sorghum bicolor*, and *Brachypodium distachyon* to find out the cross homology. Among 37 putative candidate genes, five novel candidates including cell wall invertase, G-type lectin S-receptor-like serine/threonine-protein kinase (RKS1), LECRK1, NAC transcription factor 32-like, glutamate synthase 1 and laccase-4-like were selected as potential candidates based on gene expression, SNP

analysis, and metabolic profiling to speculate the possible resistance mechanism against FHB in wheat (Table 3.2; Fig. 4.1).

4.3.4 Gene expression analysis

The rachis samples of NILs were used for the isolation of total RNA using the RNeasy plant mini kit (Qiagen Inc.). Purified total RNA (~1–2 µg) was used to synthesize cDNA using the iScript cDNA synthesis kit (BioRad, ON, Canada) for the relative quantification of transcript expression. Temperature kinetics were performed with serially diluted cDNA for the putative candidate polymorphic genes along with the reference gene (*TaActin*). Taking the standardized cDNA concentration for each sample, real-time qRT-PCR was performed using Qi SYBR Green supermix (BioRad, Canada) in a CFX384™ Real-Time system (BioRad, Canada). *TaActin* gene transcript level was used to normalize the mRNA abundance of putative candidate polymorphic genes. qRT-PCR results were analyzed using the comparative $2^{-\Delta\Delta Ct}$ method or delta-delta Ct method (2^{-CT}), and the data were analyzed for statistical significance based on the Student *t*-test (Livak and Schmittgen, 2001).

4.3.5 Phylogenetic analysis

Phylogenetic analysis for *TaLAC* was done as described previously with few modifications (Rawat et al., 2016). Protein sequences of both the candidate genes were blast searched on the NCBI BLASTp search tool. The protein sequences of more than >80 % identity were retrieved from the NCBI database and were further used to construct a phylogenetic tree. Related protein sequences for both the candidate genes were aligned using MUSCLE. MEGA 7 software was used for the evolutionary analyses with few modifications, such as bootstrap confidence value was set to 100 iterations, and the Poisson correction method was used for the evolutionary distance measurement. Followed by that, a phylogenetic tree was built in MEGA 7 software based on the maximum likelihood method. All the accession numbers of the sequences from the NCBI database used in constructing a phylogenetic tree are mentioned in the table (Table 4.2).

4.3.6 Molecular docking of TaLAC4 with lignin model compounds

TaLAC4 protein sequence retrieved from the wheat ensemble database (TraesCS3B02G392700.1) was used for the homology-based modeling. HHpred, a protein structure prediction server, used three databases such as PDB, Pfam, and NCBI conserved domain to perform homology search

(Zimmermann et al., 2018). Based on the homology search, ten best proteins were selected for multiple sequence alignment (MSA). Following that, the obtained MSA was then used to build a protein model using the MODELLER software ingrained with the MPI bioinformatics toolkit (<https://toolkit.tuebingen.mpg.de/>) (Webb and Sali, 2016). The obtained protein structure was first visualized using the PyMol® tool and then used for docking the substrate molecules to identify the docking affinities towards the receptor (TaLAC4). Mainly four lignin model compounds were selected namely, sinapyl alcohol (monomer), guaiacyl 4-O-5 guaiacyl (dimer), syringyl β -O-4 syringyl β -O-4 sinapyl alcohol (trimer), and guaiacyl β -O-4 syringyl β - β syringyl β -O-4 guaiacyl (tetramer). We could only retrieve the structure of sinapyl alcohol from the database (ZINC database (<http://zinc.docking.org/>)); the rest were sketched using ChemSketch software (<https://www.acdlabs.com/resources/freeware/chemsketch/download.php>). As suggested, energy minimization was performed using CHARMM forcefield and the BEST algorithm was used for each compound conformation generation (Awasthi et al., 2015). The target protein, the substrates to be docked, and the docking grid were all arranged using AutoDockTools (Morris et al., 2009). AutoDockTools-1.5.6, a part of the MGLTools package, is a graphical interface program that allows visualization and manipulation of molecular structures. Other modifications such as reassigning hydrogen atom to retain the polarity of hydrogen atoms, defining docking grid orientation towards the binding site, and the spacing factor was set up to 1.000 in angstrom units were made.

4.3.7 Gene cloning, sequencing, and polymorphism analysis

The genomic DNA was isolated from wheat NILs seedlings using a DNA isolation kit (Qiagen Dneasy Kit). Gene-specific primers were used to amplify putative full-length candidate genes in NILs using isolated DNA as a template (Table 4.3). Thermocycler (Bio-Rad, Mississauga, ON, Canada) was used to carry out PCR with the following steps: Initial denaturation at 95 °C for 5 min followed by 35 cycles of 94 °C for 30 s, 55 °C for 1 min, 72 °C for 2 min followed by a final extension at 72 °C for 10 min. Following that, the PCR product was loaded onto 1 % agarose gel, and the specific PCR product was then eluted from gel, purified using a Gel Extraction kit (QIAquick Gel Extraction Kit - Qiagen), further cloned into pGEM®-T Easy vector (Promega, USA). The positive clones were subjected to Sanger DNA sequencing at McGill University and Genome Quebec Innovation Center (<http://gqinnovationcenter.com/>). The retrieved DNA sequences were translated into a protein sequence using the ExPASy translate tool for sequence

analysis (<http://web.expasy.org/translate/>). The presence of functional domains was predicted using the MOTIF search tool (<http://www.genome.jp/tools/motif/>) and further confirmed based on PROSITE and NCBI Conserved Domain Database (NCBI CDD) search tool. Sequence comparison was done based on the multiple sequence alignment using MultAlin software (<http://multalin.toulouse.inra.fr/multalin/>).

4.3.8 Construction of BSMV vectors and virus-induced gene silencing (VIGS) of *TaLAC4*

For gene silencing experiment, gene fragment of size ~291 bp was selected, which includes both coding sequence and the 3' UTR region (also known as the most divergent sequence), to increase the specificity (Scofield et al., 2005). The selected gene fragment was further analyzed for siRNA generation efficiency and the absence of off-targets in the modified viral genome with the help of the siRNA Scan tool (<http://bioinfo2.noble.org/RNAiScan.htm>), and NCBI BLAST search against the GenBank database. The gene fragment was amplified from cDNA with gene-specific primers (Table S2), cloned into pGEM®-T Easy Vector (Promega Corp., WI, USA) and sequenced. The positive clones were processed further for plasmid isolation. The plasmid was restriction digested using Not1 (New England Biolabs, MA, USA), thus creating Not1 restriction sites. The cDNA fragment was subsequently cloned into a pSL038-1 vector with a modified BSMV γ genome segment along with Not1 restriction sites present downstream of γ b gene53. The pSL038-1 vector carrying either phytoene desaturase (PDS) served as a positive control, whereas the pSL038-1 vector without any gene served as a negative control. The BSMV plasmids were then linearized, where BSMV α , γ were linearized using the Mlu1 restriction enzyme and BSMV β with the Spe1 enzyme, respectively. Further, in-vitro transcription of the linearized plasmids was performed with mMessage Machine™ T7 in-vitro transcription kit (Ambion, Inc., Austin, TX, USA), as suggested in the manufacturer's protocol.

The experiment was performed as RCBD consisting of one genotype, i.e., NIL-R with two treatments (mock and pathogen) and five biological replications over time with two pots per replication. Plants were generated in the greenhouse, as discussed before. All the three in-vitro transcripts (α , β , and γ BSMV) were linearized and inoculated into the plant in the ratio of 1:1:1 (1 μ l of each) (Scofield et al., 2005). To facilitate virus entry and infection, these transcripts were rub-inoculated along with 22.5 μ l of inoculation buffer mainly onto flag leaf and spikelets to increase the efficiency of silencing (Ma et al., 2012). An experimental unit consisting of a total of

10 spikes per replication was rub-inoculated with BSMV+*TaLAC4* as a test, BSMV+PDS as a positive control, and BSMV:00 as negative control respectively.

4.3.9 Comparison of *TaLAC4* non-silenced and silenced NIL-R

4.3.9.1 qRT-PCR, fungal biomass, and disease severity

The experiment was performed as RCBD, with two treatments of NIL-R with *TaLAC* silenced or not, in three biological replications, two pots containing three plants per replication. After 15 dpi with BSMV virus, three alternate pairs of spikelets were inoculated with ten µl of *Fg* macroconidial suspension and covered with polyethylene bags sprayed with water after inoculations until 48 h and five out of ten spikes were collected at 72 hpi for qRT-PCR analysis. For fungal biomass quantification, genomic DNA was extracted from the rachis samples, and real-time qPCR was performed. Relative fungal housekeeping gene *Tri6* copy number was measured to estimate fungal biomass. *TaActin* gene was used to normalize the abundance of *Tri6* gene. Student *t*-test was applied for the statistical significance of the data.

Disease severity was evaluated using ten spikes, with one pair of spikelets in the mid-region of each spike inoculated with *Fg*. After inoculation, plants were covered with wet polyethylene bags to maintain high moisture and removed after 48 h. The number of spikelets diseased were assessed every three-day interval for 15 dpi. Spikelets discolored or bleached and brown were considered diseased. From this, the cumulative proportion of spikelets diseased (PSD), and the area under the disease progress curve (AUDPC) were calculated. Statistical significance of the data was performed using ANOVA.

4.3.9.2 Phloroglucinol-HCL staining or weisner test

Histological analysis of rachis samples inoculated with mock or pathogen, collected at 48 hpi, was conducted to reveal differential cell wall reinforcement. Samples were embedded in cryomolds using Shandon CRYOMATRIX (Richard-Allan Scientific, Kalamazoo). Further, sections of 10 µm thickness were cut using a cryotome machine (Leica, CM1850, Canada) set at -20 °C and immediately collected on slides treated with a 5 % 3-aminopropyltriethoxysilane (APES) solution. Staining was done as suggested by Hu et al. (Hu et al., 2017) with some modifications. Slides harboring sections were rinsed with distilled water and air-dried at 37 °C for 10-15 mins. Fixed sections were treated with a 3 % (w/v) phloroglucinol solution for 1 min, followed by washing

with 50 % HCL. Slides were mounted with glycerol and immediately observed under a light microscope, OLYMPUS BX51.

4.3.9.3 Acetyl bromide soluble lignin (ABSL) assay

Chemical analyses of lignin were done as described by Barnes and Anderson (2017) with some modifications (Barnes and Anderson, 2017). Rachis samples stored at -80 degrees were ground using liquid N₂ into homogenously fine powder to prepare alcohol insoluble residue (AIR). Around 100 mg of finely ground tissue was taken in a 2 mL Eppendorf tube, and 70 % ethanol was added, vortexed, and centrifuged to pellet residue. The supernatant was removed, and the pellet was resuspended in 1:1 chloroform: methanol solution. The residual pellet was further suspended in acetone as described before and air-dried in the chemical hood overnight with Eppendorf lid open until completely dry. De-starching of AIR was done by adding 90 % DMSO to the pellet, vortexing, and shaking overnight at a speed of 50 rpm on a platform rocker to facilitate proper mixing. Successively, after centrifugation, the supernatant was removed, and the pellet was washed with DMSO and later with 70 % ethanol, six times. The acetone step was repeated, and the remaining material was de-starched AIR. Lugol's iodine solution was used to verify the absence of starch. Approximately 5 mg of de-starched AIR was taken into a glass screw cap vial, and 1 mL of 25 % acetyl bromide was added where a tube containing only 25 % acetyl bromide was served as blank. For each biological sample, three technical replicates were performed. Samples were incubated at 70 degrees for 1 h with mixing every 10 mins. After the incubation, samples were kept on ice, 5 mL of glacial acetic acid was added, and vortexed inside the chemical hood. The AIR was allowed to settle down overnight at room temperature. Absorption was checked at 280 nm against a blank on a spectrophotometer by taking 300 µL of acetyl bromide from the top of each tube. Beer's law was used to calculate the percentage of acetyl bromide soluble lignin (ABSL) with the previously established extinction coefficient. The mass percentage of ABSL was converted to µg mg⁻¹ AIR using formula: %ABSL = $(A_{280} / \epsilon * L) * (D/m) * 100$, Where A₂₈₀ = Absorbance at 280 nm (Blank corrected), ϵ = extinction coefficient (g⁻¹ L cm⁻¹), L = spectrophotometer path length (cm), D = dilution factor from digested AIR, m = mass of de-starched AIR (mg). Student *t*-test was applied for the statistical significance of the data.

4.3.10 Metabolite profiling of *TaLAC4* non-silenced and silenced NIL-R

4.3.10.1 Metabolites extraction, LC-HRMS and data processing

For metabolite analysis, ten spikes containing the three alternate pairs inoculated and un-inoculated spikelets and rachis, per replication, were harvested at 72 hpi. In total, (10×6=60 pairs) 60 rachis were separated from spikelet pairs per replication. Both the samples were frozen in liquid nitrogen and stored at -80 °C until further use. Metabolites were extracted from the rachis samples initially in 60 % ice-cold aqueous methanol and then finally in 100 % ice-cold aqueous methanol (Bollina et al., 2010). About 100 uL of filtrate or sample extract was used for metabolite analysis in a negative ionization mode using a high-resolution, accurate-mass (HRAM) Q Exactive™ Hybrid Quadrupole-346 Orbitrap Mass Spectrometer (LC-MS/MS) (Thermo Fisher, USA) using a 5 cm XB-C18 kinetex column. The Xcalibur raw files obtained were converted into mzXML format using MSConverterGUI. The data processing and molecular profile data-based mass spectrometry analysis was performed using mzMine-2 tools (Pluskal et al., 2010) along with peak deconvolution, peak detection, spectral filtering, and normalization of peaks (Katajamaa and Oresic, 2005).

4.3.10.2 Statistical analysis and putative metabolite identification

The peak intensities of monoisotopic masses were subjected to pairwise analysis of treatments, based on Students *t*-test using MetaboAnalyst (<http://www.metaboanalyst.ca/>). The pair-wise treatment combinations were: RM vs. SM, RP vs. RM and SP vs. SM, where RM and RP = NIL-R+BSMV:00 (non-silenced) inoculated with water (mock) and pathogen respectively, and SM and SP = NIL-R+BSMV:*Talac4* (*TaLAC4* silenced) inoculated with water (mock) and pathogen respectively were used to identify significant metabolites in all the treatments. Peak abundances significant at $P < 0.05$, and false discovery rate threshold of 0.05 were retained for further analysis. The significant monoisotopic peaks were identified as metabolites based on three criteria; (i) accurate mass error, $AME \leq 5$ ppm (Tohge and Fernie, 2010; Gunnaiah et al., 2012), (ii) Fragmentation pattern and (iii) in-silico confirmation of fragmentation based on Masspec scissor in ChemSketch (ACD labs, Toronto) (Supp. Table 4.2) (Matsuda et al., 2009). Subsequently, these metabolites were classified as a pathogenesis-related (PR) metabolite if the fold change in abundance in the pathogen inoculated treatments were higher than in mock-inoculated treatments in resistant/non-silenced NIL-R ($PR_r = RP/RM > 1.0$) or susceptible/*TaLAC4* silenced NIL-R ($PR_s = SP/SM > 1.0$) (Bollina et al., 2010; Gunnaiah et al., 2012).

4.4 Results

4.4.1 Characterization of *TaLAC* gene

The full-length *TaLAC* gene was sequenced in NILs derived from Sumai3*5/Thatcher. FGENESH based sequence analysis revealed that *TaLAC* has six exons and five introns (Fig. 4.2a), later intron-exon boundaries were confirmed for Acceptor (AG) and Donor (GT) sites, respectively through [FSPLICE](http://linux1.softberry.com/berry.phtml?topic=fsplICE&group=programs&subgroup=gfind) (<http://linux1.softberry.com/berry.phtml?topic=fsplICE&group=programs&subgroup=gfind>). The full-length gene sequence of *TaLAC* was 4419 bp consisting of an open reading frame (ORF) of 2178bp, a 313 bp 3' untranslated region (UTR), and 128 bp 5' UTR. *TaLAC* encodes for 578 amino acids long protein sequence, comprising of three conserved domains (Cu_oxidase_3, Cu_oxidase, and Cu_oxidase_2) spanning from position 9-540 amino acids (Fig. 4.2b). The complete genomic sequence was submitted to the NCBI GenBank repository and was assigned an accession number MT587562. The *TaLAC* showed 97.23 % identity with *Aegilops tauschii* putative *TaLAC4*, 93.76 % with *Triticum Urartu*, and 86.53 % with *Brachypodium distachyon*. Also, multiple sequence alignment and phylogenetic analysis confirmed the close homology of the *TaLAC* gene sequence (unnamed protein product in *T. aestivum*) with *TaLAC4* in *Aegilops tauschii*. Based on this, we putatively designated *TaLAC* as *TaLAC4* like gene (or as *TaLAC4*) (Fig. 4.2c).

4.4.2 Molecular docking revealed binding substrates of *TaLAC4*

A three-dimensional structure of *TaLAC4* was obtained by homology detection and structure prediction by HMM-HMM (Hidden Markov Models). Homology search based ten best proteins were selected for multiple sequence alignment (MSA) are: PDB: 3SQR showing 42.4% sequence identity (id.) to *TaLAC4*; PDB: 1ZPU (26.2% id.); PDB: 1AOZ (24.8% id.); PDB: 5ZIX (29.1% id.); PDB: 1HFU (28.4% id.); PDB: 5EHF (28.6% id.); PDB: 2Q9O (34.3% id.); PDB: 3PXL (27.5% id.); and PDB: 6RI6 (28.1% id.). They have been used as templates to calculate a model for *TaLAC4* using HHpred and Modeller (Zimmermann et al., 2018; Webb & Sali, 2016).

To evaluate the binding affinity among wheat *TaLAC4* and selected lignin model compounds as substrates, molecular docking of these model compounds with their respective binding sites, sinapyl alcohol (L1: PHE`267/CA, GLN` 265\CA) (Fig. 4.3a), guaiacyl 4-O-5 guaiacyl (L2: PHE`267/CD1) (Fig. 4.3b), syringyl β -O-4 syringyl β -O-4 sinapyl alcohol (L3: TRP`316/CE2) (Fig. 4.3c), and guaiacyl β -O-4 syringyl β - β syringyl β -O-4 guaiacyl (L3:

TRP 316/CE2) (Fig. 4.3d) on TaLAC4 was performed using AutoDockTools. The best-fit ligand conformations were selected based on their minimum binding energies. Amino acid residues, which established contact with ligand and the residues involved in hydrogen bonding with ligands, were recorded using AutoDock Tools using the results obtained from AutoDock Vina. We have used Edu PyMOL v2.4.2 (<https://pymol.org/educational>) for visualizing the interactions of the ligand and modelled protein structure and for developing the respective docked images. The docking results revealed docking scores based on lignin model compounds (Supp. Table 4.1). Sinapyl alcohol, guaiacyl 4-O-5 guaiacyl and syringyl β -O-4 syringyl β -O-4 sinapyl alcohol, with the binding energy -16.02, -21.21, and -0.71 kJ/mol, respectively, bind to the inner pocket of the folded protein and showed some difference in the binding affinity with significant differences in DG, however, carrying few similar binding sites in deep inside the pocket (Fig. 4.3 a,b). On the other hand, the binding affinity recorded for guaiacyl β -O-4 syringyl β - β syringyl β -O-4 guaiacyl was 1.86 kJ/mol, along with different binding sites indicates the lesser affinity towards TaLAC4 (Fig. 4.3d). The difference in the binding affinity attributed to the binding pockets, for instance, the binding pockets for syringyl β -O-4 syringyl β -O-4 sinapyl alcohol and guaiacyl β -O-4 syringyl β - β syringyl β -O-4 guaiacyl was found to be in the shallow region on the surface of the protein. Hence, the other substrates, guaiacyl 4-O-5 guaiacyl and sinapyl alcohol bind effectively to the TaLAC4 macromolecule to facilitate the catalytic reaction. Based on the binding energy, guaiacyl 4-O-5 guaiacyl, a dimer of guaiacyl (G) lignin unit, docked more efficiently than other lignin compounds.

4.4.3 Polymorphism and differential gene expression of *TaLAC4* in NIL-R and NIL-S

Multiple sequence alignment of *TaLAC4* gene sequences identified two significant substitutions, in NIL-S, lysine to glutamate at position 250 (K250E) and histidine to aspartate at position 252 (H252D) (Fig. 4.4a). These mutations have been previously reported to be associated with affecting DNA binding ability and dissociating ligand-receptor complex, respectively (Ris-Stalpers et al., 1991; Singh et al., 2013). Although in our study, super-imposed protein three-dimensional (3D) structure prediction based on Phyre Investigator suggested no such significant conformational changes among the two NILs. However, whether the effect of mutation has a deleterious impact on protein-ligand binding needs further confirmation. The semi-quantitative PCR analysis normalized with *TaActin* indicated significantly higher expression of *TaLAC4* in NIL-R as compared to NIL-S. Further confirmation was done based on real-time quantitative PCR

(qRT-PCR), where the relative gene expression analysis of *TaLAC4* in NILs following *Fg* inoculation was higher with FC=3.13 difference in pathogen treated NIL-S as compared to mock solution treated NIL-S. Similarly, mock-treated NIL-R showed higher expression with FC=1.51 as compared to NIL-S (Fig. 4.4b). The drastic change in induced expression of *TaLAC4*, following *Fg* inoculation, suggests its role in induced defense responses against *Fg*.

4.4.4 *TaLAC4* gene expression in silenced and non-silenced NIL-R

Based on observed changes in the expression pattern of the *TaLAC4* in response to *Fg* and mock treatment, the BSMV-VIGS system was employed to transiently silence the *TaLAC4* gene in NIL-R to validate its role in resistance function (Fig. 4.5). To check the feasibility and efficacy of the BSMV-VIGS system, a wheat phytoene desaturase (*TaPDS*) genes was silenced in NIL-R as a positive control. The appearance of photo-bleaching symptoms started developing on wheat spikes at 15 dpi after silencing *TaPDS* with BSMV:*TaPDS* (Fig. 4.6). Accordingly, the BSMV-VIGS system was used to access the potential roles of *TaLAC4* in FHB resistance in wheat NILs. Similarly, BSMV:*Talac4* (test/silenced) and BSMV:00 (control/non-silenced) recombinant vectors were designed and introduced in NIL-R spikes through rub-inoculation. Resultantly, phenotypic differences could be observed in both the spike and the rachis from the point of inoculation and the spread of disease (Fig. 4.7a). Further, to study the effect of *TaLAC4* silencing on the wheat NIL-R plants, the relative gene expression study was performed based on qRT-PCR. Relative gene expression analysis revealed the significant ($P < 0.01$) reduction (FC: 6.64) in LAC4 gene expression in silenced plants (BSMV:*Talac4*) compared to non-silenced (BSMV:00) at 48 hpi with *Fg*, establishing the successful down-regulation of the target gene in wheat NILs (Fig. 4.7b).

4.4.5 Silencing of *TaLAC4* gene in NIL-R increased disease severity and fungal biomass in rachis

The effect of silencing the *TaLAC4* gene in NIL-R was evaluated following point inoculation of two florets per spike. In 80 % of the non-silenced NIL-R spikes, the pathogen did not spread beyond the inoculated spikelets, meaning high rachis resistance (Type-II), whereas in silenced it spread to almost the entire spikelet in 15 dpi. The AUDPC was significantly higher in silenced plants (6.84) as compared to non-silenced (2.31), with an FC= 2.96 (Fig. 4.8a). Also, the fungal biomass was significantly higher in silenced plants (2.95) as compared to non-silenced (0.8), with

an FC= 3.69, indicating increased susceptibility to *Fg* (Fig. 4.8b). These further confirmed the resistance in NIL-R, due to functional *TaLAC4* as compared to the non-functional.

4.4.6 Total lignin and its structure altered in NIL-R, following silencing of *TaLAC4*

In response to pathogen attack, plant secondary cell wall components, mainly lignin biosynthesis results in both growth and defense (Xie et al., 2018). Therefore, total lignin was quantified in silenced and non-silenced rachis samples, that were mock, and pathogen inoculated. The acid-soluble lignin test confirmed a 15 % higher amount of the total lignin content in the non-silenced, as compared to silenced *TaLAC4* NIL-R (Fig. 4.9a). The phloroglucinol-HCL staining (Wiesner test), which confirms the presence of coniferaldehyde groups in the lignin, revealed an increased deposition of lignin in the rachis of *TaLAC4* non-silenced NIL-R, as compared to silenced, post-*Fg* inoculation (Fig. 4.9b), meaning possible increased polymerization due to G-lignin.

4.4.7 Effect of *TaLAC4* silencing on the abundances of PRr metabolites in NIL-R

Lack of laccase activity was associated with increased upstream metabolic flux. Even when laccase was silenced in NIL-R, still it induced some resistance metabolites (PRs, pathogenesis-related metabolites), following pathogen inoculation. There was a significant increase in the accumulation of precursor metabolites, mainly the soluble phenolics such as coniferyl alcohol derivatives belonging to *Phenylpropanoids*: coniferin (FC= 2.48) with high fold change (Table 4.1); *Coumarins*: isopimpinellin (FC=13.7), 5,6,7-trimethoxycoumarin (FC=2.22); *Fatty acid*: docosanoic acid (FC=2.76); *Flavonoids*: hinokitiol glucoside (FC=2.67) and; *Hydroxycinnamic acid amides (HCAAs)* and *Phenylpropanoid conjugates*: 1-O-Vanilloyl-beta-D-glucose (FC=4.26), podorhizol beta-D-glucoside (FC=2.38) and (+)-syringaresinol O-beta-D-glucoside (FC=3.42) were found to be elevated in the silenced NIL-R, following pathogen inoculation as compared to mock-treatment. These precursor metabolites in non-silenced NIL-R may have been used to biosynthesize downstream RR metabolites; thus, no significant precursor metabolites were detected and identified.

4.5 Discussion

4.5.1 *TaLAC4* in plant defense against *Fg*

The plant cell wall components such as cellulose, hemicelluloses, lignin, and pectic polysaccharides often act as barriers to pathogen progress (Xu et al., 2011; Bellincampi et al.,

2014). Pathogens produce various CWDEs such as pectinases, xylanases, and cellulases to degrade cell walls to enable them to colonize plant tissues (Mary Wanjiru et al., 2002; Yang et al., 2012). Several studies have suggested the role of cell wall polymers contents and composition on the outcome of plant-pathogen interactions (Cantu et al., 2008; Pogorelko et al., 2013; Blümke et al., 2014). Lignin, an essential structural component of cell wall involved in pathogen defense response by providing resistance against CWDEs and preventing diffusion of toxins produced by the pathogen (Sattler and Funnell-Harris, 2013; Zhang et al., 2017). Lignin has been reported to impart resistance against multiple plant diseases, including *Fg* infection in wheat (Lionetti et al., 2015; Hu et al., 2018; Voss-Fels et al., 2018; Zhang et al., 2019). Previously, in *Arabidopsis*, plant laccases (LAC4, LAC11, and LAC17) were reported to be necessary for lignin polymerization and non-redundant with peroxidases (Berthet et al., 2011; Zhao et al., 2013). In response to verticillium wilt infection in cotton, *GhLAC15* imparts resistance by induced lignification and lignin components in plant cell walls (Zhang et al., 2019). These plant laccases oxidatively polymerize monolignols into guaiacyl (G), syringyl (S), and p-hydroxyphenyl (H) lignin units (Wang et al., 2015).

In this study, *TaLAC4* was functionally characterized as one of the candidate genes for FHB resistance in the QTL-Fhb1 based on a combined metabolo-genomics approach. Real-time qRT-PCR based differential gene expression study also revealed strong induced expression of the *TaLAC4* gene in NIL-R inoculated with *Fg*. These findings present some insights into the role of wheat laccase genes in the defense mechanism against *Fg* infection in wheat. Following that, we show that the silencing of *TaLAC4* in NIL-R led to an increased susceptibility to *Fg*. This was also associated with a significant increase in fungal biomass and cumulative progression of disease severity. Interestingly, the quantification of total lignin in rachis revealed a considerable reduction of lignin in silenced NIL-R, which also corresponds to the histochemical analysis, which clearly showed the disruption of lignin in the silenced plants, suggesting the role of laccase in catalyzing the lignin polymerization.

4.5.2 Metabolic changes in the laccase silenced NIL-R plants

Metabolites belonging to the phenylpropanoid pathway are often reported for their significance in chemical defense against *Fg* infection and DON production (Gunnaiah et al., 2012; Gauthier et al., 2015; Dhokane et al., 2016; Kage et al., 2017). Wherein, some are produced constitutively, and function as preformed antibiotics in non-host resistance to pathogens, known as phytoanticipins;

and others are induced in response to pathogen invasion and involved in plant defense mechanism, as phytoalexins (Dixon et al., 2002; Kushalappa et al., 2016). Under stress condition, previous studies reported a re-direction of metabolic flux in the phenylpropanoid pathway leading to the accumulation of a range of secondary metabolites such as flavonoids, coumarins, stilbenes and hydroxycinnamic acid conjugates that play crucial roles in plants stress response (Vogt, 2010; Fraser and Chapple, 2011; Gunnaiah et al., 2012; Dhokane et al., 2016; Kage et al., 2017; Kage et al., 2017; Yogendra et al., 2017). These studies, however, indicated a decrease in RR metabolites, downstream of the candidate gene that was silenced in a resistant genotype. Whereas in our study it was not possible to quantify metabolites downstream of *TaLAC4* as were involved in polymerization of complex lignins, which the LC-HRMS was unable to detect.

Even though our main objective was to explore the resistance mechanisms of functional *TaLAC4*, by exploring metabolites downstream of this gene, we also explored if the silenced *TaLAC4* in NIL-R had any mechanisms of resistance due to genes upstream of *TaLAC4* in the phenylpropanoid pathway, as the NILs we had resistance background. This revealed an increase in the accumulation of precursor metabolites, upstream of *TaLAC4*, and their conjugates in silenced NIL-R, following pathogen inoculation relative to mock. As a result, a coniferyl alcohol glucoside was strikingly increased in the silenced NIL-R plants (Table 1). Elevated levels of coniferyl alcohol glucoside (coniferin) and sinapyl alcohol glucoside (syringin) in the laccase triple mutant in Arabidopsis (*Lac4*, *Lac11*, and *Lac17*) have been reported, along with significant upregulation of both *UGT72E2* and *UGT72E3* genes (Miao and Liu, 2010; Zhao et al., 2013). Interestingly, *TaLAC4* silenced plants showed an increase in the abundance of precursor metabolites and their conjugates and lignans, mainly related to coumarins, HCAAs and phenylpropanoids, flavonoids and fatty acids due to lack of laccase activity with significantly high fold change (Table 4.1). Wherein, HCAAs cross-links with polysaccharides to form suberins and deposit as cell wall appositions at the inner side of plant cell walls for cell wall reinforcement (Cajka and Fiehn, 2014). In wheat, against *Fg* infection, several studies have reported HCAAs as resistance-related induced (RRI) involved in the thickening of the cell wall as defense response (Gunnaiah et al., 2012; Dhokane et al., 2016; Kage et al., 2017; Kage et al., 2017). Upon *Fg* infection, resistant wheat cultivar Sumai-3 was identified with the accumulation of N-caffeoylputrescine, 4-coumaroyl-3-hydroxyagmatine, and feruloyl-serotonin highly upregulated (Cajka and Fiehn, 2014). Against *P. infestans* infection in potato, increased expression of 4CL was

associated with increased downstream metabolites, such as HCCAs accumulation to impart resistance through cell wall thickening (Pushpa et al., 2014; Yogendra et al., 2014; Yogendra et al., 2017).

The primary transcriptional regulatory mechanism of lignin and secondary cell wall biosynthesis comprised the hierarchical network of NAC and MYB transcription factors (Nakano et al., 2015). For instance, among phenylpropanoid and lignin biosynthesis regulating related transcription factors, in Arabidopsis, MYB46 and MYB83 were found to activate the expression of PAL1, C4H, 4CL1, C30H1, HCT, CCoAOMT, CCR1, F5H1, CAD6 genes (Zhong et al., 2007; Kim et al., 2014). Apart from MYB46/MYB3, downstream, several other MYB transcription factors, including MYB58, MYB63, MYB85, MYB4, MYB32, and MYB7, were identified to specifically activate lignin biosynthesis via targeting AC elements (Zhou et al., 2009). Upstream MYB transcription factor, the NAC transcription factor including SECONDARY WALL-ASSOCIATED NAC DOMAIN PROTEIN 1/NAC SECONDARY WALL THICKENING PROMOTING FACTOR 3 (SND1/NST3) and its close homologs NST1, NST2, VASCULAR-RELATED NAC DOMAIN6 (VND6), and VND7 were also identified to regulate lignin biosynthesis in Arabidopsis (Kubo et al., 2005; Zhong et al., 2006). *TaWRKY70*, *StWRKY1*, *HvWRKY23* transcription factors regulate the downstream phenylpropanoid pathway, resulting in the accumulation of flavonoid glycoside and hydroxycinnamic acid amides to resist the spread of *Fg* infection (Kage et al., 2017; Kage et al., 2017; Yogendra et al., 2017; Karre et al., 2019). In our study, the silencing of *TaLAC4* caused a significant increase in the precursor metabolites and their conjugates, upstream of *TaLAC4*. The monolignols and their derivatives were accumulated higher in abundance in *TaLAC4* silenced NIL.

4.5.3 *TaLAC4* contributes to basal immunity by mediating induced lignins

During the onset of the secondary cell wall (SCW) formations in plants, lignin is synthesized via a complex biosynthetic pathway providing mechanical strength, hydrophobicity, and mainly contributing to defense against pests and pathogens. The elaborate process also leads to the production of a wide range of phenylpropanoid derivatives such as hydroxycinnamic acids, flavonoids, coumarins, chalcones, phenylpropenes, and stilbenes using phenylalanine as the initial substrate (Le Roy et al., 2016). However, the laccases are involved in the downstream lignification and were demonstrated in Arabidopsis based on several knockout mutants, for instance, *lac4 lac17 lac11* triple mutant showed hypolignified fibers and distorted xylem vessel phenotype along with

severe growth defects followed by failure of lignin detection in both stems and roots based on histochemical analysis (Berthet et al., 2011; Zhao et al., 2013). The lignin polymerization takes place via a combinatorial radical coupling process in the apoplastic cell wall allowing incorporation of several lignin monomers to produce different lignin polymers, such as G-lignins, in different cell types (Tobimatsu and Schuetz, 2019). The degree and nature of polymeric cross-linking are decided based on the S/G ratio. According to Chezem et al. (Chezem et al., 2017), compared to S-lignin, the G-lignin is more cross-lined and resistant to depolymerization and thus is a better defensive barrier against the pathogen. For instance, *AtMYB15* contributes to basal immunity by mediating defense-induced G-lignin synthesis (Chezem et al., 2017). However, elevated S-lignin content was found to be linked with cell wall biochemical traits in response to *Fg* infection in wheat (Lionetti et al., 2015). In this study, the histochemical analysis of pathogen inoculated *TaLAC4* non-silenced NIL-R rachis showed an increase in the total lignin deposition, especially the coniferaldehyde groups.

In the last decades, plant-pathogen relationship study has produced new information related to their interaction encompassing complex networks of molecules, signaling pathways, and strategies like recognizing the invaders and induce defense responses to protect themselves. The complex defense network involves a plethora of critical elements, regulators, and pathways associated. In conclusion, the current study functionally validated *TaLAC4* as a potential candidate gene underlying QTL-Fhb1 flanking between XSTS3B-138 and XSTS3B-142. The silencing of the *TaLAC4* gene leads to a drastic increase in fungal biomass, disease severity, and reduction in total lignin deposition. Also, over-accumulation of monolignol derivatives upon laccase silencing in the NIL-R rachis suggests *TaLAC4* is necessary for the oxidative polymerization of monolignols to biosynthesize G lignin. This study opens the opportunity to explore other laccases or cell wall biosynthetic genes involving synergistically to confer a high level of resistance against FHB in wheat.

4.6 Author contribution statement

NS wrote the manuscript and performed all the experiments; NH helped in valuable suggestions and greenhouse work; AD helped in molecular docking and statistical analysis; ACK* conceived the idea, aided in designing the experiments and edited the manuscript. All authors read and approved the manuscript.

4.7 Compliance with ethical standards

The authors declare that the experiments comply with the McGill Environment, Health and Safety guidelines, and the current laws of Canada.

4.8 Declaration of Competing Interest

The authors declare no conflict of interest.

4.9 Acknowledgments

This work was funded by the Natural Sciences and Engineering Research Council of Canada (NSERC), McGill Sustainability Systems Initiative (MSSI) and Ministère de l'Agriculture, des Pêcheries et de l'Alimentation du Québec (MAPAQ), Québec, Canada. We thank Dr. S. Fox, AAFC, Winnipeg, Canada, for providing wheat NILs and Dr. S. Rio, CEROM for providing Fg isolate. We thank Mr. Yves Dion, Centre de recherche sur les grains (CÉROM), Canada, for his guidance and support. We also acknowledge anonymous reviewers for their valuable comments and suggestions for improving the manuscript.

REFERENCES

- Adams-Phillips L, Briggs AG, Bent AF** (2010) Disruption of poly(adp-ribosyl)ation mechanisms alters responses of arabidopsis to biotic stress. *Plant Physiology* **152**: 267
- Ahuja I, Kissen R, Bones AM** (2012) Phytoalexins in defense against pathogens. *Trends Plant Sci* **17**: 73-90
- Anderson JA, Stack RW, Liu S, Waldron BL, Fjeld AD, Coyne C, Moreno-Sevilla B, Fetch JM, Song QJ, Cregan PB, Frohberg RC** (2001) DNA markers for Fusarium head blight resistance QTLs in two wheat populations. *Theoretical and Applied Genetics* **102**: 1164-1168
- Awasthi M, Jaiswal N, Singh S, Pandey VP, Dwivedi UN** (2015) Molecular docking and dynamics simulation analyses unraveling the differential enzymatic catalysis by plant and fungal laccases with respect to lignin biosynthesis and degradation. *Journal of Biomolecular Structure and Dynamics* **33**: 1835-1849
- Baayen RP** (1988) Responses related to lignification and intravascular periderm formation in carnations resistant to Fusarium wilt. *Canadian Journal of Botany* **66**: 784-792
- Barnes WJ, Anderson CT** (2017) Acetyl bromide soluble lignin (absl) assay for total lignin quantification from plant biomass. *Bio-protocol* **7**: 2149
- Bellincampi D, Cervone F, Lionetti V** (2014) Plant cell wall dynamics and wall-related susceptibility in plant-pathogen interactions. *Frontiers in plant science* **5**: 228

- Berthet S, Demont-Caulet N, Pollet B, Bidzinski P, Cézard L, Le Bris P, Borrega N, Hervé J, Blondet E, Balzergue S, Lapierre C, Jouanin L** (2011) Disruption of LACCASE4 and 17 results in tissue-specific alterations to lignification of *Arabidopsis thaliana* stems. *The Plant cell* **23**: 1124-1137
- Bhuiyan NH, Selvaraj G, Wei Y, King J** (2009) Gene expression profiling and silencing reveal that monolignol biosynthesis plays a critical role in penetration defence in wheat against powdery mildew invasion. *Journal of experimental botany* **60**: 509-521
- Blümke A, Falter C, Herrfurth C, Sode B, Bode R, Schäfer W, Feussner I, Voigt CA** (2014) Secreted fungal effector lipase releases free fatty acids to inhibit innate immunity-related callose formation during wheat head infection. *Plant physiology* **165**: 346-358
- Bollina V, Kumaraswamy GK, Kushalappa AC, Choo TM, Dion Y, Rioux S, Faubert D, Hamzehzarghani H** (2010) Mass spectrometry-based metabolomics application to identify quantitative resistance-related metabolites in barley against *Fusarium* head blight. *Mol Plant Pathol* **11**: 769-782
- Bonello P, Blodgett JT** (2003) *Pinus nigra*-*Sphaeropsis sapinea* as a model pathosystem to investigate local and systemic effects of fungal infection of pines. *Physiological and Molecular Plant Pathology* **63**: 249-261
- Cajka T, Fiehn O** (2014) Comprehensive analysis of lipids in biological systems by liquid chromatography-mass spectrometry. *Trends Analyt Chem* **61**: 192-206
- Cantu D, Vicente AR, Labavitch JM, Bennett AB, Powell AL** (2008) Strangers in the matrix: plant cell walls and pathogen susceptibility. *Trends Plant Sci* **13**: 610-617
- Cesarino I, Araújo P, Sampaio Mayer JL, Vicentini R, Berthet S, Demedts B, Vanholme B, Boerjan W, Mazzafera P** (2013) Expression of SofLAC, a new laccase in sugarcane, restores lignin content but not S:G ratio of *Arabidopsis lac17* mutant. *Journal of Experimental Botany* **64**: 1769-1781
- Chamarthi S, Kumar K, Gunnaiah R, Kushalappa A, Dion Y, Choo T** (2019) Identification of fusarium head blight resistance related metabolites specific to doubled-haploid lines in barley. *European Journal of Plant Pathology* **138**: 67-78
- Chezem WR, Memon A, Li FS, Weng JK, Clay NK** (2017) Sg2-type r2r3-myb transcription factor myb15 controls defense-induced lignification and basal immunity in *arabidopsis*. *Plant Cell* **29**: 1907-1926
- Chisholm ST, Coaker G, Day B, Staskawicz BJ** (2006) Host-microbe interactions: shaping the evolution of the plant immune response. *Cell* **124**: 803-814
- Cuthbert PA, Somers DJ, Thomas J, Cloutier S, Brule-Babel A** (2006) Fine mapping Fhb1, a major gene controlling fusarium head blight resistance in bread wheat (*Triticum aestivum* L.). *Theor Appl Genet* **112**: 1465-1472
- Dhokane D, Karre S, Kushalappa AC, McCartney C** (2016) Integrated metabolo-transcriptomics reveals fusarium head blight candidate resistance genes in wheat qtl-fhb2. *PloS one* **11**: e0155851-e0155851
- Dixon RA, Achnine L, Kota P, Liu CJ, Reddy MS, Wang L** (2002) The phenylpropanoid pathway and plant defence-a genomics perspective. *Mol Plant Pathol* **3**: 371-390
- FAO** (2019) Food outlook - biannual report on global food markets.

- Forootanfar H, Faramarzi MA** (2015) Insights into laccase producing organisms, fermentation states, purification strategies, and biotechnological applications. *Biotechnology Progress* **31**: 1443-1463
- Fraser CM, Chapple C** (2011) The phenylpropanoid pathway in Arabidopsis. *Arabidopsis Book* **9**: e0152
- Gauthier L, Atanasova-Penichon V, Chereau S, Richard-Forget F** (2015) Metabolomics to decipher the chemical defense of cereals against fusarium graminearum and deoxynivalenol accumulation. *Int J Mol Sci* **16**: 24839-24872
- Gunnaiah R, Kushalappa AC, Duggavathi R, Fox S, Somers DJ** (2012) Integrated Metabolo-Proteomic Approach to Decipher the Mechanisms by Which Wheat QTL (Fhb1) Contributes to Resistance against Fusarium graminearum. *PLOS ONE* **7**: e40695
- Hu Q, Min L, Yang X, Jin S, Zhang L, Li Y, Ma Y, Qi X, Li D, Liu H, Lindsey K, Zhu L, Zhang X** (2018) Laccase GhLac1 Modulates Broad-Spectrum Biotic Stress Tolerance via Manipulating Phenylpropanoid Pathway and Jasmonic Acid Synthesis. *Plant Physiology* **176**: 1808-1823
- Hu R, Xu Y, Yu C, He K, Tang Q, Jia C, He G, Wang X, Kong Y, Zhou G** (2017) Transcriptome analysis of genes involved in secondary cell wall biosynthesis in developing internodes of Miscanthus lutarioriparius. *Scientific Reports* **7**: 9034
- Jin F, Zhang D, Bockus W, Baenziger PS, Carver B, Bai G** (2013) Fusarium head blight resistance in u.S. Winter wheat cultivars and elite breeding lines. *Crop Science* **53**: 2006-2013
- Jones JD, Dangl JL** (2006) The plant immune system. *Nature* **444**: 323-329
- Kage U, Karre S, Kushalappa AC, McCartney C** (2017) Identification and characterization of a fusarium head blight resistance gene TaACT in wheat QTL-2DL. *Plant Biotechnology Journal* **15**: 447-457
- Kage U, Yogendra KN, Kushalappa AC** (2017) TaWRKY70 transcription factor in wheat QTL-2DL regulates downstream metabolite biosynthetic genes to resist Fusarium graminearum infection spread within spike. *Scientific Reports* **7**: 42596
- Karre S, Kumar A, Yogendra K, Kage U, Kushalappa A, Charron J-B** (2019) HvWRKY23 regulates flavonoid glycoside and hydroxycinnamic acid amide biosynthetic genes in barley to combat Fusarium head blight. *Plant Molecular Biology* **100**: 591-605
- Katajamaa M, Oresic M** (2005) Processing methods for differential analysis of LC/MS profile data. *BMC Bioinformatics* **6**: 179
- Kim WC, Kim JY, Ko JH, Kang H, Han KH** (2014) Identification of direct targets of transcription factor MYB46 provides insights into the transcriptional regulation of secondary wall biosynthesis. *Plant Mol Biol* **85**: 589-599
- Kishi-Kaboshi M, Okada K, Kurimoto L, Murakami S, Umezawa T, Shibuya N, Yamane H, Miyao A, Takatsuji H, Takahashi A, Hirochika H** (2010) A rice fungal MAMP-responsive MAPK cascade regulates metabolic flow to antimicrobial metabolite synthesis. *Plant J* **63**: 599-612
- Kitajima S, Sato F** (1999) Plant pathogenesis-related proteins: molecular mechanisms of gene expression and protein function. *J Biochem* **125**: 1-8

- Kourelis J, van der Hoorn RAL** (2018) Defended to the nines: 25 years of resistance gene cloning identifies nine mechanisms for R protein function. *Plant Cell* **30**: 285-299
- Kubo M, Udagawa M, Nishikubo N, Horiguchi G, Yamaguchi M, Ito J, Mimura T, Fukuda H, Demura T** (2005) Transcription switches for protoxylem and metaxylem vessel formation. *Genes Dev* **19**: 1855-1860
- Kushalappa AC, Yogendra KN, Karre S** (2016) Plant innate immune response: Qualitative and quantitative resistance. *Critical Reviews in Plant Sciences* **35**: 38-55
- La Camera S, Gouzerh G, Dhondt S, Hoffmann L, Fritig B, Legrand M, Heitz T** (2004) Metabolic reprogramming in plant innate immunity: the contributions of phenylpropanoid and oxylipin pathways. *Immunol Rev* **198**: 267-284
- Lacombe S, Rougon-Cardoso A, Sherwood E, Peeters N, Dahlbeck D, van Esse HP, Smoker M, Rallapalli G, Thomma BP, Staskawicz B, Jones JD, Zipfel C** (2010) Interfamily transfer of a plant pattern-recognition receptor confers broad-spectrum bacterial resistance. *Nat Biotechnol* **28**: 365-369
- Le Roy J, Huss B, Creach A, Hawkins S, Neutelings G** (2016) Glycosylation is a major regulator of phenylpropanoid availability and biological activity in plants. *Front Plant Sci* **7**: 735
- Li G, Zhou J, Jia H, Gao Z, Fan M, Luo Y, Zhao P, Xue S, Li N, Yuan Y, Ma S, Kong Z, Jia L, An X, Jiang G, Liu W, Cao W, Zhang R, Fan J, Xu X, Liu Y, Kong Q, Zheng S, Wang Y, Qin B, Cao S, Ding Y, Shi J, Yan H, Wang X, Ran C, Ma Z** (2019) Mutation of a histidine-rich calcium-binding-protein gene in wheat confers resistance to Fusarium head blight. *Nature Genetics* **51**: 1106-1112
- Liang M, Davis E, Gardner D, Cai X, Wu Y** (2006) Involvement of AtLAC15 in lignin synthesis in seeds and in root elongation of Arabidopsis. *Planta* **224**: 1185
- Lionetti V, Giancaspro A, Fabri E, Giove SL, Reem N, Zabolina OA, Blanco A, Gadaleta A, Bellincampi D** (2015) Cell wall traits as potential resources to improve resistance of durum wheat against Fusarium graminearum. *BMC Plant Biology* **15**: 6
- Livak KJ, Schmittgen TD** (2001) Analysis of relative gene expression data using real-time quantitative PCR and the 2^{(-Delta Delta C(T))} Method. *Methods* **25**: 402-408
- Ma M, Yan Y, Huang L, Chen M, Zhao H** (2012) Virus-induced gene-silencing in wheat spikes and grains and its application in functional analysis of HMW-GS-encoding genes. *BMC Plant Biology* **12**: 141
- Mary Wanjiru W, Zhensheng K, Buchenauer H** (2002) Importance of cell wall degrading enzymes produced by fusarium graminearum during infection of wheat heads. *European Journal of Plant Pathology* **108**: 803-810
- Matsuda F, Yonekura-Sakakibara K, Niida R, Kuromori T, Shinozaki K, Saito K** (2009) MS/MS spectral tag-based annotation of non-targeted profile of plant secondary metabolites. *Plant J* **57**: 555-577
- McMullen M, Bergstrom G, De Wolf E, Dill-Macky R, Hershman D, Shaner G, Van Sanford D** (2012) A unified effort to fight an enemy of wheat and barley: Fusarium head blight. *Plant Dis* **96**: 1712-1728
- McMullen M, Jones R, Gallenberg D** (1997) Scab of wheat and barley: A re-emerging disease of devastating impact. *Plant Dis* **81**: 1340-1348
- Menden B, Kohlhoff M, Moerschbacher BM** (2007) Wheat cells accumulate a syringyl-rich lignin during the hypersensitive resistance response. *Phytochemistry* **68**: 513-520

- Miao YC, Liu CJ** (2010) ATP-binding cassette-like transporters are involved in the transport of lignin precursors across plasma and vacuolar membranes. *Proc Natl Acad Sci U S A* **107**: 22728-22733
- Morris GM, Huey R, Lindstrom W, Sanner MF, Belew RK, Goodsell DS, Olson AJ** (2009) AutoDock4 and AutoDockTools4: Automated docking with selective receptor flexibility. *J Comput Chem* **30**: 2785-2791
- Mot AC, Silaghi-Dumitrescu R** (2012) Laccases: Complex architectures for one-electron oxidations. *Biochemistry (Moscow)* **77**: 1395-1407
- Mottiar Y, Vanholme R, Boerjan W, Ralph J, Mansfield SD** (2016) Designer lignins: harnessing the plasticity of lignification. *Curr Opin Biotechnol* **37**: 190-200
- Nakano Y, Yamaguchi M, Endo H, Rejab NA, Ohtani M** (2015) NAC-MYB-based transcriptional regulation of secondary cell wall biosynthesis in land plants. *Frontiers in Plant Science* **6**: 288
- Naoumkina MA, Modolo LV, Huhman DV, Urbanczyk-Wochniak E, Tang Y, Sumner LW, Dixon RA** (2010) Genomic and coexpression analyses predict multiple genes involved in triterpene saponin biosynthesis in *Medicago truncatula*. *The Plant cell* **22**: 850-866
- Pluskal T, Castillo S, Villar-Briones A, Orešič M** (2010) MZmine 2: Modular framework for processing, visualizing, and analyzing mass spectrometry-based molecular profile data. *BMC Bioinformatics* **11**: 395
- Pogorelko G, Lionetti V, Fursova O, Sundaram RM, Qi M, Whitham SA, Bogdanove AJ, Bellincampi D, Zobotina OA** (2013) *Arabidopsis* and *Brachypodium distachyon* transgenic plants expressing *Aspergillus nidulans* acetyltransferases have decreased degree of polysaccharide acetylation and increased resistance to pathogens. *Plant physiology* **162**: 9-23
- Pushpa D, Yogendra KN, Gunnaiah R, Kushalappa AC, Murphy A** (2014) Identification of late blight resistance-related metabolites and genes in potato through nontargeted metabolomics. *Plant Molecular Biology Reporter* **32**: 584-595
- Rawat N, Pumphrey MO, Liu S, Zhang X, Tiwari VK, Ando K, Trick HN, Bockus WW, Akhunov E, Anderson JA, Gill BS** (2016) Wheat *Fhb1* encodes a chimeric lectin with agglutinin domains and a pore-forming toxin-like domain conferring resistance to *Fusarium* head blight. *Nat Genet* **48**: 1576-1580
- Ris-Stalpers C, Trifiro MA, Kuiper GG, Jenster G, Romalo G, Sai T, van Rooij HC, Kaufman M, Rosenfield RL, Liao S, et al.** (1991) Substitution of aspartic acid-686 by histidine or asparagine in the human androgen receptor leads to a functionally inactive protein with altered hormone-binding characteristics. *Mol Endocrinol* **5**: 1562-1569
- Sattler S, Funnell-Harris D** (2013) Modifying lignin to improve bioenergy feedstocks: strengthening the barrier against pathogens?†. *Frontiers in Plant Science* **4**: 70
- Scofield SR, Huang L, Brandt AS, Gill BS** (2005) Development of a Virus-Induced Gene-Silencing System for Hexaploid Wheat and Its Use in Functional Analysis of the Lr21-Mediated Leaf Rust Resistance Pathway. *Plant Physiology* **138**: 2165
- Singh R, Rathore YS, Singh NS, Peddada N, Ashish, Raychaudhuri S** (2013) Substitution of glutamate residue by lysine in the dimerization domain affects DNA binding ability of *hapr* by inducing structural deformity in the DNA binding domain. *PLOS ONE* **8**: e76033

- Su Z, Bernardo A, Tian B, Chen H, Wang S, Ma H, Cai S, Liu D, Zhang D, Li T, Trick H, St. Amand P, Yu J, Zhang Z, Bai G** (2019) A deletion mutation in TaHRC confers Fhb1 resistance to Fusarium head blight in wheat. *Nature Genetics* **51**: 1099-1105
- Su Z, Jin S, Zhang D, Bai G** (2018) Development and validation of diagnostic markers for Fhb1 region, a major QTL for Fusarium head blight resistance in wheat. *Theor Appl Genet* **131**: 2371-2380
- Thomma BP, Cammue BP, Thevissen K** (2002) Plant defensins. *Planta* **216**: 193-202
- Tobimatsu Y, Schuetz M** (2019) Lignin polymerization: how do plants manage the chemistry so well? *Current Opinion in Biotechnology* **56**: 75-81
- Tohge T, Fernie AR** (2010) Combining genetic diversity, informatics and metabolomics to facilitate annotation of plant gene function. *Nature protocols* **5**: 1210-1227
- Vogt T** (2010) Phenylpropanoid biosynthesis. *Mol Plant* **3**: 2-20
- Voss-Fels KP, Qian L, Gabur I, Obermeier C, Hickey LT, Werner CR, Kontowski S, Frisch M, Friedt W, Snowden RJ, Gottwald S** (2018) Genetic insights into underground responses to Fusarium graminearum infection in wheat. *Scientific reports* **8**: 13153
- Wang W, Zhu Y, Du J, Yang Y, Jin Y** (2015) Influence of lignin addition on the enzymatic digestibility of pretreated lignocellulosic biomasses. *Bioresource Technology* **181**: 7-12
- Webb B, Sali A** (2016) Comparative protein structure modeling using MODELLER. *Curr Protoc Bioinformatics* **54**: 5.6.1-5.6.37
- Xie M, Zhang J, Tschaplinski TJ, Tuskan GA, Chen J-G, Muchero W** (2018) Regulation of lignin biosynthesis and its role in growth-defense tradeoffs. *Frontiers in plant science* **9**: 1427-1427
- Xu B, Escamilla-Trevino LL, Sathitsuksanoh N, Shen Z, Shen H, Zhang YH, Dixon RA, Zhao B** (2011) Silencing of 4-coumarate:coenzyme A ligase in switchgrass leads to reduced lignin content and improved fermentable sugar yields for biofuel production. *New Phytol* **192**: 611-625
- Yang F, Jensen JD, Svensson B, Jorgensen HJ, Collinge DB, Finnie C** (2012) Secretomics identifies Fusarium graminearum proteins involved in the interaction with barley and wheat. *Mol Plant Pathol* **13**: 445-453
- Yogendra KN, Dhokane D, Kushalappa AC, Sarmiento F, Rodriguez E, Mosquera T** (2017) StWRKY8 transcription factor regulates benzyloquinoline alkaloid pathway in potato conferring resistance to late blight. *Plant science : an international journal of experimental plant biology* **256**: 208-216
- Yogendra KN, Pushpa D, Mosa KA, Kushalappa AC, Murphy A, Mosquera T** (2014) Quantitative resistance in potato leaves to late blight associated with induced hydroxycinnamic acid amides. *Funct Integr Genomics* **14**: 285-298
- Zhang S, Liang M, Naqvi NI, Lin C, Qian W, Zhang L-H, Deng YZ** (2017) Phototrophy and starvation-based induction of autophagy upon removal of Gcn5-catalyzed acetylation of Atg7 in *Magnaporthe oryzae*. *Autophagy* **13**: 1318-1330
- Zhang Y, Wu L, Wang X, Chen B, Zhao J, Cui J, Li Z, Yang J, Wu L, Wu J, Zhang G, Ma Z** (2019) The cotton laccase gene GhLAC15 enhances *Verticillium* wilt resistance via an increase in defence-induced lignification and lignin components in the cell walls of plants. *Mol Plant Pathol* **20**: 309-322

- Zhao Q, Nakashima J, Chen F, Yin Y, Fu C, Yun J, Shao H, Wang X, Wang ZY, Dixon RA** (2013) Laccase is necessary and nonredundant with peroxidase for lignin polymerization during vascular development in Arabidopsis. *Plant Cell* **25**: 3976-3987
- Zhong R, Demura T, Ye ZH** (2006) SND1, a NAC domain transcription factor, is a key regulator of secondary wall synthesis in fibers of Arabidopsis. *Plant Cell* **18**: 3158-3170
- Zhong R, Richardson EA, Ye Z-H** (2007) The MYB46 Transcription Factor Is a Direct Target of SND1 and Regulates Secondary Wall Biosynthesis in Arabidopsis. *The Plant Cell* **19**: 2776
- Zhou J, Lee C, Zhong R, Ye ZH** (2009) MYB58 and MYB63 are transcriptional activators of the lignin biosynthetic pathway during secondary cell wall formation in Arabidopsis. *Plant Cell* **21**: 248-266
- Zimmermann L, Stephens A, Nam SZ, Rau D, Kubler J, Lozajic M, Gabler F, Soding J, Lupas AN, Alva V** (2018) A completely reimplemented mpi bioinformatics toolkit with a new hhpred server at its core. *J Mol Biol* **430**: 2237-2243

Table 4.1 List of high fold change resistance-related induced metabolites identified in NIL-R+BSMV:*Talac4* (*TaLAC4* silenced NILs).

SI No.	Observed Mass ^d	Exact Mass	AME	Database ID	Name	Fold Change	Classification
1	246.0534	246.053	2.3068	C2162	Isopimpinellin	13.7**	Coumarins
2	330.0956	330.095	1.5293	C20470	1-O-Vanilloyl-beta-D-glucose	4.26**	HCAAs
3	580.2152	580.216	-0.7401	C189	(+)-Syringaresinol O-beta-D-glucoside	3.42*	Phenylpropanoids
4	340.3344	340.334	0.7581	C8281	Docosanoic acid	2.76**	Cutin, suberine and wax biosynthesis
5	326.1349	326.137	-5.1653	C15451	Hinokitiol glucoside	2.67**	Flavonoids
6	578.2006	578.2	1.1499	C1876	Podorhizol beta-D-glucoside	2.38**	Phenylpropanoids
7	342.1315	342.132	-0.0965	C761	Coniferin	2.48*	Phenylpropanoids
8	236.0680	236.069	-1.9681	C9313	5,6,7-Trimethoxycoumarin	2.22**	Coumarins

Significance (Students *t*-test): *P < 0.05, **P < 0.01.

Detailed compound identification is presented in Supp. Table 4.2. AME: Accurate Mass Error= ((Observed mass - expected mass) / expected mass) X 10⁶, Fold-change of resistance-related induced (RRI) metabolites, where **RRI** = (NIL-R (P)+BSMV:00/ NIL-R (M)+ BSMV:00)/(NIL-R (P)+BSMV:*Talac4*/ NIL-R (M)+ BSMV:*Talac4*); R is resistant genotype, P & M are pathogen or mock inoculated; BSMV:00 is non-silenced; BSMV:*Talac4* is silenced.

Table 4.2 GenBank accession numbers of proteins used in the phylogeny study.

S.No.	Purpose	Name of gene/Protein/region	Genbank Accession number	Plant source	Reference/ Source
1	Protein phylogeny	unnamed protein product	CDM80721.1	Triticum aestivum	NCBI
2	Protein phylogeny	unnamed protein product	VAH81677.1	Triticum turgidum subsp. durum	NCBI

^d Observed Mass: To the observed mass one H mass was added because the LC/MS analysis was done in negative ionization mode.

3	Protein phylogeny	laccase-4-like	XP_020188127.1	<i>Aegilops tauschii</i> subsp. <i>tauschii</i>	NCBI
4	Protein phylogeny	predicted protein	BAJ99773.1	<i>Hordeum vulgare</i> subsp. <i>vulgare</i>	NCBI
5	Protein phylogeny	Laccase-4	EMS51326.1	<i>Triticum urartu</i>	NCBI
6	Protein phylogeny	laccase-4	XP_003564592.1	<i>Brachypodium distachyon</i>	NCBI
7	Protein phylogeny	laccase LAC5-6	AAL73968.1	<i>Lolium perenne</i>	NCBI
8	Protein phylogeny	PREDICTED: laccase-4	XP_006644993.1	<i>Oryza brachyantha</i>	NCBI
9	Protein phylogeny	laccase-4	XP_004970542.1	<i>Setaria italica</i>	NCBI
10	Protein phylogeny	laccase-4	XP_025814142.1	<i>Panicum hallii</i>	NCBI
11	Protein phylogeny	Laccase-4	PWZ31748.1	<i>Zea mays</i>	NCBI
12	Protein phylogeny	laccase-13	XP_002458747.1	<i>Sorghum bicolor</i>	NCBI
13	Protein phylogeny	laccase-13-like	XP_025814042.1	<i>Panicum hallii</i>	NCBI
14	Protein phylogeny	laccase-4-like	XP_020113582.1	<i>Ananas comosus</i>	NCBI
15	Protein phylogeny	laccase-4	XP_010920538.1	<i>Elaeis guineensis</i>	NCBI
16	Protein phylogeny	laccase-17-like	XP_021912089.1	<i>Carica papaya</i>	NCBI
17	Protein phylogeny	laccase-17	XP_006424707.1	<i>Citrus clementina</i>	NCBI
18	Protein phylogeny	laccase-17-like	XP_008785574.1	<i>Phoenix dactylifera</i>	NCBI
19	Protein phylogeny	laccase-17	XP_012064932.1	<i>Jatropha curcas</i>	NCBI
20	Protein phylogeny	Laccase 17	EOY13993.1	<i>Theobroma cacao</i>	NCBI
21	Protein phylogeny	laccase-17-like	XP_017618468.1	<i>Gossypium arboreum</i>	NCBI
22	Protein phylogeny	laccase-17	XP_011094888.1	<i>Sesamum indicum</i>	NCBI
23	Protein phylogeny	laccase-17-like	XP_021757290.1	<i>Chenopodium quinoa</i>	NCBI
24	Protein phylogeny	laccase-17-like	XP_010922297.1	<i>Elaeis guineensis</i>	NCBI
25	Protein phylogeny	laccase-17-like	XP_012465812.1	<i>Gossypium raimondii</i>	NCBI
26	Protein phylogeny	unnamed protein product	CBI16199.3	<i>Vitis vinifera</i>	NCBI

Table 4.3 List of primers used in the experiments.

	Name	Forward	Reverse
Gene sequencing	<i>TaLAC4</i>	ATGGCCATTACTATCTCCTCCGG	TCAGCATTTGGGCATGTCAGAC
Gene expression	<i>TaLAC4</i>	GAACAACGTCTCCCTAGTGC	GTGTAGTTGAACGGCGACA
VIGS Fragment amplification	<i>TaLAC4_VIGS</i>	GATACTCATGTGTGCCATGGTT	AAGAAAGTCAGCTATGAACGGG
VIGS gene expression	<i>VIGS_TaLAC4</i>	GATACTCATGTGTGCCATGGTT	AAGAAAGTCAGCTATGAACGGG
Fungal biomass	<i>Tri6</i>	TCTTTGTGAGCGGACGGGACTTTA	TGTTGGTTTGTGCTTGGACTCAT
Reference gene	<i>TaActin</i>	ACCTTCAGTTGCCAGCAAT	CAGAGTCGAGCACAAATACCAGT TG

Figure 4.1 Physical map of the QTL-Fhb1 on the short arm of wheat chromosome 3B. Location of the flanking markers (yellow color) reported by Cuthbert et al. (2006) (Cuthbert et al., 2006) are shown on the left side and location of laccase (*TaLAC4*) identified within the QTL-Fhb1 as one of the candidate genes among five potential candidates identified is shown on the right side.

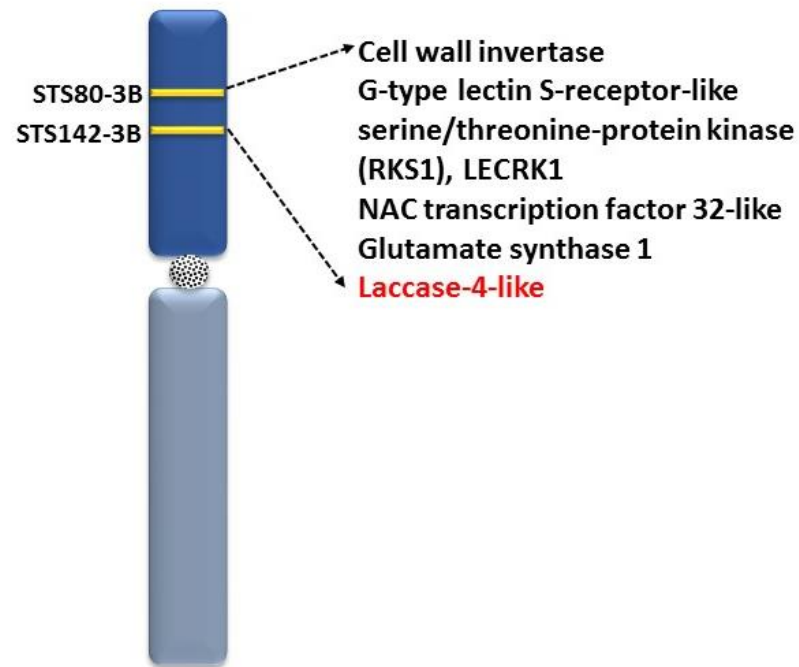
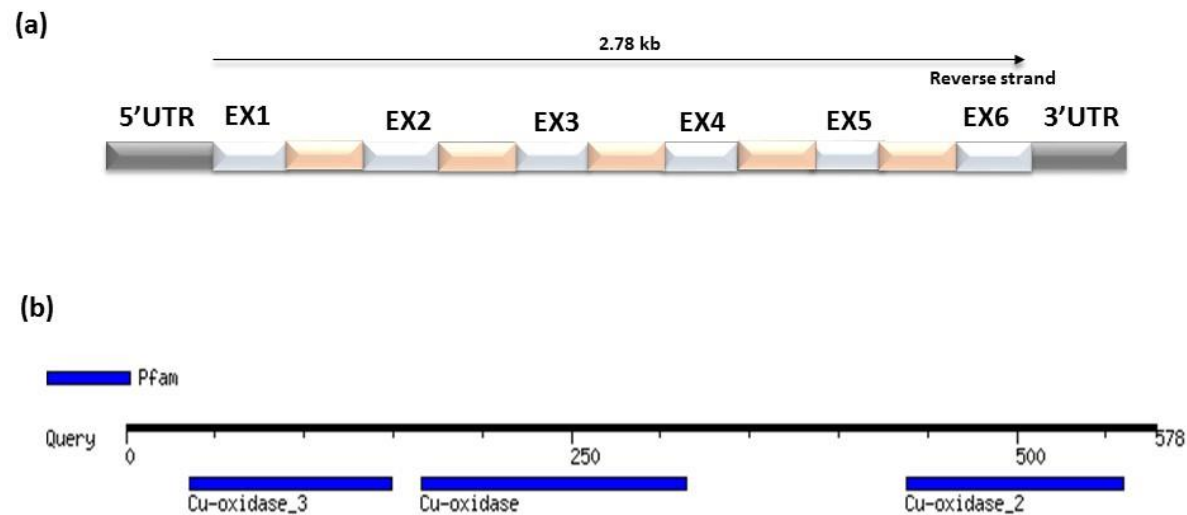
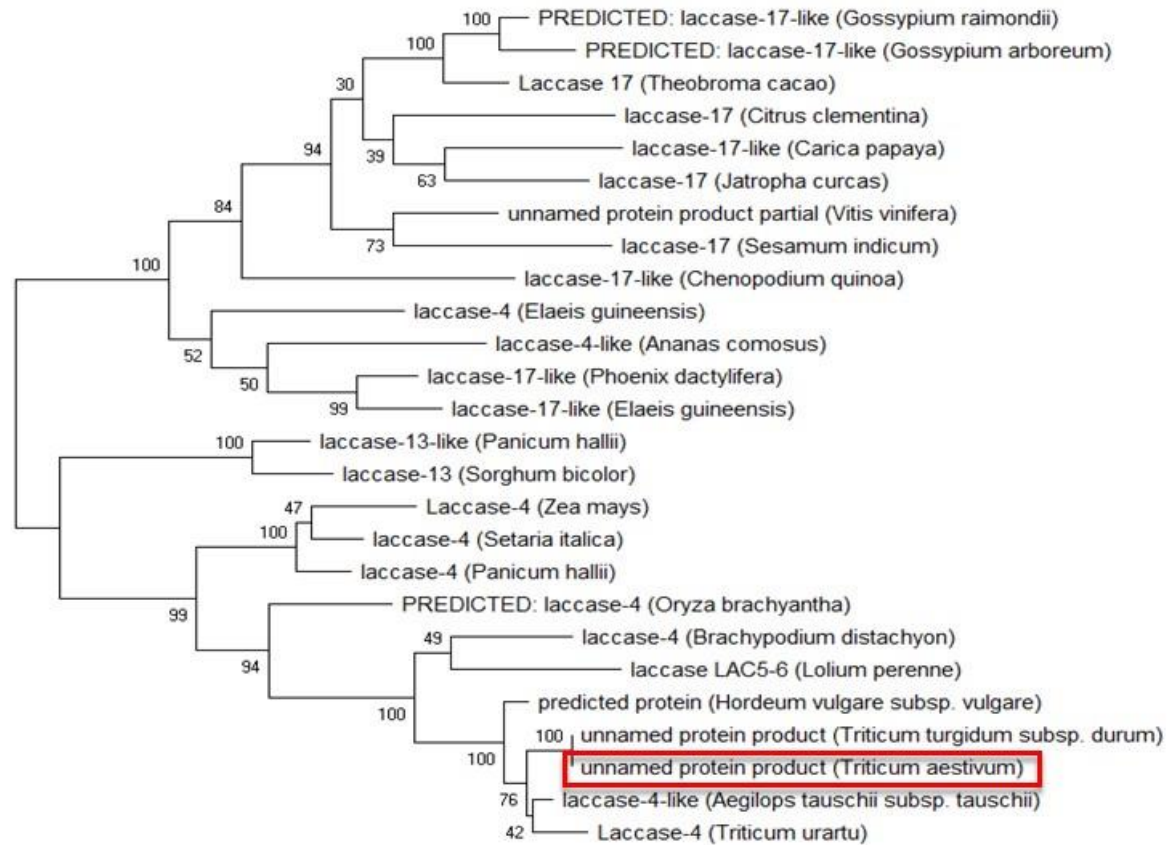


Figure 4.2 Ab-initio characterization of *TaLAC4* gene. (a) Schematic diagram depicting the *TaLAC4* gene structure containing exon, intron and coding regions; (b) Conserved domain predicted based on NCBI Conserved Domain Database Search, it shows the presence of three conserved Cu-oxidase domains; (c) The phylogenetic analysis was based on proteins like TaLAC4 protein retrieved from NCBI database BLAST search with >70 % sequence identity. Sequences were aligned with MUSCLE. Evolutionary analyses were conducted in MEGA7. Bootstrap confidence values were based on 100 iterations. The evolutionary distances were computed using the Poisson correction method. MEGA7 was used to generate the phylogenetic tree using a maximum-likelihood method. The NCBI accession numbers of all the proteins used are provided in Table 4.2.



(c)



0.050

Figure 4.3 Molecular docking of TaLAC4 with lignin model compounds. Lignin model compounds with their respective binding sites, (a) sinapyl alcohol (L1: PHE`267/CA, GLN` 265\CA), (b) guaiacyl 4-O-5 guaiacyl (L2: PHE`267/CD1), (c) syringyl β -O-4 syringyl β -O-4 sinapyl alcohol (L3: TRP`316/CE2), and (d) guaiacyl β -O-4 syringyl β - β syringyl β -O-4 guaiacyl (L3: TRP`316/CE2) on the macromolecule (TaLAC4) was performed using AutoDockTools.

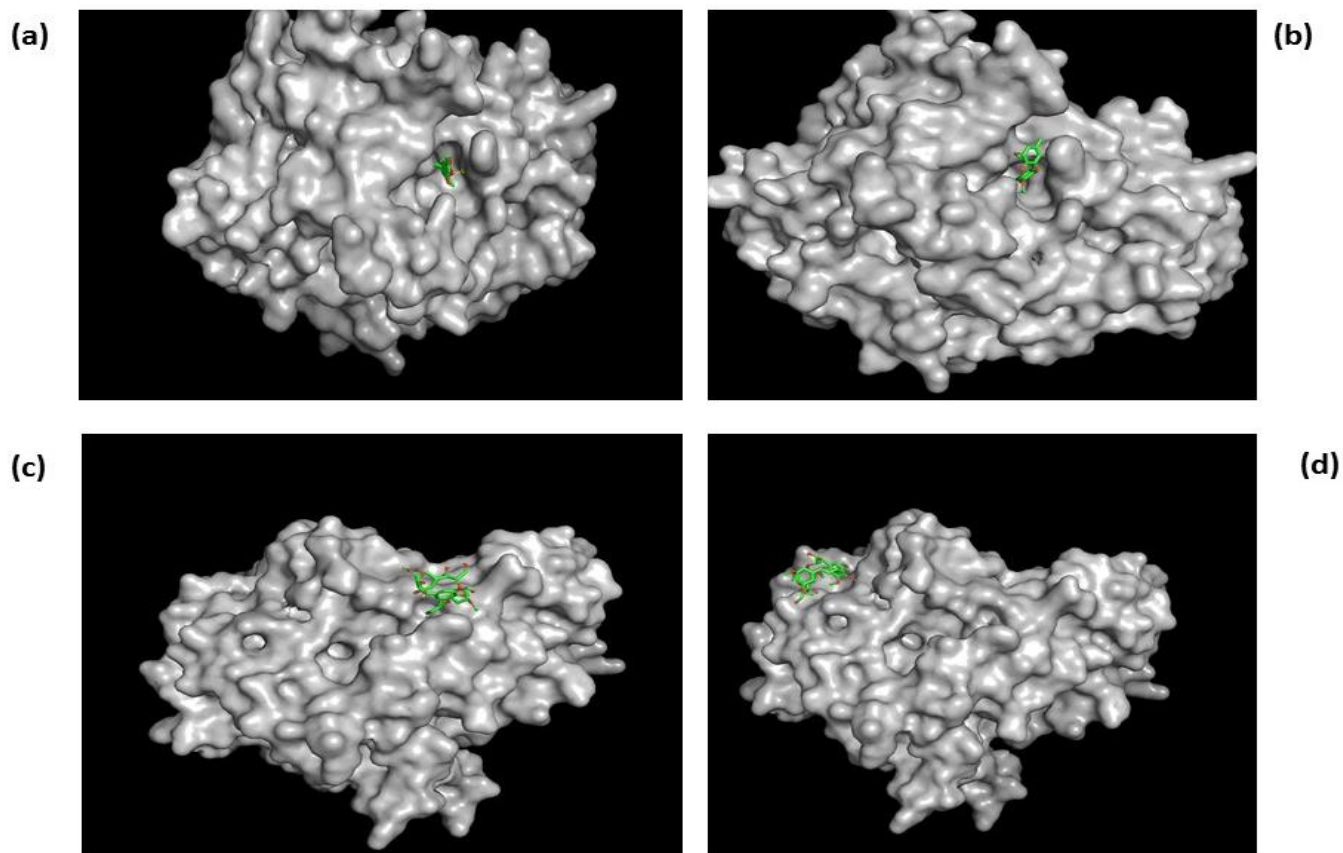


Figure 4.4 Sequencing of *TaLAC4* gene in the NILs with contrasting alleles. (a) Polymorphism screening of *TaLAC4* gene among resistant and susceptible NILs. Multiple sequence alignment of *TaLAC4* gene sequences identified two significant substitutions, lysine to glutamate at position 250 (K250E) and histidine to aspartate at position 252 (H252D) in NIL-S. These mutations have been previously reported to affect DNA binding ability and dissociating ligand-receptor complex, respectively (Ris-Stalpers et al., 1991; Singh et al., 2013); (b) Relative gene expression of *TaLAC4* in resistant and susceptible NIL induced by *F. graminearum* and mock (water) inoculation at 48 hpi based on qRT-PCR. Here target gene expression is normalized to reference gene *TaActin*. Significant differences in expression levels of RP as compared to SP using Students *t*-test: *P<0.05; **P<0.01.

(a)

```

1      10     20     30     40     50     60     70     80     90     100    110    120    130
Laccase_CS      MRLTSSGLRCSLLRHLIALLVYQRIQIIRAYDFILDMNRYTALCGTRKSELYIVAGDFPQPELLLRKLGQRVYVRYINRVAIHHGIDRAGLRDRRTGDRDGMYYTQCPIDKGGQYVYKIVYDQRGTLNHH
Laccase_SMLL    MRLTSSGLRCSLLRHLIALLVYQRIQIIRAYDFILDMNRYTALCGTRKSELYIVAGDFPQPELLLRKLGQRVYVRYINRVAIHHGIDRAGLRDRRTGDRDGMYYTQCPIDKGGQYVYKIVYDQRGTLNHH
Laccase_RNLL    MRLTSSGLRCSLLRHLIALLVYQRIQIIRAYDFILDMNRYTALCGTRKSELYIVAGDFPQPELLLRKLGQRVYVRYINRVAIHHGIDRAGLRDRRTGDRDGMYYTQCPIDKGGQYVYKIVYDQRGTLNHH
Consensus      MRLTSSGLRCSLLRHLIALLVYQRIQIIRAYDFILDMNRYTALCGTRKSELYIVAGDFPQPELLLRKLGQRVYVRYINRVAIHHGIDRAGLRDRRTGDRDGMYYTQCPIDKGGQYVYKIVYDQRGTLNHH

131    140    150    160    170    180    190    200    210    220    230    240    250    260
Laccase_CS      RNTSHFRSTVYGGVTLPKLGGVYPPFAPRQKELPPVTFGQWASGTEFATVNTALKVGGRPHTSDRFTTNGILPAPLINCGRKDTFQKVPFGKRYLLRLVHARENDLFFSVNHHITVVEVDRVYVYKPF
Laccase_SMLL    RNTSHFRSTVYGGVTLPKLGGVYPPFAPRQKELPPVTFGQWASGTEFATVNTALKVGGRPHTSDRFTTNGILPAPLINCGRKDTFQKVPFGKRYLLRLVHARENDLFFSVNHHITVVEVDRVYVYKPF
Laccase_RNLL    RNTSHFRSTVYGGVTLPKLGGVYPPFAPRQKELPPVTFGQWASGTEFATVNTALKVGGRPHTSDRFTTNGILPAPLINCGRKDTFQKVPFGKRYLLRLVHARENDLFFSVNHHITVVEVDRVYVYKPF
Consensus      RNTSHFRSTVYGGVTLPKLGGVYPPFAPRQKELPPVTFGQWASGTEFATVNTALKVGGRPHTSDRFTTNGILPAPLINCGRKDTFQKVPFGKRYLLRLVHARENDLFFSVNHHITVVEVDRVYVYKPF

261    270    280    290    300    310    320    330    340    350    360    370    380    390
Laccase_CS      VKTLVTSFGDTINALLNITKPRPGRNFYDPRPYSITDQSTFQNSIVAGLELYRNPSSPRAISFQKLPIDKPLQYFMDTDFYKFTLRLSLRATKQYPRAPQSVDRRFFFTIGLGLPCPKHATCGS
Laccase_SMLL    VKTLVTSFGDTINALLNITKPRPGRNFYDPRPYSITDQSTFQNSIVAGLELYRNPSSPRAISFQKLPIDKPLQYFMDTDFYKFTLRLSLRATKQYPRAPQSVDRRFFFTIGLGLPCPKHATCGS
Laccase_RNLL    VKTLVTSFGDTINALLNITKPRPGRNFYDPRPYSITDQSTFQNSIVAGLELYRNPSSPRAISFQKLPIDKPLQYFMDTDFYKFTLRLSLRATKQYPRAPQSVDRRFFFTIGLGLPCPKHATCGS
Consensus      VKTLVTSFGDTINALLNITKPRPGRNFYDPRPYSITDQSTFQNSIVAGLELYRNPSSPRAISFQKLPIDKPLQYFMDTDFYKFTLRLSLRATKQYPRAPQSVDRRFFFTIGLGLPCPKHATCGS

391    400    410    420    430    440    450    460    470    480    490    500    510    520
Laccase_CS      PNSTQFRRVYNSLVLPSITALLQSHITGLTSGVYRHHFPAKPLSPFNATGTPPNATVATGKLLALSFNTSVELVHQDTSLDGETSPLHLRAGNFFVYGGQFQYDVKDPKAFNLVDPVFRNTVGY
Laccase_SMLL    PNSTQFRRVYNSLVLPSITALLQSHITGLTSGVYRHHFPAKPLSPFNATGTPPNATVATGKLLALSFNTSVELVHQDTSLDGETSPLHLRAGNFFVYGGQFQYDVKDPKAFNLVDPVFRNTVGY
Laccase_RNLL    PNSTQFRRVYNSLVLPSITALLQSHITGLTSGVYRHHFPAKPLSPFNATGTPPNATVATGKLLALSFNTSVELVHQDTSLDGETSPLHLRAGNFFVYGGQFQYDVKDPKAFNLVDPVFRNTVGY
Consensus      PNSTQFRRVYNSLVLPSITALLQSHITGLTSGVYRHHFPAKPLSPFNATGTPPNATVATGKLLALSFNTSVELVHQDTSLDGETSPLHLRAGNFFVYGGQFQYDVKDPKAFNLVDPVFRNTVGY

521    530    540    550    560    570    570
Laccase_CS      PGGGAVIRFLADNPGVVFYKCHLEVHTDGLRHRHQVQGGSKPSQKLLPPSPDAPIC
Laccase_SMLL    PGGGAVIRFLADNPGVVFYKCHLEVHTDGLRHRHQVQGGSKPSQKLLPPSPDAPIC
Laccase_RNLL    PGGGAVIRFLADNPGVVFYKCHLEVHTDGLRHRHQVQGGSKPSQKLLPPSPDAPIC
Consensus      PGGGAVIRFLADNPGVVFYKCHLEVHTDGLRHRHQVQGGSKPSQKLLPPSPDAPIC

```

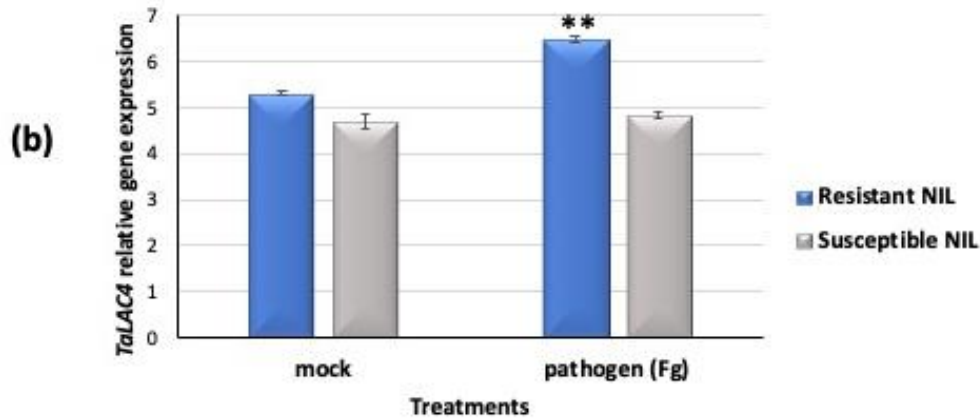


Figure 4.5 Virus-induced gene silencing (VIGS) fragments were designed to specifically knock-down the *TaLAC4* gene. The knock-down fragment comprising the coding region and 3' UTR region is boxed.

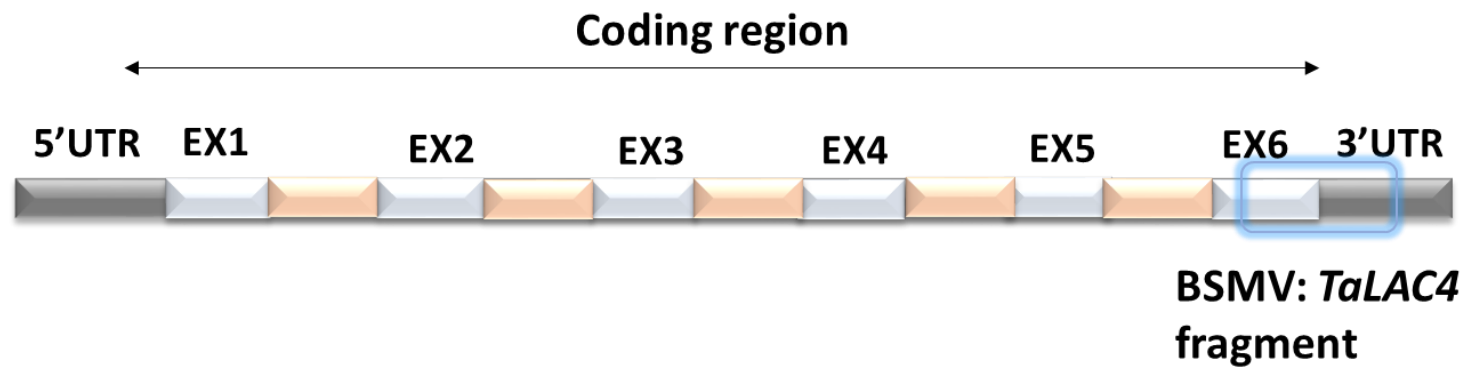


Figure 4.6 BSMV based virus-induced gene silencing of the phytoene desaturase (PDS) gene. Efficacy of BSMV based virus-induced gene silencing where resistant NIL spikes rub inoculated with PDS gene fragment (BSMV:TaPDS) shows bleaching symptom compared to the negative control (BSMV:00).



Figure 4.7 BSMV based virus-induced gene silencing of *TaLAC4* gene. (a) *F. graminearum*-infected spikes of wheat resistant NILs with *TaLAC4* non-silenced and silenced spikes and rachis samples, respectively, at 15 dpi. The red arrow indicates the spikelet inoculated; (b) Confirmation of knocking down of *TaLAC4* by assaying relative transcript expression of *TaLAC4* normalized to reference gene *TaActin* in NIL-R+BSMV: *Talac4* (silenced plant) wheat NILs compared to NIL-R+BSMV:00 (non-silenced plant) at 48 hpi post- *F. graminearum* inoculation. Significant differences in expression of BSMV:*Talac4* (silenced) as compared to BSMV:00 (non-silenced) were analyzed using Student's *t*- test: * $P < 0.05$; ** $P < 0.01$.

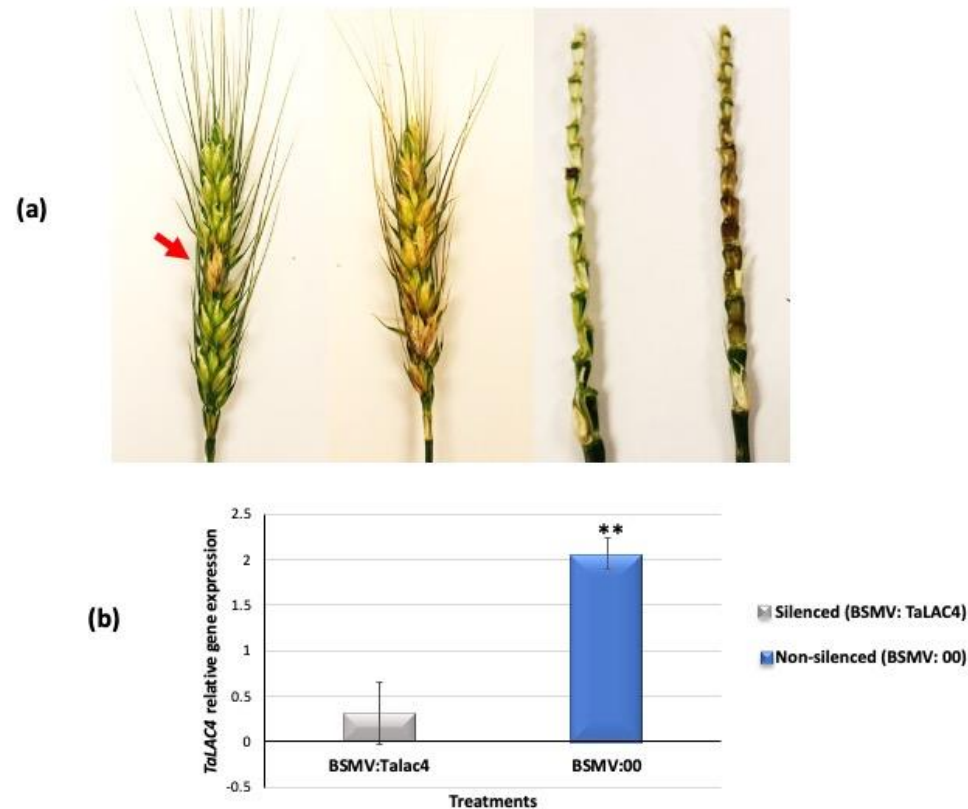


Figure 4.8 Effect of *TaLAC4* silencing in FHB resistant near-isogenic line (NIL-R), inoculated with *F. graminearum* or mock-solution. Confirmation of knocking down of *TaLAC4* by analyzing disease severity and fungal biomass in NILs, based on visual observations and qPCR following point inoculation of *F. graminearum*; (a) Proportion of spikelets diseased (PSD); (b) Fungal biomass in BSMV-infected plants at 6 dpi with *F. graminearum*. Relative copy number of *tri6* fungal housekeeping gene (=fungal biomass) was quantified in *TaLAC4* knocked down (BSMV:*Talac4*) plants and compared with control (BSMV:00). Here relative target gene copy number is normalized to reference gene *TaActin*. Significant differences in expression of BSMV:*Talac4* (silenced) as compared to BSMV:00 (non-silenced) were analyzed using Student's *t*-test: **P* < 0.05; ***P* < 0.01.

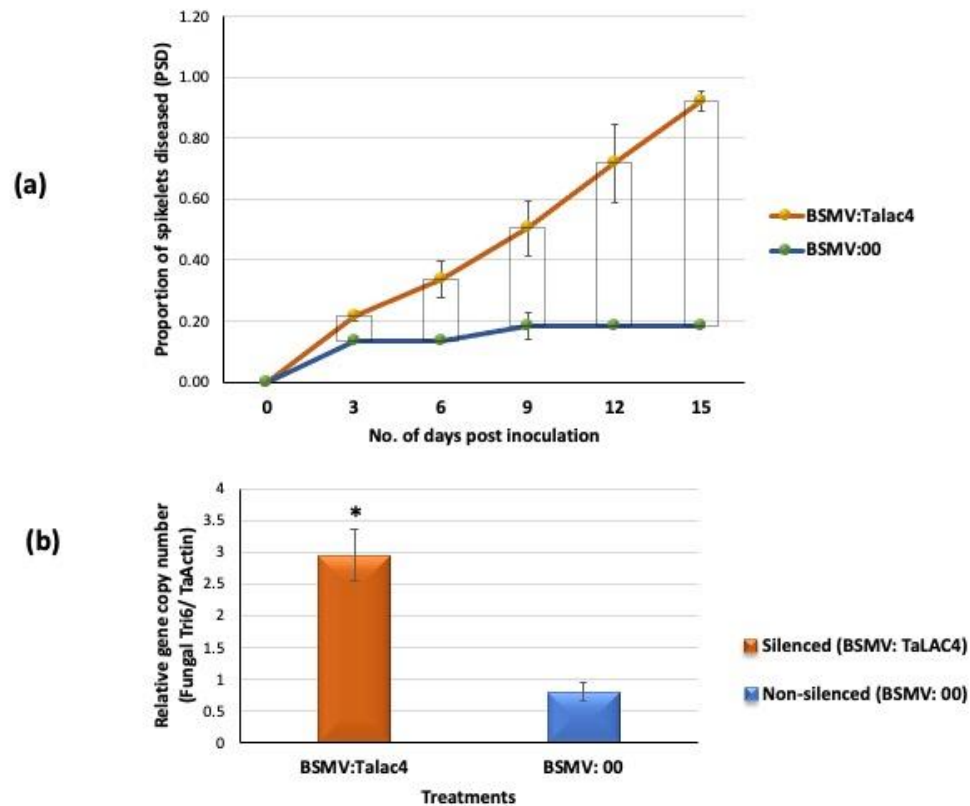
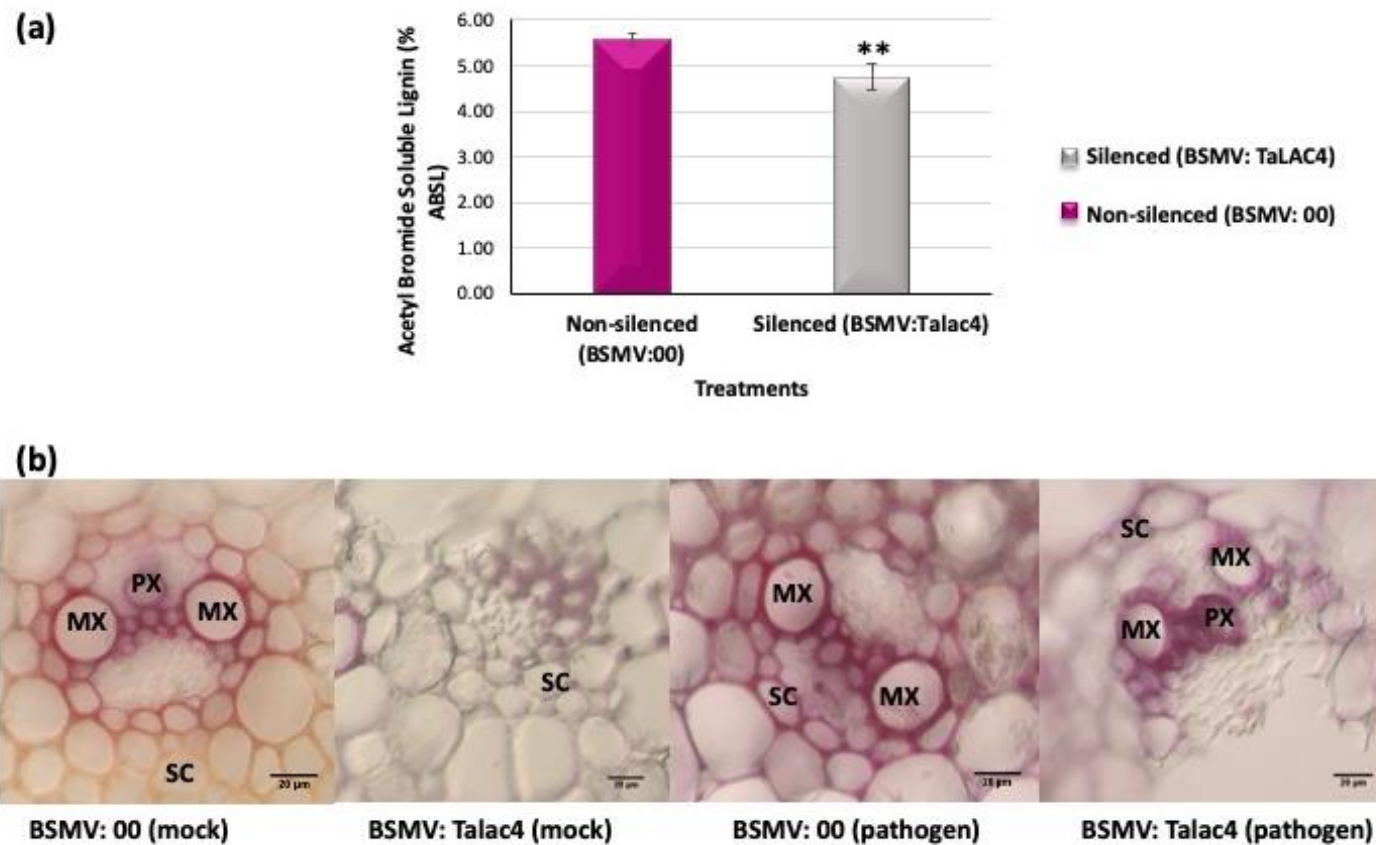


Figure 4.9 Total lignin quantification using acetyl bromide method and phloroglucinol-HCL staining. (a) the graph showing %ABSL (acetyl bromide soluble lignin) in both BSMV:*Talac4* (silenced) and BSMV:00 (non-silenced) samples; (b) Phloroglucinol-HCL staining of rachis cross-section for lignin detection. BSMV:*Talac4* (silenced) mock or pathogen inoculated; BSMV:00 (non-silenced) mock or pathogen inoculated, MX: metaxylem, PX: protoxylem, SC: sclerenchyma cells. Significant differences in %ABSL of BSMV:*Talac4* (silenced) as compared to BSMV:00 (non-silenced) using Students *t*-test: * $P < 0.05$; ** $P < 0.01$.



CONNECTING STATEMENT FOR CHAPTER V

In the previous sections, based on a combined metabolo-genomics approach, we have identified few potential candidates for FHB resistance and a higher accumulation of resistance-related induced metabolites mainly related to the phenylpropanoid pathway. In the last Chapter, we have investigated the role of *TaLAC4* associated with cell wall reinforcement due to induced G lignin deposition as the possible resistance mechanism predominant in wheat QTL-Fhb1. In Arabidopsis, secondary wall-associated NAC domain (SND) and its close homologs NAC secondary wall thickening promoting factor (NST), including vascular-related NAC-domain (VND), act as master switches to regulate the activation of the cellulose, xylan and lignin biosynthetic genes (Zhong et al., 2006; Mitsuda et al., 2007). However, the primary transcriptional regulatory mechanism of lignin and secondary cell wall biosynthesis mediated by NAC transcription factor in response to pathogen attack is less explored. Therefore, Chapter V explores the potential role of a NAC transcription factor 32-like in regulating the expression of the *TaLAC4* gene and other lignin specific pathway genes to combat *F. graminearum* infection through cell wall reinforcement. Thus, it was hypothesized that the silencing of the *TaNAC032* in the resistant NIL would compromise resistance against FHB drastically since it would be inapt to synthesize RR metabolite(s) significantly higher in abundance, which directly or indirectly limits pathogen progression. Among the potential candidates for FHB resistance discussed in Chapter III, NAC transcription factor 32-like was one of the potential candidates underlying QTL-Fhb1. Therefore, this study was aimed to characterize *TaNAC032* in wheat NILs for FHB resistance functionally and to understand the regulatory network it encompasses.

Nancy Soni wrote the first draft of the manuscript, and she conceived the experimental design, performed all the laboratory and greenhouse experiments. Mr. Bara Altartouri assisted with microscopy. Mr. Niranjana Hegde provided valuable suggestions related to the gene silencing experiment and assisted in greenhouse work. Dr. Raj Duggavathi provided lab access to perform qRT-PCR and tissue sectioning for histochemical study. Dr. Farhad Nazarian-Firouzabadi provided a protocol for qRT-PCR data analysis. Dr. Kushalappa conceived the idea, aided in designing the experiments and edited the drafts of the manuscript.

CHAPTER V

***TaNAC032* transcription factor regulates lignin-biosynthetic genes to combat *Fusarium* head blight in wheat**

Nancy Soni¹, Bara Altartouri², Niranjan Hegde¹, Raj Duggavathi³, Farhad nazarian-Firouzabadi⁴ and Ajjamada C. Kushalappa¹

¹Plant Science Department, McGill University, Quebec, Canada; ²Department of Biological Sciences, Université de Montréal, Quebec, Canada; ³Animal Science Department, McGill University, Quebec, Canada, ⁴Department of Agronomy and Plant Breeding, Lorestan University, Khorramabad, Iran

***Corresponding author:**

Dr. Ajjamada C. Kushalappa

Professor, McGill University

Ste. Anne-de-Bellevue, QC, Canada H9X3V9

Tel: 1(514-709-5874) Email: ajjamada.kushalappa@mcgill.ca

Reprinted with permission from Elsevier:

Soni N, Altartouri, B, Hegde N, Duggavathi, R, Nazarian-Firouzabadi, F. and Kushalappa AC, 2020. *TaNAC032* transcription factor regulates lignin-biosynthetic genes to combat *Fusarium* head blight in wheat. *Plant Science* p.110820.

<https://doi.org/10.1016/j.plantsci.2021.110820>

5.1 Abstract

Fusarium head blight (FHB) is a destructive disease affecting cereal crops globally due to mycotoxin contamination of grains that reduce yield and quality. Among hundreds of QTLs identified for resistance, the QTL-Fhb1 is of significant interest even today, for its major contribution to FHB resistance. Previously, QTL-Fhb1 dissection based on a combined metabolomics approach, identified a few potential resistance genes, including a NAC (NAM, ATAF and CUC) like transcription factor for FHB resistance. Sequencing and phylogenetic analysis confirmed NAC to be the wheat *TaNAC032*. Also, the quantitative RT-PCR studies revealed a greater induced expression of *TaNAC032* in resistant NIL in comparison to susceptible NIL upon *Fusarium graminearum* (*Fg*) infection. The virus-induced gene silencing (VIGS) based functional validation of *TaNAC032* in resistant NIL confirmed increased disease severity and fungal biomass. Metabolic profiling revealed low abundances of resistance-related (RR) metabolites in *TaNAC032* silenced NIL-R compared to non-silenced. Silenced plants showed decreased transcript abundances of RR metabolite biosynthetic genes associated with a reduction in total lignin content in rachis, confirming the regulatory role of *TaNAC032* in wheat in response to *Fg* infection. If *TaNAC032* is mutated in an FHB susceptible cultivar, it can be edited to enhance FHB resistance.

5.2 Introduction

Fusarium head blight (FHB) is a severe disease of wheat, barley, and maize worldwide. Among several species, *Fusarium graminearum* (*Fg*) is the most common one identified from FHB affected wheat. The FHB symptoms include discoloration or browning of kernels due to mycotoxin contamination of grains, leading to a reduction in quality and quantity (Bai and Shaner, 2004). FHB epidemics cause severe social or economic turmoil (McMullen et al., 1997). Breeding resistant wheat varieties are an environmentally safe and efficient way to reduce FHB outbreaks (Zhu et al., 2019). Hundreds of quantitative trait loci (QTLs) have been identified wherein >50 QTLs were found to be associated with resistance to *Fg* spread through rachis, following single floret inoculation (type II) (Buerstmayr et al., 2009). Among these, QTL-Fhb1 (syn. *Qfhs.ndsu.3BS*, *Fhb1*) on chromosome arm 3BS has been confirmed to be the most prominent and stable QTL, contributing up to 60% of the phenotypic variations in FHB resistance against distinct genetic backgrounds and environments (Waldron et al., 1999; Anderson et al., 2001; Buerstmayr et al., 2002). The QTL-Fhb1, initially identified in Sumai 3-derived mapping populations, was

later fine mapped to an ~1 Mb interval flanking between molecular markers sts3B-32 and sts3B-206 (Bai et al., 1999; Waldron et al., 1999; Buerstmayr et al., 2002; Choulet et al., 2010). Ever since, different research groups identified several genes and proposed various probable resistance mechanisms, but none has been confirmed without contradictions (Rawat et al., 2016; Schweiger et al., 2016; Su et al., 2019). Therefore, the genetic determinants underlying QTL-Fhb1 contributing to FHB resistance are still elusive.

Map-based cloning of QTL-Fhb1 from Sumai 3, a Chinese wheat cultivar, showed a pore-forming toxin-like (PFT) gene at QTL-Fhb1 conferring FHB resistance (Rawat et al., 2016). Other transcriptome analyses ruled out PFT as the candidate gene using yeast-based assay, including the pathogen-dependent expression analysis, where no anti-fungal activity was observed (Schweiger et al., 2016). Following that, a recent transcriptomic study confirmed putative histidine-rich calcium-binding protein (*TaHRC*) role in conferring QTL-Fhb1 resistance to FHB (Li et al., 2019; Su et al., 2019). Likewise, several genes and differentially accumulated resistance-related (RR) metabolites and proteins in response to *Fg* infection in wheat NILs have been identified based on transcriptomics, metabolomics, and proteomics approach (Liu et al., 2008; Schweiger et al., 2016). However, FHB resistance conferred by these genes has not been validated, except for PFT and *TaHRC*, in QTL-Fhb1 (Rawat et al., 2016; Su et al., 2018; Li et al., 2019).

In response to biotic stress, plants exhibit resistance through hierarchies of resistance (R) genes with roles, including immune receptors (which recognize elicitors/effectors), phytohormone biosynthetic genes, mitogen-activated protein kinases (MAPKs), and transcription factors (TFs). These genes regulate RR metabolite biosynthetic genes and RR protein-coding genes to further suppress the pathogen (Kushalappa et al., 2016). Advancements in integrated omics approaches have paved the way through FHB resistance. Therefore, approaches like metabolomics integrated with genomics or transcriptomics are considered one of the best tools to decipher the underlying mechanisms of genes. For instance, an integrated transcriptomics and metabolomics approach has unveiled the induction of resistance genes and differential accumulation of resistance-related metabolites in wheat and potato against FHB and late blight, respectively (Dhokane et al., 2016; Kage et al., 2017; Yogendra et al., 2017). Similarly, integrated metabolo-genomics studies identified the agmatine coumaroyl transferase (*TaACT*) gene and the *TaWRKY* transcription factor in QTL-2DL, imparting resistance against FHB (Kage et al., 2017; Kage et al., 2017). Our previous study, based on the combined metabolo-genomics approach, has functionally validated the role of

laccase 4 (*TaLAC4*) gene underlying QTL-Fhb1 in pathogen-induced lignification of secondary cell walls to contain the spread of *Fg* to initial infection (Soni et al., 2020).

The NAC (NAM, ATAF and CUC) proteins, which constitute an abundant plant-specific transcription factor (TFs), are characterized by the highly conserved N-terminal NAC domain. Wherein the NAC domain functions as a DNA-binding domain that is imperative for oligomerization into dimers (Olsen et al., 2005; Puranik et al., 2012), and the C-terminal domain functions as a transcriptional regulatory domain (Olsen et al., 2005; Jensen et al., 2010). Functions of several NAC TFs from other plant species have been explored against biotrophic and hemibiotrophic pathogens based on virus-induced gene silencing (VIGS) or antisense mediated suppression in host plants. For instance, the silencing of *TaNAC1*, *TaNAC21/22*, or *TaNAC30* showed enhanced resistance against *Puccinia striiformis* f. sp. *tritici*, whereas *TaNAC30* negatively regulated stripe rust resistance in wheat (Feng et al., 2014; Wang et al., 2015; Wang et al., 2018). Overexpression of *TaNAC6* suggested enhanced resistance against *Blumeria graminis* f. sp. *tritici* (*Bgt*), while silencing compromised the resistance, further confirming the role of *TaNAC6* in resistance against *Bgt* (Zhou et al., 2018).

In *Arabidopsis thaliana*, secondary wall-associated NAC domain protein (SND1) and vascular-related NAC domain 7 (VND7) functions as the master regulators of secondary wall biosynthesis in fibers and vessels (Zhong et al., 2006; Yamaguchi et al., 2011). These NACs along with other secondary walls NACs (SWNs) binds to an imperfect palindromic 19-bp consensus sequence designated as secondary wall NAC binding element (SNBE), (T/A)NN(C/T)(T/C/G)TNNNNNNNA(A/C)GN(A/C/T)(A/T), in the promoters of their direct targets (Zhong et al., 2010). The identification of SWN direct targets (SNBE sites) indicates an essential advancement in dissecting the transcriptional network regulating secondary wall biosynthesis (McCarthy et al., 2011). Subsequently, several studies have reported NAC TFs to regulate lignin biosynthesis, a crucial defense substance in plant cell walls. For instance, secondary wall-associated NAC domain protein/ NAC secondary wall thickening promoting factor 3 (SND1/NST3) and its close homolog NST1, NST2, vascular-related NAC domain 6 (VND6) and VND7 upstream of MYB46/MYB83 are involved in the regulation of lignin biosynthesis in *Arabidopsis* (Zhong et al., 2006). An ethylene response-related factor, *GbERF1*, was associated with increased resistance against *Verticillium dahlia* in *Gossypium barbadense* by activating the lignin biosynthetic pathway genes such as PAL, C4H, C3H, HCT, CoMT, CCR, and F5H (Guo et

al., 2016). However, NAC TF's role, from QTL-Fhb1, in the regulation of phenylpropanoid pathway genes leading to reinforcement of secondary cell walls, in response to *Fg* infection has not been reported.

Although there are 19997 NAC TFs in plant species, including 263 in wheat, knowledge regarding NAC TF roles in plant defense against biotic stress is still limited. Therefore, the identification and functional characterization of NAC TFs in response to pathogen attack is critical to reveal resistance in wheat against FHB. The present study identified and functionally characterized *TaNAC032* TF, in wheat resistant NIL (NIL-R) with an FHB resistance background. Our study revealed that the *TaNAC032* regulated the R genes in the phenylpropanoid pathway, increasing the abundances of RR metabolites that were deposited to reinforce the secondary cell walls around the *Fg* infection site, thus reducing the further advancement of the pathogen from the inoculated spikelet to other spikelets through rachis, conferring a high level of rachis resistance.

5.3 Materials and methods

5.3.1 Plant materials and experimental design

The near-isogenic lines (NILs) used in this study were derived from the mapping population derived from the resistant Chinese spring wheat cultivar, Sumai 3, and FHB susceptible wheat cultivar, Thatcher (Cuthbert et al., 2006). The NILs were genotyped with microsatellite markers and fine mapped within a 1.27-cM interval (S/T) to facilitate the segregation of *Fhb1*, with FHB resistance background (Cuthbert et al., 2006). The seeds of NILs with FHB resistant and susceptible alleles of QTL-Fhb1, with FHB resistance background, were obtained from Dr. S. Fox, AAFC, Winnipeg, Canada. The pots in greenhouse benches were arranged in a randomized complete block design (RCBD) consisting of resistant and susceptible NILs, pathogen and mock inoculations and five biological replications over time (Soni et al., 2020). The experimental units consisted of at least three pots with nine plants. The greenhouse was maintained at 23 ± 2 °C temperature, 16 h photoperiod, and 70 ± 10 % relative humidity throughout the growing period (Kumar et al., 2016). A compound slow-releasing fertilizer 14:14:14 (NPK) was applied once in 15 days, at the rate of 5g per pot (Kage et al., 2017; Karre et al., 2017). Essential steps were taken to prevent the development of any diseases or insects on plants.

5.3.2 Fungal inoculum production and inoculation

F. graminearum isolate (155.SLS) obtained from Dr. S. Rioux, CÉROM, Quebec was initially maintained on potato dextrose agar (PDA) medium (DIFCO Laboratories Detroit, Michigan, USA) for four days at 26 °C. It was sub-cultured on Rye B agar media for four days and exposed to near UV light for three days to produce spores. From these, macroconidia were harvested and spore concentration was adjusted to 1×10^5 macroconidia/ml using a hemocytometer (American Scientific Products, USA). Three alternate spikelets in a spike at 50 % anthesis stage (GS=65) (Zadoks et al., 1974) were point inoculated with ten μ L of either macro conidial suspension or mock solution using a syringe (GASTIGHT 1750 DAD, Reno, USA) (Kumar et al., 2016; Kage et al., 2017; Soni et al., 2020). Plants were covered with transparent bags sprayed with water to maintain high humidity and were removed after 48 hpi (Gunnaiah et al., 2012).

5.3.3 Metabolite extraction and LC-high resolution MS/MS analysis

Metabolites from rachis samples were extracted as described previously (Soni et al., 2020). Briefly, rachis samples collected at 72 hpi were weighed and ground with the pre-chilled mortar and pestle with liquid nitrogen. Metabolites were extracted from 5 replicates for each treatment, initially in 60% ice-cold aqueous methanol and subsequently with 100% ice-cold methanol to extract most of the polar, semi-polar, and non-polar metabolites from the sample (Bollina et al., 2010; Kumar et al., 2016). About 100 μ L of filtrate or sample extract was used for metabolite analysis in a negative ionization mode using a high-resolution mass spectrometer (HRMS) (Q Exactive™ Hybrid Quadrupole-Orbitrap Mass Spectrometer (LC-MS/MS) Thermo Fisher, USA) using a 5 cm XB-C18 kinetex column. The samples were analyzed in a randomized mode to avoid any structural errors associated with the LC-MS. The data files obtained from LC-MS/MS were converted to mzxml/.cdf format and were exported into a bioinformatics tool MZmine2 for peak deconvolution, peak detection, spectral filtering and normalization of peaks (Katajamaa and Oresic, 2005). The abundance of peaks was subjected to a Students *t*-test to identify significant treatment metabolites. The peaks were identified with a compound name based on monoisotopic mass match and fragmentation patterns using different databases PlantCYC, METabolite LINK (METLIN), and Kyoto encyclopedia genes and genomes (KEGG) (Gunnaiah et al., 2012). Further, RR metabolites were classified into resistance-related constitutive (RRC=RM/SM) and resistance-related induced (RRI=(RP/RM)/(SP/SM)) metabolites (Gunnaiah et al., 2012; Kumar et al., 2016).

5.3.4 Identification of NAC as a candidate gene underlying QTL-Fhb1

Our previous study, based on QTL-Fhb1 sequencing, gene expression, and metabolic profiling of resistant and susceptible NILs, identified the *TaLAC4*, in QTL-Fhb1, as a candidate gene for FHB resistance (Soni et al., 2020). This database was further explored to identify a TF that would bind to the *TaLAC4*, to enhance FHB resistance, which revealed a TF NAC 32 like, and this was further explored.

5.3.5 Sanger sequencing and genetic polymorphism analysis

The coding sequence of *TaNAC032* was amplified in wheat genotypes, including NILs derived from S/T population using gene-specific primer pairs (Table 2). A thermal cycler (Bio-Rad, Mississauga, ON, Canada) was used to carry out gene amplification set to the following conditions: initial denaturation at 95 °C for 5 min followed by 35 cycles of 94 °C for the 30 s, 56 °C for 1 min, 72 °C for 2 min and a final extension for 10 mins at 72 °C. The PCR products were run on the 1 % agarose gel, and a band size of 950bp was cut and purified from the gel, cloned into the pGEMR-T Easy vector (Promega, USA), and Sanger sequenced using the ABI Automated DNA sequencer. Followed by that, multiple sequence alignment was performed using MultAlin (<http://multalin.toulouse.inra.fr/multalin/>). Also, nucleotide sequences were translated into amino acid sequences using the ExPASy Translate Tool (<http://web.expasy.org/translate/>). The amino acid sequences were then analyzed for the conserved domain using the SMART domain prediction tool (Letunic et al., 2015) and confirmed using the NCBI Conserved Domain Database (NCBI CDD). The protein sequences of more than 80% identity were retrieved from the NCBI database and used to construct a phylogenetic tree using MEGA 7 software with bootstrap confidence value set to 100 iterations, and Poisson correction method for the evolutionary distance measurement. The maximum likelihood method was to construct the tree. All the accession numbers of the sequences from the NCBI database used in building a phylogenetic tree are given in Table 3.

5.3.6 Real-time Quantitative PCR (qRT-PCR)

Total RNA was isolated from three biological replicates using the RNeasy plant mini kit (Qiagen Inc.). Purified total RNA (1–2 µg) was then reverse transcribed into cDNA using an iScript cDNA synthesis kit (BioRad, ON, Canada). The equal quantity of cDNA (20ng) of each sample was initially used to perform semi-qPCR and later confirmed based on real-time qPCR using Qi SYBR Green supermix (BioRad, Canada) in a CFX384™ Real-Time system (BioRad, Canada). *TaActin* transcript level was used to normalize the target mRNA abundance. PCR results were analyzed

using comparative $\Delta\text{-}\Delta$ Ct method ($2\text{-}\Delta\Delta\text{CT}$) (Livak and Schmittgen, 2001). For statistical significance, the Students *t*-test was used. Primer blast software was used for designing primers for qRT-PCR analysis, listed in Table 2.

5.3.7 *In-silico* promoter analysis of RR metabolites biosynthetic genes (*R_{RRM}*) and their interaction with *TaNAC032*

The promoter regions of the phenylpropanoid pathway-related genes were analyzed for secondary wall NAC binding element (SNBE) to identify the direct downstream targets of *TaNAC032* using DNA Pattern Find software https://www.bioinformatics.org/sms2/dna_pattern.html (Zhong et al., 2010). The target gene promoters identified with SNBE sequences were further subjected to constructing a gene target network using the software Genemania v3.1.2; mainly, physical interactions between the targets were considered.

5.3.8 Constructing knockdown vectors, in vitro transcription of viral RNA, and plant inoculation

A highly conserved and unique region of 237bp fragment was used for virus-induced gene silencing experiment using target-specific forward (5'- ACGTGTATTTCTCCAGCC -3') and reverse primers (5'- GGGGATATAAACTGTCATCGATTTT -3'). The targeted region was chosen for transient gene silencing from the N-terminus region of *TaNAC032* protein comprised of the NAC domain and 3' UTR region as the most divergent sequence to increase the specificity (Scofield et al., 2005). The gene fragment was further analyzed based on BLASTX and BLASTN analysis in the NCBI and siRNA Scan tool (<http://bioinfo2.noble.org/RNAiScan.htm>) for confirming siRNA generation efficiency and the absence of off-targets in the modified viral genome. The confirmed fragment was amplified from cDNA and cloned into a pGEMT-easy vector (Promega, USA), and to confirm the target sequence, the recombinant plasmid was sent for Sanger sequencing. Simultaneously, the VIGS fragment, along with using the NotI restriction enzyme (New England BioLabs), was successfully sub-cloned into a pSL038-1 vector, which codes for the modified γ genome of barley stripe mosaic virus (Cakir and Scofield, 2008). A pSL038-1 vector carrying phytoene desaturase (PDS) gene serves as a positive control and without any plant gene as a negative control. The plasmids p α 46 (BSMV α), p γ SL038-1 was linearized with MluI restriction enzyme whereas, p β 42sp1 (BSMV β) was linearized by using SpeI enzyme. All linearized plasmids were converted to capped in vitro transcripts using mMESSAGE

mMACHINE® T7 in vitro transcription kit (Ambion, Inc., Austin, TX, USA). A 20 µL reaction contained ten µL of 2x dNTPs, 1 µg of linearized plasmid, two µL of 2X buffer, two µL of enzyme mix, and water to a final volume of 20 µL. Reaction set-up was scaled up as per the requirements of the experiment. The reaction mix was incubated at 37 °C for 3-4 h, and in vitro transcription was confirmed by running one µL of the transcript with nine µL of RNase-free water on 1 % agarose gel. During the inflorescence emergence growth stage (Zadoks et al., 1974), flag leaves and spikelets of the resistant NIL (NIL-R) were rub inoculated with all the three in vitro transcript reactions (α , β and γ BSMV) in 1:1:1 ratio (1 µL of each was used) along with 22.5 µL inoculation buffer (IB) which further facilitates viral infection due to its abrasive properties (Scofield et al., 2005; Basnet et al., 2012). The experimental units consisted of two plants, with a total of ten spikes inoculated separately with the test (BSMV: *Tanac032*) and negative control (BSMV: 00), repeated over five biological replicates. Fifteen wheat spikes were also rub inoculated with BSMV + PDS, which served as a positive control.

5.3.8.1 *TaNAC032* gene silencing confirmation and disease evaluation

After 12-15 dpi with BSMV virus, three alternate spikelets in at least five spikes per replication were inoculated with ten µL *Fg* spore suspension. Moisture was maintained for 48 h with water-sprayed plastic bags to facilitate the infection. The bags were removed, and samples were collected at 48 hpi for real-time qPCR analysis, 72 hpi for metabolite analysis, and at 7 dpi for fungal biomass quantification, and were immediately put in liquid nitrogen and stored at -80 °C until further use. Disease severity in NILs was quantified, following point inoculation of one pair of spikelets, as the proportion of spikelets diseased (PSD) in ten spikes per replicate, at 3 d intervals until 15 dpi, from which the area under the disease progress curve (AUDPC) was calculated (Hamzehzarghani et al., 2005; Soni et al., 2020). Statistical significance of the data was performed using the Students *t*-test. To assess resistance based on fungal biomass, genomic DNA was extracted, and fungal biomass was quantified using real-time qPCR by measuring the relative copy number of the fungal housekeeping gene *tri6* normalized with *TaActin*. The relative gene copy number based on real-time qPCR was used to estimate fungal biomass (Kumar et al., 2016).

5.3.8.2 Lignin detection using Weisner test

For histological analysis of lignin, initially, the rachis samples were embedded in cryomoulds using Shandon CRYOMATRIX (Richard-Allan Scientific, Kalamazoo). Following that, sections

of 10 µm thickness were cut using a cryotome machine (Leica, CM1850, Canada) set at -20 °C and immediately collected on slides treated with a 5 % 3-aminopropyltriethoxysilane (APES) solution. The samples were then mounted in phloroglucinol–HCl, a stain specific for lignin (Hu et al., 2017). Slides were mounted with glycerol and immediately observed under a light microscope, OLYMPUS BX51, and photographed (Hu et al., 2017).

5.3.8.3 Lignin quantification based on acetyl bromide soluble lignin (ABSL) assay

Lignin was quantified using acetyl bromide soluble lignin (ABSL), as described by Barnes and Anderson (Barnes and Anderson, 2017). Tissues used were rachis samples from wheat NILs. Absorption at 280 nm measurements was made on a NanoDrop Spectrophotometer ND-1000 (NanoDrop Technologies, DE, USA). A comparison of total lignin content was expressed as acetyl bromide soluble lignin (ABSL) with the previously established extinction coefficient. The mass percentage of ABSL was calculated using formula: %ABSL = $(A_{280} / \epsilon * L) * (D/m) * 100$, Where A_{280} = Absorbance at 280 nm (Blank corrected), ϵ = extinction coefficient (g⁻¹ L cm⁻¹), L = spectrophotometer path length (cm), D = dilution factor from digested AIR, m = mass of de-starched AIR (mg) and AIR = alcohol insoluble residue.

5.4 Results

5.4.1 Sequencing and *Ab-initio* characterization of a novel *TaNAC032* transcription factor identified in wheat NILs

The QTL-Fhb1 sequencing and metabolomics of resistant and susceptible NILs identified NAC transcription factor 32, like as one of the potential candidate genes conferring FHB resistance. The predicted full-length NAC gene was sequenced in nine wheat genotypes including NILs (Sumai 3, NIL-R (S/T), NIL-S (S/T), NIL-R (HC/98), NIL-S (HC/98), Frontana, Pasteur and Thatcher). BLAST analysis positioned *TaNAC* within the QTL-Fhb1 region flanking between XSTS3B-138 and XSTS3B-142 markers (Fig. 5.1a). Further, FGENESH gene-finder based sequence analysis indicated NAC comprising three exons and two introns. The full-length sequence of *TaNAC* was 2492 bp, including an open reading frame (ORF), 3' untranslated region (UTR), and 5' UTR region. A near-upstream element (NUE - AAATAA), one of the plants canonical polyadenylation signals, was found in the 3' UTR region (Loke et al., 2005). Domain analysis of *TaNAC* comprised of 308 amino acids using InterProScan program <http://www.ebi.ac.uk/Tools/InterProScan/> confirm the presence of NAC domain spanning 12-170 intervals (Quevillon et al., 2005). The complete coding

sequence was submitted to the NCBI data repository and was assigned a GenBank accession number MT512636. Phylogeny analysis among the cereal crops suggested the close homology of novel wheat NAC with *Aegilops tauschii* NAC transcription factor 32-like orthologous *Triticum aestivum* *TaNAC* with 96.92% identity, thus designated as *TaNAC032* in this study (Fig. 5.1b). Whereas BLAST search in Arabidopsis indicated a close homology with NAC domain-containing protein 29 (AT1G61110.1), which is well characterized in positive regulation of leaf senescence (Guo et al., 2006; Kim et al., 2016).

5.4.2 *TaNAC032* gene expression following pathogen inoculation

A qRT-PCR based expression analysis following *Fg* inoculation showed a significant ($P < 0.01$) increase in *TaNAC032* expression by 2.15-fold in NIL-R, as compared to NIL-S (Fig. 5.1c). Mock treated samples also showed a similar pattern wherein NIL-R represented a 1.31-fold significant increase in expression than NIL-S. Similarly, *TaNAC032* expression was higher in NIL-R pathogen treated samples when compared to mock-treated samples in both the NILs (Fig. 5.1c), suggesting *TaNAC032* as a potential candidate for FHB resistance.

5.4.3 Polymorphism in *TaNAC032* protein

Multiple sequence comparisons of the *TaNAC032* gene between wheat NILs derived from QTL-Fhb1 and differing at contrasting alleles revealed a deletion of 121 nucleotides at 179-bp position by a single nucleotide polymorphism (SNP) at the 320-bp position in NIL-S (Fig. 5.2a). The large deletion in the nucleotide sequence resulted in the deletion of 41 amino acids at the protein level, comprised of the NAC domain. Whereas, no deleterious effect was observed for the SNP on amino acid sequence analysis. The deleterious effect of deletion on protein functionality was further confirmed based on in-silico analysis by Phyre 2 Investigator (Kelley et al., 2015). The absence of alpha chain was observed in NIL-S when compared with NIL-R (Fig. 5.2b). Further, to confirm the genetic mutation leading to FHB susceptibility, the *TaNAC032* gene was amplified and sequenced from nine wheat genotypes including NILs (Sumai 3, NIL-R (S/T), NIL-S (S/T), NIL-R (HC/98), NIL-S (HC/98), Frontana, Pasteur and Thatcher) with varying levels of FHB resistance (Fig. 5.3a). Further, the three-dimensional structure prediction of both the mutated and non-mutated *TaNAC032* in the wheat genotypes was confirmed based on Phyre 2 Investigator (Fig. 5.3b).

5.4.4 In silico promoter analysis and physical interaction of RR metabolite biosynthetic genes (RRRM) with *TaNAC032*

Primarily, the promoter regions of the key RR metabolite biosynthetic genes (*RRRM*) from the phenylpropanoid pathway were searched for a 19bp consensus sequence, common cis-acting element, namely secondary wall NAC binding elements (SNBE) (Zhong et al., 2010), to study the downstream *R* gene targets of *TaNAC032* (Fig. 5.4). In silico promoter, the analysis revealed one or more characteristic secondary NAC binding elements for the following genes: *TaCCR*, *TaCAD*, *TaLAC4*, and *TaMYB* (Table 1). Subsequently, the functional significance of the SNBE sites is validated based on Arabidopsis as a search organism; the probable interaction of *TaNAC032* with these downstream *RRRM* genes using GeneMANIA software (<http://www.genemania.org/>) was confirmed. The network resulted in direct interaction between *TaNAC032* and the *RRRM* genes designated as *ATCCR2*, *ATCAD5*, *ATLAC17*, and *AtMYB97* with *ANAC029* orthologous in Arabidopsis (Fig. 5.5). Apart from confirming *in-silico* predicted interaction, these preliminary results suggest that *TaNAC032* is critical for regulating lignin pathway-specific genes such as *TaCCR*, *TaCAD*, *TaLAC4*, and *TaMYB* to biosynthesize lignin and strengthening secondary cell wall.

5.4.5 Silencing of pathogen-induced *TaNAC032* increased susceptibility in wheat resistant NIL to *Fg* infection

The *Fg* induced *TaNAC032* gene was knocked down using virus-induced gene silencing (VIGS) in NIL-R to prove the resistance functions in wheat NILs against FHB. Initially, recombinant plasmids harboring the gamma genome of the modified barley stripe mosaic virus with phytoene desaturase (positive control/ BSMV: PDS) and *TaNAC032* (test / BSMV: *Tanac032*) were developed (Fig. 5.6a). These recombinant plasmids, together with other BSMV virus plasmids harboring alpha and beta genome was linearized, *in-vitro* transcribed, and rub inoculated on wheat spikes to initiate the infection. After 12 days post rubbing, bleaching symptoms were observed on spikes treated with the positive control (BSMV: PDS), which proves the efficiency of the gene silencing system. The expression levels of *TaNAC032* transcripts were analyzed post 48 h of *Fg* infection to understand a similar effect observed on wheat spikes rubbed with the test (BSMV: *Tanac032*) (Fig. 5.6b, c). 5.64-FC reduced the mRNA levels of *Tanac032* (test gene) as compared to the negative control (BSMV: 00), thus confirming the transient silencing of the *TaNAC032*

protein (Fig. 5.7a). Upon pathogen inoculation, at seven days post-inoculation (dpi), fungal biomass was estimated in silenced and non-silenced plants using qPCR. The silenced plants were found to accumulate more fungal biomass as compared to non-silenced by 2.5-FC (Fig. 5.7b), which further suggests the crucial role played by the *TaNAC032* transcription factor in governing FHB resistance in wheat NILs. The disease severity analysis of silenced NILs (BSMV: *Tanac032*) and non-silenced NILs (BSMV: 00) was assessed by inoculating a pair of spikelets mid-region of the spike with *Fg*. The proportion of spikelets diseased (PSD) was significantly higher in silenced NIL-R (0.89) as compared to non-silenced NIL-R (0.18) (Fig. 5.7c). Furthermore, the relative gene expression levels of the downstream *RRRM* genes: *TaCCR* (3.19-FC), *TaCAD* (2.09-FC), *TaLAC4* (2.07-FC) and *TaMYB* (1.13-FC) were significantly ($P < 0.01$) lower in *Tanac032* silenced as compared to non-silenced samples upon *Fg* inoculation (Fig. 5.7d). This further confirmed that *TaNAC032* serves as a master regulator of genes related to the lignin biosynthetic process.

5.4.6 Semi-comprehensive metabolomics revealed biosynthesis of phenylpropanoids and lignan glycosides by the downstream *RRRM* genes that were regulated by *TaNAC032* in wheat

Semi-comprehensive metabolomics of wheat NIL-R, with silenced (susceptible) and control, non-silenced *TaNAC032* (resistant) samples collected at 72 hpi, was conducted using liquid chromatography and high-resolution mass spectrometry (LC-HRMS/MS). A total of 20517 monoisotopic mass peaks were consistently detected across all replicates, including adducts, of which only 337 significant peaks were retained for further analysis at p-value $P < 0.05$. The fold change (FC) of the peaks were calculated by dividing the peaks abundance in non-silenced treatment compared to silenced NILs. The RRI metabolites indicate a higher fold change in non-silenced control (resistant) is due to the reduction of abundance when silenced. The RRI metabolites mainly belonged to *monolignols*: Coniferin (FC= 5.87), *lignan glycoside*: Podorhizol beta-D-glucoside (FC= 3.19), and *phenylpropanoid biosynthesis*: 4-Hydroxycinnamyl alcohol 4-D-glucoside (FC= 1.93). The abundances of significant metabolites in silenced and non-silenced samples upon pathogen inoculation are also depicted as boxplot (BoxPlotR: a web-tool for the generation of box plots) (Fig. 5.8). Notably, all these RRI metabolites were also detected in several previous studies in Wheat- *F. graminearum* interactions. These were known to be involved in secondary cell wall modification and the lignin biosynthetic process to contain the pathogen to initial infection.

5.4.7 The silenced *Tanac032* in NIL-R revealed altered lignin composition in rachis

Phloroglucinol-HCL staining (Wiesner test) showed a significant decrease in the total lignin accumulation in the silenced (BSMV: *Tanac032*) rachis as compared to non-silenced (BSMV: 00), along with the retarded vascular bundle shape, which could be the result of reduced cell division and expansion (Fig. 5.9a, b). Also, acid-soluble lignin test of silenced and non-silenced rachis samples upon *Fg* inoculation indicated that the silencing of *TaNAC032* caused a substantial reduction of 46.98 % in the total lignin content in silenced NILs (Fig. 5.9c), which further suggests the possible involvement of *TaNAC032* in the regulation of lignin biosynthesis.

5.5 Discussion

In response to plant stress, members of the NAC gene family transcription factors (TFs) serve as the largest transcriptional regulators involved in regulating transcriptional reprogramming (Nuruzzaman et al., 2013). Several studies have reported the role of NAC TFs in the secondary cell wall (SCW) biosynthesis and biotic and abiotic stress responses (Yamaguchi et al., 2011; Nakashima et al., 2012; Puranik et al., 2012). In Arabidopsis, secondary wall-associated NAC domain (SND) and its close homologs NAC secondary wall thickening promoting factor (NST), including vascular-related NAC-domain (VND), act as master switches to regulate the activation of the cellulose, xylan and lignin biosynthetic genes (Zhong et al., 2006; Mitsuda et al., 2007). Silencing of SND1 and NST1 restricted secondary wall thickening and lignin deposition in fibres, indicating lignin biosynthesis under the control of SND1 and NST1 master switches (Zhong et al., 2006; Mitsuda et al., 2007). Among SND1 direct targets such as MYB46, SND3, and MYB103, KNAT7, the MYB46 acts as another level of the master switch to activate the entire secondary wall biosynthetic program (Zhong et al., 2007; Zhong et al., 2008). Besides, other findings identified MYB58 and MYB63 as the direct transcriptional activators of lignin biosynthesis, which are downstream targets of SND1 and MYB46, suggesting they are part of SND1 and MYB46-mediated transcriptional network regulating secondary cell wall biosynthesis (Zhou et al., 2009). A network was established between TFs and SCW metabolic genes of Arabidopsis employing protein-DNA interaction study (Taylor-Teeples et al., 2015). In these interactions, the previously reported TFs could recognize the promoter sequences of other downstream TFs and SCW metabolic genes, leading to secondary cell wall reinforcement (Taylor-Teeples et al., 2015). This implies the need to identify genes involved in SCW formation and revealing the interaction

between them. The qRT-PCR based gene expression analysis revealed higher induced expression of *TaNAC032* in NIL-R, following inoculation with *F. graminearum* (*Fg*), as compared to NIL-S (Fig. 5.1c). Transient silencing of *TaNAC032* gene in NIL-R resulted in increased susceptibility to FHB through reduced abundances of transcripts and metabolites belonging to the lignin biosynthetic pathway. The role of *TaNAC032* in regulating downstream *RRRM* genes that biosynthesize RRI metabolites, which directly or indirectly limit pathogen progression, is discussed below.

For the functionality of any organism, the gene sequences and encoding protein sequences need to be intact. However, mutations or deletions in the nucleotide sequences due to acquired changes can interrupt cellular processes and often hold the key to understand the gene functions. In this study, the *TaNAC032* gene was sequenced in eight wheat genotypes, with varying FHB resistance levels, to confirm its association with FHB resistance. The sequences from susceptible wheat genotypes, NIL-S (S/T), NIL-R (HC/98), NIL-S (HC/98), Frontana, Pasteur and Thatcher, all localized a deletion of 121 nucleotides at position 191, which corresponds to 41 amino acids constituting NAC domain (Fig. 5.3a). The NAC domain is an N-terminal module of ~160 amino acids found in proteins of the NAC family of plant-specific transcriptional regulators (Aida et al., 1997). Although NAC proteins are commonly involved in developmental processes such as the formation of the shoot apical meristem, floral organs and lateral shoots, and plant hormonal control, their role in defense still needs to be elucidated. In this study, the presence of an intact NAC domain in resistant wheat genotypes, Sumai-3 and NIL-R, suggests the possible role in conferring FHB resistance in Wheat. This was further substantiated by a three-dimensional structure prediction, which revealed the absence of alpha-helix chain in mutated genotypes, which directly act as the recognition element in regulatory and related proteins (Fig. 5.3b), further displaying the candidacy of *TaNAC032* in FHB resistance in Wheat. Interestingly, the *TaNAC032* was mutated in both NIL-R, and NIL-S derived from fixed susceptible (HC374/3*98B69-L47) (HC/98) genetic background (HC374 = Wuhan1/Nyubai) for Type II resistance. Previously, both the NILs derived from wheat genotype Nyubai were highly susceptible to *Fg*'s spread through rachis, following inoculation of one pair of spikelets (Gunnaiah et al., 2012). Whereas in the NILs derived from Sumai 3 mapping populations, only the NIL-S was mutated, confirming that the *TaNAC032* is the gene responsible for FHB resistance in wheat. This

encouraged us to functionally validate the *TaNAC032* gene for the plausible role in FHB resistance in Wheat NILs.

To affirm the role of *TaNAC032* in FHB resistance, the NILs harboring functional copy of *TaNAC032* were knocked-down based on the virus-induced gene silencing (VIGS) approach. Among several gene silencing approaches, VIGS has proven a versatile, functional genomics tool widely used in plant families such as in Wheat, barley, tobacco, tomato, and Arabidopsis to decipher the target gene(s) functions (Kage et al., 2017; Singh et al., 2019). The qRT-PCR results revealed a significant reduction in the transcript levels of *TaNAC032* in silenced FHB resistant genotype as compared to non-silenced (Fig. 5.7a), while relatively higher than susceptible NIL (NIL-S) (Fig. 5.7a). The disease severity and the fungal biomass significantly increased in the silenced NIL (Fig. 5.7b, c), confirming the role of *TaNAC032* in FHB resistance. To further unveil the exact mechanisms of *TaNAC032* TF in governing FHB resistance, a semi-targeted metabolomics study was performed.

Protein and metabolites as the end products of a functional gene can explain phenotype better than transcripts (Karre et al., 2019). To identify the downstream targets of *TaNAC032*, we did semi-targeted metabolomics combined with qRT-PCR analysis. LC-HRMS analysis revealed differential accumulation of metabolites belonging mainly to phenylpropanoids and phenylpropanoid lignan glycosides: Coniferin (FC= 5.87), Podorhizol beta-D-glucoside (FC= 3.19) and 4-Hydroxycinnamyl alcohol 4-D-glucoside (FC= 1.93). These metabolites were significantly lower in abundances in silenced compared to non-silenced NIL-R plants upon mock and pathogen (*Fg*) inoculation (Fig. 5.8). As plant cell wall is a mechanical barrier to the pathogen progression, lignin deposition leads to the reinforced cell wall that is more resistant to fungal cell wall degrading enzymes and also limits diffusion of mycotoxins produced by a pathogen (Siranidou et al., 2002; Sattler and Funnell-Harris, 2013). For instance, coniferin, a glucoside of coniferyl alcohol and 4-Hydroxycinnamyl alcohol 4-D-glucoside, a glucoside of paracoumaryl alcohol derivatives, serve as an intermediate in cell wall lignification. Likewise, lignans such as podorhizol beta-D-glucoside also exhibit antifungal phytoalexin in cell wall strengthening to prevent pathogen entry (Cho et al., 2007; Ishihara et al., 2008). Previous metabolomics study also led to the identification of several RR metabolites belonging mainly to phenylpropanoid pathway, particularly hydroxycinnamic acids (HCAAs) such as N-caffeoylputrescine, feruloyl-2-hydroxyputrescine, coumaroylagmatine, and coumaroyl-putrescine in response to *Fg* infection in

wheat NILs and RILs (Gunnaiah and Kushalappa, 2014; Dhokane et al., 2016; Kage et al., 2017). The metabolites identified in this study, mainly belonging to the phenylpropanoid related pathway directly or indirectly, are involved in the biosynthesis and polymerization of lignin as a primary component of the cell wall to orchestrate resistance to FHB infestation.

To further strengthen the leads, a histopathology study was conducted in both *TaNAC032* silenced and non-silenced rachis samples. As a result, the Wiesner test showed lesser lignin deposition in the vascular bundles in silenced samples (Fig. 5.9a, b). Following that, total lignin quantification based on acetyl bromide method revealed a significant reduction in ABSL% in silenced NIL rachis samples than in non-silenced (Fig. 5.9c), which further confirmed the role of NAC transcription factor in the regulation of lignin biosynthesis. Secondary wall NACs (SWNS) bind to an imperfect palindromic 19-bp consensus sequence known as secondary wall NAC binding element (SNBE) in the promoter region of their direct targets. These upstream regulators directly activate the downstream transcription factors leading to secondary wall biosynthesis and reinforcement (Zhong et al., 2010). As promoter region of these genes consists of multiple SNBE sites that provide insights into the sophisticated transcriptional program and the underlying evolutionary mechanism (Zhong et al., 2010). Correspondingly, the promoter region analysis of phenylpropanoid pathway-related genes identified *TaCCR*, *TaCAD*, *TaLAC4*, and a TF *TaMYB* with SNBE elements in their promoter region, suggesting *TaNAC032* regulates these downstream *RRRM* genes by binding to their cis-regulatory elements (Table 1). Also, the Genemania software revealed the physical interaction of *TaNAC032* with *RRRM* genes, *TaCCR*, *TaCAD*, *TaLAC4*, and a TF, *TaMYB* for the biosynthesis of RR metabolites mainly related to the phenylpropanoid pathway (Fig. S2). The qRT-PCR study revealed the downregulation of these genes by 3.19-, 2.09-, 2.07- and 1.13-fold change, respectively. These results combined with metabolomics study can confirm the lignin-specific pathway-related genes as a downstream target of *TaNAC032* TF and explain resistance mechanisms against FHB in wheat NILs.

The NAC TFs are known to exhibit either positive or negative transcriptional regulation of downstream genes. Like, in wheat responses to abiotic and biotic stresses, the *TaNAC4* gene functions as a transcriptional activator, whereas *ANAC032* was identified as both a negative and positive regulator of JA and SA signalling as an immune response against *Pst* (Xia et al., 2010; Allu et al., 2016). Similarly, *TaNAC1*, despite having a transcription activation domain in its C-

terminal, was unable to display transcriptional activity (Wang et al., 2015). A significant reduction in transcript levels of *R_{RRM}* genes observed along with the reduced accumulation of monolignols derivatives and lignan glycosides in *TaNAC032* silenced rachis as compared to non-silenced explains the role of *TaNAC032* TF in the positive regulation of downstream targets. The decrease in metabolite abundances in silenced rachis compared to non-silenced can be explained based on the mutation in the NAC domain of the *TaNAC032* gene in NIL-S, which alters the transcriptional activity.

Proposed model of *TaNAC032* regulatory network in response to FHB infection in wheat

Silencing study of the *TaNAC032* transcription factor combined with metabolomics, gene expression data, and gene targets interaction network analysis unveiled its novel role in regulating defense response in wheat against FHB. This interaction is represented in a working model of FHB resistance in wheat governed by *TaNAC032* (Fig. 5.10). Semi-targeted metabolomics analysis of rachis samples in silenced NIL-R suggested reduced abundances of phenylpropanoids and lignan glycosides. Further, gene expression analysis revealed the positive regulation of these genes by *TaNAC032* TF. However, future research must focus more on DNA-protein interactions based on *in vivo* observations to reveal the network dynamics because modelling based on *in vitro* data only indicates several possibilities of the network. The proposed transcriptional regulatory network of SCW reinforcement (Fig. 5.10) could be an excellent model for such advanced studies. To summarize, this study presents the role of *TaNAC032* in regulating lignin biosynthetic genes to reinforce plant secondary walls of cells around pathogen infection, which further acts as a barrier to orchestrate pathogen entry, thus providing resistance against FHB. The *TaNAC032* gene, if non-functional, can be edited in commercial cultivars, based on gene editing technologies to improve FHB resistance in wheat, provided the cultivar is also associated with rest of the hierarchy of genes to biosynthesize lignin as proposed here (Kushalappa et al., 2016). If the *TaLAC4* gene is also mutated in the cultivar, then in addition to *TaNAC32*, this gene also must be edited (Soni et al., 2020).

5.6 Author Contributions

N.S. conducted all the lab and greenhouse experiments, analyzed data, and wrote the manuscript. B.A. helped in microscopy, and N.H. helped in the VIGS experiment, FN provided helped in qRT-PCR data analysis, R.D. provided access to his lab and lab facilities, and A.K obtained funding and supervised the research.

5.7 Compliance with ethical standards

The authors declare that the experiments comply with the McGill Environment, Health and Safety guidelines and the current laws of Canada.

5.8 Declaration of Competing Interest

The authors declare no competing financial interests.

5.9 Acknowledgments

This project was funded by the Natural Sciences and Engineering Research Council of Canada (NSERC), McGill Sustainability Systems Initiative (MSSI) and Ministère de l'Agriculture, des Pêcheries et de l'Alimentation du Québec (MAPAQ), Québec, Canada. We thank Dr. S. Fox, AAFC, Winnipeg, Canada for providing wheat NILs and Dr. S. Rioux, CÉROM, Quebec, Canada for providing *Fg* isolate (155.SLS) and Mr. Yves Dion, Centre de recherche sur les grains (CÉROM) for guidance and support.

REFERENCES

- Aida M, Ishida T, Fukaki H, Fujisawa H, Tasaka M** (1997) Genes involved in organ separation in Arabidopsis: an analysis of the cup-shaped cotyledon mutant. *The Plant Cell* **9**: 841
- Allu A, Brotman Y, Xue G-P, Balazadeh S** (2016) Transcription factor ANAC032 modulates JA/SA signalling in response to *Pseudomonas syringae* infection. *EMBO reports* **17**
- Anderson JA, Stack RW, Liu S, Waldron BL, Fjeld AD, Coyne C, Moreno-Sevilla B, Fetch JM, Song QJ, Cregan PB, Frohberg RC** (2001) DNA markers for *Fusarium* head blight resistance QTLs in two wheat populations. *Theoretical and Applied Genetics* **102**: 1164-1168
- Bai G, Kolb FL, Shaner G, Domier LL** (1999) Amplified fragment length polymorphism markers linked to a major quantitative trait locus controlling scab resistance in wheat. *Phytopathology* **89**: 343-348
- Bai G, Shaner G** (2004) Management and resistance in wheat and barley to *Fusarium* head blight. *Annual Review of Phytopathology* **42**: 135-161
- Barnes WJ, Anderson CT** (2017) Acetyl bromide soluble lignin (absl) assay for total lignin quantification from plant biomass. *Bio-protocol* **7**: 2149
- Basnet BR, Glover KD, Ibrahim AMH, Yen Y, Chao S** (2012) A QTL on chromosome 2DS of 'Sumai 3' increases susceptibility to *Fusarium* head blight in wheat. *Euphytica* **186**: 91-101

- Bollina V, Kumaraswamy GK, Kushalappa AC, Choo TM, Dion Y, Rioux S, Faubert D, Hamzehzarghani H** (2010) Mass spectrometry-based metabolomics application to identify quantitative resistance-related metabolites in barley against Fusarium head blight. *Mol Plant Pathol* **11**: 769-782
- Buerstmayr H, Ban T, Anderson JA** (2009) QTL mapping and marker-assisted selection for Fusarium head blight resistance in wheat: a review. *Plant Breeding* **128**: 1-26
- Buerstmayr H, Lemmens M, Hartl L, Doldi L, Steiner B, Stierschneider M, Ruckebauer P** (2002) Molecular mapping of QTLs for Fusarium head blight resistance in spring wheat. I. Resistance to fungal spread (Type II resistance). *Theor Appl Genet* **104**: 84-91
- Cakir C, Scofield SR** (2008) Evaluating the ability of the barley stripe mosaic virus-induced gene silencing system to simultaneously silence two wheat genes. *Cereal Research Communications* **36**: 217-222
- Cho HY, Lee-Parsons CW, Yoon SY, Rhee HS, Park JM** (2007) Enhanced benzophenanthridine alkaloid production and protein expression with combined elicitor in *Eschscholtzia californica* suspension cultures. *Biotechnol Lett* **29**: 2001-2005
- Choulet F, Wicker T, Rustenholz C, Paux E, Salse J, Leroy P, Schlub S, Le Paslier MC, Magdelenat G, Gonthier C, Couloux A, Budak H, Breen J, Pumphrey M, Liu S, Kong X, Jia J, Gut M, Brunel D, Anderson JA, Gill BS, Appels R, Keller B, Feuillet C** (2010) Megabase level sequencing reveals contrasted organization and evolution patterns of the wheat gene and transposable element spaces. *Plant Cell* **22**: 1686-1701
- Cuthbert PA, Somers DJ, Thomas J, Cloutier S, Brule-Babel A** (2006) Fine mapping Fhb1, a major gene controlling fusarium head blight resistance in bread wheat (*Triticum aestivum* L.). *Theor Appl Genet* **112**: 1465-1472
- Dhokane D, Karre S, Kushalappa AC, McCartney C** (2016) Integrated metabolo-transcriptomics reveals fusarium head blight candidate resistance genes in wheat qtl-fhb2. *PloS one* **11**: e0155851-e0155851
- Feng H, Duan X, Zhang Q, Li X, Wang B, Huang L, Wang X, Kang Z** (2014) The target gene of taе-miR164, a novel NAC transcription factor from the NAM subfamily, negatively regulates resistance of wheat to stripe rust. *Mol Plant Pathol* **15**: 284-296
- Gunnaiah R, Kushalappa AC** (2014) Metabolomics deciphers the host resistance mechanisms in wheat cultivar Sumai-3, against tricothecene producing and non-producing isolates of *Fusarium graminearum*. *Plant Physiol Biochem* **83**: 40-50
- Gunnaiah R, Kushalappa AC, Duggavathi R, Fox S, Somers DJ** (2012) Integrated Metabolo-Proteomic Approach to Decipher the Mechanisms by Which Wheat QTL (Fhb1) Contributes to Resistance against *Fusarium graminearum*. *PLOS ONE* **7**: e40695
- Guo P-G, Bai G-H, Li R-H, Shaner G, Baum M** (2006) Resistance gene analogs associated with Fusarium head blight resistance in wheat. *Euphytica* **151**: 251-261
- Guo W, Jin L, Miao Y, He X, Hu Q, Guo K, Zhu L, Zhang X** (2016) An ethylene response-related factor, GbERF1-like, from *Gossypium barbadense* improves resistance to *Verticillium dahliae* via activating lignin synthesis. *Plant Mol Biol* **91**: 305-318

- Hamzehzarghani H, Kushalappa AC, Dion Y, Rioux S, Comeau A, Yaylayan V, Marshall WD, Mather DE** (2005) Metabolic profiling and factor analysis to discriminate quantitative resistance in wheat cultivars against fusarium head blight. *Physiological and Molecular Plant Pathology* **66**: 119-133
- Hu R, Xu Y, Yu C, He K, Tang Q, Jia C, He G, Wang X, Kong Y, Zhou G** (2017) Transcriptome analysis of genes involved in secondary cell wall biosynthesis in developing internodes of *Miscanthus lutarioriparius*. *Scientific Reports* **7**: 9034
- Ishihara A, Hashimoto Y, Tanaka C, Dubouzet JG, Nakao T, Matsuda F, Nishioka T, Miyagawa H, Wakasa K** (2008) The tryptophan pathway is involved in the defense responses of rice against pathogenic infection via serotonin production. *The Plant Journal* **54**: 481-495
- Jensen MK, Kjaersgaard T, Nielsen MM, Galberg P, Petersen K, O'Shea C, Skriver K** (2010) The *Arabidopsis thaliana* NAC transcription factor family: structure-function relationships and determinants of ANAC019 stress signalling. *The Biochemical journal* **426**: 183-196
- Kage U, Karre S, Kushalappa AC, McCartney C** (2017) Identification and characterization of a fusarium head blight resistance gene TaACT in wheat QTL-2DL. *Plant Biotechnology Journal* **15**: 447-457
- Kage U, Yogendra KN, Kushalappa AC** (2017) TaWRKY70 transcription factor in wheat QTL-2DL regulates downstream metabolite biosynthetic genes to resist *Fusarium graminearum* infection spread within spike. *Scientific Reports* **7**: 42596
- Karre S, Kumar A, Dhokane D, Kushalappa AC** (2017) Metabolo-transcriptome profiling of barley reveals induction of chitin elicitor receptor kinase gene (HvCERK1) conferring resistance against *Fusarium graminearum*. *Plant Mol Biol* **93**: 247-267
- Karre S, Kumar A, Yogendra K, Kage U, Kushalappa A, Charron J-B** (2019) HvWRKY23 regulates flavonoid glycoside and hydroxycinnamic acid amide biosynthetic genes in barley to combat *Fusarium head blight*. *Plant Molecular Biology* **100**: 591-605
- Katajamaa M, Oresic M** (2005) Processing methods for differential analysis of LC/MS profile data. *BMC Bioinformatics* **6**: 179
- Kelley LA, Mezulis S, Yates CM, Wass MN, Sternberg MJ** (2015) The Phyre2 web portal for protein modeling, prediction and analysis. *Nat Protoc* **10**: 845-858
- Kim HJ, Nam HG, Lim PO** (2016) Regulatory network of NAC transcription factors in leaf senescence. *Curr Opin Plant Biol* **33**: 48-56
- Kumar A, Yogendra KN, Karre S, Kushalappa AC, Dion Y, Choo TM** (2016) WAX INDUCER1 (HvWIN1) transcription factor regulates free fatty acid biosynthetic genes to reinforce cuticle to resist *Fusarium head blight* in barley spikelets. *Journal of experimental botany* **67**: 4127-4139
- Kushalappa AC, Yogendra KN, Karre S** (2016) Plant innate immune response: Qualitative and quantitative resistance. *Critical Reviews in Plant Sciences* **35**: 38-55
- Kushalappa AC, Yogendra KN, Sarkar K, Kage U, Karre S** (2016) Gene discovery and genome editing to develop cisgenic crops with improved resistance against pathogen infection. *Canadian Journal of Plant Pathology* **38**: 279-295

- Letunic I, Doerks T, Bork P** (2015) SMART: recent updates, new developments and status in 2015. *Nucleic acids research* **43**: D257-D260
- Li G, Zhou J, Jia H, Gao Z, Fan M, Luo Y, Zhao P, Xue S, Li N, Yuan Y, Ma S, Kong Z, Jia L, An X, Jiang G, Liu W, Cao W, Zhang R, Fan J, Xu X, Liu Y, Kong Q, Zheng S, Wang Y, Qin B, Cao S, Ding Y, Shi J, Yan H, Wang X, Ran C, Ma Z** (2019) Mutation of a histidine-rich calcium-binding-protein gene in wheat confers resistance to Fusarium head blight. *Nature Genetics* **51**: 1106-1112
- Liu S, Pumphrey M, Gill B, Trick H, Zhang J, Dolezel J, Chalhoub B, Anderson J** (2008) Toward positional cloning of Fhb1 , a major QTL for Fusarium head blight resistance in wheat. *Cereal Research Communications* **36**: 195-201
- Livak KJ, Schmittgen TD** (2001) Analysis of relative gene expression data using real-time quantitative PCR and the 2⁻(Delta Delta C(T)) Method. *Methods* **25**: 402-408
- Loke JC, Stahlberg EA, Strenski DG, Haas BJ, Wood PC, Li QQ** (2005) Compilation of mrna polyadenylation signals in arabidopsis revealed a new signal element and potential secondary structures. *Plant Physiology* **138**: 1457
- McCarthy RL, Zhong R, Ye Z-H** (2011) Secondary wall NAC binding element (SNBE), a key cis-acting element required for target gene activation by secondary wall NAC master switches. *Plant Signaling & Behavior* **6**: 1282-1285
- McMullen M, Jones R, Gallenberg D** (1997) Scab of wheat and barley: A re-emerging disease of devastating impact. *Plant Dis* **81**: 1340-1348
- Mitsuda N, Iwase A, Yamamoto H, Yoshida M, Seki M, Shinozaki K, Ohme-Takagi M** (2007) NAC Transcription Factors, NST1 and NST3, Are Key Regulators of the Formation of Secondary Walls in Woody Tissues of Arabidopsis. *The Plant Cell* **19**: 270
- Nakashima K, Takasaki H, Mizoi J, Shinozaki K, Yamaguchi-Shinozaki K** (2012) NAC transcription factors in plant abiotic stress responses. *Biochim Biophys Acta* **1819**: 97-103
- Nuruzzaman M, Sharoni AM, Kikuchi S** (2013) Roles of NAC transcription factors in the regulation of biotic and abiotic stress responses in plants. *Frontiers in microbiology* **4**: 248
- Olsen AN, Ernst HA, Leggio LL, Skriver K** (2005) NAC transcription factors: structurally distinct, functionally diverse. *Trends Plant Sci* **10**: 79-87
- Puranik S, Sahu PP, Srivastava PS, Prasad M** (2012) NAC proteins: regulation and role in stress tolerance. *Trends Plant Sci* **17**: 369-381
- Quevillon E, Silventoinen V, Pillai S, Harte N, Mulder N, Apweiler R, Lopez R** (2005) InterProScan: protein domains identifier. *Nucleic Acids Research* **33**: W116-W120
- Rawat N, Pumphrey MO, Liu S, Zhang X, Tiwari VK, Ando K, Trick HN, Bockus WW, Akhunov E, Anderson JA, Gill BS** (2016) Wheat Fhb1 encodes a chimeric lectin with agglutinin domains and a pore-forming toxin-like domain conferring resistance to Fusarium head blight. *Nat Genet* **48**: 1576-1580
- Sattler S, Funnell-Harris D** (2013) Modifying lignin to improve bioenergy feedstocks: strengthening the barrier against pathogens?†. *Frontiers in Plant Science* **4**: 70

- Schweiger W, Steiner B, Vautrin S, Nussbaumer T, Siegwart G, Zamini M, Jungreithmeier F, Gratl V, Lemmens M, Mayer KFX, Bérghès H, Adam G, Buerstmayr H** (2016) Suppressed recombination and unique candidate genes in the divergent haplotype encoding Fhb1, a major Fusarium head blight resistance locus in wheat. *Theoretical and Applied Genetics* **129**: 1607-1623
- Scofield SR, Huang L, Brandt AS, Gill BS** (2005) Development of a Virus-Induced Gene-Silencing System for Hexaploid Wheat and Its Use in Functional Analysis of the Lr21-Mediated Leaf Rust Resistance Pathway. *Plant Physiology* **138**: 2165
- Singh B, Kukreja S, Salaria N, Thakur K, Gautam S, Taunk J, Goutam U** (2019) VIGS: a flexible tool for the study of functional genomics of plants under abiotic stresses. *Journal of Crop Improvement* **33**: 567-604
- Siranidou E, Kang Z, Buchenauer H** (2002) Studies on symptom development, phenolic compounds and morphological defence responses in wheat cultivars differing in resistance to fusarium head blight. *Journal of Phytopathology* **150**: 200-208
- Soni N, Hegde N, Dhariwal A, Kushalappa AC** (2020) Role of laccase gene in wheat NILs differing at QTL-Fhb1 for resistance against Fusarium head blight. *Plant Science* **298**: 110574
- Su Z, Bernardo A, Tian B, Chen H, Wang S, Ma H, Cai S, Liu D, Zhang D, Li T, Trick H, St. Amand P, Yu J, Zhang Z, Bai G** (2019) A deletion mutation in TaHRC confers Fhb1 resistance to Fusarium head blight in wheat. *Nature Genetics* **51**: 1099-1105
- Su Z, Jin S, Zhang D, Bai G** (2018) Development and validation of diagnostic markers for Fhb1 region, a major QTL for Fusarium head blight resistance in wheat. *Theor Appl Genet* **131**: 2371-2380
- Taylor-Teeple M, Lin L, De Lucas M, Turco G, Toal TW, Gaudinier A, Young NF, Trabucco GM, Veling MT, Lamothe R** (2015) An Arabidopsis gene regulatory network for secondary cell wall synthesis. *Nature* **517**: 571-575
- Waldron BL, Moreno-Sevilla B, Anderson JA, Stack RW, Froberg RC** (1999) RFLP mapping of QTL for Fusarium head blight resistance in wheat. *Crop Science* **39**: 805-811
- Wang F, Lin R, Feng J, Chen W, Qiu D, Xu S** (2015) TaNAC1 acts as a negative regulator of stripe rust resistance in wheat, enhances susceptibility to *Pseudomonas syringae*, and promotes lateral root development in transgenic *Arabidopsis thaliana*. *Frontiers in plant science* **6**: 108-108
- Wang Y, Xu L, Shen H, Wang J, Liu W, Zhu X, Wang R, Sun X, Liu L** (2015) Metabolomic analysis with GC-MS to reveal potential metabolites and biological pathways involved in Pb & Cd stress response of radish roots. *Scientific reports* **5**: 18296
- Wang Z, Xia Y, Lin S, Wang Y, Guo B, Song X, Ding S, Zheng L, Feng R, Chen S, Bao Y, Sheng C, Zhang X, Wu J, Niu D, Jin H, Zhao H** (2018) Osa-miR164a targets OsNAC60 and negatively regulates rice immunity against the blast fungus *Magnaporthe oryzae*. *The Plant Journal* **95**: 584-597
- Xia N, Zhang G, Liu XY, Deng L, Cai GL, Zhang Y, Wang XJ, Zhao J, Huang LL, Kang ZS** (2010) Characterization of a novel wheat NAC transcription factor gene involved in defense response against stripe rust pathogen infection and abiotic stresses. *Mol Biol Rep* **37**: 3703-3712

- Yamaguchi M, Mitsuda N, Ohtani M, Ohme-Takagi M, Kato K, Demura T** (2011) VASCULAR-RELATED NAC-DOMAIN7 directly regulates the expression of a broad range of genes for xylem vessel formation. *Plant J* **66**: 579-590
- Yogendra KN, Dhokane D, Kushalappa AC, Sarmiento F, Rodriguez E, Mosquera T** (2017) StWRKY8 transcription factor regulates benzyloisoquinoline alkaloid pathway in potato conferring resistance to late blight. *Plant science : an international journal of experimental plant biology* **256**: 208-216
- Zadoks JC, Chang TT, Konzak CF** (1974) A decimal code for the growth stages of cereals. *Weed Research* **14**: 415-421
- Zhong R, Demura T, Ye ZH** (2006) SND1, a NAC domain transcription factor, is a key regulator of secondary wall synthesis in fibers of Arabidopsis. *Plant Cell* **18**: 3158-3170
- Zhong R, Lee C, Ye ZH** (2010) Global analysis of direct targets of secondary wall NAC master switches in Arabidopsis. *Mol Plant* **3**: 1087-1103
- Zhong R, Lee C, Zhou J, McCarthy RL, Ye Z-H** (2008) A Battery of Transcription Factors Involved in the Regulation of Secondary Cell Wall Biosynthesis in *Arabidopsis*. *The Plant Cell* **20**: 2763
- Zhong R, Richardson EA, Ye Z-H** (2007) The MYB46 Transcription Factor Is a Direct Target of SND1 and Regulates Secondary Wall Biosynthesis in Arabidopsis. *The Plant Cell* **19**: 2776
- Zhou J, Lee C, Zhong R, Ye Z-H** (2009) MYB58 and MYB63 Are Transcriptional Activators of the Lignin Biosynthetic Pathway during Secondary Cell Wall Formation in *Arabidopsis*. *The Plant Cell* **21**: 248
- Zhou W, Qian C, Li R, Zhou S, Rui-qi Z, Xiao J, Wang X, Zhang S, Xing L, Cao A** (2018) TaNAC6s are involved in the basal and broad-spectrum resistance to powdery mildew in wheat. *Plant Science* **277**
- Zhu Z, Hao Y, Mergoum M, Bai G, Humphreys G, Cloutier S, Xia X, He Z** (2019) Breeding wheat for resistance to Fusarium head blight in the Global North: China, USA, and Canada. *The Crop Journal* **7**: 730-738

Table 5.1 Promoter sequence analysis of downstream resistance-related metabolite biosynthetic genes (R_{RRM}) harboring secondary wall NAC binding element (SNBE).

Gene	UniProtKB/TrEMBL;Acc	SNBE Sequences	Position (bp)
<i>TaCCR</i>	Q4KUK8	TTCTCTTATATATAAGAAA	-976
<i>TaCAD</i>	D7PGW0	AATTTTATTTGGCAAGCAT	-933
<i>TaLAC4</i>	A0A077RUW0	AATTGTGGGCATGAAGCTA	-901
<i>TaMYB</i>	G9DR80	TTTCGTTCTCCGAAGAAT	-133

TaCCR = *T. aestivum* cinnamoyl-CoA reductase gene; *TaCAD* = *T. aestivum* cinnamyl alcohol dehydrogenase gene; *TaLAC4* = *T. aestivum* laccase gene; *TaMYB* = *T. aestivum* R2R3-MYB transcription factor gene. Position = is the localization of SNBE upstream to the ATG start site.

Table 5.2 List of primers used in this study.

	Name	Forward	Reverse
Gene sequencing	<i>TaNAC</i>	CCGACTCCGAGCTAGTGCCGTG	TCGTGCGCAAGGCAACACCTAA
Gene expression	<i>TaNAC_qRT-PCR</i>	TCAAGAGGGACCTCTCGTTC	CCTCGAACATGGACAAGGAC
	<i>TaACTIN</i>	ACCTTCAGTTGCCAGCAAT	CAGAGTCGAGCACAATACCAGTTG
Promoter sequencing	<i>TaCCR_pro</i>	ATATGAGATGTCGTGCTATTCTCTT	CCGGAGTTGGTGGGAAACT
	<i>TaCAD_pro</i>	TGCCCCGTGATTTACTTGCCT	GGGATGGATGGAAGGGTTGC
	<i>TaLAC4_pro</i>	ATATGCGCGCACGTAAGTAGA	TAGGGTGTGTGTGTCAAGCC
	<i>TaMyb_pro</i>	ACTCTGATTCCAGGCTTCCG	AGTGCTTGCCTTGTACTGTG
VIGS gene expression	<i>TaNAC-VIGSqPCR</i>	ACGTGTATTTCTCCAGCC	GGGGATATAAACTGTCATCGATTTT
	<i>TaCCR</i>	TGTCCATTCGATCGGTCATA	TGTGCGTCATACAGCACTGA
	<i>TaCAD</i>	GGCATTGCTGAACTTGAT	TAAGGCCGGATTTTCATACCA
	<i>TaLAC4</i>	TCGCGGCTGATGTTTAATTT	GCTATGAACGGGCTAAACACA

	<i>TaMyb</i>	CCCTCACCCCTGATTGTTTTG	GGCTTAGTTGCATGGAGAGC
	<i>TaACTIN</i>	ACCTTCAGTTGCCAGCAAT	CAGAGTCGAGCACAATACCAGTTG
	<i>Tri6</i>	TCTTTGTGAGCGGACGGGACTTTA	TGTTGGTTTGTGCTTGGACTCAT

Table 5.3 Genbank accession numbers of proteins used in the phylogeny study.

S.No.	Purpose	Name of gene/Protein/region	Genbank Accession number	Plant source	Reference/ Source
1	Protein phylogeny	unnamed protein product	CDM82556.1	Triticum aestivum	NCBI
2	Protein phylogeny	unnamed protein product	VAH75368.1	Triticum turgidum subsp. durum	NCBI
3	Protein phylogeny	NAC transcription factor 32-like	XP_020200711.1	Aegilops tauschii subsp. tauschii	NCBI
4	Protein phylogeny	NAC transcription factor 56	XP_003565559.1	Brachypodium distachyon	NCBI
5	Protein phylogeny	NAC transcription factor 25	XP_002454866.1	Sorghum bicolor	NCBI
6	Protein phylogeny	NAC domain-containing protein 72-like	RLM91813.1	Panicum miliaceum	NCBI
7	Protein phylogeny	NAC transcription factor 32-like	XP_025815776.1	Panicum hallii	NCBI
8	Protein phylogeny	NAC transcription factor 32	XP_004971462.1	Setaria italica	NCBI
9	Protein phylogeny	NAC domain-containing protein 2	XP_010904917.1	Elaeis guineensis	NCBI
10	Protein phylogeny	NAC transcription factor 29-like	XP_008782049.1	Phoenix dactylifera	NCBI
11	Protein phylogeny	NAC transcription factor 29-like	XP_020256631.1	Asparagus officinalis	NCBI
12	Protein phylogeny	NAC transcription factor 56-like	XP_020099751.1	Ananas comosus	NCBI
13	Protein phylogeny	NAC domain-containing protein 2-like	XP_020689086.1	Dendrobium catenatum	NCBI
14	Protein phylogeny	NAC transcription factor NAM-2	PKA47255.1	Apostasia shenzhenica	NCBI
15	Protein phylogeny	NAC transcription factor 29	XP_020688947.1	Dendrobium catenatum	NCBI
16	Protein phylogeny	NAC domain-containing protein 18	XP_020701043.1	Dendrobium catenatum	NCBI
17	Protein phylogeny	NAC transcription factor 29-like	XP_020597561.1	Phalaenopsis equestris	NCBI

18	Protein phylogeny	NAC transcription factor 29-like	XP_021637435.1	Hevea brasiliensis	NCBI
19	Protein phylogeny	NAC transcription factor 29-like	XP_028088451.1	Camellia sinensis	NCBI
20	Protein phylogeny	NAC transcription factor 32-like	XP_020585190.1	Phalaenopsis equestris	NCBI

Figure 5.1 *In silico* analysis of the *TaNAC032* gene. (a) QTL-Fhb1 representation on the short arm of wheat chromosome 3B. The location of *TaNAC* identified within the QTL-Fhb1 region is presented on the right side of the 3B chromosome; (b) Neighbor-joining phylogenetic analysis of *TaNAC* protein (highlighted in the red box) with already reported homology proteins from other crop plants, identified close homology with NAC designated as *TaNAC032* in *Aegilops tauschii* (c) Relative transcriptional changes of *TaNAC032* at 48 hpi in wheat NILs. RM & SM: resistant and susceptible NIL mock-treated; RP & SP: resistance and susceptible NIL pathogen (*Fg*) treated. *TaActin* was used to normalize the target gene expression. Significance between resistant NIL (NIL-R) and susceptible NIL (NIL-S) treatments were analyzed using student's *t*-test *P<0.05, **P<0.01, ***P<0.001, ****P<0.0001.

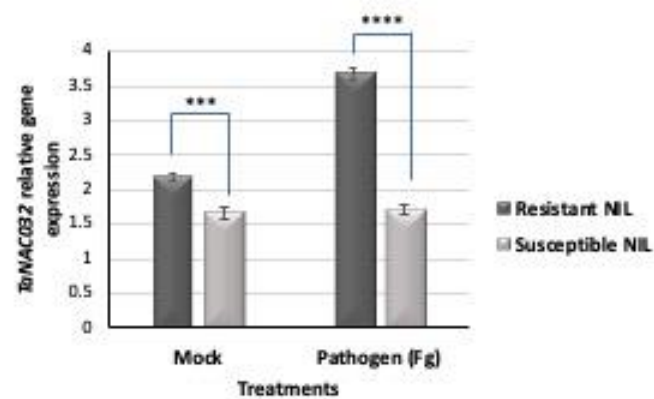
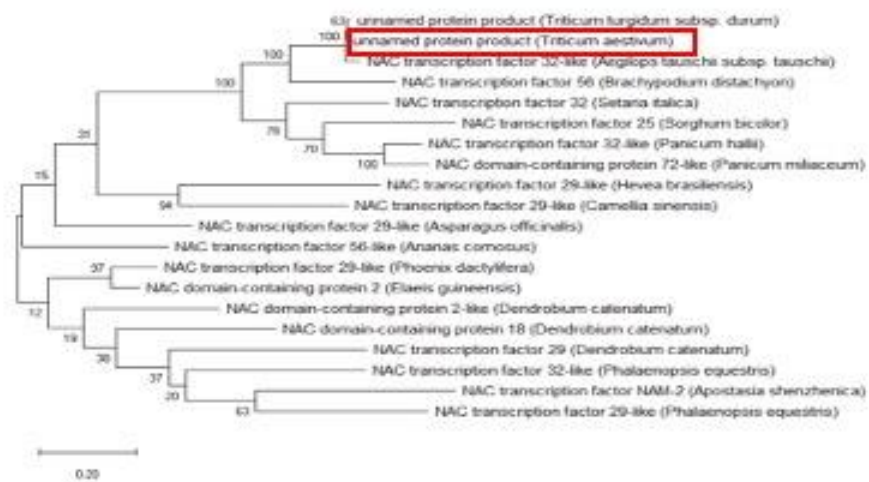
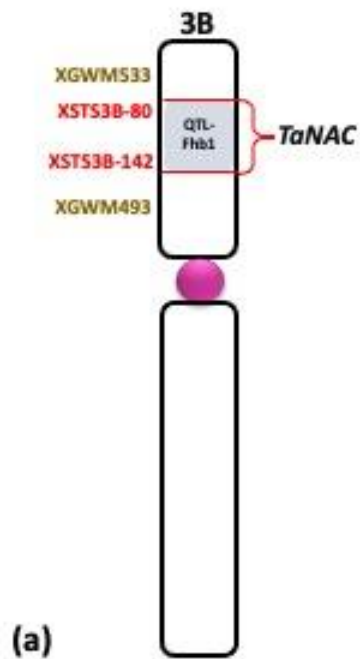


Figure 5.2 *TaNAC032* sequencing and sequence analysis. (a) Sequence alignment of *TaNAC032* DNA sequence variation between resistant NIL (NIL-R) and susceptible NIL (NIL-S) presented a deletion of 121-bp at 179 nucleotide position highlighted in blue; (b) MultAlin based amino acid sequence comparison revealed 41 amino acids deletion in NIL-S at the corresponding position highlighted in green depicts deletion of conserved NAC domain spanning 12 - 170 intervals.

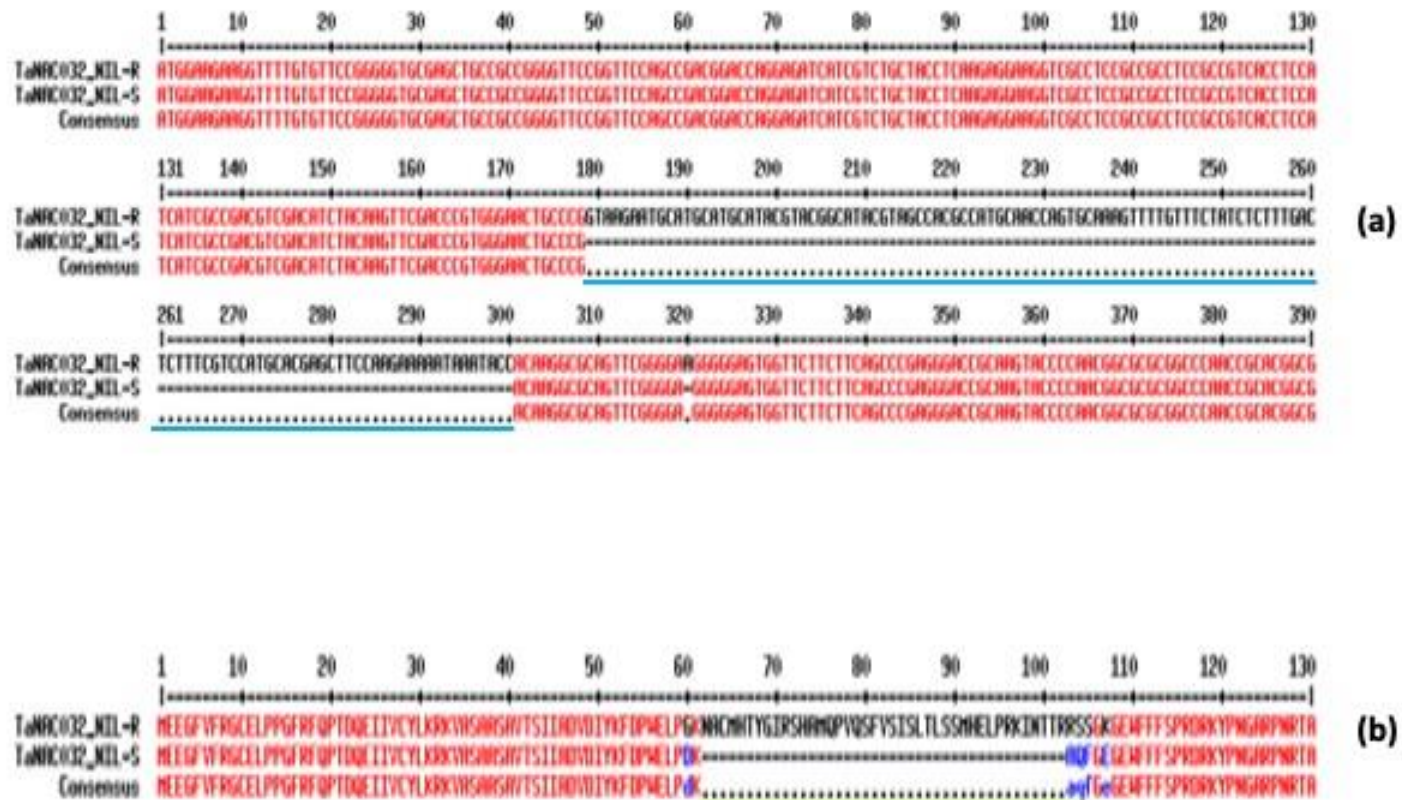
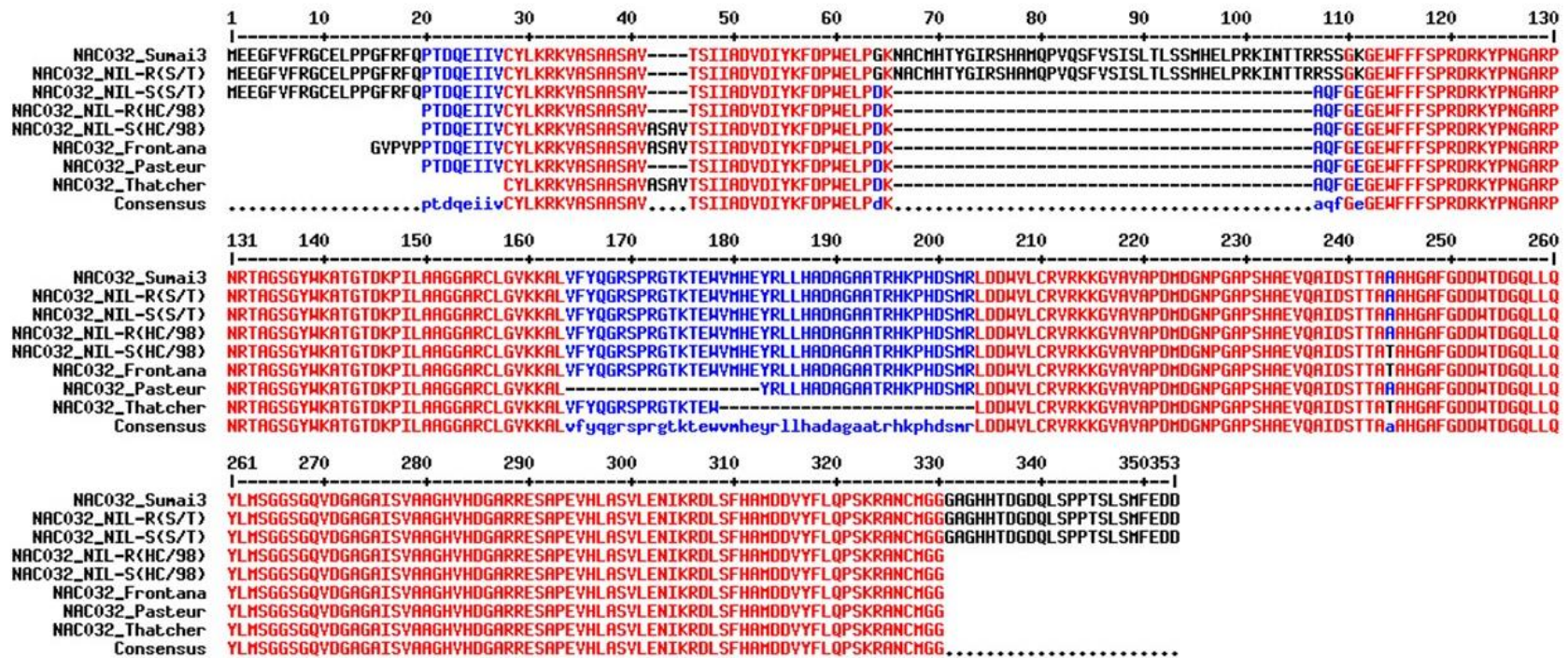


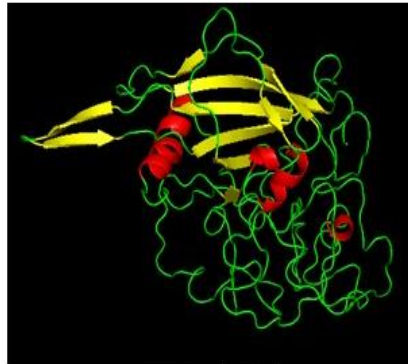
Figure 5.3 *TaNAC032* sequencing and sequence analysis in wheat genotypes (Sumai 3, NIL-R (S/T), NIL-S (S/T), NIL-R (HC/98), NIL-S (HC/98), Frontana, Pasteur and Thatcher) with varying levels of FHB resistance. (a) MultiAlin based *TaNAC032* gene sequence comparison in nine wheat genotypes including Sumai3, NIL-R (S/T), NIL-S (S/T), NIL-R (HC/98), NIL-S (HC/98), Frontana, Pasteur and Thatcher; (b) Phyre 2 Investigator software based 3D-structure prediction of both the mutated and non-mutated *TaNAC032* in the wheat genotypes.



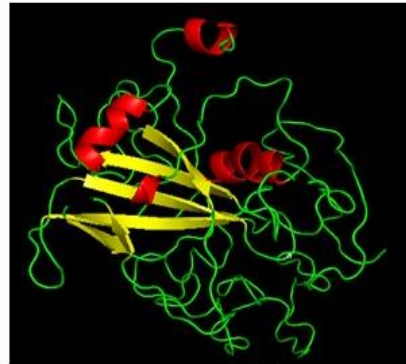
(a)



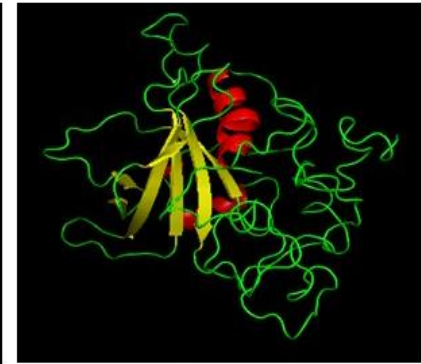
Sumai3



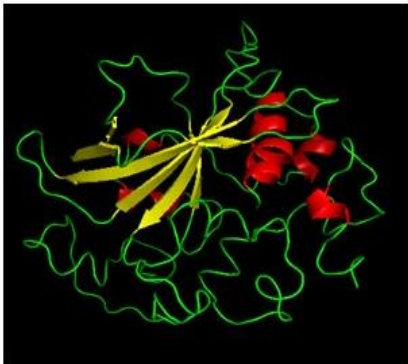
NIL-R (S/T)



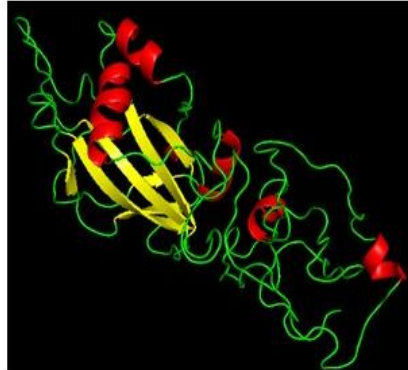
NIL-S (S/T)



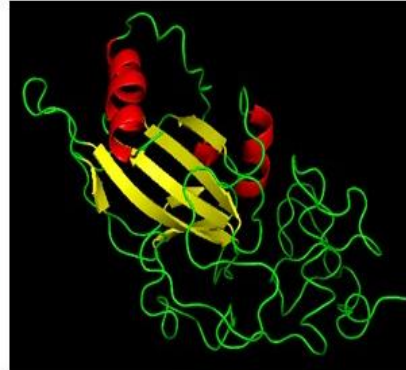
NIL-R (HC/98)



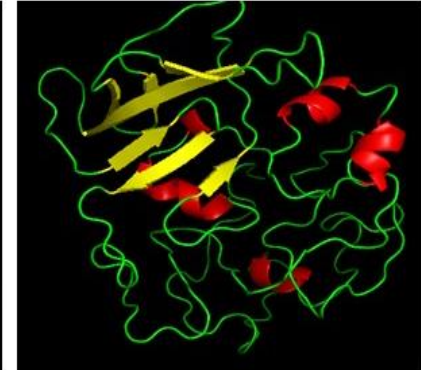
NIL-S (HC/98)



Frontana



Pasteur



Thatcher

(b)

Figure 5.4 Canonical lignin biosynthesis pathway in plants. In the phenylpropanoid pathway, PAL (phenylalanine ammonia-lyase), C4H (cinnamate 4-hydroxylase), and 4CL (4-coumarate: CoA ligase) catalyzes the formation of hydroxycinnamoyl-CoA thioesters (p-HCA-CoA), which are then reduced by CCR (cinnamoyl-CoA reductase) and CAD (cinnamyl alcohol dehydrogenase) to give p-hydroxycinnamyl alcohols (monolignols). The monolignols synthesized in the cytosol, transported into cell walls, and polymerized into lignin via oxidative coupling reactions catalyzed by oxidases such as LAC* (laccase) and PRX (peroxidase). The precursors highlighted in blue were found containing SNBE sites.

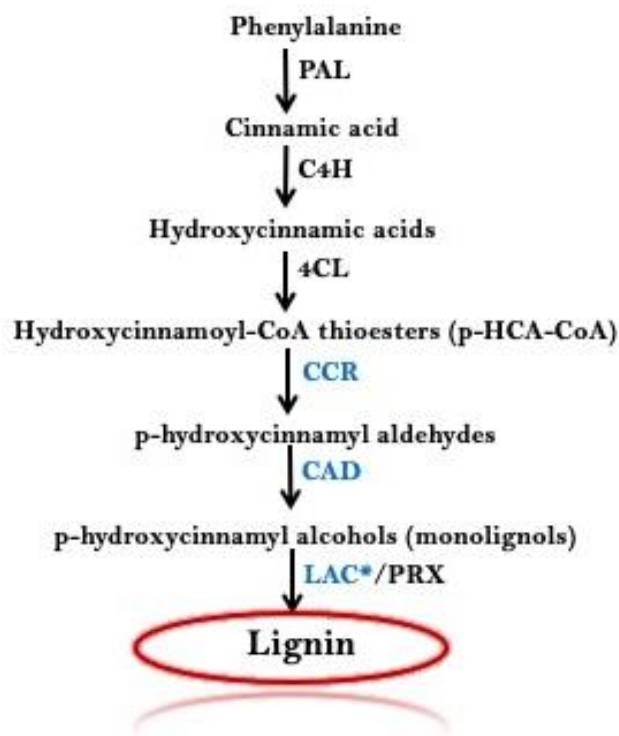


Figure 5.5 *In-silico* DNA-protein interaction using the GeneMANIA server. Here dark-colored rounds indicate target genes, *ATCCR2* (*TaCCR*), *ATCAD5* (*TaCAD*), *ATLAC17* (*TaLAC4*), and *AtMYB97* (*TaMYB*).

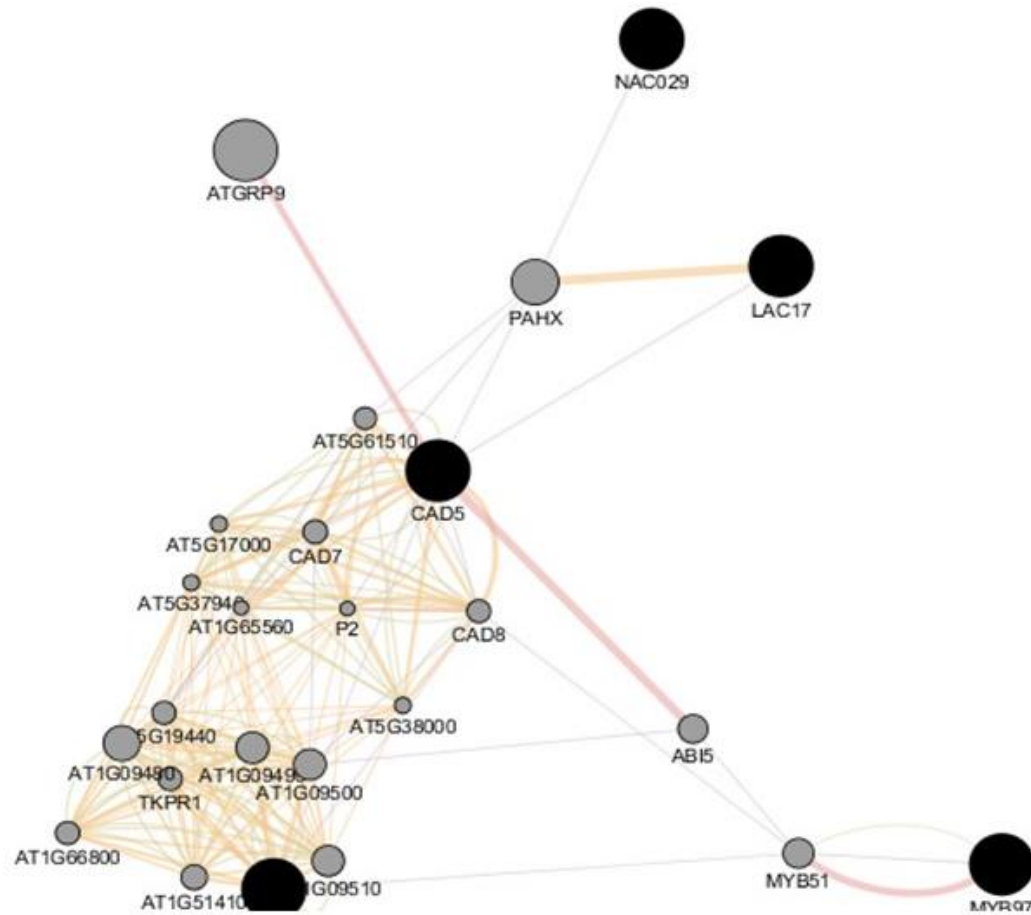


Figure 5.6 Virus-induced gene silencing (VIGS) of the *TaNAC032* gene. (a) Illustrations of constructs used in silencing study, where γ -vector of BSMV virus with *TaNAC032* gene fragment is used as a test; PDS (Phytoene desaturase) as positive control and empty γ -vector as negative control; (b) & (c) Phenotype of NILs spike and rachis section showing the efficacy of BSMV based virus-induced gene silencing of *TaNAC032* after inoculation with *F. graminearum* (*Fg*) based on discoloration or browning symptoms in silenced (BSMV: *Tanac032*) as compared to non-silenced (BSMV: 00) NIL-R plants respectively. Here, the red arrow indicates the point of inoculation.

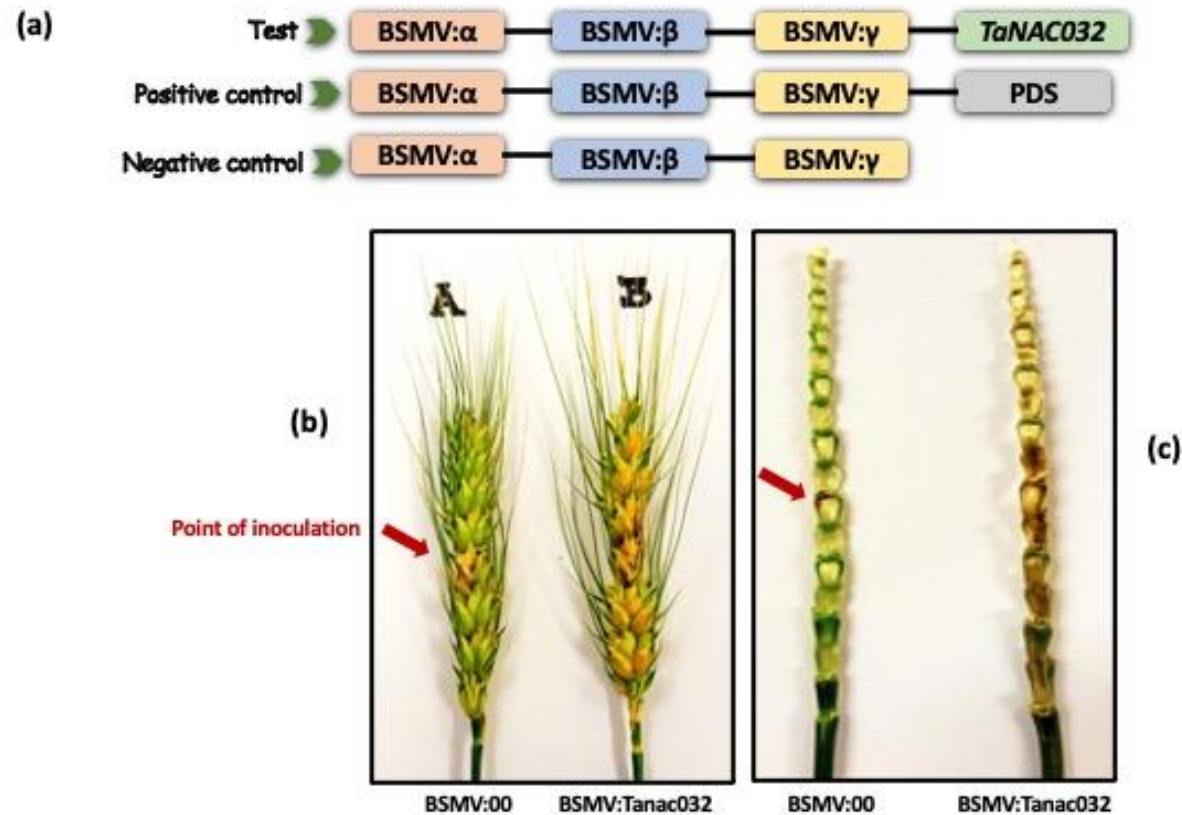
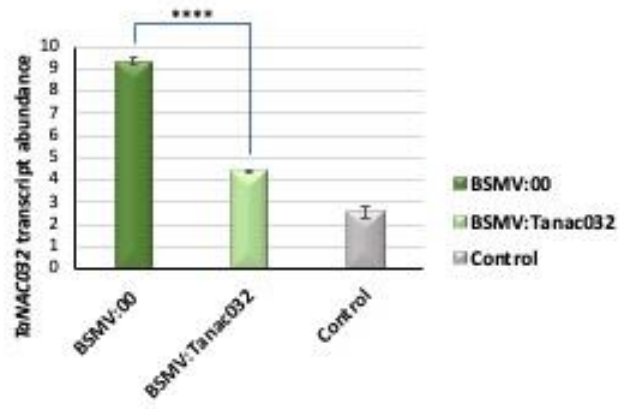
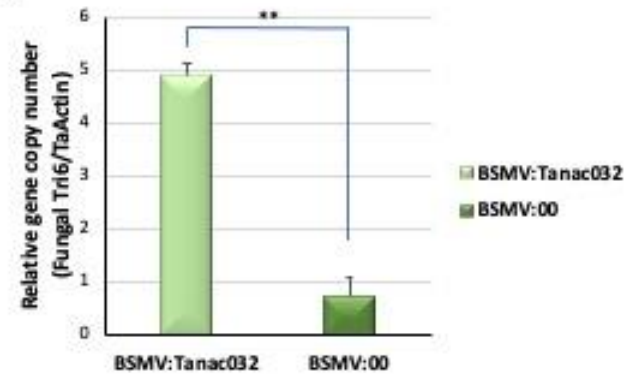


Figure 5.7 Effect of *TaNAC032* silencing in FHB resistant near-isogenic line (NIL-R), inoculated with *F. graminearum* or mock-solution. (a) Confirmation of *TaNAC032* knock-down based on relative transcript expression levels of *TaNAC032* normalized to reference gene *TaActin* in the silenced plant (BSMV: *Tanac032*) compared to non-silenced (BSMV: 00) at 48 hpi after *Fg* inoculation; The control here represents susceptible NIL (NIL-S); (b) Fungal biomass in BSMV-infected plants at 6 dpi with *Fg*, the relative copy number of *Tri6* fungal housekeeping gene (= fungal biomass) was quantified in *TaNAC032* knocked down (BSMV: *Tanac032*) plants and compared with control (BSMV: 00). *TaActin* was used to normalize the target gene copy number; (c) Disease severity analysis in NILs, based on visual observations of the proportion of spikelets diseased (PSD) (d) Relative transcript levels of *TaCCR*, *TaCAD*, *TaLAC4*, and *TaMYB* in *TaNAC032* knocked down (BSMV: *Tanac032*) plants compared to non-silenced (BSMV: 00) at 48 hpi after *Fg* inoculation. *TaActin* was used to normalize the target gene expression. Significance between silenced and non-silenced treatments were analyzed using student's *t*-test *P<0.05, **P<0.01, *P<0.001, ****P<0.0001.**

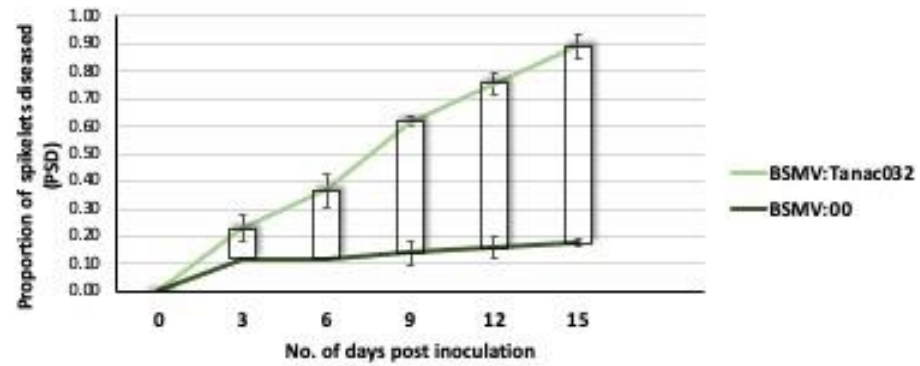
(a)



(b)



(c)



(d)

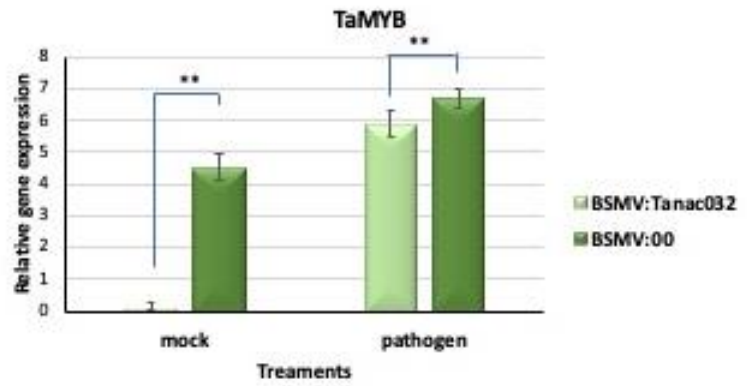
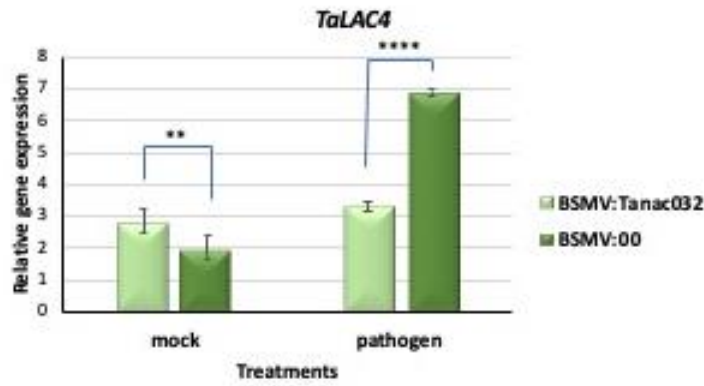
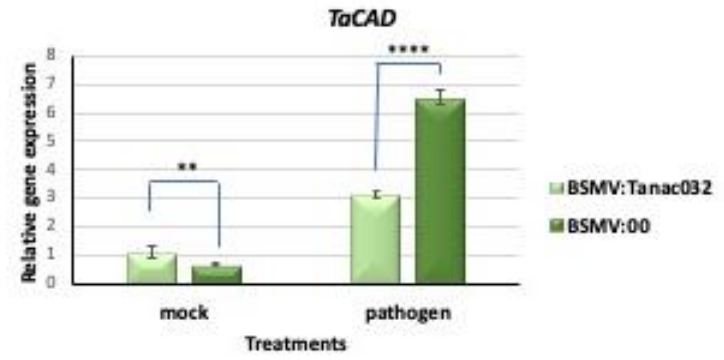
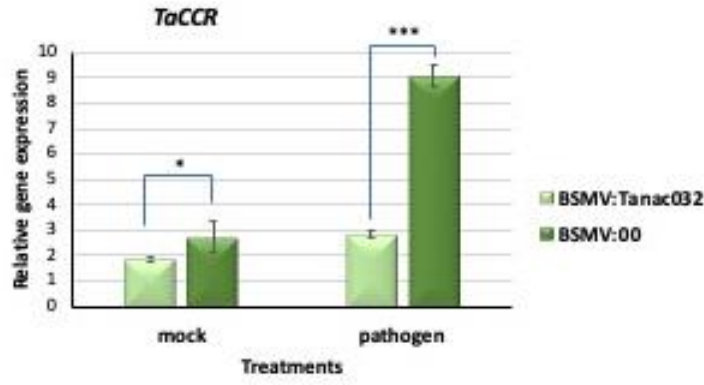


Figure 5.8 BoxPlot represents relative metabolite abundances of RRI metabolites in silenced (BSMV: *Tanac032*) and non-silenced (BSMV: 00) NIL-R at 3 dpi after *Fg* inoculation. Coniferin, Podorhizol beta-D-glucoside, and 4- Hydroxycinnamyl alcohol 4-D-glucoside. Significant differences in expression levels as compared in silenced (BSMV: *TaNAC032*) with non-silenced (BSMV: 00) upon *Fg* inoculation using Students t-test: *P < 0.05; **P < 0.01. Here, EM: non-silenced (mock-treated), EP: non-silenced (pathogen (*Fg*) treated), NM: *TaNAC032* silenced (mock-treated), NP: *TaNAC032* silenced (pathogen (*Fg*) treated).

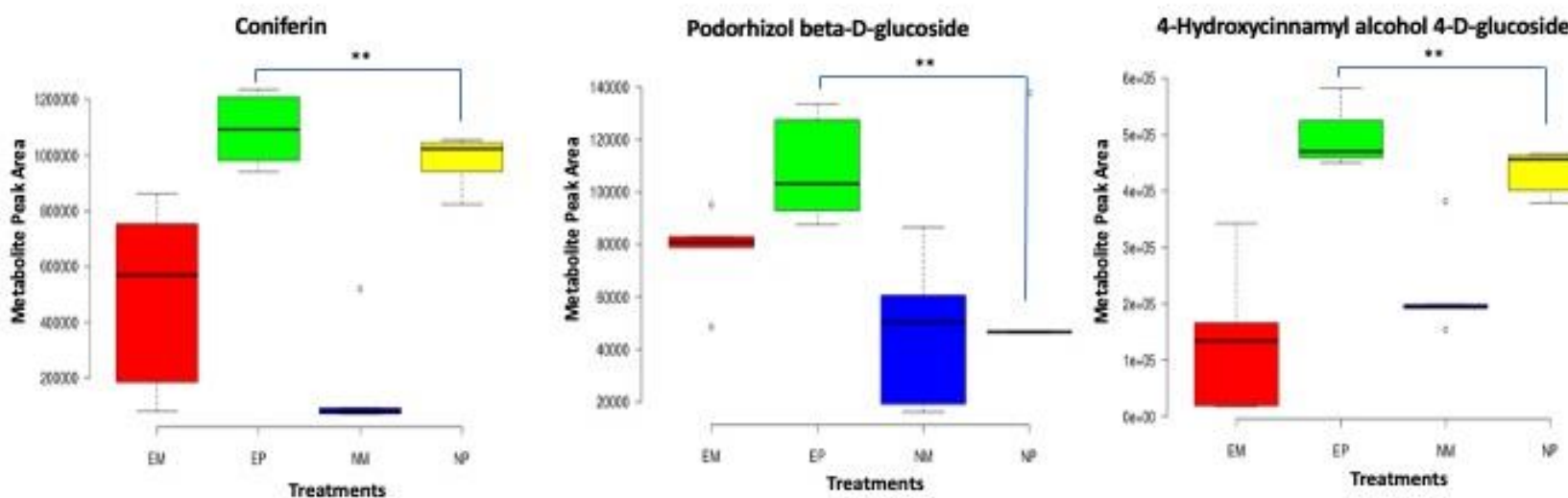
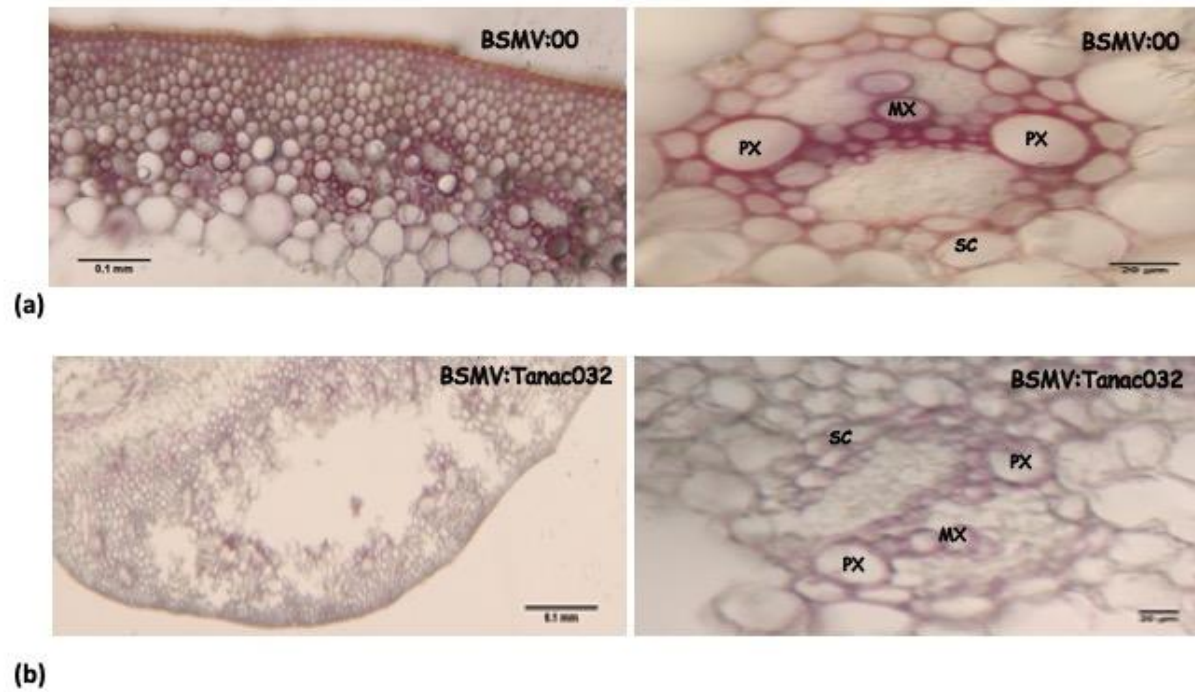


Figure 5.9 Lignification induced by *TaNAC032* in rachis. (a) & (b) Phloroglucinol-HCL staining of non-silenced (BSMV: 00) and silenced (BSMV: *Tanac032*) rachis cross-section (Scale bar 0.1mm, 20µm) respectively. Here, MX: metaxylem, PX: protoxylem, SC: sclerenchyma cells; (c) Total lignin quantification based on acetyl bromide soluble lignin test. The graph showing %ABSL (acetyl bromide soluble lignin percentage) in both BSMV: *Tanac032* (silenced) and BSMV: 00 (non-silenced) rachis samples. The control here represents susceptible NIL (NIL-S). Significance between silenced and non-silenced treatments were analyzed using student's *t*-test * $P < 0.05$, ** $P < 0.01$, * $P < 0.001$.**



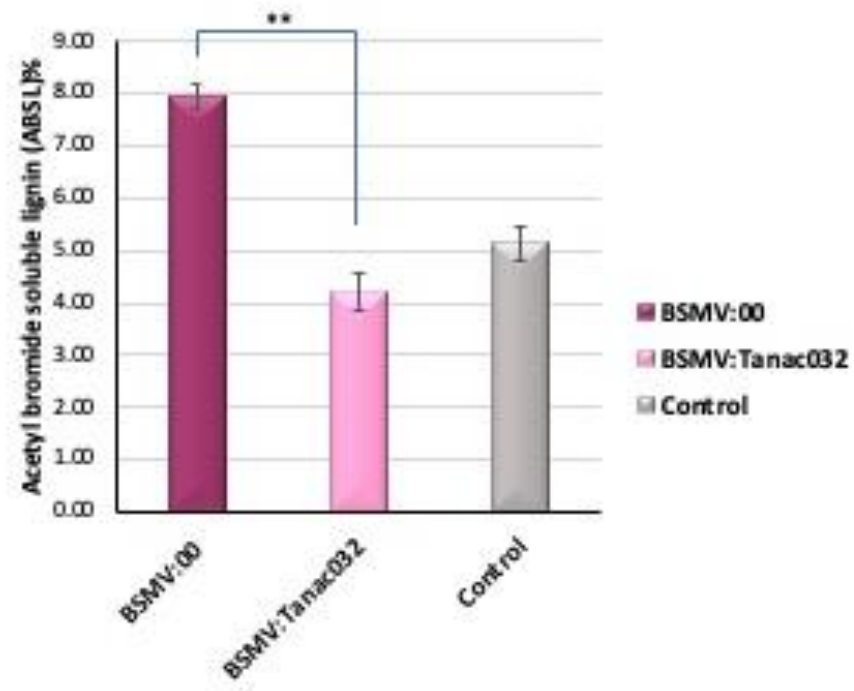
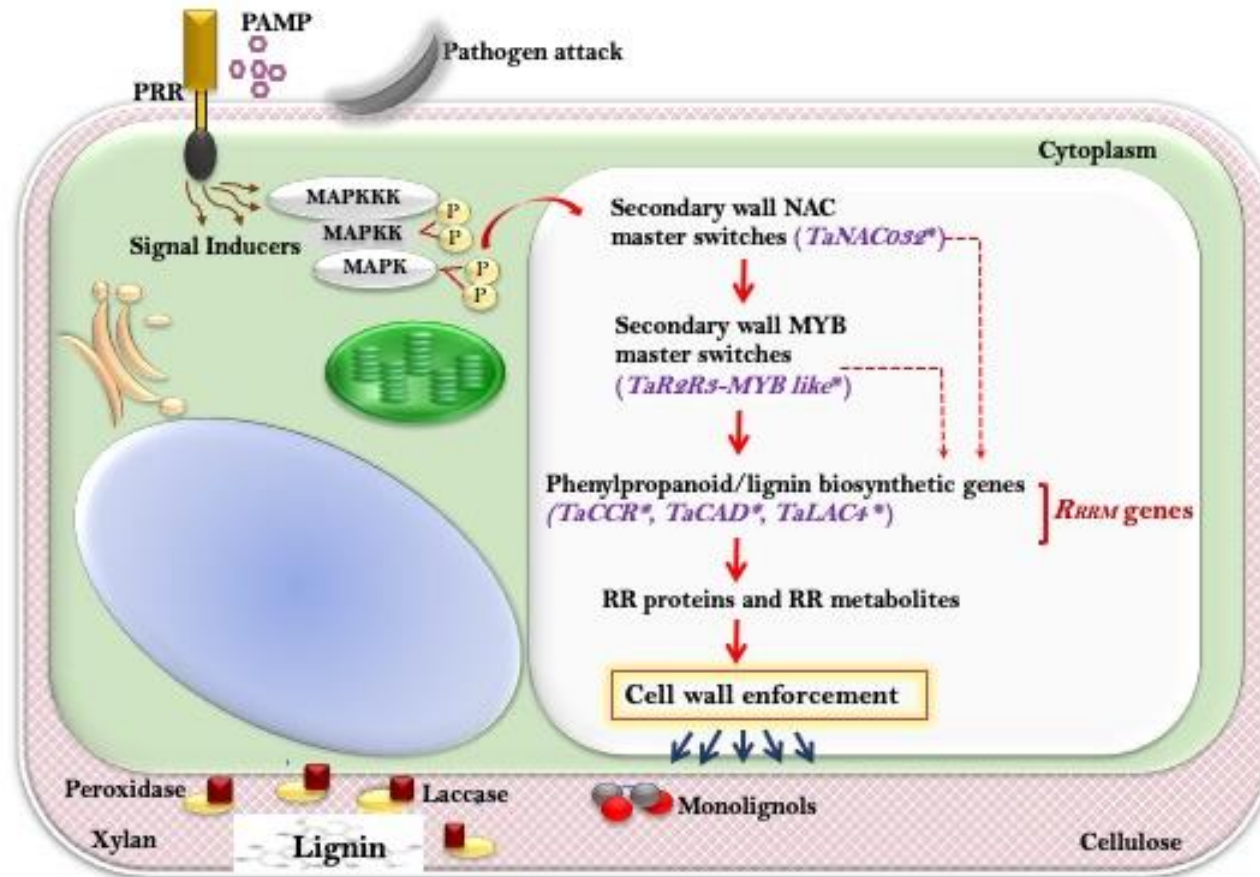


Figure 5.10 Proposed model showing *TaNAC032* transcription factor regulating the biosynthesis of lignin specific pathway biosynthetic *R_{RRM}* genes to produce resistant-related metabolites (RMs). These (RMs) are phytoanticipins and phytoalexins, or their conjugate products deposited to reinforce secondary cell wall to combat against Fusarium head blight. Red-colored bold arrows indicate the regulatory gene network, including receptors, MAPK, transcription factor (TFs), and downstream genes. Broken arrows indicate *TaNAC032* TF mediated direct regulation of downstream genes.



CHAPTER VI

GENERAL DISCUSSION, CONCLUSION AND FUTURE DIRECTIONS

6.1 General discussion and conclusions

Fusarium head blight (FHB) is a severe fungal disease affecting small grains such as bread wheat (*Triticum aestivum L.*), durum wheat (*T. durum L.*), oat (*Avena sativa L.*), and barley (*Hordeum vulgare L.*). In warm and humid regions, *Fusarium graminearum* is the primary pathogen among several other *Fusarium* species. FHB infection leads to reduced yields, shriveled grains, mycotoxin contamination, and reduction in seed quality, which accounts for economic losses over billions of US dollar since 1990 (Snijders and Perkowski, 1990; Desjardins and Hohn, 1997; McMullen et al., 1997; Windels, 2000; Dahl and Wilson, 2018; Wilson et al., 2018). The primary mycotoxin produced by *F. graminearum* in the infected grain is Deoxynivalenol (DON), which remains in processed food and causes health risks in humans and animals (Desjardins and Hohn, 1997; Pestka, 2010).

Developing resistant cultivars by utilizing host resistance is the most promising approach to control FHB. Type I and type II are the two widely accepted types of resistance; Type I resistance is known as the resistance to initial infection, whereas Type II infection is the resistance to the spread of infection within the spike (Schroeder and Christensen, 1963). Type I resistance is mainly contributed by spike morphology and systemic innate immune response activation, which is more common in barley as compared to wheat (Mesterhazy, 1995; Foroud et al., 2012). Contrastingly, Type II resistance is controlled by several resistance genes with major and minor effects based on numerous genetic studies on various resistant sources (Rejesus et al., 1996; Ma et al., 2006). Molecular mapping of quantitative trait loci (QTLs) has been extensively studied and reported for Type II resistance. Hundreds of QTLs associated with FHB resistance have been mapped in all wheat chromosomes, except 7D (Buerstmayr et al., 2009). Several candidate genes were identified from some key QTLs which contributed towards a better understanding of the pathogenesis and the underlying resistance mechanisms (Liu et al., 2008; Zhuang et al., 2013; Rawat et al., 2016; Schweiger et al., 2016; Li et al., 2019; Su et al., 2019; Paudel et al., 2020).

The FHB resistance QTL-Fhb1 (formerly named as *Qfhs.ndsu-3BS*) was first identified from Chinese cultivar Sumai 3 on chromosome arm 3BS (Anderson et al., 2001). QTL-Fhb1 accounts for 20-60 % of the phenotypic variation in FHB resistance and has been well defined as the most effective and stable QTL across different genetic backgrounds and various environment (Anderson et al., 2001; Buerstmayr et al., 2002; Zhou et al., 2002; Somers et al., 2003; Buerstmayr et al., 2009; Basnet et al., 2012). Thus, QTL-Fhb1 is considered the primary resistance QTL in wheat breeding to improve FHB resistance. Several resistance mechanisms of QTL-Fhb1 have been proposed by various studies (discussed in Chapter II), but none has been validated without contradiction. Therefore, wheat QTL-Fhb1 still interests researchers worldwide to understand the underlying resistance mechanism.

This thesis was written with two broad objectives in mind; to identify Fusarium head blight (FHB) resistance genes based on a combined metabolo-genomics approach and, functionally characterize the candidate gene(s) in response to *F. graminearum* infection in resistant near-isogenic lines to unravel the underlying resistance mechanism. The functionally validated gene(s) can be corrected in the susceptible wheat cultivar based on genome editing approaches to improve FHB resistance.

The current study reported the novel candidates associated with FHB resistance in wheat major QTL-Fhb1. It functionally characterized both *TaLAC4* and *TaNAC032* in response to *F. graminearum* infection in wheat NILs. Although several FHB resistance candidates have been identified and functionally validated, the mechanism of resistance underlying QTL-Fhb1 has not been entirely understood. This study has taken the initiative to understand the resistance mechanism by focusing on metabolomics and genomics' combined approach. We have identified several resistance-related induced, and constitutive metabolites present significantly higher in abundance through the LC-HRMS-based metabolomics approach, mainly related to the phenylpropanoid pathway. This study functionally validated the laccase gene's role in the oxidative polymerization of monolignols to biosynthesize G lignin.

Further, the NAC transcription factor has been explored to be involved in the secondary cell wall biosynthesis. This study presents the role of *TaNAC032* in regulating lignin biosynthetic genes and biosynthesizing cell wall-related metabolites during pathogen infection, which further acts as a barrier to orchestrate pathogen entry, thus providing resistance against FHB. The

proposed transcriptional regulatory network of secondary cell wall reinforcement could be an excellent model for advanced plant studies related to biotic stress.

Following the candidate gene expression analysis in both resistant and susceptible NILs upon mock and pathogen inoculation, *in-silico* characterization and polymorphism detection, the candidate gene(s) were subjected to virus-induced based gene silencing to characterize their role in FHB resistance. The silenced NILs were studied for increased disease severity and fungal biomass, metabolic changes, gene expression analysis of RR metabolite biosynthetic genes, and lignin quantification. This study further opens the opportunity to explore other candidate genes involved in the hierarchy affect the reinforcement of SCW synergistically to confer a high level of resistance against FHB in wheat.

This study elucidates the lignin biosynthetic pathway's role and its biosynthetic gene(s) in conferring resistance against FHB through secondary cell wall thickening. The role of candidate genes such as *TaLAC4* was characterized in the response of *F. graminearum* infection. The biochemical characterization of rachis based on phloroglucinol-HCL staining and acetyl bromide soluble lignin quantitation has been explored. Besides, the role of *TaNAC032* in the regulation of lignin biosynthetic genes, including *TaLAC4*, was deciphered. Overall, this thesis identified and functionally characterized two resistant genes in the hierarchy, significantly contributing to enhanced resistance to FHB. The genes functionally validated in this study can be used to replace a mutated or non-functional gene in susceptible cultivar based on genome editing tools to improve FHB resistance in wheat and related species.

6.2 Future works

Analysis of enzyme kinetics

Chapter IV attributed the role of *TaLAC4* in oxidative polymerization of monolignols to biosynthesize guaiacyl (G) lignin that reinforce plant secondary cell walls to confer enhanced resistance against FHB in wheat QTL-Fhb1. We proposed a basis for this substrate based on molecular modeling/docking experiments wherein *TaLAC4* binds more effectively to guaiacyl 4-O-5 guaiacyl (L2: PHE`267/CD1). Transient silencing of *TaLAC4* in wheat resistant NILs significantly increased lignin precursor metabolite accumulation. These metabolites were mainly soluble phenolics such as coniferyl alcohol derivatives known to be used as a substrate for Laccase enzyme to biosynthesize G lignin subunit. These findings speculated the role of *TaLAC4* in basal immunity and induced G lignin units during the infection. However, future studies can be focussed

on detailed enzymatic studies to test the laccase catalytic properties. This can be studied by HPLC based analysis by analyzing the oxidation of different monolignols as substrates in the presence of recombinant *TaLAC4*. This HPLC based study could further confirm that the *TaLAC4* oxidizes only coniferyl alcohol and not hydroxyphenyl and sinapyl alcohol.

Genomics study of the candidate genes

A combined metabolo-genomics approach paved the way for identifying novel candidates that might confer a significant role in FHB resistance. In Chapter IV, the *TaLAC4* role has been deciphered based on virus-induced gene silencing for its role in pathogen-induced secondary cell wall lignification. This study opens the opportunity to explore other laccases in wheat and other FHB QTLs involving synergistically to confer a high level of resistance against FHB in wheat. Among five novel candidates identified in Chapter III, *TaLAC4* and *TaNAC032* have been functionally validated to their FHB resistance role. However, other candidate genes such as Cell Wall Invertase (CWIN), G-type lectin S-receptor-like serine/threonine-protein kinase (RKS1), and Glutamate synthase 1 (GLT1), needs to be investigated for their roles in FHB resistance to facilitate breeding programs.

In Chapter V, the role of *TaNAC032* TF in the positive regulation of lignin-biosynthetic genes to combat Fusarium head blight has been reported based on promoter analysis, gene interaction network and gene expression analysis. However, modelling based on in vitro data only indicates several possibilities of the network; therefore, future research must focus more on DNA-protein interactions based on in vivo observations to reveal the network dynamics.

Signaling pathway and related genes in FHB resistance

Plants have developed several defense mechanisms, including pre-formed mechanisms, such as physical barriers provided by the cell wall and cuticle and inducible mechanisms to control diseases (Makandar et al., 2015). Among inducible defense responses, pathogen attack induces several defense-related pathogenesis-related (PR) genes, wherein some of them encode for antimicrobial proteins (van Loon et al., 2006). Regulation of these genes depends on signaling molecules such as salicylic acid (SA) and jasmonic acid (JA). These phytohormones may bind to nuclear proteins harboring specific domains to activate further downstream regulatory and resistance-related metabolite (RRM) genes (Lumba et al., 2010). Among defense pathways, SA

mainly confers resistance against biotrophs, which derive nutrients from live host cells. In contrast, methyl JA and ethylene (ET) play a significant role in resistance to necrotrophic pathogens, which derive their nutrients from dead host cells.

This study has functionally characterized *TaLAC4* and *TaNAC032* genes in the underlying hierarchy QTL-Fhb1. The regulation of these genes may depend upon signaling molecules such as salicylic acid (SA) that may confer resistance against biotrophs by deriving nutrients from live host cells. In contrast, jasmonic acid (JA) and ethylene (ET) play a significant role in resistance to necrotrophic pathogens, which derive their nutrients from dead host cells. Thus, it would be fascinating to explore other genes underlying QTL-Fhb1, mainly related to signaling pathways that might be involved in regulating the potential candidates identified in the QTL-Fhb1 in this study. Functional characterization of signaling pathway-related genes and understanding the hierarchical network of gene regulation would unveil the FHB resistance mechanism.

CRISPR/Cas9-induced targeted mutagenesis and gene replacement to enhance FHB resistance in wheat

Clustered regularly interspaced short palindromic repeats (CRISPR)/Cas9 is a rapidly emerging genome editing technique that revolutionized fundamental and applied research in plant breeding. It has been successfully demonstrated in many cereal crops, including rice, wheat, maize, and barley (Ansari et al., 2020). The candidate genes such as *TaLAC4* and *TaNAC032* identified and functionally validated in this study can be cloned and sequenced in other wheat cultivars. Suppose the gene or transcript is mutated in the selected cultivar. In that case, the mutated alleles can be replaced with functional alleles of the genes using the CRISPR-Cas9 genome editing tool that enables editing parts of the genome by making single nucleotide changes or removing, adding or altering sections of the DNA sequence. Enhanced FHB resistance can be proved, providing both *TaNAC032* and *TaLAC4* must be edited in commercial cultivars associated with the rest of the genes' hierarchy to biosynthesize lignin.

Large scale field study

The edited genome cultivars need to be screened for the FHB occurrence under field conditions to facilitate breeding programs. This is crucial to evaluate the disease severity both

phenotypically and genotypically under favorable environmental conditions to help the wheat growers practically.

REFERENCES

- Anderson JA, Stack RW, Liu S, Waldron BL, Fjeld AD, Coyne C, Moreno-Sevilla B, Fetch JM, Song QJ, Cregan PB, Frohberg RC** (2001) DNA markers for Fusarium head blight resistance QTLs in two wheat populations. *Theoretical and Applied Genetics* **102**: 1164-1168
- Ansari WA, Chandanshive SU, Bhatt V, Nadaf AB, Vats S, Katara JL, Sonah H, Deshmukh R** (2020) Genome editing in cereals: approaches, applications and challenges. *International Journal of Molecular Sciences* **21**: 4040
- Atanasov D** (1920) Fusarium-blight (scab) of wheat and other cereals. US Government Printing Office
- Avila CM, Atienza SG, Moreno MT, Torres AM** (2007) Development of a new diagnostic marker for growth habit selection in faba bean (*Vicia faba* L.) breeding. *Theoretical and Applied Genetics* **115**: 1075
- Bacon CW, Hinton DM** (2007) Potential for control of seedling blight of wheat caused by *Fusarium graminearum* and related species using the bacterial endophyte *Bacillus mojavenis*. *Biocontrol science and technology* **17**: 81-94
- Bai G, Shaner G** (1994) Scab of wheat: prospects for control. *Plant Disease* **78**: 760-766
- Bai G, Shaner G** (2004) Management and resistance in wheat and barley to fusarium head blight. *Annual Review of Phytopathology* **42**: 135-161
- Bai G-H, Shaner G** (1996) Variation in *Fusarium graminearum* and cultivar resistance to wheat scab. *Plant disease* **80**: 975-979
- Bai GH, Shaner G, Ohm H** (2000) Inheritance of resistance to *Fusarium graminearum* in wheat. *Theoretical and Applied Genetics* **100**: 1-8
- Basnet BR, Glover KD, Ibrahim AMH, Yen Y, Chao S** (2012) A QTL on chromosome 2DS of 'Sumai 3' increases susceptibility to *Fusarium* head blight in wheat. *Euphytica* **186**: 91-101
- Bateman GL, Gutteridge RJ, Gherbawy Y, Thomsett MA, Nicholson P** (2007) Infection of stem bases and grains of winter wheat by *Fusarium culmorum* and *F. graminearum* and effects of tillage method and maize-stalk residues. *Plant Pathology* **56**: 604-615
- Benton HP, Wong DM, Trauger SA, Siuzdak G** (2008) XCMS2: processing tandem mass spectrometry data for metabolite identification and structural characterization. *Analytical chemistry* **80**: 6382-6389
- Bergstrom GC, Kalb DW, Schilder AMC, Cox WJ, Harman GE, Samimy C** (1986) Assessment of the 1986 winter-wheat scab epidemic in new-york. *In*, Ed 11 Vol 77. Amer phytopathological soc 3340 pilot knob road, st paul, mn 55121, p 1613
- Bhuiyan NH, Selvaraj G, Wei Y, King J** (2009) Gene expression profiling and silencing reveal that monolignol biosynthesis plays a critical role in penetration defence in wheat against powdery mildew invasion. *Journal of experimental botany* **60**: 509-521
- Bisht NC, Gupta V, Ramchiary N, Sodhi YS, Mukhopadhyay A, Arumugam N, Pental D, Pradhan AK** (2009) Fine mapping of loci involved with glucosinolate biosynthesis in oilseed mustard (*Brassica juncea*) using genomic information from allied species. *Theoretical and Applied Genetics* **118**: 413-421

- Bollina V, Kumaraswamy GK, Kushalappa AC, Choo TM, Dion Y, Rioux S, Faubert D, Hamzehzarghani H** (2010) Mass spectrometry-based metabolomics application to identify quantitative resistance-related metabolites in barley against Fusarium head blight. *Mol Plant Pathol* **11**: 769-782
- Bollina V, Kushalappa AC, Choo TM, Dion Y, Rioux S** (2011) Identification of metabolites related to mechanisms of resistance in barley against Fusarium graminearum, based on mass spectrometry. *Plant molecular biology* **77**: 355
- Bradley CA, McMullen MP** (2008) Fungicides for FHB management: Past, present, and future. *In*. Citeseer, p 12
- Buerstmayr H, Ban T, Anderson JA** (2009) QTL mapping and marker-assisted selection for Fusarium head blight resistance in wheat: a review. *Plant Breeding* **128**: 1-26
- Buerstmayr H, Lemmens M, Hartl L, Doldi L, Steiner B, Stierschneider M, Ruckebauer P** (2002) Molecular mapping of QTLs for Fusarium head blight resistance in spring wheat. I. Resistance to fungal spread (Type II resistance). *Theor Appl Genet* **104**: 84-91
- Buerstmayr M, Huber K, Heckmann J, Steiner B, Nelson JC, Buerstmayr H** (2012) Mapping of QTL for Fusarium head blight resistance and morphological and developmental traits in three backcross populations derived from Triticum dicoccum × Triticum durum. *Theoretical and Applied Genetics* **125**: 1751-1765
- Burch-Smith TM, Schiff M, Liu Y, Dinesh-Kumar SP** (2006) Efficient virus-induced gene silencing in Arabidopsis. *Plant physiology* **142**: 21-27
- Cakir C, Gillespie ME, Scofield SR** (2010) Rapid determination of gene function by virus-induced gene silencing in wheat and barley. *Crop science* **50**: S-77
- Cao A, Xing L, Wang X, Yang X, Wang W, Sun Y, Qian C, Ni J, Chen Y, Liu D, Wang X, Chen P** (2011) Serine/threonine kinase gene Stpk-V, a key member of powdery mildew resistance gene Pm21, confers powdery mildew resistance in wheat. *Proc Natl Acad Sci U S A* **108**: 7727-7732
- Champeil A, Doré T, Fourbet J-F** (2004) Fusarium head blight: epidemiological origin of the effects of cultural practices on head blight attacks and the production of mycotoxins by Fusarium in wheat grains. *Plant science* **166**: 1389-1415
- Choulet F, Alberti A, Theil S, Glover N, Barbe V, Daron J, Pingault L, Sourdille P, Couloux A, Paux E** (2014) Structural and functional partitioning of bread wheat chromosome 3B. *Science* **345**
- Cummins GB** (1978) JC Arthur: The man and his work. *Annual Review of Phytopathology* **16**: 19-30
- Curtis TY, Muttucumaru N, Shewry PR, Parry MA, Powers SJ, Elmore JS, Mottram DS, Hook S, Halford NG** (2009) Effects of genotype and environment on free amino acid levels in wheat grain: implications for acrylamide formation during processing. *J Agric Food Chem* **57**: 1013-1021
- Cuthbert PA, Somers DJ, Thomas J, Cloutier S, Brule-Babel A** (2006) Fine mapping Fhb1, a major gene controlling fusarium head blight resistance in bread wheat (*Triticum aestivum* L.). *Theor Appl Genet* **112**: 1465-1472
- Dahl B, Wilson WW** (2018) Risk premiums due to Fusarium Head Blight (FHB) in wheat and barley. *Agricultural Systems* **162**: 145-153

- Das S, Upadhyaya HD, Bajaj D, Kujur A, Badoni S, Kumar V, Tripathi S, Gowda CLL, Sharma S, Singh S** (2015) Deploying QTL-seq for rapid delineation of a potential candidate gene underlying major trait-associated QTL in chickpea. *DNA research* **22**: 193-203
- De Vos RC, Moco S, Lommen A, Keurentjes JJ, Bino RJ, Hall RD** (2007) Untargeted large-scale plant metabolomics using liquid chromatography coupled to mass spectrometry. *Nature protocols* **2**: 778
- De Wolf ED, Madden LV, Lipps PE** (2003) Risk assessment models for wheat Fusarium head blight epidemics based on within-season weather data. *Phytopathology* **93**: 428-435
- Del Ponte EM, Fernandes JMC, Bergstrom GC** (2007) Influence of growth stage on Fusarium head blight and deoxynivalenol production in wheat. *Journal of Phytopathology* **155**: 577-581
- Desjardins AE, Hohn TM** (1997) Mycotoxins in plant pathogenesis. *Molecular Plant-Microbe Interactions* **10**: 147-152
- Dexter JE, Clear RM, Preston KR** (1996) Fusarium head blight: effect on the milling and baking of some Canadian wheats. *Cereal Chemistry* **73**: 695-701
- Dhokane D, Karre S, Kushalappa AC, McCartney C** (2016) Integrated metabolo-transcriptomics reveals fusarium head blight candidate resistance genes in wheat qtl-fhb2. *PloS one* **11**: e0155851-e0155851
- Duan Y, Zhang X, Ge C, Wang Y, Cao J, Jia X, Wang J, Zhou M** (2014) Development and application of loop-mediated isothermal amplification for detection of the F167Y mutation of carbendazim-resistant isolates in *Fusarium graminearum*. *Scientific reports* **4**: 7094
- Duveiller E, Singh RP, Singh PK, Dababat AA, Mezzalama M** (2012) Wheat diseases and pests: a guide for field identification. *CIMMYT*: 138
- FAO** (2016) World food situation.
- Fiehn O** (2002) Metabolomics—the link between genotypes and phenotypes. *In* *Functional genomics*. Springer, pp 155-171
- Fiehn O, Kopka J, Dörmann P, Altmann T, Trethewey RN, Willmitzer L** (2000) Metabolite profiling for plant functional genomics. *Nature biotechnology* **18**: 1157-1161
- Foroud NA, Ouellet T, Laroche A, Oosterveen B, Jordan MC, Ellis BE, Eudes F** (2012) Differential transcriptome analyses of three wheat genotypes reveal different host response pathways associated with Fusarium head blight and trichothecene resistance. *Plant Pathology* **61**: 296-314
- Francia E, Tacconi G, Crosatti C, Barabaschi D, Bulgarelli D, Dall'Aglio E, Valè G** (2005) Marker assisted selection in crop plants. *Plant Cell, Tissue and Organ Culture* **82**: 317-342
- Gilbert J, Tekauz A** (2011) Strategies for management of fusarium head blight (FHB) in cereals. *Prairie Soils Crops J* **4**: 97-104
- Golkari S, Gilbert J, Prashar S, Procnier JD** (2007) Microarray analysis of *Fusarium graminearum*-induced wheat genes: identification of organ-specific and differentially expressed genes. *Plant Biotechnology Journal* **5**: 38-49
- Goswami RS, Kistler HC** (2004) Heading for disaster: *Fusarium graminearum* on cereal crops. *Molecular plant pathology* **5**: 515-525

- Gunnaiah R** (2013) Functional characterization of wheat fusarium head blight resistance qtl (fhb1) based on non-targeted metabolomics and proteomics. *McGill University*
- Gunnaiah R, Kushalappa AC, Duggavathi R, Fox S, Somers DJ** (2012) Integrated Metabolo-Proteomic Approach to Decipher the Mechanisms by Which Wheat QTL (Fhb1) Contributes to Resistance against Fusarium graminearum. *PLOS ONE* **7**: e40695
- Hall R, Beale M, Fiehn O, Hardy N, Sumner L, Bino R** (2002) Plant metabolomics: the missing link in functional genomics strategies. *In. Am Soc Plant Biol*
- Ireta MJ, Gilchrist L** (1994) Fusarium head scab of wheat (*Fusarium graminearum* Schwabe). *CIMMYT*
- Jang C, Chen L, Rabinowitz JD** (2018) Metabolomics and isotope tracing. *Cell* **173**: 822-837
- Jia H, Cho S, Muehlbauer GJ** (2009) Transcriptome analysis of a wheat near-isogenic line pair carrying fusarium head blight-resistant and-susceptible alleles. *Molecular plant-microbe interactions* **22**: 1366-1378
- Jia H, Zhou J, Xue S, Li G, Yan H, Ran C, Zhang Y, Shi J, Jia L, Wang X, Luo J, Ma Z** (2018) A journey to understand wheat Fusarium head blight resistance in the Chinese wheat landrace Wangshuibai. *The Crop Journal* **6**: 48-59
- Jiang GL, Shi J, Ward RW** (2007) QTL analysis of resistance to Fusarium head blight in the novel wheat germplasm CJ 9306. I. Resistance to fungal spread. *Theor Appl Genet* **116**: 3-13
- Jiang GL, Ward RW** (2006) Inheritance of resistance to Fusarium head blight in the wheat lines ‘CJ 9306’ and ‘CJ 9403’. *Plant breeding* **125**: 417-423
- Jonah PM, Bello LL, Lucky O, Midau A, Moruppa SM, Moruppa Ω** (2011) Review: The importance of molecular markers in plant breeding programmes. *Global Journal of Science Frontier Research* **11**: 4-12
- Kage U, Karre S, Kushalappa AC, McCartney C** (2017) Identification and characterization of a fusarium head blight resistance gene TaACT in wheat QTL-2DL. *Plant Biotechnology Journal* **15**: 447-457
- Kage U, Yogendra KN, Kushalappa AC** (2017) TaWRKY70 transcription factor in wheat QTL-2DL regulates downstream metabolite biosynthetic genes to resist Fusarium graminearum infection spread within spike. *Scientific Reports* **7**: 42596
- Kang G, Li G, Ma H, Wang C, Guo T** (2013) Proteomic analysis on the leaves of TaBTF3 gene virus-induced silenced wheat plants may reveal its regulatory mechanism. *Journal of proteomics* **83**: 130-143
- Karre S, Kumar A, Dhokane D, Kushalappa AC** (2017) Metabolo-transcriptome profiling of barley reveals induction of chitin elicitor receptor kinase gene (HvCERK1) conferring resistance against Fusarium graminearum. *Plant Mol Biol* **93**: 247-267
- Kaspar S, Peukert M, Svatos A, Matros A, Mock HP** (2011) MALDI-imaging mass spectrometry—an emerging technique in plant biology. *Proteomics* **11**: 1840-1850
- Katajamaa M, Miettinen J, Orešič M** (2006) MZmine: toolbox for processing and visualization of mass spectrometry based molecular profile data. *Bioinformatics* **22**: 634-636
- Kugler KG, Siegwart G, Nussbaumer T, Ametz C, Spannagl M, Steiner B, Lemmens M, Mayer KF, Buerstmayr H, Schweiger W** (2013) Quantitative trait loci-dependent analysis of a gene co-expression

- network associated with Fusarium head blight resistance in bread wheat (*Triticum aestivum*L.). *BMC Genomics* **14**: 728
- Kumar A, Karre S, Dhokane D, Kage U, Hukkeri S, Kushalappa AC** (2015) Real-time quantitative PCR based method for the quantification of fungal biomass to discriminate quantitative resistance in barley and wheat genotypes to fusarium head blight. *Journal of Cereal Science* **64**: 16-22
- Kumar A, Yogendra KN, Karre S, Kushalappa AC, Dion Y, Choo TM** (2016) WAX INDUCER1 (HvWIN1) transcription factor regulates free fatty acid biosynthetic genes to reinforce cuticle to resist Fusarium head blight in barley spikelets. *Journal of experimental botany* **67**: 4127-4139
- Kumaraswamy GK, Bollina V, Kushalappa AC, Choo TM, Dion Y, Rioux S, Mamer O, Faubert D** (2011) Metabolomics technology to phenotype resistance in barley against *Gibberella zeae*. *European Journal of Plant Pathology* **130**: 29-43
- Kushalappa AC, Gunnaiah R** (2013) Metabolo-proteomics to discover plant biotic stress resistance genes. *Trends in plant science* **18**: 522-531
- Kwon SJ, Jin HC, Lee S, Nam MH, Chung JH, Kwon SI, Ryu CM, Park OK** (2009) GDSL lipase-like 1 regulates systemic resistance associated with ethylene signaling in *Arabidopsis*. *Plant J* **58**: 235-245
- Lahlali R, Karunakaran C, Wang L, Willick I, Schmidt M, Liu X, Borondics F, Forseille L, Fobert PR, Tanino K** (2015) Synchrotron based phase contrast X-ray imaging combined with FTIR spectroscopy reveals structural and biomolecular differences in spikelets play a significant role in resistance to Fusarium in wheat. *BMC plant biology* **15**: 24
- Lahlali R, Kumar S, Wang L, Forseille L, Sylvain N, Korbas M, Muir D, Swerhone G, Lawrence JR, Fobert PR** (2016) Cell wall biomolecular composition plays a potential role in the host type II resistance to Fusarium head blight in wheat. *Frontiers in microbiology* **7**: 910
- Lee W-S, Rudd JJ, Kanyuka K** (2015) Virus induced gene silencing (VIGS) for functional analysis of wheat genes involved in *Zymoseptoria tritici* susceptibility and resistance. *Fungal Genetics and Biology* **79**: 84-88
- Legrand F, Picot A, Cobo-Díaz JF, Chen W, Le Floch G** (2017) Challenges facing the biological control strategies for the management of Fusarium Head Blight of cereals caused by *F. graminearum*. *Biological Control* **113**: 26-38
- Leonard KJ, Bushnell WR** (2003) Fusarium head blight of wheat and barley. American Phytopathological Society (APS Press)
- Li G, Zhou J, Jia H, Gao Z, Fan M, Luo Y, Zhao P, Xue S, Li N, Yuan Y, Ma S, Kong Z, Jia L, An X, Jiang G, Liu W, Cao W, Zhang R, Fan J, Xu X, Liu Y, Kong Q, Zheng S, Wang Y, Qin B, Cao S, Ding Y, Shi J, Yan H, Wang X, Ran C, Ma Z** (2019) Mutation of a histidine-rich calcium-binding-protein gene in wheat confers resistance to Fusarium head blight. *Nature Genetics* **51**: 1106-1112
- Ling H** (2008) Sequence analysis of GDSL lipase gene family in *Arabidopsis thaliana*. *Pak J Biol Sci* **11**: 763-767
- Lisec J, Schauer N, Kopka J, Willmitzer L, Fernie AR** (2006) Gas chromatography mass spectrometry-based metabolite profiling in plants. *Nature protocols* **1**: 387

- Liu S, Abate ZA, Lu H, Musket T, Davis GL, McKendry AL** (2007) QTL associated with Fusarium head blight resistance in the soft red winter wheat Ernie. *Theoretical and Applied Genetics* **115**: 417-427
- Liu S, Anderson JA** (2003) Targeted molecular mapping of a major wheat QTL for Fusarium head blight resistance using wheat ESTs and synteny with rice. *Genome* **46**: 817-823
- Liu S, Pumphrey M, Gill B, Trick H, Zhang J, Dolezel J, Chalhoub B, Anderson J** (2008) Toward positional cloning of Fhb1 , a major QTL for Fusarium head blight resistance in wheat. *Cereal Research Communications* **36**: 195-201
- Liu X, Locasale JW** (2017) Metabolomics: a primer. *Trends in biochemical sciences* **42**: 274-284
- Lommen A, Kools HJ** (2012) MetAlign 3.0: performance enhancement by efficient use of advances in computer hardware. *Metabolomics* **8**: 719-726
- Lu H, Lin T, Klein J, Wang S, Qi J, Zhou Q, Sun J, Zhang Z, Weng Y, Huang S** (2014) QTL-seq identifies an early flowering QTL located near Flowering Locus T in cucumber. *Theoretical and applied genetics* **127**: 1491-1499
- Lumba S, Cutler S, McCourt P** (2010) Plant nuclear hormone receptors: a role for small molecules in protein-protein interactions. *Annual review of cell and developmental biology* **26**: 445-469
- Ma HX, Zhang KM, Gao L, Bai GH, Chen HG, Cai ZX, Lu WZ** (2006) Quantitative trait loci for resistance to fusarium head blight and deoxynivalenol accumulation in Wangshuibai wheat under field conditions. *Plant pathology* **55**: 739-745
- Ma M, Yan Y, Huang L, Chen M, Zhao H** (2012) Virus-induced gene-silencing in wheat spikes and grains and its application in functional analysis of HMW-GS-encoding genes. *BMC Plant Biology* **12**: 141
- Makandar R, Nalam VJ, Chowdhury Z, Sarowar S, Klossner G, Lee H, Burdan D, Trick HN, Gobbato E, Parker JE** (2015) The combined action of ENHANCED DISEASE SUSCEPTIBILITY1, PHYTOALEXIN DEFICIENT4, and SENESCENCE-ASSOCIATED101 promotes salicylic acid-mediated defenses to limit Fusarium graminearum infection in Arabidopsis thaliana. *Molecular Plant-Microbe Interactions* **28**: 943-953
- Manmathan H, Shaner D, Snelling J, Tisserat N, Lapitan N** (2013) Virus-induced gene silencing of Arabidopsis thaliana gene homologues in wheat identifies genes conferring improved drought tolerance. *Journal of experimental botany* **64**: 1381-1392
- Marcussen T, Sandve SR, Heier L, Spannagl M, Pfeifer M, Jakobsen KS, Wulff BBH, Steuernagel B, Mayer KFX, Olsen O-A** (2014) Ancient hybridizations among the ancestral genomes of bread wheat. *Science* **345**: 1250092
- Matny ON** (2015) Fusarium head blight and crown rot on wheat & barley: losses and health risks. *Adv Plants Agric Res* **2**: 00039
- McMullen M, Jones R, Gallenberg D** (1997) Scab of wheat and barley: A re-emerging disease of devastating impact. *Plant Dis* **81**: 1340-1348
- Mesterhazy A** (1995) Types and components of resistance to Fusarium head blight of wheat. *Plant breeding* **114**: 377-386

- Mesterházy Á, Bartók T, Mirocha CG, Komoroczy R** (1999) Nature of wheat resistance to Fusarium head blight and the role of deoxynivalenol for breeding. *Plant breeding* **118**: 97-110
- Miller JD, Young JC, Sampson DR** (1985) Deoxynivalenol and Fusarium head blight resistance in spring cereals. *Journal of Phytopathology* **113**: 359-367
- Miller SS, Watson EM, Lazebnik J, Gulden S, Balcerzak M, Fedak G, Ouellet T** (2011) Characterization of an alien source of resistance to Fusarium head blight transferred to Chinese Spring wheat. *Botany* **89**: 301-311
- Mitsuda N, Iwase A, Yamamoto H, Yoshida M, Seki M, Shinozaki K, Ohme-Takagi M** (2007) NAC Transcription Factors, NST1 and NST3, Are Key Regulators of the Formation of Secondary Walls in Woody Tissues of *Arabidopsis*. *The Plant Cell* **19**: 270
- Mohan M, Nair S, Bhagwat A, Krishna TG, Yano M, Bhatia CR, Sasaki T** (1997) Genome mapping, molecular markers and marker-assisted selection in crop plants. *Molecular breeding* **3**: 87-103
- Mueller DS** (2006) Fungicides: triazoles.
- Nadeem MA, Nawaz MA, Shahid MQ, Doğan Y, Comertpay G, Yıldız M, Hatipoğlu R, Ahmad F, Alsaleh A, Labhane N** (2018) DNA molecular markers in plant breeding: current status and recent advancements in genomic selection and genome editing. *Biotechnology & Biotechnological Equipment* **32**: 261-285
- Nicholson RL, Hammerschmidt R** (1992) Phenolic compounds and their role in disease resistance. Annual review of phytopathology **30**: 369-389
- Ogbonnaya FC, Subrahmanyam NC, Moullet O, De Majnik J, Eagles HA, Brown JS, Eastwood RF, Kollmorgen J, Appels R, Lagudah ES** (2001) Diagnostic DNA markers for cereal cyst nematode resistance in bread wheat. *Australian Journal of Agricultural Research* **52**: 1367-1374
- Okazaki Y, Saito K** (2012) Recent advances of metabolomics in plant biotechnology. *Plant biotechnology reports* **6**: 1-15
- Palazzini JM, Ramirez ML, Torres AM, Chulze SN** (2007) Potential biocontrol agents for Fusarium head blight and deoxynivalenol production in wheat. *Crop Protection* **26**: 1702-1710
- Parry DW, Jenkinson P, McLeod L** (1995) Fusarium ear blight (scab) in small grain cereals—a review. *Plant pathology* **44**: 207-238
- Paudel B, Zhuang Y, Galla A, Dahal S, Qiu Y, Ma A, Raihan T, Yen Y** (2020) WFhb1-1 plays an important role in resistance against Fusarium head blight in wheat. *Scientific reports* **10**: 1-15
- Paux E, Sourdille P, Salse J, Saintenac C, Choulet F, Leroy P, Korol A, Michalak M, Kianian S, Spielmeier W** (2008) A physical map of the 1-gigabase bread wheat chromosome 3B. *science* **322**: 101-104
- Perry JN** (1995) Spatial analysis by distance indices. *Journal of Animal Ecology*: 303-314
- Pestka JJ** (2008) Mechanisms of deoxynivalenol-induced gene expression and apoptosis. *Food additives and contaminants* **25**: 1128-1140
- Pestka JJ** (2010) Deoxynivalenol: mechanisms of action, human exposure, and toxicological relevance. *Archives of toxicology* **84**: 663-679
- Pluskal T, Castillo S, Villar-Briones A, Orešič M** (2010) MZmine 2: Modular framework for processing, visualizing, and analyzing mass spectrometry-based molecular profile data. *BMC Bioinformatics* **11**: 395

- Rafalski A** (2002) Applications of single nucleotide polymorphisms in crop genetics. *Current opinion in plant biology* **5**: 94-100
- Ramegowda V, Mysore KS, Senthil-Kumar M** (2014) Virus-induced gene silencing is a versatile tool for unraveling the functional relevance of multiple abiotic-stress-responsive genes in crop plants. *Frontiers in plant science* **5**: 323
- Ratcliff F, Harrison BD, Baulcombe DC** (1997) A similarity between viral defense and gene silencing in plants. *Science* **276**: 1558-1560
- Rawat N, Pumphrey MO, Liu S, Zhang X, Tiwari VK, Ando K, Trick HN, Bockus WW, Akhunov E, Anderson JA, Gill BS** (2016) Wheat Fhb1 encodes a chimeric lectin with agglutinin domains and a pore-forming toxin-like domain conferring resistance to Fusarium head blight. *Nat Genet* **48**: 1576-1580
- Rejesus RM, Ginkel MV, Smale M** (1996) Wheat breeders' perspectives on genetic diversity and germplasm use: Findings from an international survey. *International Wheat Conference 5; Ankara (Turkey)*. In, Ed 633.11 IWC No. 5. CIMMYT.
- Ris-Stalpers C, Trifiro MA, Kuiper GG, Jenster G, Romalo G, Sai T, van Rooij HC, Kaufman M, Rosenfield RL, Liao S, et al.** (1991) Substitution of aspartic acid-686 by histidine or asparagine in the human androgen receptor leads to a functionally inactive protein with altered hormone-binding characteristics. *Mol Endocrinol* **5**: 1562-1569
- Robertson D** (2004) VIGS vectors for gene silencing: many targets, many tools. *Annu. Rev. Plant Biol.* **55**: 495-519
- Rudd JC, Horsley RD, McKendry AL, Elias EM** (2001) Host plant resistance genes for Fusarium head blight: sources, mechanisms, and utility in conventional breeding systems. *Crop Science* **41**: 620-627
- Šafář J, Bartoš J, Janda J, Bellec A, Kubaláková M, Valárik M, Pateyron S, Weiserová J, Tušková R, Číhalíková J** (2004) Dissecting large and complex genomes: flow sorting and BAC cloning of individual chromosomes from bread wheat. *The Plant Journal* **39**: 960-968
- Schauer N, Zamir D, Fernie AR** (2005) Metabolic profiling of leaves and fruit of wild species tomato: a survey of the *Solanum lycopersicum* complex. *Journal of experimental botany* **56**: 297-307
- Schmale DG, Munkvold GP** (2009) Mycotoxins in crops: A threat to human and domestic animal health. *The plant health instructor* **3**: 340-353
- Schroeder HW, Christensen JJ** (1963) Factors affecting resistance of Wheat to scab caused by *Gibberella zeae*. *Phytopathology* **53**: 831-838
- Schweiger W, Steiner B, Vautrin S, Nussbaumer T, Siegwart G, Zamini M, Jungreithmeier F, Gratl V, Lemmens M, Mayer KFX, Bérghès H, Adam G, Buerstmayr H** (2016) Suppressed recombination and unique candidate genes in the divergent haplotype encoding Fhb1, a major Fusarium head blight resistance locus in wheat. *Theoretical and Applied Genetics* **129**: 1607-1623
- Scofield SR, Huang L, Brandt AS, Gill BS** (2005) Development of a Virus-Induced Gene-Silencing System for Hexaploid Wheat and Its Use in Functional Analysis of the *Lr21*-Mediated Leaf Rust Resistance Pathway. *Plant Physiology* **138**: 2165

- Senthil-Kumar M, Gowda HVR, Hema R, Mysore KS, Udayakumar M** (2008) Virus-induced gene silencing and its application in characterizing genes involved in water-deficit-stress tolerance. *Journal of plant physiology* **165**: 1404-1421
- Shaner G, Buechley G** (2001) New sources of resistance to Fusarium head blight of wheat. Canty SM et al. Eds: 203-203
- Shewry PR, Hey SJ** (2015) The contribution of wheat to human diet and health. *Food and energy security* **4**: 178-202
- Shulaev V** (2006) Metabolomics technology and bioinformatics. *Briefings in bioinformatics* **7**: 128-139
- Shulaev V, Cortes D, Miller G, Mittler R** (2008) Metabolomics for plant stress response. *Physiologia plantarum* **132**: 199-208
- Singh R, Rathore YS, Singh NS, Peddada N, Ashish, Raychaudhuri S** (2013) Substitution of glutamate residue by lysine in the dimerization domain affects DNA binding ability of hpr by inducing structural deformity in the DNA binding domain. *PLOS ONE* **8**: e76033
- Smith CA, Want EJ, O'Maille G, Abagyan R, Siuzdak G** (2006) XCMS: processing mass spectrometry data for metabolite profiling using nonlinear peak alignment, matching, and identification. *Analytical chemistry* **78**: 779-787
- Snijders CHA, Perkowski J** (1990) Effects of head blight caused by *Fusarium culmorum* on toxin content and weight of wheat kernels. *Phytopathology* **80**: 566-570
- Soga T, Baran R, Suematsu M, Ueno Y, Ikeda S, Sakurakawa T, Kakazu Y, Ishikawa T, Robert M, Nishioka T** (2006) Differential metabolomics reveals ophthalmic acid as an oxidative stress biomarker indicating hepatic glutathione consumption. *Journal of Biological Chemistry* **281**: 16768-16776
- Somers DJ, Fedak G, Savard M** (2003) Molecular mapping of novel genes controlling Fusarium head blight resistance and deoxynivalenol accumulation in spring wheat. *Genome* **46**: 555-564
- Stack RW** (2000) Return of an old problem: Fusarium head blight of small grains. *Plant health progress* **1**: 19
- Su Z, Bernardo A, Tian B, Chen H, Wang S, Ma H, Cai S, Liu D, Zhang D, Li T, Trick H, St. Amand P, Yu J, Zhang Z, Bai G** (2019) A deletion mutation in TaHRC confers Fhb1 resistance to Fusarium head blight in wheat. *Nature Genetics* **51**: 1099-1105
- Su Z, Jin S, Zhang D, Bai G** (2018) Development and validation of diagnostic markers for Fhb1 region, a major QTL for Fusarium head blight resistance in wheat. *Theor Appl Genet* **131**: 2371-2380
- Sutton PN, Gilbert MJ, Williams LE, Hall J** (2007) Powdery mildew infection of wheat leaves changes host solute transport and invertase activity. *Physiologia Plantarum* **129**: 787-795
- Tai Y-S, Bragg J, Edwards MC** (2005) Virus vector for gene silencing in wheat. *Biotechniques* **39**: 310-314
- Takagi H, Abe A, Yoshida K, Kosugi S, Natsume S, Mitsuoka C, Uemura A, Utsushi H, Tamiru M, Takuno S** (2013) QTL-seq: rapid mapping of quantitative trait loci in rice by whole genome resequencing of DNA from two bulked populations. *The Plant Journal* **74**: 174-183

- Urano K, Maruyama K, Ogata Y, Morishita Y, Takeda M, Sakurai N, Suzuki H, Saito K, Shibata D, Kobayashi M** (2009) Characterization of the ABA-regulated global responses to dehydration in Arabidopsis by metabolomics. *The Plant Journal* **57**: 1065-1078
- Van Eck L, Schultz T, Leach JE, Scofield SR, Peairs FB, Botha AM, Lapitan NLV** (2010) Virus-induced gene silencing of WRKY53 and an inducible phenylalanine ammonia-lyase in wheat reduces aphid resistance. *Plant biotechnology journal* **8**: 1023-1032
- van Loon LC, Rep M, Pieterse CMJ** (2006) Significance of inducible defense-related proteins in infected plants. *Annu. Rev. Phytopathol.* **44**: 135-162
- Van Loon LC, Van Kammen A** (1970) Polyacrylamide disc electrophoresis of the soluble leaf proteins from *Nicotiana tabacum* var. 'Samsun' and 'Samsun NN': II. Changes in protein constitution after infection with tobacco mosaic virus. *Virology* **40**: 199-211
- Van Sanford D, Anderson J, Campbell K, Costa J, Cregan P, Griffey C, Hayes P, Ward R** (2001) Discovery and deployment of molecular markers linked to Fusarium head blight resistance: an integrated system for wheat and barley. *Crop science* **41**: 638-644
- Vance CP, Kirk TK, Sherwood RT** (1980) Lignification as a mechanism of disease resistance. *Annual review of phytopathology* **18**: 259-288
- Várallyay É, Giczey G, Burgyán J** (2012) Virus-induced gene silencing of Mlo genes induces powdery mildew resistance in *Triticum aestivum*. *Archives of virology* **157**: 1345-1350
- Vinaixa M, Schymanski EL, Neumann S, Navarro M, Salek RM, Yanes O** (2016) Mass spectral databases for LC/MS- and GC/MS-based metabolomics: State of the field and future prospects. *TrAC Trends in Analytical Chemistry* **78**: 23-35
- Waldron BL, Moreno-Sevilla B, Anderson JA, Stack RW, Frohberg RC** (1999) RFLP mapping of QTL for Fusarium head blight resistance in wheat. *Crop Science* **39**: 805-811
- Wang Y, Xu L, Shen H, Wang J, Liu W, Zhu X, Wang R, Sun X, Liu L** (2015) Metabolomic analysis with GC-MS to reveal potential metabolites and biological pathways involved in Pb & Cd stress response of radish roots. *Scientific reports* **5**: 18296
- Ward JL, Baker JM, Beale MH** (2007) Recent applications of NMR spectroscopy in plant metabolomics. *The FEBS journal* **274**: 1126-1131
- Ward JL, Baker JM, Miller SJ, Deborde C, Maucourt M, Biais B, Rolin D, Moing A, Moco S, Vervoort J** (2010) An inter-laboratory comparison demonstrates that [1 H]-NMR metabolite fingerprinting is a robust technique for collaborative plant metabolomic data collection. *Metabolomics* **6**: 263-273
- Weigel D, Ahn JH, Blázquez MA, Borevitz JO, Christensen SK, Fankhauser C, Ferrándiz C, Kardailsky I, Malancharuvil EJ, Neff MM** (2000) Activation tagging in Arabidopsis. *Plant physiology* **122**: 1003-1014
- Wilson W, Dahl B, Nganje W** (2018) Economic costs of fusarium head blight, scab and deoxynivalenol. *World Mycotoxin Journal* **11**: 291-302
- Windels CE** (2000) Economic and social impacts of Fusarium head blight: changing farms and rural communities in the Northern Great Plains. *Phytopathology* **90**: 17-21

- Xiao J, Jin X, Jia X, Wang H, Cao A, Zhao W, Pei H, Xue Z, He L, Chen Q, Wang X** (2013) Transcriptome-based discovery of pathways and genes related to resistance against Fusarium head blight in wheat landrace Wangshuibai. *BMC Genomics* **14**: 197
- Xiao X, Ohm HW, Hunt GJ, Poland JA, Kong L, Nemacheck JA, Williams CE** (2016) Genotyping-by-sequencing to remap QTL for type II Fusarium head blight and leaf rust resistance in a wheat–tall wheatgrass introgression recombinant inbred population. *Molecular Breeding* **36**: 51
- Xue A, Chen Y, Voldeng H, Savard M, Tian X** (2008) Biological control of Fusarium head blight of wheat with *Clonostachys rosea* strain ACM941. *Cereal Research Communications* **36**: 695-699
- Yang ZP, Gilbert J, Somers DJ, Fedak G, Procnier JD, McKenzie IH** (2003) Marker assisted selection of Fusarium head blight resistance genes in two doubled haploid populations of wheat. *Molecular Breeding* **12**: 309-317
- Yogendra KN, Dhokane D, Kushalappa AC, Sarmiento F, Rodriguez E, Mosquera T** (2017) StWRKY8 transcription factor regulates benzyloquinoline alkaloid pathway in potato conferring resistance to late blight. *Plant science : an international journal of experimental plant biology* **256**: 208-216
- Yogendra KN, Pushpa D, Mosa KA, Kushalappa AC, Murphy A, Mosquera T** (2014) Quantitative resistance in potato leaves to late blight associated with induced hydroxycinnamic acid amides. *Funct Integr Genomics* **14**: 285-298
- Yu J-B, Bai G-H, Cai S-B, Ban T** (2006) Marker-assisted characterization of Asian wheat lines for resistance to Fusarium head blight. *Theoretical and Applied Genetics* **113**: 308-320
- Yu JB, Bai GH, Zhou WC, Dong YH, Kolb FL** (2008) Quantitative trait loci for Fusarium head blight resistance in a recombinant inbred population of Wangshuibai/Wheaton. *Phytopathology* **98**: 87-94
- Zhao XE, Zhu S, Liu H** (2020) Recent progresses of derivatization approaches in the targeted lipidomics analysis by mass spectrometry. *Journal of Separation Science* **43**: 1838-1846
- Zhong R, Demura T, Ye ZH** (2006) SND1, a NAC domain transcription factor, is a key regulator of secondary wall synthesis in fibers of Arabidopsis. *Plant Cell* **18**: 3158-3170
- Zhou W, Kolb FL, Bai G, Shaner G, Domier LL** (2002) Genetic analysis of scab resistance QTL in wheat with microsatellite and AFLP markers. *Genome* **45**: 719-727
- Zhu Z, Bonnett D, Ellis M, He X, Heslot N, Dreisigacker S, Gao C, Singh P** (2016) Characterization of Fusarium head blight resistance in a CIMMYT synthetic-derived bread wheat line. *Euphytica* **208**: 367-375
- Zhuang Y, Gala A, Yen Y** (2013) Identification of functional genic components of major fusarium head blight resistance quantitative trait loci in wheat cultivar Sumai 3. *Mol Plant Microbe Interact* **26**: 442-450
- Zou Z, Ishida M, Li F, Kakizaki T, Suzuki S, Kitashiba H, Nishio T** (2013) QTL analysis using SNP markers developed by next-generation sequencing for identification of candidate genes controlling 4-methylthio-3-butenyl glucosinolate contents in roots of radish, *Raphanus sativus* L. *PLoS One* **8**: e53541

APPENDICES

Supplementary Tables

Supplementary Table 3. 1 Resistance related (RR) metabolites (P<0.05) detected in the wheat NILs rachis following *F. graminearum* (*Fg*) or mock-solution inoculation.

Observed mass (Da) ^e	Retention time	ID	Name	Observed fragments	Database fragmentation	Chemical group	PubMed ID
248.1122	14.83	C05643	6-Hydroxymelatonin	80.16, 93.22, 101.29, 113.10, 119.12, 119.85, 132.13, 141.12, 164.16, 177.25, 190.26, 205.27, 219.19, 231.21, 249.27	131.06, 132.04, 141.04, 203.08, 205.09, 231.07	Tryptophan metabolism	26331804, 26927635
102.0329	32.68	LMFA01030978	3-hydroxybut-2-enoic acid	57.249775,59.163879,85.135574,59.13623,71.027458	No MS	Fatty acids	
290.1544	15.94	C09492	Laurenobiolide	85.34, 93.16, 112.17, 119.13, 127.20, 135.22, 154.17, 171.18, 185.32, 197.12, 209.21, 232.23, 249.24, 263.30, 274.24, 291.38, 298.99	68.99, 171.13, 185.13, 231.10, 232.13, 243.13, 245.08	Sesquiterpenoids	
476.2644	16.69	C09420	Emetamine	57.01, 61.99, 78.96, 101.02, 137.06, 153.00, 174.28, 197.12, 247.21, 291.20, 309.28, 339.05, 381.90, 416.06, 431.08, 462.09, 477.12	15.02,43.05,57.03,101.05, 262.18,272.16,274.18, 421.25,423.26,431.26,447.26,450.26,451.26,452.28,462.26,463.26	Alkaloids biosynthesis	
161.0491	15.4	C06330	Quinoline-3,4-diol	101.02, 113.02,119.05,120.04,131.03, 144.04,148.05,161.02,162.05, 163.06,180.48	104.05,105.03,106.06,107.05,120.04,132.04,134.02,134.06,136.04,146.02,162.05		https://doi.org/10.1101/2020.10.30.363010

^e Raw mass - 1.008 (atomic mass of hydrogen) = Observed mass, as the metabolite analysis was based on positive mode

118.0 239	1.32	SUC	succinate	No MS	No MS	Carboxylate	17032043, 30084118
164.0 473	4.99	KOX001 42	4-Coumaric acid	148.25, 135.11, 131.14,119.16, 91.45	163.03, 147.04, 135.05,119.05, 91.05	Phenylprop anoid	https://doi.org/10.1111/ ijfs.12898 , 32560111
206.0 579	18.97	CPD- 12208	p- coumaroyldiket ide	No MS	No MS	phenylprop anoid	32471084
210.0 891	16.29	44805	Sinapyl-alcohol	No MS	194.05, 179.03, 161.02,151.03, 133.02, 105.03	Phenylprop anoid	26811086
238.0 84	18.95	6705	Sinapic acid methyl ester	No MS	237.07, 133.06,103.05	phenylprop anoid	33412688, 12590493
356.1 104	14.48	64481, C17759	1-O-feruloyl- β - D-glucose	337.08, 295.18, 235.29,217.25,193.16, 175.17, 160.19, 134.16	No MS	Phenylprop anoid	12569404, 19721758
372.1 203	20.12	CPD- 8927	(+)-sesamolinal	No MS	No MS	Phenylpropanoid	
376.1 361	9.4	LOGAN ATE	Loganate	325.76, 331.00, 315.21,221.32, 217.02, 161.12,153.25, 143.25	375.12, 339.13, 329.08,213.07, 169.08, 113.08	Alkaloid	28922750
376.1 516	15.3	C08747	Ailanthone	356.93, 345.19, 327.23,195.27, 179.33, 165.28	No MS	Terpenoid	29899752
414.1 277	11.45		(-)- Podophyllotoxi n	267.2,163.23	No MS	Phenylpropanoid	
440.2 766	23.56	LMGP1 0050002	PA(17:1(9Z)/0: 0);1-(9Z- heptadecenoyl)- sn-glycero-3- phosphate	No MS	No MS	Glyceroph spholipids	27663684
520.1 936	18.56	C17529, 71761	(-)-Pinoresinol glucoside	501.23,357.28,267.28,179.18	No MS	Phenylprop anoid	17030818, 18030664
540.1 623	25.61	C10548	Cleistanthin A	No MS	No MS	Phenylpropanoid	
564.1 068	16.48		Isorhamnetin 3- (6"- malonylglucosi de)	473.19,443.18,383.26,353.18, 503.17,545.18	No MS	Flavonoid	6948582
580.2 147	17.56	C10890	(+)- Syringaresinol	339.2,327.2,356.54,459.16	No MS	Lignan	26492237

			O-beta-D-glucoside				
592.2 638	28.2	LMGP0 6050017	PI(18:4(6Z,9Z, 12Z,15Z)/0:0)	No MS	No MS	Glycerophospholipids	27194736
654.1 786	19.4	LMPK1 2050397	Iristectorigenin A 7-O-gentiobioside	329.19,314.10,299.21	No MS	Flavonoid	28922750

Supplementary Table 3. 2 Putative candidate genes and gene ontology (GO) underlying QTL-Fhb1.

Gene	Second Annotation (<i>Aegilops Tauschii</i>)	UniProtKB			Gene Ontology			
		Gene No.	Final Annotation	UniProt ID	Gene name	Protein Name	GO accession number	GO term name
#1	EXECUTER 2		No gene annotated		Uncharacterized protein	GO:0000304	response to singlet oxygen	
#2	Sarcoplasmic reticulum histidine-rich calcium-binding protein	D8L9 U3	TAA_ctg0954 b.00390.1		Sarcoplasmic reticulum histidine-rich calcium-binding protein	GO:0005509	calcium ion binding	
#3	Glycosyltransferase, HGA-like	D8L9 S8	hga2		Glycosyltransferase	GO:0016021	integral component of membrane	
#4	Glutamate decarboxylase	D8L9 S2	gad1		Glutamate decarboxylase	GO:0030170	pyridoxal phosphate binding	glutamate metabolic process, carboxylic acid metabolic process
#5	Polygalacturonase 3	D8L9 S1	pg3		Uncharacterized protein	GO:0003824	catalytic activity	
#6	F-box like domain superfamily containing protein	A0A3 B6FE 66	TRAES_3BF0 50600020CFD _c1		Uncharacterized protein	GO:0005515	protein binding	
#7	Phosphatidylserine synthase	D8L9 R0	TAA_ctg0954 b.00080.1		Phosphatidylserine synthase	GO:0016021	integral component of membrane	
#8	Fructose-bisphosphate aldolase 1	A0A3 B6FH K1	No gene annotated		Fructose-bisphosphate aldolase	GO:0003824	catalytic activity	response to oxidative stress

#9	Cell wall invertase	A0A3 B6FE A8	No gene annotated	Uncharacterized protein	GO:000 4553	hydrolase activity, hydrolyzing O- glycosyl compounds	carbohydrate metabolic process, metabolic process
#10	Uncharacterized protein		No gene annotated	Uncharacterized protein	GO:000 5524	ATP binding	protein amino acid phosphorylation
#11	Rust resistance kinase Lr10	A0A3 B6FE Y5	No gene annotated	Protein kinase domain- containing protein	GO:001 6021	integral component of membrane	protein amino acid phosphorylation
#12	Ubiquitin-conjugating enzyme E2 conversed domain	A0A0 77RU H6	TRAES_3BF1 71700050CFD _c1	Uncharacterized protein			
#13	Putative disease resistance protein RGA3			Uncharacterized protein	GO:004 3531	ADP binding	
#14	NAC domain-containing protein 75	A0A0 77RQ D0	TRAES_3BF0 96900070CFD _c1	Uncharacterized protein	GO:000 3677	DNA binding	regulation of transcription, DNA- dependent
#15	G-patch domain containing protein	W5C ZF8	TRAES_3BF0 96900030CFD _c1	Uncharacterized protein	GO:000 3676	nucleic acid binding	
#16	G-type lectin S-receptor-like serine/threonine-protein kinase (RKS1), LECRK1	A0A0 77RZ C2	TRAES_3BF0 87100050CFD _c1	Uncharacterized protein	GO:001 6021	integral component of membrane	phosphorylation, protein amino acid phosphorylation
#17	NAC transcription factor 32- like	A0A0 77RZ D5	TRAES_3BF1 00600040CFD _c1	Uncharacterized protein	GO:000 5634	nucleus	regulation of transcription, DNA- dependent
#18	Purple acid phosphatase	F6MI W5, C4PK L0	TRAES_3BF0 26700100CFD _c1, PAPHy	Purple acid phosphatase	GO:004 6872	metal ion binding	
#19	Calmodulin TaCaM2-2	P9405 8	TRAES_3BF0 79400020CFD _c1	Calmodulin TaCaM2-2	GO:000 5509	calcium ion binding	
#20	Cytochrome P450 72A14-like	W5D6 D0	TRAES_3BF0 21100050CFD _c1	Uncharacterized protein	GO:002 0037	heme binding	oxidation reduction
#21	Peroxidase 19-like	A0A3 B6FS 14	No gene annotated	Peroxidase	GO:004 6872	metal ion binding	response to oxidative stress, oxidation reduction

#22	Acetyl-CoA carboxylase (Acc-1)	A0A3B6FN69	No gene annotated	Uncharacterized protein	GO:0005524	ATP binding	protein amino acid phosphorylation
#23	Violaxanthin de-epoxidase (VDE) domain containing protein	W5D6Y2	TRAES_3BF093600100CFD_c1	Uncharacterized protein	GO:0055114	oxidation-reduction process	oxidation reduction
#24	WD40 repeat domain containing protein	W5D4F5	TRAES_3BF007900030CFD_c1	Uncharacterized protein	GO:0005737	cytoplasm	
#25	Glutamate synthase 1	A0A3B6FNM9	No gene annotated	Uncharacterized protein	GO:0016491	oxidoreductase activity	nitrogen compound metabolic process, oxidation reduction
#26	1,3-beta-glucan synthase	A0A077RZR5	TRAES_3BF046100040CFD_c1	Uncharacterized protein	GO:0016021	integral component of membrane	
#27	DUF1421 domain containing protein	W5CSZ6	TRAES_3BF046100050CFD_c1	Uncharacterized protein			
#28	Potassium channel KAT3-like	W5D6C9	TRAES_3BF090300160CFD_c1	Cyclic nucleotide-binding domain-containing protein	GO:0016021	integral component of membrane	
#29	Heat shock protein 70	W5CXB0	TRAES_3BF023000010CFD_c1	Uncharacterized protein	GO:0006457		
#30	UDP-arabinopyranose mutase 1-like	A0A077RVB3	TRAES_3BF003200130CFD_c1	Uncharacterized protein	GO:0016866	intramolecular transferase activity	
#31	Beta-glucosidase BoGH3B-like	W5D309	TRAES_3BF074800100CFD_c1	Uncharacterized protein	GO:0004553	hydrolase activity, hydrolyzing O-glycosyl compounds	carbohydrate metabolic process
#32	Scarecrow-like protein 9	A0A3B6FT64	No gene annotated	Uncharacterized protein			
#33	Laccase-4-like	A0A077RUW0	TRAES_3BF090100140CFD_c1	Laccase	GO:0005507	copper ion binding	oxidation reduction
#34	Protein PELOTA 1-like	W5D2Z2	TRAES_3BF056100010CFD_c1	Protein pelota homolog	GO:0046872	metal ion binding	

#35	NB-ARC domain-containing protein	A0A077S3Y9	TRAES_3BF041300010CFD_c1	Uncharacterized protein	GO:0043531	ADP binding	
#36	Two-component response regulator ORR25-like	A0A3B6G0N7	No gene annotated	Two-component response regulator	GO:0003700	DNA-binding transcription factor activity	regulation of transcription, DNA-dependent
#37	SKP1-like protein	W5D522	TRAES_3BF052700010CFD_c1	Uncharacterized protein	GO:0006511	ubiquitin-dependent protein catabolic process	

Supplementary Table 4.1 Lists the predicted minimum binding energy scores (kJ/mol), RMSD of best-fit predicted laccase models with lignin model compounds obtained from AutoDock Vina software.

Ligand (Modelled Protein-ID)	L1	L2	L3	L4
Binding energies (kJ/mol)	-16.02472	-21.21288	-0.71128	1.86
Amino acid residues of modelled laccase in contact	GLN265, ASP207	PHE267, GLN265	GLN188, ARG185, VAL138, ASN170	THR442, LEU306
root mean square deviation (RMSD) (nm)	0.64	0.7	0.79	0.84

Supplementary Table 4.2 List of high fold change metabolites identified in NIL-R+BSMV:*Talac4* (*TaLAC4* silenced NILs).

ID	Observed Fragmentation	Database Fragmentation
Ex AM DA Name Fo Cl ass ific ati on Observed Fragmentation Database Fragmentation		

4729	246053368	246053368	2	C	Iso pim pin elli n	137*	Co um ari ns	61.99,74.02,78.96,88.04,96.97,110.02,129.10,145.06,153,163.07,171.01,183.11,201.12,210.08,227.11,244.03,245.04,246.05	31.01838972,44.99765427,55.01838972,163.04,173.0602545,177.0551691,183.0395191,191.0344337,203.0708192,227.0500838,247.0606485
968	330955605	330955605	1	C	1- O- Van illo yl- beta -D- glu cos e	426*	HC AA s	61.99,78.96,83.05,87.01,99.08,99.92,113.10,127.11,137.10,139.11,145.06,155.11,167.14,171.10,176.93,183.14,193.12,201.11,211.13,212.14,214.89,229.14,230.15,241,255.23,256.24	No MS
11844	580215171	580215171	-	C	(+)- Syri nga resi nol O- beta -D- glu cosi de	342*	Ph eny lpr opa noi ds	61.99,78.96,89.02,123.04,153,163.04,165.05,193.05,207,225.01,243.02,255.23,279.23,299.04,314.04,329.07,355.12,368.09,383.08,411.31,476.10,491.13,509.79,558.03,579.29,600.37	No MS
12457	34034381	34034381	0	C	Doc osa noi c acid	276*	Cut in, sub eri ne and wa x bio	61.99,75.56,83.05,97.03,114.02,125,10,139.11,163.11,171.10,183.01,184.02,199.13,225.15,245.19,252.08,281.08,289.18,309.08,324.10,339.20,340.20,341.20,355.83	17.00273965,41.00273965,43.01838972,43.05477522,44.99765427,57.07042529,59.01330434,71.08607535,75.10172542,99.11737548,114.1330255,127.1486756,141.1643257,155.1799757,169.1956258,183.2112759,197.2269259,211.242576,225.2582261,239.2738761,253.2895262,267.3051762,279.3051762,291.3051762,293.3208263,295.3364764,303.3051762,311.2950055,321.3157409,323.2950055,339.3263056

							syn the sis		
1 5 7	3 2 6. 1 3 4 9 1 5	3 2 6. 1 3 6 6 3	- 5 . 5 1 6 5 3	C 1 5 4 1	Hin okit iol glu cosi de	2 . 6 7 * *	Fla vo noi ds	59.01,71.01,85.03,97.06,125.10,127. 05,128.03,145.06,146.07,171.10,183. 01,185.12,209.12,211.13,221.12,229. 14,239.13,247.21,265.22	No MS
8 5 4	5 7 8. 2 0 0 5 6 5	5 7 8. 1 9 9 9	1 . 1 4 9 9 9	C 1 8 7 6	Pod orhi zol beta -D- glu cosi de	2 . 3 8 * *	Ph eny lpr opa noi ds	59.01,80.96,94.98,125.02,152.98,164 .99,183,207,225.01,243.02,277.22,29 9.04,310.08,322.09,325.11,337.11,35 3.07,383.08,415.18,439.10,476.10,49 7.21,513.48,567.67,577.27,607.34	No MS
3 6 8 6	3 4 2. 1 3 1 4 6 7	3 4 2. 1 3 1 5	- 0 . 0 9 6 5	C 7 6 1	Con iferi n	2 . 4 8 *	Ph eny lpr opa noi ds	59.01,60.02,71.01,85.03,89.02,96.97, 101.02,113.02,131.05,145.03,161.04, 171.10,179.06,201.11,209.12,225.15, 252.08,267.10,283.26,291.20,292.20, 313.04,328.06,343.25,355.48,363.43	45.0334912,137.0597059,145.0647913,149.0597059,161.0597059,163.06009 99,163.075356,165.0910061,181.0859207,297.0968793,307.1176147,311.112 5294,325.1281794,343.1387441
1 1 5 7 5	2 3 6. 0 6 8 0 3 5	2 3 6. 0 6 8 8 5	- 1 . 9 6 6 8 1	C 9 3 1 3	5,6, 7- Tri met hox yco um arin	2 . 2 2 * *	Co um ari ns	53.13,61.99,72.99,78.96,94.98,113.0 2,119.05,125.02,145.03,147,160.09,1 66.95,168.10,190.99,206.42,217.16,2 20.15,221.15,233.15,235.17,236.17,2 36.91,247	93.97,124.93,141.85,154.95,168.96,186.92,217.07

Supplementary Text

Figure 4.2 c Phylogenetic analysis for *TaLAC*. The phylogenetic study was performed to understand the *TaLAC* gene relation with other laccases in the wheat genomes and other plant species such as *Hordeum vulgare*, *Brachypodium distachyon*, *Zea mays*, *Oryza brachyantha*, *Setaria italica*, *Panicum hallii* etc. The *TaLAC* sequence was used to search against the NCBI protein database to extract similar sequences in other plant species. The phylogenetic tree was constructed using MEGA7.0 software. The *TaLAC* gene (unnamed protein product in *T. aestivum*) is grouped along with the laccase-13-like or laccase-4 in other cereal crops. However, they were distinctly divided into two separate subgroups, indicating similarity among the laccases. Nevertheless, they have specific differences between them when it comes to the evolutionarily closed species. The *TaLAC* gene sequence (unnamed protein product in *T. aestivum*) having a recent common ancestor with laccase-4-like in *A. tauschii* and laccase-4 in *T. urartu*, suggested it be laccase-4 in *T. aestivum*.

Figure 5.1 b Phylogenetic analysis for NAC transcription factor 32-like. An unrooted phylogenetic tree was constructed by performing multiple sequence alignments of NAC proteins from several plants using the Neighbor-Joining method with well-supported bootstrap values with MEGA7.0 to confirm the phylogenetic relationships between the wheat NAC transcription factors and evaluate the evolutionary history of the *TaNAC* gene families among other related plant species. From the phylogenetic analysis, it can be concluded that the *TaNAC* (characterized as unnamed protein product) in *Triticum aestivum* have certain close homology with NAC transcription factor-32 like in *Aegilops tauschii subsp. tauschii*. Also, it can be seen that *TaNAC* is closely grouped with NAC transcription factor 56, NAC transcription factor 32, NAC transcription factor 25, NAC transcription factor-32 like, and NAC domain-containing protein 72-like in *Brachypodium distachyon*, *Setaria italica*, *Sorghum bicolor*, *Panicum hallii*, and *Panicum miliaceum* respectively. This further indicated that *TaNAC* in *Triticum aestivum* shares a close phylogenetic relationship with other wheat genomes and cereal crops during the evolutionary process. Furthermore, the phylogenetic relationship analysis can provide novel insights into the evolution of diverse NAC transcription factor gene family members, gene multiplicity and their putative functions in wheat.

Figure 5.8 BoxPlot represents relative metabolite abundances of RRI metabolites in silenced (BSMV: *Tanac032*) and non-silenced (BSMV: 00) NIL-R at 3 dpi after *Fg* inoculation. Coniferin, Podorhizol beta-D-glucoside, and 4-Hydroxycinnamyl alcohol 4-D-glucoside. Significant differences in expression levels as compared in silenced (BSMV: *TaNAC032*) with non-silenced (BSMV: 00) upon *Fg* inoculation using Students *t*-test: **P* < 0.05; ***P* < 0.01. The box plots show the normalized values or concentration (mean +/- one standard deviation). The boxes range from the 25% and the 75% percentiles; the 5% and 95% percentiles are indicated as error bars; circles indicate single data points. Horizontal lines indicate medians within each box. Here, EM: non-silenced (mock-treated), EP: non-silenced (pathogen (*Fg*) treated), NM: *TaNAC032* silenced (mock-treated), NP: *TaNAC032* silenced (pathogen (*Fg*) treated).

PERMISSION FOR MANUSCRIPT USE

Personal use

Authors can use their articles, in full or in part, for a wide range of scholarly, non-commercial purposes as outlined below:

- Use by an author in the author's classroom teaching (including distribution of copies, paper or electronic)
- Distribution of copies (including through e-mail) to known research colleagues for their personal use (but not for Commercial Use)
- Inclusion in a thesis or dissertation (provided that this is not to be published commercially)
- Use in a subsequent compilation of the author's works
- Extending the Article to book-length form
- Preparation of other derivative works (but not for Commercial Use)
- Otherwise using or re-using portions or excerpts in other works

These rights apply for all Elsevier authors who publish their article as either a subscription article or an open access article. In all cases we require that all Elsevier authors always include a full acknowledgement and, if appropriate, a link to the final published version hosted on Science Direct.

Commercial use

This is defined as the use or posting of articles:

- **For commercial gain without a formal agreement with the publisher.**
 - For example by associating advertising with the full-text of the article, by providing hosting services to other repositories or to other organizations (including where an otherwise non-commercial site or repository provides a service to other organizations or agencies), or charging fees for document delivery or access
- **To substitute for the services provided directly by the journal.**
 - For example article aggregation, systematic distribution of articles via e-mail lists or share buttons, posting, indexing, or linking for promotional/marketing activities,

by commercial companies for use by customers and intended target audiences of such companies (e.g. pharmaceutical companies and healthcare professionals/physician-prescribers).

If you would like information on how to obtain permission for such uses [click here](#) or if you would like to make commercial use of the article please visit the [Permissions Support Center](#).

Internal institutional use

- Use by the author's institution for classroom teaching at the institution and for internal training purposes (including distribution of copies, paper or electronic, and use in coursepacks and courseware programs, but not in Massive Open Online Courses)
- Inclusion of the Article in applications for grant funding
- For authors employed by companies, the use by that company for internal training purposes

BIOSAFETY RELATED DOCUMENTS

McGill University
Environmental Health and Safety

Room 426, McTavish 3610 Montreal, Quebec H3A 1Y2

THIS IS TO CERTIFY THAT

Nancy Soni

Department of Plant Science

SUCCESSFULLY COMPLETED CORE TRAINING IN

Workplace Hazardous Materials Information System (W.H.M.I.S.)

ON 23-Aug-16



Joseph Vincelli
EHS Operations Manager

Valid Until Friday, August 23, 2019



Wayne Wood
Director, EHS

McGill University Environmental Health and Safety

Room 426, McTavish 3610 Montreal, Quebec H3A 1Y2

THIS IS TO CERTIFY THAT

Nancy Soni

Department of Plant Science

SUCCESSFULLY COMPLETED CORE TRAINING IN

Introduction to Biosafety

ON 13-May-16



Joseph Vincelli
EHS Operations Manager

Valid Until Monday, May 13, 2019



Wayne Wood
Director, EHS